STABLE AMORPHOUS CALCIUM CARBONATE:

CRYSTALLIZATION BEHAVIOUR AND STABLE ISOTOPES

STABLE AMORPHOUS CALCIUM CARBONATE:

CRYSTALLIZATION BEHAVIOUR AND STABLE ISOTOPES

By KATHERINE ALLAN, B.Sc.

A Thesis
Submitted to the School of Earth, the Environment & Society
In Partial Fulfillment of the Requirements for the Degree Master of Science

McMaster University

MASTER OF SCIENCE (2022), McMaster University, Hamilton, Ontario

School of Earth, Environment & Society

TITLE: Stable Amorphous Calcium Carbonate: Crystallization Behaviour and Stable Isotopes

AUTHOR: Katherine Allan

SUPERVISOR: Dr. Sang-Tae Kim

Number of Pages: X, 218

Abstract

Amorphous Calcium Carbonate (ACC) is a naturally occurring amorphous form of the widely distributed mineral calcium carbonate ($CaCO_3$). ACC has been found increasingly as a precursor phase, calcium storage site, or strengthening structural phase in a wide array of different biomineralizing organisms. An accurate understanding of the widely used classic carbonate-water paleothermometry relies on formation of $CaCO_3$ minerals and associated oxygen isotope effects. Moreover, ACC has oft been pointed to as a possible reason for non-equilibrium isotope effects, also called vital effects, in biogenic carbonates. It is, therefore, vital to understand whether ACC can reach equilibrium with its surrounding solution, as well as the role of ACC precursors in the isotopic composition and evolution of the final crystalline phase they transform into. This study is designed to answer these questions through the precipitation of stable ACC by two methods, the alkaline method (AM) which utilizes high pH to precipitate ACC, and the silica method (SM) which envelopes precipitating ACC particles in silica vesicles to prevent crystallization. These differently precipitated ACCs are then subjected to several different experimental treatments. This is achieved by monitoring the crystallization by X-ray Diffraction (XRD), and isotopic evolution of the ACC precipitates by Isotope Ratio Mass Spectrometry (IRMS) as they age and concurrently crystallize in parent solution, or in ^{18}O enriched re-equilibration solution.

This research indicated a marked difference in the crystallization behaviour, isotopic composition, and isotopic evolution of ACC produced by these two precipitation methods. With the AM method, ACC precipitates (AM-ACC) crystallized more predictably to calcite and maintained $\delta^{18}O$ signatures that were slightly lower than the equilibrium CO_3^{2-} and resisted further isotopic exchange with surrounding solution. We propose that the former is mostly due to an incomplete DIC-water oxygen isotope equilibrium prior to the AM-ACC precipitation and the latter is a result of the high pH of the precipitating solution decreasing the solubility of the precipitated ACC phase, disallowing isotope exchange, and favouring crystallization by solid-state transformation. Conversely, while ACC precipitated using the SM (SM-ACC) yielded much more variable results, both in terms of mineralogical identity upon crystallization, and $\delta^{18}O$ values. Isotopic results were much closer to the expected equilibrium $\delta^{18}O$ value for calcite, hinting at an expedited oxygen isotope exchange between SM-ACC and parent solution. Furthermore, SM-ACC was capable of isotopic exchange with the ^{18}O enriched re-equilibration solution, a feat corresponding AM-ACC was incapable of. Overall, our experimental results gleaned here that precipitation method or precipitation environment play a critical role in the isotopic evolution of precursor ACC to crystalline $CaCO_3$, suggesting ACC as an important source of the vital effect.

Acknowledgements

First and foremost, I would like to thank Dr. Sang-Tae Kim. I cannot understate how much I valued having you as a supervisor. I was inspired by your passion for the field and your tireless pursuit of excellence. Without your support, and guidance my research and academic writing would surely have been impossible. One often finds with academic writing an almost purposeful opaqueness, sacrificing clarity and comprehensibility to cater only to certain readers. I feel I must commend you on your commitment to scientific communication that is inclusive and understandable, inviting anyone who cares to learn. I hope to bring these lessons with me both in my career and in my life. I am very thankful for the funding provided to me by the School of Earth, Environment and Society at McMaster University, the Natural Science and Engineering Research Council (NSERC) discovery grant, and McMaster University through Dr. Sang-Tae Kim. I am incredibly thankful to my committee members Dr. Greg Slater and Dr. Henry Schwarcz for their time, recommendations, and insight into my research.

I would also like to especially thank Martin Knyf, who taught me everything I know about the lab, working with you was always a joy. Your expertise, optimism, and occasional book recommendations were instrumental to my research efforts. You not only guided me in performing these laboratory techniques but passed on your knowledge and took the time to teach me, for which I'll always be grateful. Thanks also goes to Soujung Kim, my colleague and friend, who was always there to help, or offer a sympathetic ear when I needed it. Thanks also to my lab-mates Savio Manaj, Nick Randazzo, and Justin Chan I appreciated your advice, assistance, and continued support. I'd also like to thank Victoria Jarvis, James Britten, and Maureen Fitzpatrick for their assistance with XRD characterization, your expertise and hard work was invaluable. I'd also like to acknowledge Salome Santos-Blaguski, Cassandra Lo, and the rest of the SEES office staff, who always looked out for us grad students and answered any questions I had.

Finally, thank you to my family and friends for their support throughout my academic career. Mom and Dad, I can't thank you enough for the love and support you provided me during this time, and for teaching me the importance of hard work and perseverance. Thank you also to my siblings Mike and Liz for always being there for me. Michael Klowak, Morgan, and Jordan, you are absolute angels, I don't know what I would have done without you.

- Kate

Table of Contents

List of Figures

List of Tables

CHAPTER 1: INTRODUCTION & BACKGROUND

CHAPTER 1: INTRODUCTION AND BACKGROUND

1.1 Amorphous Calcium Carbonate: Properties & Precipitation/Characterization Techniques

1.1.1 Properties of Amorphous Calcium Carbonate

Calcium carbonate, or $CaCO_3$, is one of the most abundant minerals on earth, both in terms of mass and biological production (Weiner, 2003). The $CaCO_3$ mineral exists in a number of different forms including crystalline polymorphs (i.e., calcite, aragonite and vaterite), hydrated polymorphs (i.e., monohydrocalcite and ikaite), and amorphous poly*a*morphs. Details regarding the stoichiometry and structure of these $CaCO_3$ polymorphs, hydrated polymorphs and polyamorphs, referred to collectively as poly(a)morphs can be viewed in Figure 1.1. Many marine organisms produce calcite- or aragonite-based skeletal hard parts through the process of biomineralization, whereby precipitation of $CaCO_3$ is biologically induced (Cölfen, 2010; Weiner, 2003; Weiner et al., 2003). Recent scholarship, however, has increasingly noted the use of Amorphous Calcium Carbonate (ACC) as a precursor phase to more stable polymorphs of $CaCO_3$ in biomineralization processes (e.g., Aizenberg, 1996; Aizenberg et al., 2003a; Jacob et al., 2011; Politi et al., 2004). Unlike more stable crystalline $CaCO_3$ polymorphs, which have a defined structure and crystal orientation, ACC can vary dramatically in terms of its morphology, size, stability, and level of hydration (Lam et al., 2007). Therefore, a simple definition of the stoichiometry and ordering of ACC is virtually impossible, as depending on its precipitating environment (contributing factors will be discussed later in this chapter) the structure of ACC will vary considerably. Generally, biogenic ACC can be found in two different polyamorphic forms, one hydrated and one dehydrated. These two forms vary stoichiometrically in the fact that hydrated ACC – also called stable ACC – has one mole of water per mole of calcium carbonate, while dehydrated ACC – also called transient ACC – does not have bound water (Addadi et al.,

2003). These forms are considered stable or transient due to the stabilizing effect of bound water on ACC, and the fact that ACC crystallization is often linked to dehydration.

Despite variability in ACC structure depending on precipitation conditions, there are a few features that remain consistent. First, it is isotropic in polarized light, meaning it does not diffract X-rays, an important factor when discussing how to characterize ACC or confirm its presence (Lowenstam, 1972), and second, ACC exhibits no structural order at atomic distances greater than 15 Å (Michel et al., 2008). Some short-range order below these atomic distances can be expected, indicating proto-structures, which are short-range structures that sometimes correspond to the final crystalline $CaCO_3$ polymorph the ACC eventually crystallizes into (Cartwright et al., 2012; Levi-Kalisman et al., 2002; Raz et al., 2003). This pre-structuring of ACC to yield a certain crystalline $CaCO_3$ polymorph is specifically controlled in nature by the biomineralizing organism, and is often done through a complex interplay of additive ions, macromolecules, proteins and possible interaction with an organic matrix (Politi et al., 2006). The imposition of a proto structure on ACC has also been achieved in lab using additive ions, which will be discussed in forthcoming sections.

1.1.2 ACC in Nature

A study by Beniash et al. in 1997 documented the first evidence of ACC as a precursor phase in biomineralization, noting that sea urchin larval spicule growth proceeded first by deposition of ACC which then crystallized to calcite over time. Before this point biogenic ACC had been observed rarely as temporary $CaCO_3$ storage sites in mollusc granules, gastroliths and spicules (Akiva-Tal et al., 2011; Beniash et al., 2009; Politi et al., 2006), as structural stiffeners in larval shells, and crustacean cuticles (Raz et al., 2002; Weiss et al., 2002), as well as being found in leaf Cystoliths of certain plants (Levi-Kalisman et al., 2002; Setoguchi, 1989).

However, all these ACC deposits were uncharacteristically stable, and remained part of the host organism for long periods of time, in some cases for the entire lifetime of the organism (Gal et al., 2010). Conversely, the discovery that ACC could exist as a temporally transient precursor phase indicated that ACC could be much more widespread throughout taxa than originally thought. Its existence was likely obscured by its transient nature when removed from the stabilizing environment of its host organism.

This supposition proved accurate, and an increasing number of organisms were found to utilize ACC as a precursor phase to calcite or aragonite biomineralization. The larva of the gastropod *Biomphalaria* was later reported to be composed of entirely ACC (Hasse et al., 2000). Larval shells of marine bivalves *Mercenaria* and *Crassostrea gigas* were found to employ ACC as the first deposited $CaCO_3$ phase prior to its crystallization to aragonite and calcite (Weiss et al., 2002). Furthermore, it was noted that the striking similarities in the behaviour of these two bivalves indicate that this crystallization strategy is likely shared by other, similar taxa (Weiss et al., 2002). A detailed distribution of biogenic ACC is provided in Table 1.1.

Inorganic $CaCO_3$ sources have also been found to harbour ACC. For example, ACC has been found within speleothems, $CaCO_3$ deposits which precipitate from drip-water solution in limestone caves, and commonly take on the forms of stalagmites, stalactites, or flow-stone deposits (Fairchild et al., 2006; Frisia et al., 2002). The isotopic composition of these speleothems offer a great deal of useful information about the climate in which deposition occurred. For instance, the $\delta^{18}O$ of the speleothem calcite can provide information about rainfall (Lachniet, 2009), while $\delta^{13}C$ can help infer the type and coverage of vegetation over a cave, assuming that chemical and isotopic equilibrium was met during precipitation (Fairchild et al., 2006; Labuhn et al., 2015). One feature of speleothems is that they often contain small pores of trapped water within their mass, these are known as fluid inclusions (McDermott, 2004; Swart,

2015). Recently ACC has been discovered to co-exist with calcite and aragonite within these cave deposits (Demény, Czuppon, et al., 2016; Demény, Németh, et al., 2016). This can complicate the isotopic record relayed by the speleothem as the fluid inclusion can re-equilibrate with the ACC as it crystallizes to aragonite, and then to calcite via a dissolution-reprecipitation reaction (Demény, Czuppon, et al., 2016; Zhang et al., 2014)

1.1.3 In-Lab ACC Precipitation

With the discovery of ACC-producing organisms there has been a concurrent increase in molecules, ions, and environmental conditions that are found to stabilize ACC in vitro. The precipitation of ACC and its subsequent transformation to increasingly metastable crystalline $CaCO_3$ phases is suggested to occur according to Ostwald's step rule (Navrotsky, 2004; Wang & Xu, 2013). This rule, first proposed by Ostwald in 1897 posits that an initial reaction product will continuously undergo reactions to form new phases that increase in metastability with each crystallization, until the most stable phase precipitates. This process is often referred to as Ostwald ripening (Ostwald, 1901; Voorhees, 1985). In the case of ACC this might occur, for example, as an initial ACC deposition followed by a transformation to aragonite, and a final transformation to calcite. This has been directly illustrated in the calciferous glands of earthworms, where ACC has been observed in the initial deposited phase, then dissolving and partially recrystallizing as calcite, which in turn transforms to a polycrystalline calcite and then finally to a single calcite crystal (Versteegh et al., 2017). This process is thought to be less energetically expensive than a direct precipitation of calcite without the intervening steps. Rather than overcoming the large energetic barrier associated with this immediate single-crystal precipitation, smaller barriers to increasingly metastable $CaCO_3$ polymorphs are subsequently overcome. This rule also forms the basis for understanding how ACC precipitation techniques

can reduce the free energy of the precipitating system to produce ACC rather than a more stable polymorph of $CaCO_3$

Observations regarding the macromolecules and ions present in biogenically stable ACC were used to extrapolate their use as synthetic ACC stabilizing agents. For example, in one study, Wang & Xu, (2013) prepared and stabilized synthetic ACC by creating a polymerized dopamine layer on which ACC could form, synthetically mimicking the way stable ACC forms with adhesive proteins on mussel shells. There has been a number of similar studies over the past two decades analyzing the efficacy of different ACC-stabilization methods (Blue et al., 2013; Cai et al., 2010; Kellermeier et al., 2010; Lam et al., 2007; Ross et al., 2011; Tester et al., 2014). These methods can be broken down into two broad groups – (I) The use of additives, and (II) local environmental controls.

1.1.3.1 Additive Method

An additive is a relatively broad term that applies to any soluble ion or macromolecule that prevents the formation of crystalline $CaCO_3$ and helps ACC persist as the primary phase in solution (Jung et al., 2019). Different additives achieve this goal by various means, such as preventing dehydration, altering coordination geometries, and preventing nucleation (Albéric et al., 2018; Bewernitz et al., 2012; Jung et al., 2019). Many stabilizing additives were initially found by looking to organic producers of ACC (Ihli, Kim, et al., 2013). It was often found that biogenic ACC was stabilized in environments rich in magnesium and phosphate, as well as mineral phases with glycoproteins high in glutamic acid and hydroxyamino acids (Politi et al., 2010; Raz et al., 2003; Wang & Xu, 2013). While many studies introduce synthetic versions of these additives, some experiments have isolated actual proteins and molecules from ACC-producing organisms and successfully used them to stabilize synthetic ACC in vitro (Bentov et

al., 2010; Gayathri et al., 2007). Furthermore, when utilizing biogenically produced additives, the structure of the ACC and the resultant $CaCO_3$ crystal it becomes are often structurally similar to the true biomineral that crystallized in vivo.

For the purposes of this thesis the addition of OH^- ions to achieve manipulation of parent solution pH, was one of the primary methods of ACC stabilization. This precipitation method was called the Alkaline Method (AM), based on the method used by Koga et al. (1998). The high concentration of NaOH in the carbonate (CO_3^{2-}-) donor solution creates a highly alkaline environment for ACC precipitation. If viewed from a thermodynamic perspective, this high pH changes several conditions within ACC-water system that consequently decrease the likelihood of $CaCO_3$ mineral crystallization. This, therefore, allows for ACC to precipitate before any crystalline $CaCO_3$ polymorphs, and to persist for much longer in the system compared to the ambient conditions. Koga et al. (1998) noted that the activation energy for the induction of crystallization rose from 152 to 304 kj mol $^{-1}$, which was facilitated by the observation that the crystallization temperature in the $CaCl_2$-Na_2CO_3-NaOH system varied depending upon the pH of the system or the concentration of NaOH (Kojima et al., 1994). This also revealed that pH drastically affects the particle size, morphology, and crystallization dynamics of ACC. As pH increases there is a concurrent rise in the content of $Ca(OH)_2$ as a crystallization product, and the ACC crystallizes at increasing dehydration temperatures as well as decreasing in overall particle size. This is all evidence of increasing disorder within the ACC-solution system, and the decreased number of possible nucleation sites. This was further characterized by an observed increase in the activation energy of crystallization. In later studies (Rao et al., 2016; Rodriguez-Blanco et al., 2012), it has been asserted that this pH dependence is linked to a short-range structure of ACC, and the binding strength of the Ca^{2+} and CO_3^{2+} ions within precursor clusters. As pH and the binding strength of these ions are inversely related to the stability of the ACC,

higher pH leads to a lengthened metastable phase in the crystallization landscape (Ogino et al., 1987; Rodriguez-Blanco et al., 2012; Rodriguez-Blanco et al., 2011). Furthermore, solutions containing ACC have a higher relative supersaturation with respect to $CaCO_3$ with increasing pH levels (Rodriguez-Blanco et al., 2011). There is also evidence that pH affects the local environment of stable prenucleation clusters that form prior to transformation to a metastable polymorph of $CaCO_3$, preventing them from reaching an appropriate, or critical, size to induce further particle aggregation or crystallization (Gebauer et al., 2008).

Furthermore, one of the known factors that induces the formation of an amorphous mineral is a highly rapid increase in Ca^{2+} and CO_3^{2-} ion concentration – i.e. dumping of $CaCl_2$ (Ca^{2+}-donor) parent solution into Na_2CO_3 (CO_3^{2-}-donor) solution rather than slow, precise pouring – in the system, as this is known to inhibit larger crystal growth (Simkiss, 1991). This rapid nucleation rate favours a smaller particle size, another common trait of amorphous minerals. Another factor considered for AM was the solution used to clean the precipitate. Ethanol has been used successfully in ACC stabilization in various experiments (e.g., Chen et al., 2013; Koga & Yamane, 2008; Lee et al., 2005; Seo et al., 2005). Organic solvents, such as ethanol among other light alcohols, can significantly reduce the solubility of carbonates, and stabilize the ACC phase, causing it to remain the primary phase in solution (Li et al., 1999).

1.1.3.2 Environmental Control Method

The alternative to the additive method of stabilizing ACC is controlling the local environment in which it precipitates. The use of additives in stabilizing ACC is associated with a few problems, specifically, post-precipitation treatments such as drying or washing that often mitigate the additives' ability to stabilize ACC. Therefore, the use of a specific environment that favours the precipitation of ACC and helps it persist can be very useful in creating ACC that is

stable, and relatively "pure" in the sense that there is no contamination by additive chemicals or ions. One study by Ihli et al. (2013) uses freeze-drying to yield pure ACC that remains stable over long periods of time. This was achieved by immersing a container of supersaturated $CaCO_3$ solution in a liquid nitrogen bath. As the solution freezes the reacting ions, CO_3^{2-} and Ca^{2+} are pushed closer and closer together by the encroaching ice front resulting in high supersaturation and causing ACC to form, which is then stabilized by the cold temperatures. Other works using aerosol precipitation similarly seek to form additive-free, stable ACC (Xto et al., 2019).

One of the most popular methods in environmental-control ACC stabilization is isolation, where the volume in which ACC precipitates is limited. This method of reaction volume restriction is also known as 'confinement', which can be seen as any environment that limits the number of dimensions in which nucleation is allowed to occur, thereby changing the thermodynamics and kinetics of the mineralizing system (Meldrum & O'Shaughnessy, 2020). A great deal of crystallization processes in nature are known to occur in vesicles or other isolating environments, away from bulk solutions (Stephens et al., 2010). This provides a great many advantages to a biomineralizing organisms, such as depression of freezing and melting points, a control over crystal formation locality, and most importantly, stabilization of metastable phases and assistance in polymorph selection (Meldrum & O'Shaughnessy, 2020).

To understand the effect of isolation on ACC stabilization, a basic understanding of nucleation is necessary. Classical biomineralization of $CaCO_3$ begins with precipitation of a mineral phase from a solution that is supersaturated with respect to a specific polymorph, calcite, for example. The initial stage of polymorph precipitation is characterized by fluctuations in concentration of ions in the solution, and the formation of clusters of the new phase once ion concentrations exceed the solubility constant of the phase of interest. Classical nucleation theory tells us that if these clusters reach a certain size (or a critical size). they will grow to reduce the

free energy of the system. This requires the system to summit a free energy barrier to nucleation, the height of this barrier relies on several factors such as spatial concerns and heterogeneous nucleators (Whittaker et al., 2016). For example, in a bulk solution at ambient temperature and pressure with sufficient available ions of Ca^{2+} and CO_3^{2-}, calcite will readily precipitate as it has the lowest solubility product of the $CaCO_3$ polymorphs (Simkiss, 1991). However, with an increasing number of organisms known to employ amorphous precursors it is becoming clear that the direct precipitation of the most stable polymorph is not nearly as common in nature as once believed (Addadi et al., 2003; Akiva-Tal et al., 2011; Beniash et al., 2009; Jacob et al., 2011; Politi et al., 2006; Raz et al., 2003)

Precipitation of carbonates in confinement provides a number of environmental factors that favour the persistence of an amorphous phase and disfavour the formation of more stable crystalline phases. This is achieved through several thermodynamic and kinetic methods. Firstly, the nucleation rate is greatly reduced, small volumes both exclude impurities and greatly reduce the probability of nucleation sites forming (Meldrum & O'Shaughnessy, 2020; Simkiss, 1991). If a nucleus of critical size is unable to form, then supersaturation can increase past the solubility product of any crystalline $CaCO_3$ polymorph allowing for ACC to form instead. This also leads to a strong dependence of polymorph selection on the pore-size, or volume-size in which precipitation occurs. For example, when researchers utilized the contact point between two crossed glass cylinders as spaces for carbonate growth, vaterite, rather than calcite, was observed to precipitate in pores of sufficiently small diameter (Wang et al., 2017). For another example, ACC tended to be the persistent phase when 10-50 μm liposomes were used as the precipitating environment (Tester et al., 2011). Various confining environments have been successfully used to isolate and confine growing ACC particles, including glass, phospholipid bilayers consisting of 1,2-dioleoyl-sn-glycero-3-phosphocholine (DOPC) or 1,2-dipalmitoyl-sn-glycero-3-

phosphocholine (DPPC), as well as collagen fibrils and silica coatings (Kellermeier et al., 2010; Ping et al., 2016; Ross et al., 2011; Wang et al., 2017). Interestingly, these methods have been utilized not only to study the effect of confinement on crystallization, but also to create these confined spaces to assist in industrial methods, and pharmaceutical delivery. The silica method, or SM, relies on limiting the volume in which mineralization occurs to control the amorphous phase and prevent aggregation and nucleation of ACC particles.

1.1.4 Characterization of ACC

1.1.4.1 Considerations when Characterizing ACC

Characterizing ACC can be a somewhat complicated endeavor. The technique used is dependent on the feature of ACC being examined – most commonly, amorphousness, topography and appearance, short-range order, and relative fractions of the $CaCO_3$ poly(a)morphs present in the precipitate. Most characterization techniques involve some measure of sample preparation such as grinding, mounting, coating, heating, or purification (Atkins, 1978; Goldstein et al., 1975; Smith, 2011). This presents a problem when characterizing ACC due to its unstable nature. For example, scanning electron microscopy (SEM) is a popular technique for imaging $CaCO_3$ crystals, as it elucidates surface topography, chemical composition, and crystalline structure at magnifications as high as 1 μm (Goldstein et al., 1975). However, to perform this characterization using typical SEM machines, the sample is bombarded by incident electrons that are usually accelerated to energies between 2 and 1000 keV (Henini, 2000). Both sample storage prior to characterization, and sample preparation for characterization involve heating samples to temperatures above 100 °C. This can make SEM a poor candidate for unstable ACC characterization as these preparatory steps are likely to crystallize an ACC sample before it is even transported to the SEM facility. Therefore, characterizing ACC using SEM is

only appropriate given that the precipitate is sufficiently stabilized, either by additives or precipitation environment, to prevent crystallization during preparation or characterization. When such additives are present SEM has been used successfully to image both biogenic (e.g., Aizenberg et al., 2002; Gago-Duport et al., 2008; Gayathri et al., 2007; Lee et al., 2008), and synthetically produced (e.g., Günther et al., 2005; Huang et al., 2007; Ihli et al., 2013; Zou et al., 2015) ACC. These issues could be solved using an alternative imaging process, such as an environmental SEM (ESEM) which operates using specialized apertures to minimize electron loss and requires minimal sample preparation. This addresses the need to image materials in conditions as close to their natural settings as possible, however, typical SEM machines can take images at higher spatial resolutions (Wang & Lee, 2008).

ACC is known to sometimes display short-range order that has some predictive power in terms of the final polymorph it transforms into. These differences in short-range order (over areas of < 0.5 nm) can be elucidated by extended X-ray absorption fine structure (EXAFS) analysis (Addadi et al., 2003; Levi-Kalisman et al., 2002). This characterization technique provides a quantitative impression of the local atomic structure of the material being analyzed (O'Day et al., 1994). Through mathematical manipulation of the EXAFS results, the arrangement of atoms around the central calcium ion of ACC and accurate interatomic distances can be determined, as well as differences in short-range order (Becker et al., 2003). For example, a study by Weiner et al. (2003) showed the short-range order of three different biogenic ACCs illustrating how they differed and theorizing that this difference was subject to biological control. Likewise, another study by Becker et al. (2003) using EXAFS, showed that deposits of biogenic ACC had a short-range order (structure of first coordination shell) that corresponded to the crystalline phase it crystallized into. Figure 1.3 features examples of the typical characterization techniques used to confirm ACC amorphousness and investigate topography and appearance.

For the purpose of this study verifying amorphousness of precipitates, or polymorphic identity upon crystallization was considered to be of the greatest import. The characterization techniques and considerations are outlined below.

1.1.4.2 Characterizing Amorphousness

Possibly the most important, and obvious, feature of ACC is its amorphousness, or whether it lacks long-range order (> 15 Å), this is also the most relevant to this thesis. This is a useful diagnostic test to confirm the presence of ACC either as a stable mineral, or as a precursor phase to more crystalline $CaCO_3$ polymorphs. As there are no telltale signs of the amorphousness of ACC visible to the human eye, confirming a precipitate as ACC is an essential step in most studies of this polyamorph of $CaCO_3$. There are three basic methods typically used to determine the presence of ACC – X-ray diffraction (XRD), Fourier Transform Infrared Spectroscopy (FTIR), and Raman spectroscopy.

XRD is most commonly used to determine the orientation of a single crystal, to determine the identity of an unknown material, and to measure the size, internal stress, and shape of small crystalline regions (Kontoyannis & Vagenas, 2000). A brief description of the nature of this method of testing is required to illuminate its use as an ACC characterisation method. The required radiation is produced in an X-ray tube. An X-ray tube must always contain two electrodes, an anode (the target metal) which is almost always at ground potential, and a cathode which is at high negative potential. The cathode is normally on the order of 30,000-50,000 volts for XRD work. Upon the release of this radiation, the beam of electrons will strike the target at high velocity and produce X-rays which radiate in all directions. These rays will consist of several different wavelengths of varying intensities. These differences are a product of the tube

itself and the material the electrons interacted with. Electrons are either produced using gas, or hot filaments (Atkins, 1978).

Typically, CuKα X-ray diffraction is used to analyze the various poly(a)morphs of calcium carbonate. In this case, copper as its target metal, producing characteristic K lines on the continuous spectrum (Atkins, 1978). The copper anode is chosen over other possible target metals such as molybdenum, iron, or cobalt because the wavelengths produced by the Cu anode are reasonably long (1.5406 Å). Furthermore, this wavelength notably matches the interatomic distance of crystalline solids, and thus provides the highest resolutions for the materials in question for this study. This is also the most commonly used anode for the identification of $CaCO_3$ poly(a)morph character for both synthetic and biological samples (e.g., Aizenberg et al., 2002; Demény, Németh, et al., 2016; Rodriguez-Blanco et al., 2011). Indeed, when alternative methods are used, they are often corrected to Cu-Kα radiation to normalize their data with the existing literature (e.g., Gago-Duport et al., 2008; Levi-Kalisman et al., 2000). XRD can be incredibly useful as a method for confirming amorphousness of a precipitate, being both fast, and relatively simple.

The typical spectra of all amorphous and crystalline $CaCO_3$ poly(a)morphs can be viewed in Figure 1.1. XRD spectra can not only differentiate between poly(a)morphs but elucidate the molar fraction of each polymorph within the system by comparing the reflection peaks that are individual to that polymorph. This evaluation cannot be applied to the molar fraction of polyamorphs to polymorphs. For instance, the fraction of calcite to aragonite in a mineral sample can be determined by comparing the 104-reflection peak unique to calcite, and the 221-peak for aragonite. However, due to the lack of peaks, the XRD spectra cannot, for example, estimate the relative fraction of ACC to calcite.

The XRD results for ACC typically feature large hump-like peaks, referred to as broad diffuse maxima, or sometimes as haloes, centered at the 2θ around 20° and 45° (Figure 1.3-(C)), hinting that there is some order within the ACC precipitate, even if this is not expressed as crystalline peaks. XRD spectra can be reported in either relative intensities or counts, both are a measure of the intensity of the deflected X-rays, but relative intensities will correct all spectra to the same scale, which is useful for displaying polymorphic identity (Atkins, 1978). When reported in counts, an observer can see the actual intensity of the scattered X-rays increase with transformation from ACC to a crystalline polymorph of $CaCO_3$, corresponding with an increase in long-range order (Radha et al., 2010). XRD can also be useful for studies of ACC because it can be used in conjunction with a programmable heating apparatus and the crystallization of ACC with dehydration can be directly monitored (Koga & Yamane, 2008).

The difficulty with the XRD method is the unstable nature of ACC, and its tendency to crystallize. For this reason, there are both timing and methodology constraints on characterizing ACC using XRD (Kontoyannis & Vagenas, 2000). Though XRD hints at a short-range order, there is no indication of what that may be. For example, XRD might tell you that the precipitate is amorphous, however, it would not be able to differentiate between proto-vaterite and proto-calcite. Moreover, ACC is generally destabilized by dehydration, and can be caused to crystallize by manual grinding (Radha et al., 2010). When using XRD, the sample must be ground into a fine powder to be mounted. Due to the unstable nature of ACC grinding of precipitates was performed immediately before characterization to limit post-filtration crystallization as structural water may cause interference on the spectra.

FTIR and Raman spectroscopy are also widely used to characterize ACC. Raman spectroscopy provides the molecular fingerprint of the sample of interest using inelastic scattering phenomenon (Lewis & Edwards, 2001), while FTIR is a form of vibrational

spectroscopy, relying on either the absorption, reflection, or transmission of infrared light (Smith, 2011). Raman spectroscopy can be highly useful in confirming or dismissing amorphousness in a $CaCO_3$ sample, furthermore, sample preparation for this technique is relatively non-destructive. Like XRD the appearance of the Raman and FTIR ACC spectra are distinct from that of crystalline $CaCO_3$ polymorphs, showing broad humps rather than sharp peaks (Figure 1.2C) (Aizenberg et al., 2003; Koga & Yamane, 2008; Raz et al., 2002). FTIR is also capable of illustrating amorphousness, in a process similar to both of the aforementioned techniques. ACC spectra are characterized by broad humps at around 3400-3500, if the ACC is hydrated, and 1400-1500 cm^{-1} rather than sharp peaks (Figure 1.2-A) (Evans et al., 2019; Koga & Yamane, 2008). The locations of these broad humps, correspond to specific vibrations, O-H stretching of bound water (if ACC is hydrated), and the carbonate ion respectively (Koga et al., 1998; Politi et al., 2004). Many studies have used all three (i.e., XRD, Raman and FTIR) characterization techniques simultaneously (e.g., Ajikumar et al., 2005; Blue et al., 2013; Rodriguez-Navarro et al., 2015), to illustrate the presence of ACC, and often, the change in each corresponding spectrum as it crystallizes. For the purposes of this study XRD was used as the primary characterization technique as it sufficiently illustrates amorphousness of freshly precipitated ACC while limiting sample damage associated with preparation. Furthermore, this technique determines which $CaCO_3$ polymorphs are present in a sample after ACC crystallizes.

1.2 Classic Carbonate-Water Oxygen Isotope Thermometry – Successes & Challenges

Calcium Carbonate ($CaCO_3$) minerals – the most abundant biologically-produced minerals – have, for some time, made up the backbone of various fields of Earth and Environmental study (Addadi et al., 2003; Meldrum & O'Shaughnessy, 2020; Weiner et al., 2003). Decades of research into these minerals has created an increasingly robust understanding

of how formation conditions can imprint themselves upon these forming minerals and record certain conditions such as temperature (Samuel Epstein et al., 1951; S. T. Kim et al., 2007), and ocean chemistry (Immenhauser et al., 2016; Zeebe, 1999). The study of stable isotope geochemistry has been widely used in the reconstruction of paleoclimate environments for over half a century. In the early 1950s it was observed that, if in isotopic equilibrium with precipitating water, calcite's oxygen isotope composition is temperature dependent (McCrea, 1950). Two substances, i.e., calcite and water, attain isotopic equilibrium when the exchange of stable isotopes between the two phases ceases to occur. This state is reached when chemical equilibrium has been established (Epstein & Mayeda, 1953). Therefore, a calibration can be established between formation temperature and carbonate oxygen isotopes – allowing for the estimation of past ocean temperatures based upon biogenic marine carbonates that formed at that time. These calibration curves are typically created using inorganic mineral synthesis in lab at precisely controlled temperatures (Coplen, 2007; Epstein et al., 1951; S.-T. Kim & O'Neil, 1997; S. T. Kim et al., 2007; McCrea, 1950) Accurate use of these temperature calibrations requires knowledge of the original oxygen isotope composition of the precipitating solution, as well as a supposition that isotopic equilibrium between precipitating solution and precipitating carbonate was established (S.-T. Kim & O'Neil, 1997). Reaching this point of isotopic equilibrium is a requirement for the calculation of an effective temperature-dependent equilibrium oxygen isotope fractionation factor between the precipitating solution, and the carbonate mineral (S.-T. Kim & O'Neil, 1997; S. T. Kim et al., 2007).

Problems arise with using this calibration when the precipitating carbonate is not in isotopic equilibrium with its surrounding solution, which can lead to the carbonate bearing a disequilibrium, or kinetic, isotope signature. These kinetic isotope effects are normally linked to rapid, one-way, incomplete processes, which can impart the resultant carbonate with high

magnitude fractionations that do not reflect environmental conditions of formation (McConnaughey, 1989b, 1989a). There are many reasons why a precipitating carbonate may fail to reach equilibrium with its precipitating solution including carbonate nucleation kinetics (Given & Wilkinson, 1985), insufficient growth rates (Gabitov et al., 2012), or relative proportions of dissolved inorganic carbon (DIC) species in precipitating solution (Devriendt et al., 2017; Zeebe et al., 1999). Perhaps most ambiguously, some kinetic isotope effects are attributed to the specific biology and metabolism of the biomineralizing organisms itself, summarized in literature by the catch-all term "vital effect" (Addadi et al., 2003; Erez, 1978; Pérez-Huerta & Fred, 2010; Ziveri et al., 2003).

Among the variety of possible sources for this vital effect is the role of non-classical biomineralization pathways, specifically the precipitation first of an amorphous precursor phase prior to transformation to a more stable crystalline biomineral. Here lies the potential relevance of ACC to our current understanding of $CaCO_3$ stable isotope geochemistry, and to a more robust understanding of classic oxygen isotope carbonate-water paleothermometer. Specifically, uncertainty remains regarding whether ACC can reach isotope equilibrium with its surrounding water, and perhaps more importantly, once this ACC transforms to a more stable crystalline polymorph of $CaCO_3$ will it still bear the isotopic signature of the initially precipitated ACC.

1.2.1 Isotopic Geochemistry of ACC: A review of existing scholarship

Despite the widespread use of ACC by various taxa, little is understood about its' isotopic composition and evolution, and more specifically, the geochemical importance of these features. Very few studies have, to date, probed how the use of an amorphous precursor phase effects the incorporation and evolution of stable isotopes as it transforms to a more stable crystalline mineral. Furthermore, though these studies did investigate stable isotopes of either

magnesium, calcium, or oxygen, only brief mention is made regarding the potential relevance of these studies to a more nuanced understanding of stable isotope geochemistry. Instead, the majority of current research revolves around identifying crystallization pathways in these systems. Furthermore, most of these studies have investigated magnesium-rich ACC (Mg-ACC) as a precursor to magnesium rich calcite (Mg-calcite) or dolomite.

One early study performed by Schmidt et al. (2005) synthesized dolomite ($CaMg(CO_3)_2$) at various temperatures via an Mg-ACC precursor to determine the effect on the $\delta^{18}O$ signature of the resulting dolomite. When Mg-ACC was synthesized at low temperatures (20 ˚C), there was an enrichment in ^{18}O compared to the precipitation solution, the Mg-ACC maintained this signature even when the temperature of the system was raised to 60 ˚C following precipitation. Significantly, the dolomite that the Mg-ACC eventually transformed was more depleted with respect to the ^{18}O isotope than the precursor Mg-ACC, and comparable to isotopic equilibrium fractionation of water and dolomite at 60 ˚C. However, this dolomite-water equilibrium value was extrapolated from the high temperatures equation (200-800 ˚C) developed by Northrop & Clayton, 2015 making its efficacy at low temperatures unclear. This study also precipitated Mg-ACC at 60 ˚C and maintained this temperature as it transformed to dolomite. In this case the resultant dolomite's isotopic composition compares well to the dolomite in the previous experiment where the temperature was changed to 60˚C following initial Mg-ACC formation. However, the initial Mg-ACC precipitated at 60 ˚C is isotopically lighter than its 20˚C counterpart. It was also found that when dolomite transformed from higher relative amounts of Mg-ACC, the resulting dolomite would be isotopically heavier, closer to the isotopic composition of the initially precipitated Mg-ACC. From this study researchers indicated that the $\delta^{18}O$ composition of Mg-ACC is temperature dependant, that crystallization of Mg-ACC to dolomite proceeds by a dissolution-reprecipitation reaction, as well as the possible effect of

relative amount of Mg-ACC to water on the $\delta^{18}O$ value of the final dolomite (Schmidt et al., 2005).

Other studies used synthetically enriched isotopes to probe the crystallization pathway of ACC. Giuffre et al. (2015) added ACC to solutions that were "spiked" with especially high amounts of the heavy ^{43}Ca and ^{25}Mg isotopes. This was done to determine whether the crystallization of ACC to calcite proceeded via a direct precipitation, or dissolution-reprecipitation pathway, and therefore, whether the final calcite would ultimately record the isotopic signature of the initial precipitating solutions, or the solution in which ACC transformed to calcite. It was found that this depended upon the amount of ACC added to the secondary solution, with decreasing amount of ACC relative to surrounding solution, the final isotopic signature would be increasingly consistent with the secondary spiked solution rather than the natural-abundance solution in which the ACC was originally precipitated. This indicates that ACC likely crystallizes to calcite by completely dissolving in solution and reprecipitating as calcite, bolstering the claims of the previous study by Schmidt et al. (2005) (Giuffre et al., 2015).

A subsequent study by Mavromatis et al. (2017) looked at the influence of a precursor Mg-ACC phase upon the magnesium isotope signature of the subsequent Mg-calcite it transformed into (Mavromatis et al., 2017). They noted a high initial magnesium isotope fractionation between the Mg-ACC and precipitating water which grew subsequently more negative as it transformed to crystalline Mg-calcite. The Mg-calcite that had transformed via the Mg-ACC precursor notably bore a more negative magnesium isotope signature than the Mg-calcite that was precipitated directly from solution.

Some isotopic investigation has been performed in vivo on ACC produced by earthworms (Versteegh et al., 2017). The earthworm *L. terrestris* produces ACC as a milky fluid in specialized organs, called gastroliths, within its calciferous glands. This ACC then crystallizes

to an ACC-calcite granule before being deposited into the soil as calcite. The $\delta^{13}C$ values of the various $CaCO_3$ transformation precipitates were monitored and were found to become significantly more negative with each subsequent crystallization. These differences in isotopic signatures are again, used to infer that the transformation of ACC to calcite was likely to have occurred via dissolution-reprecipitation, rather than direct precipitation.

Most recently Dietzel et al. (2020) examined oxygen and clumped isotope fractionation during the formation of Mg-calcite from an Mg-ACC precursor. Clumped isotope fractionation is a relatively recent advancement in isotopic investigation and monitors the fractionation of doubly substituted isotopologues, in this case $Ca^{13}C^{18}O^{16}O_2$, which form temperature dependant stochastic abundances of the rare ^{13}C-^{18}O bond (Ghosh et al., 2006). This is especially useful because clumped isotope composition is independent of the isotopic composition of the precipitating solution, a dependence that is a common complication with traditional stable isotope fractionation (Ghosh et al., 2006). Samples in this case were monitored for isotopic composition as the Mg-ACC crystallized in solution, and in air. The researchers found that the $\delta^{18}O$ values of the Mg-calcite that formed via the Mg-ACC precursor were highly variable, and very dependent upon the primary DIC species present in solution. This caused a very high initial fractionation between Mg-ACC and precipitating solution; however, there was a subsequent rapid exchange between the Mg-ACC and water as crystallization to Mg-calcite occurred resulting in a final crystalline precipitate that was almost in equilibrium with water. This suggests the crystallization of ACC occurs via dissolution-reprecipitation. Finally, the clumped isotopes of the Mg-calcite seemed to be unaffected by the crystallization pathway, and are therefore suggested as an attractive alternative for paleoclimate reconstruction when amorphous precursor phases are at play (Dietzel et al., 2020)

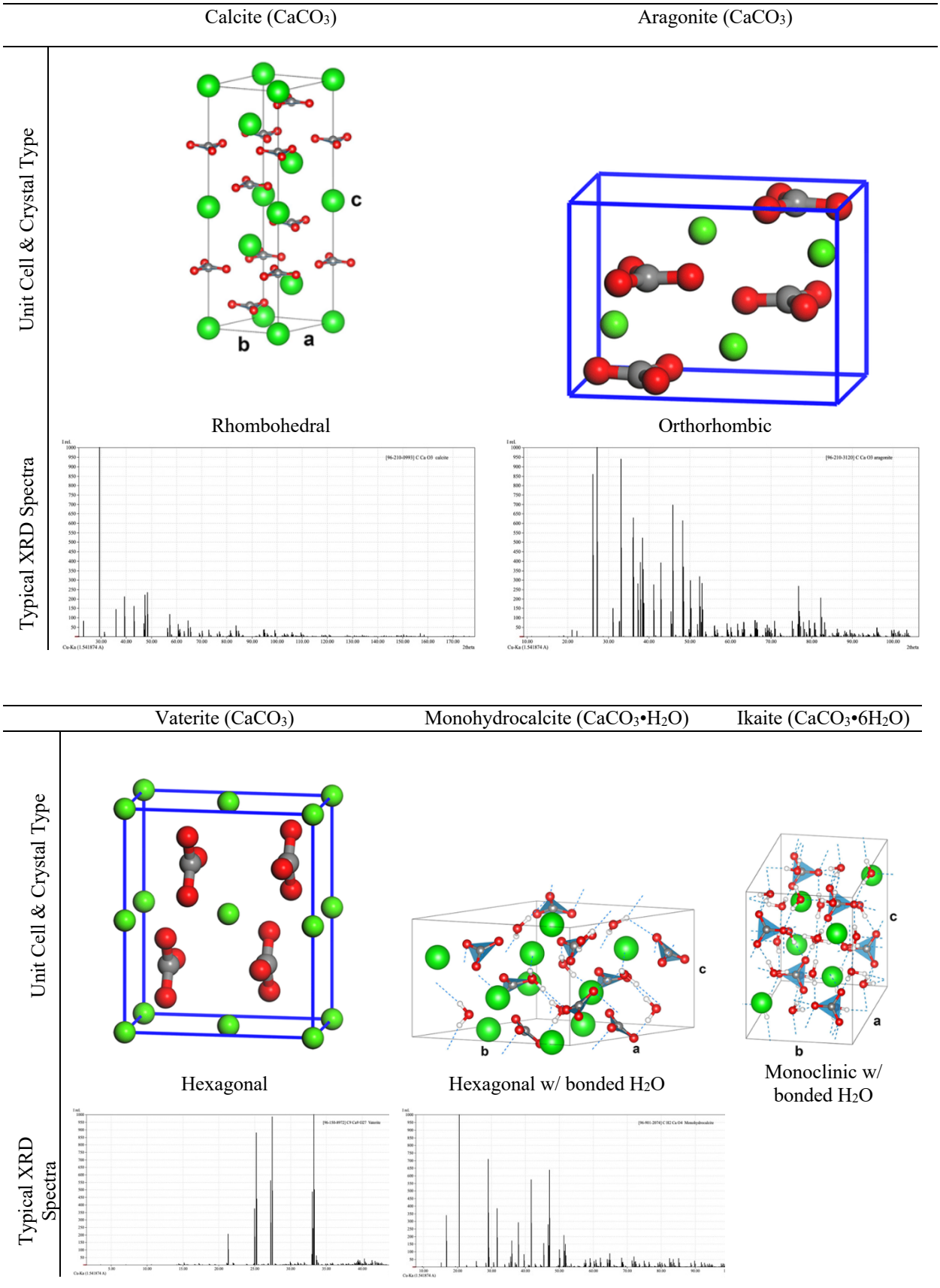

Figure 1.1. Unit cell rendering, crystal orientation type and typical XRD spectra of $CaCO_3$ polymorphs. Unit cells – Calcite, Monohydrocalcite, Ikaite - (Costa et al., 2016), Vaterite, Aragonite - (M. Zhang et al., 2020). XRD spectra from ICDD database (ICDD. PDF-2+, 2002)

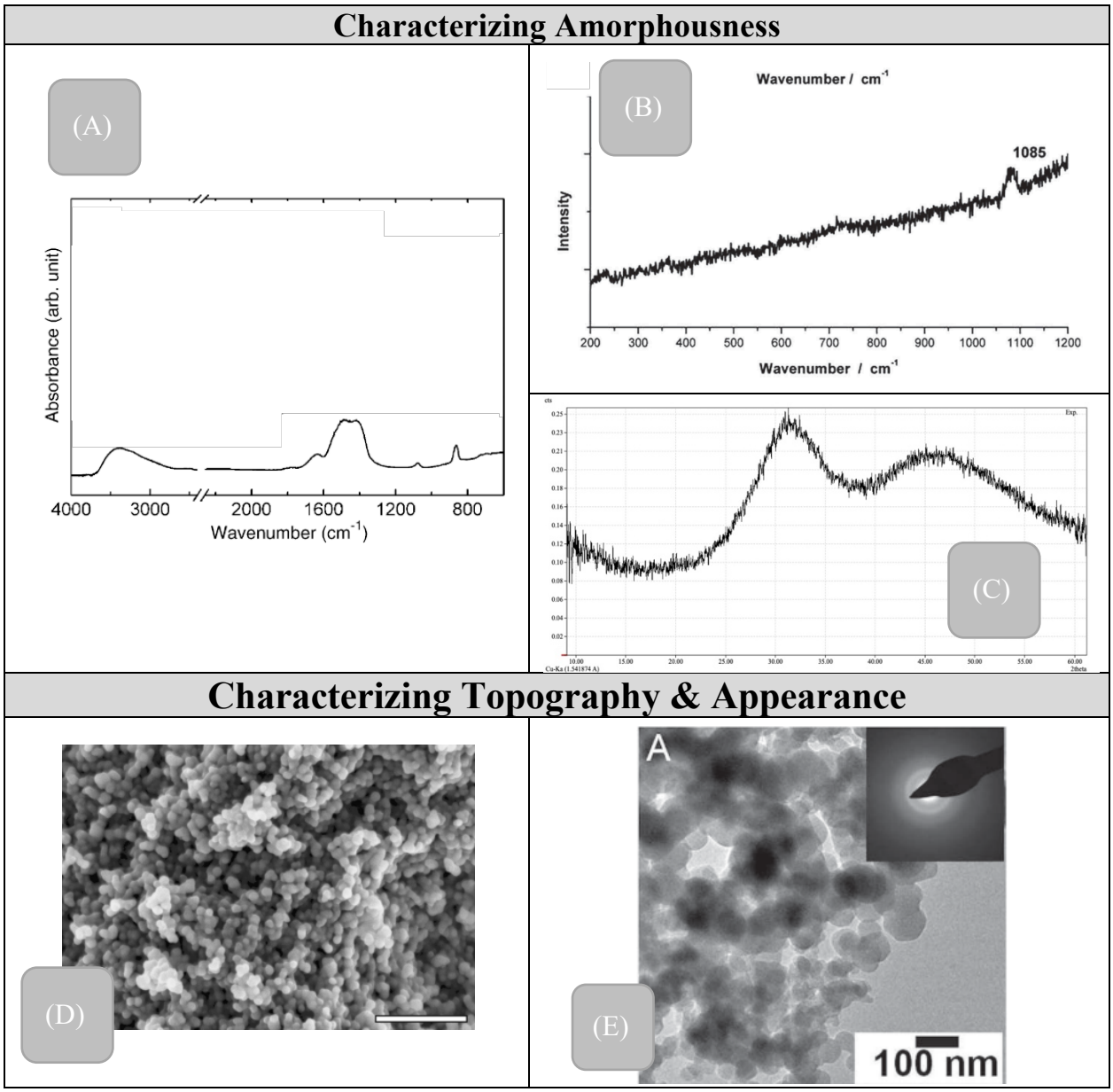

Figure 1.2. Common ACC characterization techniques and examples. (A) Typical Fourier Transform Infrared (FTIR) Spectroscopy of pure ACC (H. S. Lee et al., 2005). (B) Raman spectra of pure ACC (Ihli, Kim, et al., 2013). (C) X-Ray Diffraction (XRD) spectra of ACC from this study. (D) Scanning Electron Microscopy (SEM) of Silica stabilized ACC (Kellermeier et al., 2010) and (E) Transmission Electron Microscopy of additive-free ACC (top right shows corresponding XRD output) (Ihli, Kim, et al., 2013).

KINGDOM		PHYLUM	ORGANISM	LOCATION OF ACC	SUSPECTED BIOLOGICAL FUNCTION	REFERENCE
	Animalia	Annelida	Lumbricus friendi	gastroliths in calciferous glands	easily mobilized ion reservoir, precursor phase	(Gago-Duport et al., 2008)
			Lumbricus terrestris	gastroliths in calciferous glands	Regulation of pH and CO2 concentrations in bodily fluids	(Versteegh et al., 2017)
		Athropoda	Cherax quadricarinatus	gastroliths in calciferous glands	easily mobilized ion reservoir	(Akiva-Tal et al., 2011)
			Armadillidium vulgare	cuticles	structural properties	(Vinogradov, 1953)
			Carcinus maenas,	cuticle	structural properties	
			Crangon vulgaris	cuticle	structural properties	
			Homarus americanus	cuticle	structural properties	
			Homarus vulgaris	cuticle	structural properties	
			Homola spinifrons	cuticle	structural properties	
			Potamobius fluviatilis	cuticle	structural properties	
			Orchestia cavimana	spheruliths	easily mobilized ion reservoir	(Raz et al., 2002)
			Orconectes virilis	gastrolith	easily mobilized ion reservoir	(Travis, 1963)
			Porcellio scaber	cuticles	easily mobilized ion reservoir	(Becker et al., 2005)
			Porcellio scaber	sternal plates	easily mobilized ion reservoir	(Ziegler, 1994)
		Chordata	Pyura pachydermatina	tunic spicules	structural properties	(Aizenberg et al., 2003; Aizenberg, 1996; Aizenberg et al., 2002; Lowenstam, 1989)
				antler spicules	structural properties	
				spicule (body)	precursor mineral phase for spicule formation	
				spicule core (tunic)	precursor mineral phase for spicule formation	
			Sparus aurata	intestinal lumen	easily mobilized ion reservoir	(Foran et al., 2013)
		Cnidaria	Stylophora pistillata	coral tissue	fast growth precursor	(Mass et al., 2017)
		Echinodermata	Paracentrotus lividus	ACC-containing granules in spicules	precursor mineral phase for spicule formation, transport of material, controlling mineralization	(Beniash et al., 1997; Beniash et al., 1999; Politi et al., 2004; Wang et al., 1997)
				Particles at site of spinal injury	precursor phase for spine regeneration	
				larval spicule	precursor mineral phase for spicule formation	
				adult teeth	structural properties	
			Strongylocentrotus purpuratus	spicules	precursor mineral phase for spicule formation	(Radha et al., 2010, Raz et al., 2003)
		Mollusca	Hyriopsis cumingii	vesicles near crystallization face	transient precursor phase	(Jacob et al., 2008)
			Anguispira alternata	intracellular spherules in major arteries	unclear - links to blood buffering and Calcium release	(Tompa & Watabe, 1977)
			Biomphalaria glabrata	larval shell	precursor phase	(Hasse et al., 2000)
			Crassostrea gigas	larval shell	precursor phase	(Weiss et al., 2002)
			Dorid nudibranch	spicules	shell formation/repair	(Weiner et al., 2003)
			Haliotis laevigata	nacre from the shell ACC surrounding aragonite	unclear - maybe linked to lower energy surface interactions	(Nassif et al., 2005)
			Hyriopsis schlegeli	vesicles near crystallization face	transient precursor phase	(Jacob et al., 2008)
			Mercenaria mercenaria	larval shell	precursor phase	(Weiss et al., 2002)
			Pinctada maxima	vesicles near crystallization face	transient precursor phase	(Gower, 2008)
		Porifera	Clathrina	spicule	structural properties	(Aizenberg et al., 2003; Aizenberg, 1996)
				spicule core	precursor mineral phase for spicule formation	
	Plantae	Tracheophyta	Ficus microcarpa	cystoliths in leaves	uncertain (maybe photosynthesis?)	(Gal et al., 2010)
			Ficus retusa	cystoliths in leaves	uncertain (maybe photosynthesis?)	(Taylor et al., 1993)
			Morus alba	cystoliths in leaves	uncertain (maybe photosynthesis?)	(Gal et al., 2010)

Table 1.1. Distribution of biogenic producers of ACC and known of proposed function.

References

Addadi, L., Raz, S., & Weiner, S. (2003). Taking Advantage of Disorder: Amorphous Calcium Carbonate and Its Roles in Biomineralization. *Advanced Materials*, *15*(12), 959–970. https://doi.org/10.1002/adma.200300381

Aizenberg, J. (1996). Stabilization of amorphous calcium carbonate by specialized macromolecules in biological and synthetic precipitates. *Advanced Materials*, *8*(3), 222–226. https://doi.org/10.1002/adma.19960080307

Aizenberg, J., Addadi, L., Weiner, S., & Lambert, G. (1996). Stabilization of amorphous calcium carbonate by specialized macromolecules in biological and synthetic precipitates. *Advanced Materials*, *8*(3), 222–226. https://doi.org/10.1002/adma.19960080307

Aizenberg, J., Lambert, G., Weiner, S., & Addadi, L. (2002). Factors Involved in the Formation of Amorphous and Crystalline Calcium Carbonate: A Study of an Ascidian Skeleton. *Journal of the American Chemical Society*, *124*(1), 32–39. https://doi.org/10.1021/ja016990l

Aizenberg, J., Weiner, S., & Addadi, L. (2003). Coexistence of amorphous and crystalline calcium carbonate in skeletal tissues. *Connective Tissue Research*, *44*(SUPPL. 1), 20–25. https://doi.org/10.1080/03008200390152034

Ajikumar, P. K., Ling, G. W., Subramanyam, G., Lakshminarayanan, R., & Valiyaveettil, S. (2005). Synthesis and characterization of monodispersed spheres of amorphous calcium carbonate and calcite spherules. *Crystal Growth and Design*, *5*(3), 1129–1134. https://doi.org/10.1021/cg049606f

Akiva-Tal, A., Kababya, S., Balazs, Y. S., Glazer, L., Berman, A., Sagi, A., & Schmidt, A. (2011). In situ molecular NMR picture of bioavailable calcium stabilized as amorphous CaCO 3 biomineral in crayfish gastroliths. *Proceedings of the National Academy of Sciences of the United States of America*, *108*(36), 14763–14768. https://doi.org/10.1073/pnas.1102608108

Al-Horani, F. A., Al-Moghrabi, S. M., & De Beer, D. (2003). The mechanism of calcification and its relation to photosynthesis and respiration in the scleractinian coral Galaxea fascicularis. *Marine Biology*, *142*(3), 419–426. https://doi.org/10.1007/S00227-002-0981-8/FIGURES/7

Albéric, M., Bertinetti, L., Zou, Z., Fratzl, P., Habraken, W., & Politi, Y. (2018). The Crystallization of Amorphous Calcium Carbonate is Kinetically Governed by Ion Impurities and Water. *Advanced Science*, *5*(5), 1701000. https://doi.org/10.1002/advs.201701000

Atkins, E. (1978). Elements of X-ray Diffraction. *Physics Bulletin*, *29*(12), 572–572. https://doi.org/10.1088/0031-9112/29/12/034

Beck, W. C., Grossman, E. L., & Morse, J. W. (2005). Experimental studies of oxygen isotope fractionation in the carbonic acid system at 15°, 25°, and 40°C. *Geochimica et Cosmochimica Acta*, *69*(14), 3493–3503. https://doi.org/10.1016/j.gca.2005.02.003

Becker, A., Bismayer, U., Epple, M., Fabritius, H., Hasse, B., Shi, J., & Ziegler, A. (2003). Structural characterisation of X-ray amorphous calcium carbonate (ACC) in sternal deposits of the crustacea Porcellio scaber. *Journal of the Chemical Society. Dalton Transactions*, *3*(4), 551–555. https://doi.org/10.1039/b210529b

Becker, A., Ziegler, A., & Epple, M. (2005). The mineral phase in the cuticles of two species of Crustacea consists of magnesium calcite, amorphous calcium carbonate, and amorphous calcium phosphate. *Dalton Transactions*, *10*, 1814. https://doi.org/10.1039/b412062k

Beniash, E., Addadi, L., & Weiner, S. (1999). Cellular Control Over Spicule Formation in Sea Urchin Embryos: A Structural Approach. *Journal of Structural Biology*, *125*(1), 50–62. https://doi.org/10.1006/jsbi.1998.4081

Beniash, E., Aizenberg, J., Addadi, L., & Weiner, S. (1997). Amorphous calcium carbonate transforms into calcite during sea urchin larval spicule growth. *Proceedings of the Royal Society of London. Series B: Biological Sciences*, *264*(1380), 461–465. https://doi.org/10.1098/rspb.1997.0066

Beniash, E., Metzler, R. A., Lam, R. S. K., & Gilbert, P. U. P. A. (2009). Transient amorphous calcium phosphate in forming enamel. *Journal of Structural Biology*, *166*(2), 133–143. https://doi.org/10.1016/j.jsb.2009.02.001

Bentov, S., Brownlee, C., & Erez, J. (2009). The role of seawater endocytosis in the biomineralization process in calcareous foraminifera. *Proceedings of the National Academy of Sciences of the United States of America*, *106*(51), 21500–21504. https://doi.org/10.1073/pnas.0906636106

Bentov, S., Weil, S., Glazer, L., Sagi, A., & Berman, A. (2010). Stabilization of amorphous calcium carbonate by phosphate rich organic matrix proteins and by single phosphoamino acids. *Journal of Structural Biology*, *171*(2), 207–215. https://doi.org/10.1016/j.jsb.2010.04.007

Bergwerff, L., & van Paassen, L. A. (2021). Review and recalculation of growth and nucleation kinetics for calcite, vaterite and amorphous calcium carbonate. In *Crystals* (Vol. 11, Issue 11, p. 1318). Multidisciplinary Digital Publishing Institute. https://doi.org/10.3390/cryst11111318

Bewernitz, M. A., Gebauer, D., Long, J., Cölfen, H., & Gower, L. B. (2012). A metastable liquid precursor phase of calcium carbonate and its interactions with polyaspartate. *Faraday Discussions*, *159*, 291–312. https://doi.org/10.1039/c2fd20080e

Blue, C. R., Rimstidt, J. D., & Dove, P. M. (2013). A Mixed Flow Reactor Method to Synthesize Amorphous Calcium Carbonate Under Controlled Chemical Conditions. In *Methods in Enzymology* (Vol. 532, pp. 557–568). Academic Press Inc. https://doi.org/10.1016/B978-0-12-416617-2.00023-0

Brecevic, L., & Kralj, D. (2008). ChemInform Abstract: On Calcium Carbonates: From Fundamental Research to Application. *ChemInform*, *39*(5), 467–484. https://doi.org/10.1002/chin.200805226

Cai, G. Bin, Zhao, G. X., Wang, X. K., & Yu, S. H. (2010). Synthesis of polyacrylic acid stabilized amorphous calcium carbonate nanoparticles and their application for removal of toxic heavy metal ions in water. *Journal of Physical Chemistry C*, *114*(30), 12948–12954. https://doi.org/10.1021/jp103464p

Cartwright, J. H. E., Checa, A. G., Gale, J. D., Gebauer, D., & Sainz-Díaz, C. I. (2012). Calcium Carbonate Polyamorphism and Its Role in Biomineralization: How Many Amorphous Calcium Carbonates Are There? *Angewandte Chemie International Edition*, *51*(48), 11960–11970. https://doi.org/10.1002/anie.201203125

Chen, S. F., Cölfen, H., Antonietti, M., & Yu, S. H. (2013). Ethanol assisted synthesis of pure and stable amorphous calcium carbonate nanoparticles. *Chemical Communications*, *49*(83), 9564–9566. https://doi.org/10.1039/c3cc45427d

Cohn, M., & Urey, H. C. (1938). Oxygen Exchange Reactions of Organic Compounds and Water. *Journal of the American Chemical Society*, *60*(3), 679–687. https://doi.org/10.1021/ja01270a052

Cölfen, H. (2010). A crystal-clear view. In *Nature Materials* (Vol. 9, Issue 12, pp. 960–961). https://doi.org/10.1038/nmat2911

Coplen, T.B., & Schlanger, S. O. (1973). Oxygen and Carbon Isotope Studies of Carbonate Sediments from Site 167, Magellan Rise, Leg 17. In *Initial Reports of the Deep Sea Drilling Project, 17*. U.S. Government Printing Office. https://doi.org/10.2973/dsdp.proc.17.115.1973

Coplen, Tyler B. (2007). Calibration of the calcite-water oxygen-isotope geothermometer at Devils Hole, Nevada, a natural laboratory. *Geochimica et Cosmochimica Acta*, *71*(16), 3948–3957. https://doi.org/10.1016/j.gca.2007.05.028

Coronado, I., Fine, M., Bosellini, F. R., & Stolarski, J. (2019). Impact of ocean acidification on crystallographic vital effect of the coral skeleton. *Nature Communications*, *10*(1). https://doi.org/10.1038/s41467-019-10833-6

Costa, S. N., Freire, V. N., Caetano, E. W. S., Maia, F. F., Barboza, C. A., Fulco, U. L., & Albuquerque, E. L. (2016). DFT Calculations with van der Waals Interactions of Hydrated Calcium Carbonate Crystals CaCO3·(H2O, 6H2O): Structural, Electronic, Optical, and Vibrational Properties. *Journal of Physical Chemistry A*, *120*(28), 5752–5765. https://doi.org/10.1021/acs.jpca.6b05436

Cullity, B. D. (Bernard D. (2001). Elements of x-ray diffraction / B.D. Cullity, S.R. Stock. In *Book*. Prentice Hall,. https://discovery.mcmaster.ca/iii/encore/record/C__Rb1167916__SElements of x-ray diffraction__Orightresult__U__X6?lang=eng&suite=def

Darkins, R., Côté, A. S., Freeman, C. L., & Duffy, D. M. (2013). Crystallisation rates of calcite from an amorphous precursor in confinement. *Journal of Crystal Growth*, *367*, 110–114. https://doi.org/10.1016/j.jcrysgro.2012.12.027

De Nooijer, L. J., Toyofuku, T., & Kitazato, H. (2009). Foraminifera promote calcification by elevating their intracellular pH. *Proceedings of the National Academy of Sciences*, *106*(36), 15374–15378. https://doi.org/10.1073/PNAS.0904306106

De Yoreo, J. J., Gilbert, P. U. P. A., Sommerdijk, N. A. J. M., Penn, R. L., Whitelam, S., Joester, D., Zhang, H., Rimer, J. D., Navrotsky, A., Banfield, J. F., Wallace, A. F., Michel, F. M., Meldrum, F. C., Cölfen, H., & Dove, P. M. (2015). Crystallization by particle attachment in synthetic, biogenic,

and geologic environments. In *Science* (Vol. 349, Issue 6247). https://doi.org/10.1126/science.aaa6760

Demény, A., Czuppon, G., Kern, Z., Leél-Őssy, S., Németh, A., Szabó, M., Tóth, M., Wu, C. C., Shen, C. C., Molnár, M., Németh, T., Németh, P., & Óvári, M. (2016). Recrystallization-induced oxygen isotope changes in inclusion-hosted water of speleothems – Paleoclimatological implications. *Quaternary International*, *415*, 25–32. https://doi.org/10.1016/j.quaint.2015.11.137

Demény, A., Németh, P., Czuppon, G., Leél-Ossy, S., Szabó, M., Judik, K., Németh, T., & Stieber, J. (2016). Formation of amorphous calcium carbonate in caves and its implications for speleothem research. *Scientific Reports*, *6*(1), 39602. https://doi.org/10.1038/srep39602

Devriendt, L. S., Watkins, J. M., & McGregor, H. V. (2017). Oxygen isotope fractionation in the CaCO3-DIC-H2O system. *Geochimica et Cosmochimica Acta*, *214*, 115–142. https://doi.org/10.1016/j.gca.2017.06.022

Dietzel, M., Purgstaller, B., Kluge, T., Leis, A., & Mavromatis, V. (2020). Oxygen and clumped isotope fractionation during the formation of Mg calcite via an amorphous precursor. *Geochimica et Cosmochimica Acta*, *276*, 258–273. https://doi.org/10.1016/j.gca.2020.02.032

DIFFRAC.EVA | Bruker. (n.d.). Retrieved December 3, 2021, from https://www.bruker.com/en/products-and-solutions/diffractometers-and-scattering-systems/x-ray-diffractometers/diffrac-suite-software/diffrac-eva.html

Douglas, R. C., & Savin, S. M. (1975). Oxygen and Carbon Isotope Analyses of Tertiary and Cretaceous Microfossils from Shatsky Rise and Other Sites in the North Pacific Ocean. In *Initial Reports of the Deep Sea Drilling Project, 32*. U.S. Government Printing Office. https://doi.org/10.2973/dsdp.proc.32.115.1975

Emiliani, C. (1966). Isotopic Paleotemperatures. *Science*, *154*(3751), 851–857. https://doi.org/10.1126/science.154.3751.851

Epstein, S., & Mayeda, T. (1953). Variation of O18 content of waters from natural sources. *Geochimica et Cosmochimica Acta*, *4*(5), 213–224. https://doi.org/10.1016/0016-7037(53)90051-9

Epstein, Samuel, Buchsbaum, R., Lowenstam, H., & Urey, H. C. (1951). Carbonate-water isotopic

temperature scale. *Bulletin of the Geological Society of America*, *62*(4), 417–426. https://doi.org/10.1130/0016-7606(1951)62[417:CITS]2.0.CO;2

Erez, J. (1978). *Vital Effect in Coral & Foram*.

Evans, D., Webb, P. B., Penkman, K., Kröger, R., & Allison, N. (2019). The Characteristics and Biological Relevance of Inorganic Amorphous Calcium Carbonate (ACC) Precipitated from Seawater. *Crystal Growth and Design*, *19*(8), 4300–4313. https://doi.org/10.1021/acs.cgd.9b00003

Fairchild, I. J., Smith, C. L., Baker, A., Fuller, L., Spötl, C., Mattey, D., & McDermott, F. (2006). Modification and preservation of environmental signals in speleothems. *Earth-Science Reviews*, *75*(1–4), 105–153. https://doi.org/10.1016/j.earscirev.2005.08.003

Farhadi Khouzani, M., Chevrier, D. M., Güttlein, P., Hauser, K., Zhang, P., Hedin, N., & Gebauer, D. (2015). Disordered amorphous calcium carbonate from direct precipitation. *CrystEngComm*, *17*(26), 4842–4849. https://doi.org/10.1039/c5ce00720h

Frisia, S., Borsato, A., Fairchild, I. J., McDermott, F., & Selmo, E. M. (2002). Aragonite-Calcite Relationships in Speleothems (Grotte De Clamouse, France): Environment, Fabrics, and Carbonate Geochemistry. *Journal of Sedimentary Research*, *72*(5), 687–699. https://doi.org/10.1306/020702720687

Gabitov, R. I., Watson, E. B., Sadekov, A., Watson, B. E., & Sadekov, A. (2012). Oxygen isotope fractionation between calcite and fluid as a function of growth rate and temperature: An in situ study. *Chemical Geology*, *306–307*, 92–102. https://doi.org/10.1016/j.chemgeo.2012.02.021

Gago-Duport, L., Briones, M. J. I., Rodríguez, J. B., & Covelo, B. (2008). Amorphous calcium carbonate biomineralization in the earthworm's calciferous gland: Pathways to the formation of crystalline phases. *Journal of Structural Biology*, *162*(3), 422–435. https://doi.org/10.1016/j.jsb.2008.02.007

Gal, A., Weiner, S., & Addadi, L. (2010). The stabilizing effect of silicate on biogenic and synthetic amorphous calcium carbonate. *Journal of the American Chemical Society*, *132*(38), 13208–13211. https://doi.org/10.1021/ja106883c

Gayathri, S., Lakshminarayanan, R., Weaver, J. C., Morse, D. E., Manjunatha Kini, R., & Valiyaveettil, S. (2007). In vitro study of magnesium-calcite biomineralization in the skeletal materials of the

seastar Pisaster giganteus. *Chemistry - A European Journal*, *13*(11), 3262–3268. https://doi.org/10.1002/chem.200600825

Gebauer, D., Gunawidjaja, P. N., Ko, J. Y. P., Bacsik, Z., Aziz, B., Liu, L., Hu, Y., Bergström, L., Tai, C. W., Sham, T. K., Edén, M., & Hedin, N. (2010). Proto-calcite and proto-vaterite in amorphous calcium carbonates. *Angewandte Chemie - International Edition*, *49*(47), 8889–8891. https://doi.org/10.1002/anie.201003220

Gebauer, D., Völkel, A., & Cölfen, H. (2008). Stable prenucleation calcium carbonate clusters. *Science*, *322*(5909), 1819–1822. https://doi.org/10.1126/science.1164271

Ghosh, P., Adkins, J., Affek, H., Balta, B., Guo, W., Schauble, E. A., Schrag, D., & Eiler, J. M. (2006). 13C-18O bonds in carbonate minerals: A new kind of paleothermometer. *Geochimica et Cosmochimica Acta*, *70*(6), 1439–1456. https://doi.org/10.1016/j.gca.2005.11.014

Giuffre, A. J., Gagnon, A. C., De Yoreo, J. J., & Dove, P. M. (2015). Isotopic tracer evidence for the amorphous calcium carbonate to calcite transformation by dissolution-reprecipitation. *Geochimica et Cosmochimica Acta*, *165*, 407–417. https://doi.org/10.1016/j.gca.2015.06.002

Given, R. K., & Wilkinson, B. H. (1985). Kinetic control of morphology, composition, and mineralogy of abiotic sedimentary carbonates. *Journal of Sedimentary Petrology*, *55*(1), 109–119. https://doi.org/10.1306/212f862a-2b24-11d7-8648000102c1865d

Goldstein, J. I., Yakowitz, H., Newbury, D. E., Lifshin, E., Colby, J. W., & Coleman, J. R. (1975). Practical Scanning Electron Microscopy. In *Practical Scanning Electron Microscopy*. https://doi.org/10.1007/978-1-4613-4422-3

Gower, L. B. (2008). Biomimetic model systems for investigating the amorphous precursor pathway and its role in biomineralization. *Chemical Reviews*, *108*(11), 4551–4627. https://doi.org/10.1021/cr800443h

Günther, C., Becker, A., Wolf, G., & Epple, M. (2005). In vitro Synthesis and Structural Characterization of Amorphous Calcium Carbonate. *Zeitschrift Für Anorganische Und Allgemeine Chemie*, *631*(13–14), 2830–2835. https://doi.org/10.1002/zaac.200500164

Hasse, B., Ehrenberg, H., Marxen, J. C., Becker, W., & Epple, M. (2000). Calcium carbonate

modifications in the mineralized shell of the freshwater snail Biomphalaria glabrata. *Chemistry - A European Journal*, *6*(20), 3679–3685. https://doi.org/10.1002/1521-3765(20001016)6:20<3679::AID-CHEM3679>3.0.CO;2-#

Henini, M. (2000). Scanning electron microscopy: An introduction. *III-Vs Review*, *13*(4), 40–44. https://doi.org/10.1016/S0961-1290(00)80006-X

Hillaire-Marcel, C., Kim, S.-T., Landais, A., Ghosh, P., Assonov, S., Lécuyer, C., Blanchard, M., Meijer, H. A. J., & Steen-Larsen, H. C. (2021). A stable isotope toolbox for water and inorganic carbon cycle studies. *Nature Reviews Earth & Environment*, *2*(10), 699–719. https://doi.org/10.1038/s43017-021-00209-0

Hodson, M. E., Benning, L. G., Demarchi, B., Penkman, K. E. H., Rodriguez-Blanco, J. D., Schofield, P. F., & Versteegh, E. A. A. (2015). Biomineralisation by earthworms – an investigation into the stability and distribution of amorphous calcium carbonate. *Geochemical Transactions*, *16*(1), 4. https://doi.org/10.1186/s12932-015-0019-z

Huang, S. C., Naka, K., & Chujo, Y. (2007). A carbonate controlled-addition method for amorphous calcium carbonate spheres stabilized by poly(acrylic acid)s. *Langmuir*, *23*(24), 12086–12095. https://doi.org/10.1021/la701972n

ICDD. PDF-2+. (2002). *ICDD Database Search – ICDD*. International Centre for Diffraction Data, Newtown Square. https://www.icdd.com/pdfsearch/

Ihli, J., Kim, Y. Y., Noel, E. H., & Meldrum, F. C. (2013). The effect of additives on amorphous calcium carbonate (ACC): Janus behavior in solution and the solid state. *Advanced Functional Materials*, *23*(12), 1575–1585. https://doi.org/10.1002/adfm.201201805

Ihli, J., Kulak, A. N., & Meldrum, F. C. (2013). Freeze-drying yields stable and pure amorphous calcium carbonate (ACC). *Chemical Communications*, *49*(30), 3134–3136. https://doi.org/10.1039/c3cc40807h

Immenhauser, A., Schöne, B. R., Hoffmann, R., & Niedermayr, A. (2016). Mollusc and brachiopod skeletal hard parts: Intricate archives of their marine environment. *Sedimentology*, *63*(1), 1–59. https://doi.org/10.1111/sed.12231

Jacob, D. E., Soldati, A. L., Wirth, R., Huth, J., Wehrmeister, U., & Hofmeister, W. (2008). Nanostructure, composition and mechanisms of bivalve shell growth. *Geochimica et Cosmochimica Acta*, *72*(22), 5401–5415. https://doi.org/10.1016/j.gca.2008.08.019

Jacob, D. E., Wirth, R., Soldati, A. L., Wehrmeister, U., & Schreiber, A. (2011). Amorphous calcium carbonate in the shells of adult Unionoida. *Journal of Structural Biology*, *173*(2), 241–249. https://doi.org/10.1016/j.jsb.2010.09.011

Jung, G. Y., Shin, E., Park, J. H., Choi, B. Y., Lee, S. W., & Kwak, S. K. (2019). Thermodynamic Control of Amorphous Precursor Phases for Calcium Carbonate via Additive Ions. *Chemistry of Materials*, *31*(18), 7547–7557. https://doi.org/10.1021/acs.chemmater.9b02346

Kellermeier, M., Melero-García, E., Glaab, F., Klein, R., Drechsler, M., Rachel, R., García-Ruiz, J. M., & Kunz, W. (2010). Stabilization of Amorphous Calcium Carbonate in Inorganic Silica-Rich Environments. *Journal of the American Chemical Society*, *132*(50), 17859–17866. https://doi.org/10.1021/ja106959p

Kim, S.-T., Coplen, T. B., & Horita, J. (2015). Normalization of stable isotope data for carbonate minerals: Implementation of IUPAC guidelines. *Geochimica et Cosmochimica Acta*, *158*, 276–289. https://doi.org/10.1016/j.gca.2015.02.011

Kim, S.-T., Hillaire-Marcel, C., & Mucci, A. (2006). Mechanisms of equilibrium and kinetic oxygen isotope effects in synthetic aragonite at 25 °C. *Geochimica et Cosmochimica Acta*, *70*(23 SPEC. ISS.), 5790–5801. https://doi.org/10.1016/j.gca.2006.08.003

Kim, S.-T., & O'Neil, J. R. (1997). Equilibrium and nonequilibrium oxygen isotope effects in synthetic carbonates. *Geochimica et Cosmochimica Acta*, *61*(16), 3461–3475. https://doi.org/10.1016/S0016-7037(97)00169-5

Kim, S. T., O'Neil, J. R., Hillaire-Marcel, C., & Mucci, A. (2007). Oxygen isotope fractionation between synthetic aragonite and water: Influence of temperature and Mg2+ concentration. *Geochimica et Cosmochimica Acta*, *71*(19), 4704–4715. https://doi.org/10.1016/j.gca.2007.04.019

Kimura, T., & Koga, N. (2011). Monohydrocalcite in comparison with hydrated amorphous calcium carbonate: Precipitation condition and thermal behavior. *Crystal Growth and Design*, *11*(9), 3877–

3884. https://doi.org/10.1021/cg200412h

Kitano, Y., Okumura, M., & Idogaki, M. (1979). Behavior of dissolved silica in parent solution at the formation of calcium carbonate. *Geochemical Journal*, *13*(6), 253–260. https://doi.org/10.2343/geochemj.13.253

Koga, N., Nakagoe, Y., & Tanaka, H. (1998). Crystallization of amorphous calcium carbonate. *Thermochimica Acta*, *318*(1–2), 239–244. https://doi.org/10.1016/S0040-6031(98)00348-7

Koga, N., & Yamane, Y. (2008). Thermal behaviors of amorphous calcium carbonates prepared in aqueous and ethanol media. *Journal of Thermal Analysis and Calorimetry*, *94*(2), 379–387. https://doi.org/10.1007/s10973-008-9110-3

Köhler-Rink, S., & Kühl, M. (2007). The chemical microenvironment of the symbiotic planktonic foraminifer Orbulina universa. *Http://Dx.Doi.Org/10.1080/17451000510019015*, *1*(1), 68–78. https://doi.org/10.1080/17451000510019015

Kojima, Y., Sakama, K., Toyama, T., Yasue, T., & Arai, Y. (1994). Dehydration of the Water Molecule in Amorphous Calcium Phosphate. *Phosphorus Research Bulletin*, *4*, 47–52. https://doi.org/10.3363/prb1992.4.0_47

Konrad, F., Gallien, F., Gerard, D. E., & Dietzel, M. (2016). Transformation of Amorphous Calcium Carbonate in Air. *Crystal Growth and Design*, *16*(11), 6310–6317. https://doi.org/10.1021/acs.cgd.6b00906

Kontoyannis, C. G., & Vagenas, N. V. (2000). Calcium carbonate phase analysis using XRD and FT-Raman spectroscopy. *The Analyst*, *125*(2), 251–255. https://doi.org/10.1039/a908609i

Labuhn, I., Genty, D., Vonhof, H., Bourdin, C., Blamart, D., Douville, E., Ruan, J., Cheng, H., Edwards, R. L., Pons-Branchu, E., & Pierre, M. (2015). A high-resolution fluid inclusion δ18O record from a stalagmite in SW France: Modern calibration and comparison with multiple proxies. *Quaternary Science Reviews*, *110*, 152–165. https://doi.org/10.1016/j.quascirev.2014.12.021

Lachniet, M. S. (2009). Climatic and environmental controls on speleothem oxygen-isotope values. *Quaternary Science Reviews*, *28*(5–6), 412–432. https://doi.org/10.1016/j.quascirev.2008.10.021

Lam, R. S. K., Charnock, J. M., Lennie, A., & Meldrum, F. C. (2007). Synthesis-dependant structural

variations in amorphous calcium carbonate. *CrystEngComm*, *9*(12), 1226–1236. https://doi.org/10.1039/b710895h

Lee, H. S., Ha, T. H., & Kim, K. (2005). Fabrication of unusually stable amorphous calcium carbonate in an ethanol medium. *Materials Chemistry and Physics*, *93*(2–3), 376–382. https://doi.org/10.1016/j.matchemphys.2005.03.037

Lee, M. R., Hodson, M. E., & Langworthy, G. N. (2008). Crystallization of calcite from amorphous calcium carbonate: earthworms show the way. *Mineralogical Magazine*, *72*(1), 257–261. https://doi.org/10.1180/minmag.2008.072.1.257

Levi-Kalisman, Y., Raz, S., Weiner, S., Addadi, L., & Sagi, I. (2002). Structural differences between biogenic amorphous calcium carbonate phases using X-ray absorption spectroscopy. *Advanced Functional Materials*, *12*(1), 43–48. https://doi.org/10.1002/1616-3028(20020101)12:1<43::AID-ADFM43>3.0.CO;2-C

Levi-Kalisman, Yael, Raz, S., Weiner, S., Addadi, L., & Sagi, I. (2000). X-Ray absorption spectroscopy studies on the structure of a biogenic "amorphous" calcium carbonate phase †. *Journal of the Chemical Society, Dalton Transactions*, *21*, 3977–3982. https://doi.org/10.1039/b003242p

Lewis, I. R., & Edwards, H. (2001). Handbook of Raman Spectroscopy. *Handbook of Raman Spectroscopy*. https://doi.org/10.1201/9781420029253

Li, J., Chen, Z., Wang, R. J., & Proserpio, D. M. (1999). Low temperature route towards new materials: solvothermal synthesis of metal chalcogenides in ethylenediamine. *Coordination Chemistry Reviews*, *190–192*, 707–735. https://doi.org/10.1016/S0010-8545(99)00107-1

Lowenstam, H. A, & Epstein, S. (1954). Paleotemperatures of the Post-Aptian Cretaceous as Determined by the Oxygen Isotope Method. *The Journal of Geology*, *62*(3), 207–248. https://doi.org/10.1086/626160

Lowenstam, Heinz A. (1972). Phosphatic hard tissues of marine invertebrates: Their nature and mechanical function, and some fossil implications. *Chemical Geology*, *9*(1–4), 153–166. https://doi.org/10.1016/0009-2541(72)90053-8

Mass, T., Giuffre, A. J., Sun, C. Y., Stifler, C. A., Frazier, M. J., Neder, M., Tamura, N., Stan, C. V.,

Marcus, M. A., & Gilbert, P. U. P. A. (2017). Amorphous calcium carbonate particles form coral skeletons. *Proceedings of the National Academy of Sciences of the United States of America*, *114*(37), E7670–E7678. https://doi.org/10.1073/pnas.1707890114

Mavromatis, V., Purgstaller, B., Dietzel, M., Buhl, D., Immenhauser, A., & Schott, J. (2017). Impact of amorphous precursor phases on magnesium isotope signatures of Mg-calcite. *Earth and Planetary Science Letters*, *464*, 227–236. https://doi.org/10.1016/j.epsl.2017.01.031

McConnaughey, T. (1989a). 13C and 18O isotopic disequilibrium in biological carbonates: I. Patterns. *Geochimica et Cosmochimica Acta*, *53*(1), 151–162. https://doi.org/10.1016/0016-7037(89)90282-2

McConnaughey, T. (1989b). 13C and 18O isotopic disequilibrium in biological carbonates: II. In vitro simulation of kinetic isotope effects. *Geochimica et Cosmochimica Acta*, *53*(1), 163–171. https://doi.org/10.1016/0016-7037(89)90283-4

McCrea, J. M. (1950). On the Isotopic Chemistry of Carbonates and a Paleotemperature Scale. *The Journal of Chemical Physics*, *18*(6), 849–857. https://doi.org/10.1063/1.1747785

McDermott, F. (2004). Palaeo-climate reconstruction from stable isotope variations in speleothems: A review. *Quaternary Science Reviews*, *23*(7–8), 901–918. https://doi.org/10.1016/j.quascirev.2003.06.021

Meldrum, F. C. (2003). Calcium carbonate in biomineralisation and biomimetic chemistry. In *International Materials Reviews* (Vol. 48, Issue 3, pp. 187–224). https://doi.org/10.1179/095066003225005836

Meldrum, F. C., & O'Shaughnessy, C. (2020). Crystallization in Confinement. In *Advanced Materials* (Vol. 32, Issue 31, p. 2001068). John Wiley & Sons, Ltd. https://doi.org/10.1002/adma.202001068

Michel, F. M., MacDonald, J., Feng, J., Phillips, B. L., Ehm, L., Tarabrella, C., Parise, J. B., & Reeder, R. J. (2008). Structural characteristics of synthetic amorphous calcium carbonate. *Chemistry of Materials*, *20*(14), 4720–4728. https://doi.org/10.1021/cm800324v

Nakashima, Y., Takai, C., Razavi-Khosroshahi, H., Suthabanditpong, W., & Fuji, M. (2018). Synthesis of ultra-small hollow silica nanoparticles using the prepared amorphous calcium carbonate in one-pot process. *Advanced Powder Technology*, *29*(4), 904–908. https://doi.org/10.1016/j.apt.2018.01.006

Navrotsky, A. (2004). Energetic clues to pathways to biomineralization: Precursors, clusters, and nanoparticles. *Proceedings of the National Academy of Sciences of the United States of America*, *101*(33), 12096–12101. https://doi.org/10.1073/pnas.0404778101

Neumann, M., & Epple, M. (2007). Monohydrocalcite and its relationship to hydrated amorphous calcium carbonate in biominerals. *European Journal of Inorganic Chemistry*, *2007*(14), 1953–1957. https://doi.org/10.1002/ejic.200601033

Njegić-Džakula, B., Brečević, L., Falini, G., & Kralj, D. (2011). Kinetic Approach to Biomineralization: Interactions of Synthetic Polypeptides with Calcium Carbonate Polymorphs. *Croatica Chemica Acta*, *84*(2), 301–314. https://doi.org/10.5562/cca1809

Northrop, D. A., & Clayton, R. N. (1966). Oxygen-Isotope Fractionations in Systems Containing Dolomite. *The Journal of Geology*, *74*(2), 174–196. https://doi.org/10.1086/627153

O'Day, P. A., Rehr, J. J., Zabinsky, S. I., & Brown, G. E. (1994). Extended X-ray Absorption Fine Structure (EXAFS) Analysis of Disorder and Multiple-Scattering in Complex Crystalline Solids. *Journal of the American Chemical Society*, *116*(7), 2938–2949. https://doi.org/10.1021/ja00086a026

Ogino, T., Suzuki, T., & Sawada, K. (1987). The formation and transformation mechanism of calcium carbonate in water. *Geochimica et Cosmochimica Acta*, *51*(10), 2757–2767. https://doi.org/10.1016/0016-7037(87)90155-4

Ostwald, W. (1901). Reviews-On the assumed isomerism between red and yellow mercuric oxide and on the surface-tension of solids. *The Journal of Physical Chemistry*, *5*(1), 75–75. https://doi.org/10.1021/j150028a603

Paquin, F., Rivnay, J., Salleo, A., Stingelin, N., & Silva, C. (2015). Multi-phase semicrystalline microstructures drive exciton dissociation in neat plastic semiconductors. *J. Mater. Chem. C*, *3*, 10715–10722. https://doi.org/10.1039/b000000x

Pérez-Huerta, A., & C. Fred, T. A. (2010). Vital effects in the context of biomineralization. *Seminarios de La Sociedad Española de Mineralogía*, *7*, 35–45.

Ping, H., Xie, H., Wan, Y., Zhang, Z., Zhang, J., Xiang, M., Xie, J., Wang, H., Wang, W., & Fu, Z. (2016). Confinement controlled mineralization of calcium carbonate within collagen fibrils. *Journal*

of Materials Chemistry B, *4*(5), 880–886. https://doi.org/10.1039/C5TB01990G

Politi, Y., Batchelor, D. R., Zaslansky, P., Chmelka, B. F., Weaver, J. C., Sagi, I., Weiner, S., & Addadi, L. (2010). Role of Magnesium Ion in the Stabilization of Biogenic Amorphous Calcium Carbonate: A Structure−Function Investigation. *Chemistry of Materials*, *22*(1), 161–166. https://doi.org/10.1021/cm902674h

Politi, Y., Levi-Kalisman, Y., Raz, S., Wilt, F., Addadi, L., Weiner, S., & Sagi, I. (2006). Structural Characterization of the Transient Amorphous Calcium Carbonate Precursor Phase in Sea Urchin Embryos. *Advanced Functional Materials*, *16*(10), 1289–1298. https://doi.org/10.1002/adfm.200600134

Purgstaller, B., Mavromatis, V., Immenhauser, A., & Dietzel, M. (2016). Transformation of Mg-bearing amorphous calcium carbonate to Mg-calcite - In situ monitoring. *Geochimica et Cosmochimica Acta*, *174*, 180–195. https://doi.org/10.1016/j.gca.2015.10.030

Radha, A. V., Forbes, T. Z., Killian, C. E., Gilbert, P. U. P. A., & Navrotsky, A. (2010). Transformation and crystallization energetics of synthetic and biogenic amorphous calcium carbonate. *Proceedings of the National Academy of Sciences*, *107*(38), 16438–16443. https://doi.org/10.1073/pnas.1009959107

Rao, A., Vásquez-Quitral, P., Fernández, M. S., Berg, J. K., Sánchez, M., Drechsler, M., Neira-Carrillo, A., Arias, J. L., Gebauer, D., & Cölfen, H. (2016). PH-Dependent Schemes of Calcium Carbonate Formation in the Presence of Alginates. *Crystal Growth and Design*, *16*(3), 1349–1359. https://doi.org/10.1021/acs.cgd.5b01488

Raz, S., Hamilton, P. C., Wilt, F. H., Weiner, S., & Addadi, L. (2003). The Transient Phase of Amorphous Calcium Carbonate in Sea Urchin Larval Spicules: The Involvement of Proteins and Magnesium Ions in Its Formation and Stabilization. *Advanced Functional Materials*, *13*(6), 480–486. https://doi.org/10.1002/adfm.200304285

Raz, S., Testeniere, O., Hecker, A., Weiner, S., & Luquet, G. (2002). Stable amorphous calcium carbonate is the main component of the calcium storage structures of the crustacean Orchestia cavimana. *Biological Bulletin*, *203*(3), 269–274. https://doi.org/10.2307/1543569

Rodriguez-Blanco, J. D., Shaw, S., Bots, P., Roncal-Herrero, T., & Benning, L. G. (2012). The role of pH and Mg on the stability and crystallization of amorphous calcium carbonate. *Journal of Alloys and Compounds*, *536*(SUPPL.1), S477–S479. https://doi.org/10.1016/j.jallcom.2011.11.057

Rodriguez-Blanco, Juan Diego, Shaw, S., & Benning, L. G. (2011). The kinetics and mechanisms of amorphous calcium carbonate (ACC) crystallization to calcite, viavaterite. *Nanoscale*, *3*(1), 265–271. https://doi.org/10.1039/C0NR00589D

Rodriguez-Navarro, C., Kudłacz, K., Cizer, Ö., & Ruiz-Agudo, E. (2015). Formation of amorphous calcium carbonate and its transformation into mesostructured calcite. *CrystEngComm*, *17*(1), 58–72. https://doi.org/10.1039/c4ce01562b

Ross, E. E., Mok, S. W., & Bugni, S. R. (2011). Assembly of lipid bilayers on silica and modified silica colloids by reconstitution of dried lipid films. *Langmuir*, *27*(14), 8634–8644. https://doi.org/10.1021/la200952c

Roy, R. N., Roy, L. N., Vogel, K. M., Porter-Moore, C., Pearson, T., Good, C. E., Millero, F. J., & Campbell, D. M. (1993). The dissociation constants of carbonic acid in seawater at salinities 5 to 45 and temperatures 0 to 45°C. *Marine Chemistry*, *44*(2–4), 249–267. https://doi.org/10.1016/0304-4203(93)90207-5

Saenger, C., & Wang, Z. (2014). Magnesium isotope fractionation in biogenic and abiogenic carbonates: Implications for paleoenvironmental proxies. In *Quaternary Science Reviews* (Vol. 90, pp. 1–21). Elsevier Ltd. https://doi.org/10.1016/j.quascirev.2014.01.014

Savin, S. M. (1977). The History of the Earth's Surface Temperature During the Past 100 Million Years. *Annual Review of Earth and Planetary Sciences*, *5*(1), 319–355. https://doi.org/10.1146/annurev.ea.05.050177.001535

Schmidt, M., Xeflide, S., Botz, R., & Mann, S. (2005). Oxygen isotope fractionation during synthesis of CaMg-carbonate and implications for sedimentary dolomite formation. *Geochimica et Cosmochimica Acta*, *69*(19), 4665–4674. https://doi.org/10.1016/j.gca.2005.06.025

Schwartz, A. M. (2002). Handbook of Industrial Crystallization - Chapter 01 - Solutions and solution properties. *Handbook of Industrial Crystallization*, *7*, 1–31.

http://www.sciencedirect.com/science/article/pii/B9780750670128500033

Seo, K. S., Han, C., Wee, J. H., Park, J. K., & Ahn, J. W. (2005). Synthesis of calcium carbonate in a pure ethanol and aqueous ethanol solution as the solvent. *Journal of Crystal Growth*, *276*(3–4), 680–687. https://doi.org/10.1016/j.jcrysgro.2004.11.416

Setoguchi, H. (1989). Origin, Evolution, and Modern Aspects of Biomineralization in Plants and Animals. *Origin, Evolution, and Modern Aspects of Biomineralization in Plants and Animals*, *December*. https://doi.org/10.1007/978-1-4757-6114-6

Simkiss, K. (1991). Amorphous Minerals and Theories of Biomineralization. In *Mechanisms and Phylogeny of Mineralization in Biological Systems* (pp. 375–382). Springer Japan. https://doi.org/10.1007/978-4-431-68132-8_60

Smith, B. C. (2011). Fundamentals of fourier transform infrared spectroscopy, second edition. In *Fundamentals of Fourier Transform Infrared Spectroscopy, Second Edition*.

Stephens, C. J., Ladden, S. F., Meldrum, F. C., & Christenson, H. K. (2010). Amorphous calcium carbonate is stabilized in confinement. *Advanced Functional Materials*, *20*(13), 2108–2115. https://doi.org/10.1002/adfm.201000248

Swart, P. K. (2015). The geochemistry of carbonate diagenesis: The past, present and future. *Sedimentology*, *62*(5), 1233–1304. https://doi.org/10.1111/sed.12205

Taylor, M. G., Simkiss, K., Greaves, G. N., Okazaki, M., & Mann, S. (1993). An X-ray absorption spectroscopy study of the structure and transformation of amorphous calcium carbonate from plant cystoliths. *Proceedings of the Royal Society B: Biological Sciences*, *252*(1333), 75–80. https://doi.org/10.1098/rspb.1993.0048

Tester, C. C., Brock, R. E., Wu, C.-H., Krejci, M. R., Weigand, S., & Joester, D. (2011). In vitro synthesis and stabilization of amorphous calcium carbonate (ACC) nanoparticles within liposomes. *CrystEngComm*, *13*(12), 3975. https://doi.org/10.1039/c1ce05153a

Tester, C. C., Whittaker, M. L., & Joester, D. (2014). Controlling nucleation in giant liposomes. *Chemical Communications*, *50*(42), 5619–5622. https://doi.org/10.1039/c4cc01457j

Tobler, D. J., Rodriguez-Blanco, J. D., Sørensen, H. O., Stipp, S. L. S., & Dideriksen, K. (2016). Effect of

pH on Amorphous Calcium Carbonate Structure and Transformation. *Crystal Growth and Design*, *16*(8), 4500–4508. https://doi.org/10.1021/acs.cgd.6b00630

Tompa, A. S., & Watabe, N. (1977). Calcified arteries in a gastropod. *Calcified Tissue Research*, *22*(1), 159–172. https://doi.org/10.1007/BF02010355

Townsend, D., Lahankar, S. A., Lee, S. K., Chambreau, S. D., Suits, A. G., Zhang, X., Rheinecker, J., Harding, L. B., & Bowman, J. M. (2004). The Roaming Atom: Straying from the Reaction Path in Formaldehyde Decomposition. *Science*, *306*(5699), 1158–1161. https://doi.org/10.1126/science.1104386

Travis, D. F. (2006). Structural features of mineralization from tissue to macromolecular levels of organization in the decapod crustacea. *Annals of the New York Academy of Sciences*, *109*(1), 177–245. https://doi.org/10.1111/j.1749-6632.1963.tb13467.x

Venn, A., Tambutté, E., Holcomb, M., Allemand, D., & Tambutté, S. (2011). Live tissue imaging shows reef corals elevate pH under their calcifying tissue relative to seawater. *PLoS ONE*, *6*(5). https://doi.org/10.1371/JOURNAL.PONE.0020013

Versteegh, E. A. A., Black, S., & Hodson, M. E. (2017). Carbon isotope fractionation between amorphous calcium carbonate and calcite in earthworm-produced calcium carbonate. *Applied Geochemistry*, *78*, 351–356. https://doi.org/10.1016/j.apgeochem.2017.01.017

Vinogradov, A. P. (1953). *The elementary chemical composition of marine organisms / A.P. Vinogradov.* https://discovery.mcmaster.ca/iii/encore/record/C__Rb2252090__SVinogradov, A. P. The Elementary Chemical Composition of Marine Organisms__Orightresult__U__X2?lang=eng&suite=def

Voorhees, P. W. (1985). The theory of Ostwald ripening. *Journal of Statistical Physics*, *38*(1–2), 231–252. https://doi.org/10.1007/BF01017860

Wang, S. S., & Xu, A. W. (2013). Amorphous calcium carbonate stabilized by a flexible biomimetic polymer inspired by marine mussels. *Crystal Growth and Design*, *13*(5), 1937–1942. https://doi.org/10.1021/cg301759t

Wang, Y., Zeng, M., Meldrum, F. C., & Christenson, H. K. (2017). Using confinement to study the

crystallization pathway of calcium carbonate. *Crystal Growth and Design*, *17*(12), 6787–6792. https://doi.org/10.1021/acs.cgd.7b01359

Wang, Z. L., & Lee, J. L. (2008). Electron Microscopy Techniques for Imaging and Analysis of Nanoparticles. In *Developments in Surface Contamination and Cleaning: Second Edition* (Vol. 1, pp. 395–443). William Andrew Publishing. https://doi.org/10.1016/B978-0-323-29960-2.00009-5

Weiner, S. (2003). An Overview of Biomineralization Processes and the Problem of the Vital Effect. *Reviews in Mineralogy and Geochemistry*, *54*(1), 1–29. https://doi.org/10.2113/0540001

Weiner, S., Levi-Kalisman, Y., Raz, S., & Addadi, L. (2003). Biologically Formed Amorphous Calcium Carbonate. *Connective Tissue Research*, *44*(1), 214–218. https://doi.org/10.1080/03008200390181681

Weiss, I. M., Tuross, N., Addadi, L., & Weiner, S. (2002). Mollusc larval shell formation: amorphous calcium carbonate is a precursor phase for aragonite. *Journal of Experimental Zoology*, *293*(5), 478–491. https://doi.org/10.1002/jez.90004

Whittaker, M. L., Dove, P. M., & Joester, D. (2016). Nucleation on surfaces and in confinement. *MRS Bulletin*, *41*(5), 388–392. https://doi.org/10.1557/mrs.2016.90

Wombacher, F., Eisenhauer, A., Böhm, F., Gussone, N., Regenberg, M., Dullo, W. C., & Rüggeberg, A. (2011). Magnesium stable isotope fractionation in marine biogenic calcite and aragonite. *Geochimica et Cosmochimica Acta*, *75*(19), 5797–5818. https://doi.org/10.1016/j.gca.2011.07.017

Xto, J. M., Borca, C. N., van Bokhoven, J. A., & Huthwelker, T. (2019). Aerosol-based synthesis of pure and stable amorphous calcium carbonate. *Chemical Communications*, *55*(72), 10725–10728. https://doi.org/10.1039/c9cc03749g

Xu, N., Li, Y., Zheng, L., Gao, Y., Yin, H., Zhao, J., Chen, Z., Chen, J., & Chen, M. (2014). Synthesis and application of magnesium amorphous calcium carbonate for removal of high concentration of phosphate. *Chemical Engineering Journal*, *251*, 102–110. https://doi.org/10.1016/j.cej.2014.04.037

Xu, X. R., Cai, A. H., Liu, R., Pan, H. H., Tang, R. K., & Cho, K. (2008). The roles of water and polyelectrolytes in the phase transformation of amorphous calcium carbonate. *Journal of Crystal Growth*, *310*(16), 3779–3787. https://doi.org/10.1016/j.jcrysgro.2008.05.034

Zeebe, R. E. (1999). An explanation of the effect of seawater carbonate concentration on foraminiferal oxygen isotopes. *Geochimica et Cosmochimica Acta*, *63*(13–14), 2001–2007. https://doi.org/10.1016/S0016-7037(99)00091-5

Zeebe, R. E., & Wolf-Gladrow, D. A. (2001). CO2 in Seawater: Equilibrium, Kinetics, Isotopes. In *Elsevier*. https://linkinghub.elsevier.com/retrieve/pii/S0924796302001793

Zeebe, R. E., Wolf-Gladrow, D. A., & Jansen, H. (1999). On the time required to establish chemical and isotopic equilibrium in the carbon dioxide system in seawater. *Marine Chemistry*, *65*, 135–153.

Zhang, H., Cai, Y., Tan, L., Qin, S., & An, Z. (2014). Stable isotope composition alteration produced by the aragonite-to-calcite transformation in speleothems and implications for paleoclimate reconstructions. *Sedimentary Geology*, *309*, 1–14. https://doi.org/10.1016/j.sedgeo.2014.05.007

Zhang, M., Li, J., Zhao, J., Cui, Y., & Luo, X. (2020). Comparison of CH4and CO2Adsorptions onto Calcite(10.4), Aragonite(011)Ca, and Vaterite(010)CO3Surfaces: An MD and DFT Investigation. *ACS Omega*, *5*(20), 11369–11377. https://doi.org/10.1021/acsomega.0c00345

Ziveri, P., Stoll, H., Probert, I., Klaas, C., Geisen, M., Ganssen, G., & Young, J. (2003). Stable isotope "vital effects" in coccolith calcite. *Earth and Planetary Science Letters*, *210*(1–2), 137–149. https://doi.org/10.1016/S0012-821X(03)00101-8

Zou, Z., Bertinetti, L., Politi, Y., Jensen, A. C. S., Weiner, S., Addadi, L., Fratzl, P., & Habraken, W. J. E. M. (2015). Supplementary - Opposite Particle Size Effect on Amorphous Calcium Carbonate Crystallization in Water and during Heating in Air. *Chemistry of Materials*, *27*(12), 4237–4246. https://doi.org/10.1021/acs.chemmater.5b00145

CHAPTER 2

Precipitation and Characterization of Stable Amorphous Calcium Carbonate (ACC)

Katherine Allan[a]

allank2@mcmcaster.ca

&

Sang-Tae Kim[a]

sangtae@mcmaster.ca

School of Earth, Environment & Society, McMaster University, 1280 Main Street West, Hamilton, ON, L8S 4K1, Canada

Abstract

Over the past several years Amorphous Calcium Carbonate (ACC) has been identified as a precursor phase in calcium carbonate ($CaCO_3$) biomineralization, as calcium storage reservoir, or a structural component of organisms spanning various phyla of the animal and plant kingdoms. As a result, the past few decades have seen abundant research into the ways by which one can synthesize stable ACC. This study presents the first, to the best of our knowledge, direct comparison of two different ACC precipitation methods in terms of their ability to stabilize ACC, and the way in which they direct ACC crystallization. Firstly, ACC is precipitated by increasing the pH of the parent solution to such a point that transformation to a more stable crystalline polymorph of $CaCO_3$ is disfavoured, this was referred to as the Alkaline Method (AM). Alternatively, precipitation was achieved by utilizing SiO_2 to form isolating envelopes or vesicles around precipitating ACC, preventing the particle nucleation needed for ACC crystallization, this technique was referred to as the Silica Method (SM). Both precipitation methods produce ACC-containing solutions which are either immediately filtered or left sealed in parent solution from periods ranging from 1 to 5 weeks. As a result, we were able to monitor the ACC precipitates as they transformed to crystalline $CaCO_3$ in air or in parent solution.

These AM and SM precipitates are compared using X-Ray Diffraction (XRD) analysis, to discern whether they remain ACC with increased time in parent solution or air. Significant differences are found in the success with which these two methods stabilize ACC, as well as differences in the poly(a)morphic evolution of the respective AM and SM-ACC precipitates as they begin to crystallize. Our results indicate that the high pH conditions of the AM favour a faster and more predictable transformation from ACC to calcite in parent solution. Conversely, SM-precipitated ACC is both slower, and more variable in terms of crystallization with time aging in parent solution, often transforming to $CaCO_3$ that features a mix of different polymorphs and hydrated polymorphs of $CaCO_3$, including calcite, vaterite and monohydrocalcite. When AM and SM-ACC precipitates were allowed to crystallize in air they also displayed different behaviour, with AM-ACC maintaining complete amorphousness for a period of 48 hours, while SM-ACC began to transform to crystalline $CaCO_3$ within 24 hours. However, this same SM-ACC was able to resist complete crystallization in air for longer than AM-ACC precipitates. The results of this study may help direct further research with regard to the study of ACC in particular, as longer ACC-lifetimes, and higher ACC-stability is vital to understanding ACC on its own, as opposed to ACC as a transient precursor to more stable polymorphs of $CaCO_3$.

CHAPTER 2: PRECIPITATION AND CHARACTERIZATION OF STABLE AMORPHOUS CALCIUM CARBONATE (ACC)

2.1 Introduction

In recent years, there has been a marked interest in the behaviour of minerals that crystallize via a non-classical pathway, or by a method other than direct precipitation (Addadi et al., 2003; Bewernitz et al., 2012; Jacob et al., 2011; Mass et al., 2017; Radha et al., 2010) Indeed, many unanswered questions, including the mystery of the "vital effect" – where the isotopic signal conveyed by a biogenic carbonate is in clear disequilibrium with its formation environment - can possibly be explained by alternative precipitation pathways – more specifically, $CaCO_3$ transformation via an amorphous calcium carbonate (ACC) precursor (e.g., Addadi et al., 2003; Weiner, 2003). There have been numerous studies investigating different ways to precipitate ACC precursors in the laboratory by using a variety of additives (e.g., Bentov et al., 2010; Blue et al., 2013; Ihli et al., 2013; Xu et al., 2008) and/or a wide range of precipitation conditions (Ihli, Kulak, et al., 2013; Konrad et al., 2016; Meldrum & O'Shaughnessy, 2020; Stephens et al., 2010), which both promote the formation of ACC, a poly*a*morph of $CaCO_3$ and prevent subsequent transformation to one of the many crystalline polymorphs of $CaCO_3$ (i.e., calcite, aragonite, vaterite) or hydrated crystalline $CaCO_3$ polymorphs (i.e., monohydrocalcite, ikaite). These many forms, (i.e., amorphous, crystalline, hydrated crystalline) of $CaCO_3$ can be collectively referred to as poly(a)morphs.

Isotopic "doping" has been a popular method for tracking this alternative crystallization pathway and involves "spiking" different components of parent materials with heavy isotopes, such as ^{43}Ca and ^{25}Mg, to track how these isotopes are incorporated into the final crystal structure in order to trace the exact crystallization pathway (Giuffre et al., 2015). This spiking method successfully illustrates that the crystallization of ACC to calcite occurs via a dissolution-reprecipitation pathway (Giuffre et al., 2015).

With implications for industry, mineralogy, geochemistry, and paleoclimatology, among many others, it is no wonder that a deep and nuanced understanding of biomineralization, or how organisms develop their mineral shell parts, is an essential field of scientific study. The utility of an amorphous phase in biomineralization is obvious as it possesses a number of interesting physicochemical qualities when compared to its more stable and mature crystalline counterpart. These include higher solubility, an ability to incorporate a variety of inclusions, and fewer spatial concerns. This means that ACC-producing organisms do not have to accommodate a specific crystal structure until there is a need for new crystalline $CaCO_3$ biominerals, making an amorphous phase (e.g., ACC) an ideal precursor to biomineralization (Simkiss, 1991). To use a metaphor, consider a piece of Ikea furniture – a customer is provided with the raw materials and instructions to assemble the final product, but transport and maneuvering of the piece is made much easier by the fact that it is disassembled. Likewise, an amorphous phase may be stored and transported before it gains the rigid and relatively immobile crystal structure that it was destined for. Furthermore, due to the use of an additive, interaction with an organic matrix, or an environmental condition, an amorphous phase will crystallize into a predictable and intricate mineral phase by a biomineralizing organism (Bentov et al., 2010; Weiner et al., 2003). More and more biomineralizing organisms are found to produce such amorphous precursors (Gago-Duport et al., 2008; Gal et al., 2010; Jacob et al., 2011; Jung et al., 2019; Mass et al., 2017; Weiss et al., 2002).

ACC forms in nature in conjunction with several different stabilizing agents, which make synthesizing and quantifying an amorphous phase in the laboratory an intricate and many-faceted problem because there are many avenues of stabilization that could be used. It is therefore beneficial to consider the problem at the energetic level. In the classical understanding biomineralization, the final mineral phase precipitates directly from ions in solution, and ion

concentrations in the solution must exceed the solubility product to induce the nucleation of the mineral phase in question (Simkiss, 1991). For example, the solubility product of calcite ($K_{sp} = [Ca^{2+}][CO_3^{2-}]$) is 3.36×10^{-9} at 25 ˚C (Schwartz, 2002) while the reported solubility product of ACC ($K_{sp} = [Ca^{2+}][CO_3^{2-}]$) ranges from 4.0×10^{-7} (Brecevic & Kralj, 2008) to 1.35×10^{-6} (Bergwerff & van Paassen, 2021). Therefore, at this temperature, the phase with the lower solubility product, or the less soluble phase (i.e., calcite) is expected to precipitate first. However, it is often found in nature that organisms do not achieve nucleation in the simple and ambient conditions typical in lab-based mineralization experiments. Biomineralization is generally achieved by some interaction between ion pumps that maintain a selective concentration of ions, and nucleation is induced by a charged surface or due to interaction with a heterogenous nucleator (Bentov et al., 2009). Therefore, organisms may biomineralize within specialized, isolated areas of their bodies, or perhaps induce the crystallization of an amorphous precursor such as ACC (Akiva-Tal et al., 2011; Bentov et al., 2010; Meldrum, 2003). If a system either lacks sufficient additives or is not under precipitation conditions to allow ACC to persist, then the crystalline phase will form immediately (I to IV in Figure 2.1) because the energy barrier to this crystallization process is lower than the corresponding solubility product of the amorphous phase (Simkiss, 1991). In order to prevent direct precipitation of the crystalline phase, and instead, favour the formation of an amorphous precursor (I to II in Figure 2.1), there must be an energetic barrier to the nucleation of the more stable crystalline phase. This allows the mineralization to occur in a more controlled manner based on the Ostwald step-rule. This rule states that the initial reaction products will continuously undergo a series of reactions that form new products, each less soluble and more stable than the previous product (Ostwald, 1901), a principle that is illustrated in Figure 2.1.

ACC precipitation is almost always performed in conjunction with an additive or a local precipitation condition that provides an energetic barrier to prohibit spontaneous nucleation of a crystalline phase (Aizenberg et al., 2002; Bentov et al., 2010; Blue et al., 2013; Gower, 2008; Kellermeier et al., 2010; Njegić-Džakula et al., 2011). Additives are soluble ions or macromolecules, such as magnesium ions (Mg^{2+}), phosphate, or poly(aspartic) acid, that interact with the crystallizing system in a myriad of ways to prevent crystallization and assist ACC in persisting in the system (Ihli et al., 2013). In addition, the crystallization of ACC can also be prevented by controlling its precipitating environment. For instance, very cold temperatures (Ihli et al., 2013), and physical isolation (e.g., Meldrum & O'Shaughnessy, 2020; Tester et al., 2011), have both been successful in preventing the crystallization of ACC. Researchers have examined natural processes to aid in identifying potential additives and precipitation conditions that provide a barrier to spontaneous crystallization such as using either matrix proteins isolated from ACC-producing organisms (e.g. Aizenberg, 1996; Bentov et al., 2010). Biomineralized structures in nature play incredibly intricate roles that are often exquisitely tailored to specific organisms. This high level of control over the structure of these biominerals serve to confute the widespread use of spontaneous, uncontrolled crystallization in nature. Overall, the methods by which ACC can be stabilized fall into 5 broad categories - (I) high supersaturations, (II) isolation, (III) low temperatures, (IV) presence of additives/interaction with a biological matrix and (V) interaction with heterogeneous nucleators (See Chapter 1 for more detailed information). These complex interactions allow a biomineralizing organism to exert precise control over the final crystal form, tailoring it to their individual needs (Addadi et al., 2003).

Despite recent studies that use different stabilization methods to investigate the transformation pathways of ACC to calcite (Giuffre et al., 2015; Konrad et al., 2016; Rodriguez-Blanco et al., 2012; Versteegh et al., 2017), or to probe how long these methods successfully

stabilize ACC (Kellermeier et al., 2010; Lee et al., 2005; Ross et al., 2011; Stephens et al., 2010; Xu et al., 2014), there has not yet been a study which directly compares ACC precipitation methods, monitoring their success in stabilizing ACC, and probing their crystallization behaviour. This is notable considering the increasing number of organisms that are found to use an amorphous phase as a metastable step in the development of their own mineral parts, whether they are composed of $CaCO_3$ or some other biominerals (e.g., calcium phosphates), Therefore, this study aims to investigate the crystallization behaviour of calcium carbonate minerals ($CaCO_3$) when the initial precipitated phase is ACC. This is achieved by using two different stabilization methods that stabilize the metastable ACC phase preventing its transformation to crystalline $CaCO_3$: (1) the additive method and (2) the environmental control method.

2.2 Experimental Methods

2.2.1 Preparation of Thermally and Isotopically equilibrated Ca^{2+} or CO_3^{2-} donating Parent Solutions

A series of 20 mmolal calcium ion (Ca^{2+}) donor parent solutions were prepared by dissolving $CaCl_2$ in deionized water (ID: KW-15Mar21) and were stored in 1 L Pyrex® bottles at 25 °C ± 0.1 ˚C. These Ca^{2+}-donor parent solutions were used for both of the two separate stabilizing methods described in Sections 2.2.2 and 2.2.3 to supply Ca^{2+} ions for ACC precipitation. In addition, two separate sets of carbonate ion (CO_3^{2-})-donor parent solutions were prepared to supply an equimolar supply of CO_3^{2-} ions and facilitate the precipitation of ACC. For the Alkaline Method (hereafter referred to as the AM), a solution of 20 mmolal Na_2CO_3 and 200 mmolal NaOH was prepared by dissolving first NaOH pellets, followed by anhydrous Na_2CO_3 powder in 1 L deionized water (ID:KW-15Mar21). For the Silica Method (SM), a solution of 20 mmolal Na_2CO_3 was first prepared by dissolving anhydrous Na_2CO_3 in 1L deionized water (ID:

KW-15Mar21). Subsequently, several millilitres of sodium metasilicate ($Na_2O(SiO_2)\cdot H_2O$) solution with 26.8 % wt% as SiO_2 was added to the Na_2CO_3 solution to yield a Na_2CO_3-SiO_2 solution of 31 mmolal SiO_2. All of the Ca^{2+}- and AM-/SM-CO_3^{2-}-donor parent solutions were sealed in Pyrex® media bottles, wrapped with Parafilm® to avoid evaporation, and then placed in a 25 ± 0.1°C water bath for 58 days. A minimum of 44 days was estimated to establish oxygen isotope equilibrium among DIC species and water in the AM-/SM-CO_3^{2-}-donor parent solutions at 25 °C given their pH range (> 10) (Beck et al., 2005)

All chemicals used in this study were ACS-grade and they were weighed out using a Sartorious® weighing scale, while the volumes of the solutions were accurately measured by using a volumetric flask. A pipette was also used to remove excess water if necessary. Deionized (DI) water (κ = ~ 0.6 µS cm-1 or ~18 MΩ) was used for all solution preparation. This water was kept in a High Density Polyethylene (HDPE) carboy with a cap and was labelled as "KW-(date prepared)". The stock DI water was regularly tested for its oxygen isotope composition (relevant to Chapter 3) whenever it was used or refilled. Prior to use all Pyrex® media bottles were cleaned in an acid bath containing ~5 % hydrochloric acid (HCl) for 2-7 days. Following this acid cleaning, the media bottles were removed, rinsed thrice with tap water, twice with reversed osmosis (RO) water, and once with DI water before being placed in a drying oven for a minimum of 24 hours.

2.2.2. The Alkaline Method

The AM utilized (1) a high alkalinity solution for higher supersaturation, (2) temporally quick ion concentration increase – in this case a rapid Ca^{2+} and CO_3^{2-} concentration increase, and (3) anhydrous ethanol as a stabilizing precipitate wash. 50 mL of the Ca^{2+}-donor parent solution was rapidly dumped into the 50 mL AM-CO_3^2-donor parent solution in a glass beaker (see

Figure 2.3). Initial attempts of parent solution mixing, utilizing a reaction chamber instead of a glass beaker, were not sufficiently fast, and always resulted in calcite formation without an initial amorphous phase. This was due to the reaction chamber structure, specifically the small mouth through which donor parent solutions had to be poured, necessitating careful transferring of two donor solutions together, rather than the immediate pouring utilized in traditional ACC precipitation. Therefore, this method of using glass breakers, over the reaction chamber, was favoured.

Upon immediate mixing of the Ca^{2+}- and AM-CO_3^{2-}-donor parent solutions the resultant solution is referred to as an AM-ACC solution, as XRD later confirms that all solutions contain ACC at this time point. Following donor parent solution mixing the ACC-solution was measured using an Oakton® pH electrode. The ACC-solution was then subjected to 2 post-ACC-treatments in which precipitated AM-ACC was either (1) left in parent solution, or (2) transferred to an ^{18}O enriched re-equilibration solution (relevant to Chapter 3). Both post-ACC-treatments also necessitate the immediate filtration of several AM-ACC precipitates without aging in parent or re-equilibration solution. When the crystallization of AM-ACC in solution over time was investigated, the AM-ACC-solution was decanted from the beaker to a 100 mL Pyrex bottle, wrapped in Parafilm™ and placed in the 25 ± 0.1 °C water bath for 1-5 weeks.

Upon immediate filtration and subsequent X-Ray Diffraction (henceforth, XRD) analysis (see section 2.2.4) of some AM precipitates (~30 % total precipitates), all of them were confirmed to be amorphous. Therefore, it was assumed that the primary precipitate in the solution is ACC. All immediately filtered, unaged AM precipitates are referred to as AM-ACC precipitates, following any time aging in solution they are known as AM-$CaCO_3$ solutions prior to filtration and AM-$CaCO_3$ precipitates post-vacuum filtration due to their variable poly(a)morphic nature, as confirmed by XRD. AM-$CaCO_3$ precipitates were vacuum filtered

through a Millipore® 0.45 μm polyvinylidene difluoride (PVDF) membrane disc filter, and subsequently rinsed with ~50 mL of anhydrous ethanol. The resulting solid AM-ACC or AM-$CaCO_3$ precipitates, were then dried in a 70 °C oven for a minimum of 24 hours (see Figure 2.3). Unless the resulting precipitates were set aside for XRD analysis, they were then finely ground using a mortar and pestle, weighed, and stored in a glass carbonate storage vial.

2.2.3 The Silica Method

Kellermeier et al. (2010)'s precipitation method resulted in ACC that was highly volumetrically constrained with respect to its crystallizing environment, and ACC tended to persist in solution for an indefinite period with sufficient metasilicate concentrations of >1870 ppm (~31 mmolal). Notably, this method was not intended to synthesize ACC, but was rather to create hollow silica nanoparticles and subsequently destroy the ACC within. These silica vesicles, collected by removing ACC, can be used for industrial purposes. Therefore, Kellermeier et al. (2010)'s method had to be modified in this study to maintain ACC in solution by using ethanol to stabilize ACC during filtration.

When precipitating ACC by the SM, 50 mL of the Ca^{2+}-donor parent solution was first rapidly transferred into the 50 mL of the SM-CO_3^{2-}-donor parent solution. Following brief mixing, the pH of the SM-ACC-solution was measured using an Oakton® pH electrode. This solution was then either immediately vacuum filtered through a Millipore 0.45 μm PVDF membrane disc filter, and subsequently rinsed with ~50 mL of anhydrous ethanol or sealed in a 100 mL Pyrex glass bottle and returned to the water bath (25 ± 0.1 ˚ C) for aging experiments. The vacuum filtered precipitates, whether ACC upon immediate filtration (SM-ACC precipitates), or some mix of poly(a)morphs of $CaCO_3$ (henceforth SM-$CaCO_3$ precipitates), for all experiments were placed in a glass petri dish and dried in a 70 ˚C ± 0.3 ˚C oven for ≥ 24

hours prior to grinding with a mortar and pestle and storage. Please refer to Figure 2.2 for an illustration of this method.

2.2.4 XRD Characterization of Calcium Carbonate Poly(a)morphs

Following the precipitation and vacuum filtration a number of the resultant AM-$CaCO_3$ or SM-$CaCO_3$ precipitates were washed with anhydrous ethanol and immediately taken to the McMaster Analytical X-Ray Diffraction Facility (MAX) without drying in the oven. The solid AM-$CaCO_3$/SM-$CaCO_3$ precipitates were not ground until immediately prior to XRD analysis. The mineralogy of each precipitate was identified using a Bruker D8 DISCOVER diffractometer equipped with a Bruker Vantex600 and a CuKα sealed tube source which produces a wavelength of 1.5406 Å.

To analyze the precipitates with CuKα radiation, small amounts (less than ~1 mg) of the dried and ground AM/SM-$CaCO_3$ precipitates were flattened and packed onto a small glass rod and mounted into the instrument (See Figure 2.4 for reference). The raw diffraction data from the XRD analyses was corrected into a plot of 2θ versus relative intensity patterns, which is a typical plot for mineral identification and composition. Some diffraction data was corrected to a plot of 2θ versus counts because it this is useful for tracking the precipitate progression from amorphous to partially or fully crystalline, because the values in counts are not normalized to the same scale. Mineral phases, if present, were identified using the International Center for Diffraction Data (ICDD) PDF-4+ 2021 Diffraction Database (ICDD. PDF-2+, 2002), which provides diffraction and instrument data for a large number of organic and inorganic materials. The search or match was performed in Diffrac.EVA V5.2 from Bruker (*DIFFRAC.EVA | Bruker*, n.d.) for mineral analysis.

2.3 Results and Discussion

2.3.1: Overview of XRD Analysis for ACC and crystalline $CaCO_3$

The instability, and likelihood of rapid crystallization of ACC, required an analytical test that is quick and relatively simple for its characterization (Günther et al., 2005). XRD analysis provides this quality even though it has some drawbacks. Typically, Cu-Kα X-ray diffraction is used to analyze the various polymorphs of $CaCO_3$. This subset of XRD uses Copper as its target metal, producing characteristic K lines on the continuous spectrum (Cullity, 2001). Copper is chosen over other possible anode metals such as Molybdenum, Iron or Cobalt because the wavelengths produced by the Cu anode are reasonably long, around 1.5406 Å (Cullity, 2001). Furthermore, this anode tends to be the most commonly available, with the most useful wavelength and is therefore favoured for more mundane concerns such as budget and accessibility. This wavelength of the Cu anode notably matches the interatomic distance of crystalline solids, and thus provides the highest resolutions for the $CaCO_3$ polymorphs being characterized. The Cu anode is also the most commonly used for the identification of both synthetic and biogenic $CaCO_3$ poly(a)morphs (e.g., Aizenberg et al., 2002; Demény et al., 2016; Rodriguez-Blanco et al., 2011). Indeed, when alternative methods are used, the spectra are often corrected to Cu-Kα radiation directly compare their data with the existing literature (Gago-Duport et al., 2008; Levi-Kalisman et al., 2000).

The typical spectra of four common polymorphs of calcium carbonate ($CaCO_3$) as well as the polyamorph of stable ACC, are displayed in Figure 2.3 and summarized in Table 2.1. XRD can not only differentiate different polymorphs, but also elucidate the molar percent of each polymorph within the precipitate by comparing the reflection peaks that correspond to a specific polymorph. For instance, the fraction of calcite to aragonite in a can be determined by comparing the fractions of the 104-reflection peak unique to calcite, and the 221-peak for aragonite

(Kontoyannis & Vagenas, 2000). This peak-comparison method can be helpful in monitoring the transformation from an amorphous precursor phase to a crystal form, as well as determining the effect of different additives and precipitation conditions upon the crystallization. Furthermore, XRD can be incredibly useful as a method for confirming the presence of an amorphous material. For example, amorphousness can be confirmed in about 10 minutes because any crystalline peaks that exist would have already been evident typically within the first few minutes of XRD analysis.

The XRD spectrum of ACC is notable for the fact that despite being called amorphous, there is some spectral characteristics, meaning ACC does not scatter light randomly in all directions as it would if it fit the true definition of "amorphous". Large hump-like peaks, referred to as broad diffuse maxima, centered at around the 2θ of 20^{o} and 45^{o} are typical of an ACC-XRD spectrum. (Figure 2.3), which indicate that there is some semblance of order even though there is no express crystalline character. When these broad diffuse maxima in the XRD patterns are lower, it indicates relatively less short-range order (Radha et al., 2010). XRD can also be useful, especially in conjunction with a programmable heating apparatus, to monitor the crystallization of ACC with dehydration (Koga & Yamane, 2008).

In terms of the drawbacks, there are both timing and methodological constraints on the characterization of ACC using XRD owing to the unstable nature of ACC (Kontoyannis & Vagenas, 2000). Although XRD hints at the short-range order of an ACC precipitate, there is no clear indication of what exactly this is – for example, this short-range structure might correspond to proto-calcite-, proto-aragonite-, or a mixture (Khouzani et al., 2015; Gebauer et al., 2010). Moreover, ACC is generally destabilized by dehydration and structural water may cause interference on the spectra. ACC can perhaps lose its orientation by manual grinding, too (Radha et al., 2010). This presents an issue as the precipitate being characterized must be ground into a

fine powder when using XRD. X-ray absorption extended fine structure (EXAFS) and Fourier Transform Infrared Spectroscopy (FTIR) methods can more clearly elucidate the aforementioned low-level order, discern between stable and unstable ACC, and even predict the final polymorph the amorphous phase may crystallize into through study of the short-range order (Addadi et al., 2003; Cartwright et al., 2012). FTIR also allows us to calculate the ACC/calcite ratio in a precipitate that is midway through crystallization (Hodson et al., 2015). However, it should be noted that XRD analysis was sufficient in this study as a $CaCO_3$ characterization technique among ACC and three polymorphs of $CaCO_3$.

2.3.2: General Observation of ACC Formation and Crystallization

Our findings directly illustrate a significant effect of two different ACC stabilization methods (i.e., the AM & the SM) on $CaCO_3$ transformation in the $CaCO_3$-H_2O system. Upon immediate filtration following precipitation the SM produced an ACC precipitate with a partially transparent colour and gel-like consistency, which dried to a white powder when left in the 70 ˚C ± 0.3 ˚C drying oven (Figure 2.5). In contrast, the immediate precipitate by the AM (AM-ACC) showed an appearance of a white powder, rather than a gel-like appearance (Figure 2.5). The SM-$CaCO_3$ precipitates maintained their initial appearance regardless of their aging time in parent solution; however, the AM-$CaCO_3$ precipitates began to show a distinctly yellowish colour after 1 week of aging in parent solution. This change in colour, from white to yellow, was found to correspond the transformation of ACC to crystalline calcite, as confirmed by XRD.

In this study, the XRD spectra were used to identify the mineralogy as well as the amorphous nature of the AM/SM-$CaCO_3$ precipitate. All dried $CaCO_3$ precipitates spontaneously transformed to either entirely calcite, or a mix of calcite and other $CaCO_3$ poly(a)morphs. It was observed that the manual grinding prior to the XRD analysis appeared to induce or expedite

crystallization – as early AM/SM-$CaCO_3$ precipitates that had undergone manual grinding hours prior to XRD analysis were much more likely to be crystalline upon XRD analysis than those that were ground immediately prior to XRD analysis. This grinding-related crystallization can mostly be avoided by waiting until the last possible moment to grind the precipitate for XRD analysis and manual grinding of the precipitates was thus carried out as close to the time of the XRD analysis as possible. Figures 2.6 and 2.7 show an example of the spontaneous crystallization in air where precipitates are observed to crystallize when left undisturbed, these are all images of the same precipitate (1 AM, 1 SM) extracted from the same petri dishes. They display the crystallization of AM-/SM-ACC precipitates to crystalline $CaCO_3$, showing XRD spectra (a) immediately after filtration, (b) after 1 hour on the XRD stage, and (c) after 24 hours following the initial precipitation and vacuum filtration. It should be noted that each time stage represents a different collection from the same precipitate, rather than the exact same collected precipitate characterized repeatedly.

2.3.3: Progression of AM-ACC Crystallization

The AM-$CaCO_3$ precipitates showed a predictable transformation from ACC to the most stable $CaCO_3$ polymorph – calcite - with increasing aging time both in air (Figure 2.6) and in parent solution (Figure 2.7). Figure 2.6 illustrates that AM-ACC precipitates in air did not show any evident crystalline components (a) upon immediate filtration, (b) after 1 hour and (c) after 24 hours. On the contrary, they became entirely calcite (d) after 48 hours. Accordingly, all the precipitates from the AM are believed to spontaneously crystallize to calcite when they are left undisturbed outside of solution. Figure 2.6-(d) clearly shows this spontaneous transformation as the increasing peak intensities of the XRD spectra indicates the transformation to crystalline calcite.

Meanwhile, the AM-$CaCO_3$ precipitates aged in parent solution showed a completely calcitic nature almost immediately (Figure 2.8-(a) vs Figure 2.8-(b)). Figure 2.7 shows that some of the AM-$CaCO_3$ precipitates had crystallized to calcite within 24 hours, which was evident from both the appearance of calcite peaks and a sharp increase in the peak intensities. However, Figure 2.8 shows that other $CaCO_3$ crystalline phases, aside from calcite, were present in a few of the AM-$CaCO_3$ precipitates. More specifically, there was XRD evidence of traces of vaterite (~3%) within AM-$CaCO_3$ precipitates that had aged for 24 or 48 hours in parent solution (Figures 2.8-(b), 2.8-(c) and 2.8-(d)). Following this 48-hour aging time, almost all AM-$CaCO_3$ precipitates characterized are found to be calcite, with the exception of one, (AM•1W•NS•2), that had some evidence of vaterite, perhaps because this was the precipitate most recently filtered, but the second one characterized using XRD, therefore, it was the youngest precipitate and had less time to undergo crystallization (see Figure 2.8(e)-(f)).

2.3.4: Progression of SM-ACC Crystallization

In contrast to the AM-$CaCO_3$ precipitates, the SM-$CaCO_3$ precipitates crystallized much less readily and remained somewhat amorphous, with evidence of multiple $CaCO_3$ poly(a)morphic phases within most precipitates. Figure 2.9 shows that the SM precipitates aged in air were completely ACC at up to 1 hour but contained both ACC, vaterite and calcite after 24 hours. These precipitates also showed a steady progression towards higher crystallinity when they remained in air. This on-going crystallization process was evident from a steady increase in peak intensity and the gradual disappearance of the large humps associated with the presence of ACC. However, this crystallization process was not complete and there was still a great deal of amorphous material left after 24 hours despite the appearance of some small peaks (Figure 2.9-(c)).

For the SM-$CaCO_3$ precipitates aged in parent solution, ACC crystallization occurred in a much more gradual manner when compared to the identically treated AM-$CaCO_3$ precipitates (Figures 2.7 vs 2.10). Immediate filtration predictably produced SM precipitates that were entirely amorphous and this was confirmed by the lack of XRD peaks, as well as extremely low XRD spectrum intensity (Figure 2.10-(a)). After 24-hours aging in parent solution, some small XRD peaks appeared; however, these SM precipitates were mostly amorphous and maintained a relatively low peak intensity (Figure 2.10-(b)). SM precipitates that stayed in solution for 48 hours (Figure 2.10-(c)) have an almost identical XRD pattern to their 24-hour counterpart. SM-$CaCO_3$ precipitates, after 1 week aging in parent solution, show much more intense peaks, implying a more crystalline nature (Figure 2.10-(d)). Nevertheless, Figures 2.10-(d)-(e) still show a low intensity curvature pattern of ACC, along with the stronger crystalline $CaCO_3$ peaks. This spectrum resembles the ACC curvature pattern from 1 and 2-week aged precipitates in parent solution, with higher crystalline peaks; this mixed poly(a)morphic character - mostly crystalline with evidence of ACC - is still seen in the SM-$CaCO_3$ precipitates that had been aged in parent solution for 2 weeks. After 48 hours in parent solution peaks corresponding to the monohydrocalcite phase appear and remain present in SM-$CaCO_3$ precipitates until dehydration occurs and these peaks disappear. It is interesting to note that SM-$CaCO_3$ precipitates that had been in dry storage for two months following an initial 4 weeks of aging in parent solution (used in re-equilibration experiments in Chapter 3), still showed a "mixed" character of containing both ACC and calcite (Figure 2.10-(f)).

The SM-$CaCO_3$ precipitates had yielded a variable mix of $CaCO_3$ poly(a)morphs. Unlike the precipitates prepared by the AM, no SM-$CaCO_3$ precipitates characterized in this study were entirely calcite. Indeed, SM-$CaCO_3$ precipitates that were aged in parent solution consistently showed an interesting mix of ACC and calcite, often with a third crystalline polymorph, either

aragonite (Figures 2.11-(e)) or most commonly monohydrocalcite (Figures 2.11-(c),(e),(f)). This is particularly interesting because monohydrocalcite ($CaCO_3 \cdot H_2O$), one of two hydrated polymorphs of $CaCO_3$, is a relatively rare and an unstable phase of $CaCO_3$ (Kimura & Koga, 2011; Neumann & Epple, 2007). Monohydrocalcite was consistently observed the XRD-characterized SM-$CaCO_3$ precipitates, and it appeared in almost all precipitates after 2 weeks.

2.3.5: Comparison with previous literature

The crystallization behaviour, and poly(a)morphic evolution of ACC precipitated using the AM were fairly uniform and predictable, while the behavior of SM precipitates was more variable. To assess the impact of these observations, they must be compared to previous studies that prepared ACC using similar methods. ACC precipitated via the AM transformed rather quickly and predictably to calcite – after 24 hours aged in solution, and after 48 hours aged in air (see Figure 2.6, 2.8 (a)-(b)). The study by Koga et al. (1998) served as inspiration for this method, precipitating ACC in aqueous solutions that varied in pH. However, this study heated its resultant ACC precipitates to directly test how pH affected crystallization temperature; the final crystalline product was stated to be calcite (Koga et al., 1998). A later study, by Koga & Yamane (2008) compared two types of ACC – one prepared in water (ACC-AQ) and one prepared in ethanol (ACC-ET) – gradual heating was applied to dehydrated precipitates of each to monitor the crystallization process. The ACC-AQ crystallized at around 600 K to calcite in a single step corresponding to thermal dehydration, conversely, ACC-ET underwent two steps – first at ~ 600 K when a poorly crystalline calcite phase with traces of vaterite formed, and then at 825 K when the precipitate was fully crystalline and calcitic in nature (Koga & Yamane, 2008).

Though these studies both observed ACC as it was subjected to increased heat as opposed to the constant temperature conditions maintained in this study (25 ˚C ± 0.1 ˚C), parallels can be

drawn between these precipitates, and those from this study. Firstly, a similar, rapid crystallization to calcite is observed both in parent solution, and in air (Koga & Yamane, 2008; Koga et al., 1998). Secondly, the traces of vaterite in crystallized ACC-ET noted in the study by Koga and Yamane (2008) were also observed in AM-$CaCO_3$ precipitates – although these were washed with ethanol during vacuum filtration rather than precipitated within it. This might indicate that ethanol can initiate this intermediate dehydration step even if it is not the parent solution. Overall, the AM-$CaCO_3$ precipitates of this study behaved comparably to ACC prepared in similar manners in previous studies. However, it must be noted that this is the first study to monitor ACC prepared in highly alkaline solution as it ages in parent solution at constant temperature (25 ± 0.1 ˚C)

Several studies have observed the influence of the silica on the ACC system (e.g., Gal et al., 2010; Kellermeier et al., 2010; Kitano et al., 1979; Nakashima et al., 2018). These have been performed both biogenically, such as in the case of Cystoliths – small calcified bodies that form with in special cells of certain plant leaves (Gal et al., 2010), as well as inorganically by adding silica ions to supersaturated solutions of $CaCO_3$ (e.g., Gal et al., 2010; Kellermeier et al., 2010; Nakashima et al., 2018). These studies all illustrated the stabilizing effect of silica ions – specifically how they surround and isolate ACC and stabilize it for periods of time. A few studies synthesized silica-stabilized ACC similarly to the SM and several similarities can be noted between the precipitation and crystallization behaviour of the precipitated ACC. One study by Gal et al. (2010) tests the thermal stability of silica-stabilized ACC at increasing silica ion concentrations; it was observed that increasing concentrations corresponded with an increase in the crystallization temperature of the precipitates and with increasing periods of co-existence of ACC and calcite within the same precipitate. This matches well with the observed co-existence of ACC and calcite observed in this study, though this previous study observed none of the

metastable crystalline polymorphs of $CaCO_3$ as noted in SM-$CaCO_3$ precipitates. This may be due to the inherent differences in methodology, as this experiment did not age ACC in parent solution, but rather applied heat to filtered and dried ACC precipitates (Gal et al., 2010). The study by Kellermeier et al. (2010) assessed silica-coated ACC's crystallization by repeatedly washing the same precipitates until only crystal remained. They indicated that ACC would be permanently stabilized at concentrations of > 1870 ppm, and found precipitates to be still fully amorphous and coated in silica after 1 year (Kellermeier et al., 2010). However, solutions with lower SiO_2 concentrations were observed to crystallize to calcite, with some vaterite detected. This was not observed in this study, as ACC prepared using the SM had these same high silica concentrations (31 mmolal or 1870 ppm) but predictably began showing evidence of crystalline $CaCO_3$ polymorphs within 24 hours in parent solution – see Figure 2.9, 2.11-(a)-(b). Furthermore, there is no mention made in this previous study regarding the potential for this method to produce monohydrocalcite, which was often observed in SM-$CaCO_3$ precipitates alongside calcite and ACC – see Figure 2.11-(c),(d),(f). This may have been due to the effect of aging in parent solution, as all of the precipitates in the Kellermeier et al. (2010) study were subjected to immediate filtration and drying. Nakashima et al. (2018) prepared ACC similarly but did not report the crystallization behaviour of the ACC they prepared, though they noted that preparation in a methanol solution aided in stabilizing ACC. It appears that the environment in which ACC crystallizes plays a very important role in its path to crystallization, and immediate filtration may simplify a more complex process.

2.4. Conclusions

While the AM and SM were both intended to stabilize ACC, they differed greatly in the manner in which they achieved this goal, as well as their overall success. Furthermore, they

showed differing behaviour when comparing precipitates that were aged in air as opposed to aging in parent solution, as well as showing very different results in terms of the $CaCO_3$ poly(a)morphs that each ACC precipitate eventually transformed into. Results here show that the AM is possibly more successful, over short periods, in stabilizing ACC in air – as AM-ACC precipitates saw no appearance of crystalline XRD peaks with 48 hours exposed to air, while with the SM-ACC precipitates, crystalline peaks appeared after a 48-hour period. This could mean that the SM-ACC is more susceptible to the effects of dehydration that occur under such ambient conditions. However, the SM was seen to be more successful at maintaining some fraction of an ACC phase, as well as a monohydrocalcite phase, even after several months following filtration as seen in Figure 2.8-(b). Therefore, it is likely that SM-ACC precipitates may begin crystallizing sooner in air than AM-ACC precipitates, however, they resist complete crystallization to calcite in air with much greater success.

With aging in parent solution results are somewhat different. AM-$CaCO_3$ precipitates crystallize almost immediately with time in solution and are completely calcite within 1 week aging in solution. However, SM-$CaCO_3$ precipitates display a much more gradual crystallization process with time in parent solution. AM-$CaCO_3$ precipitates show consistent evidence of vaterite when allowed to age in solution for 24 and 48 hours, as confirmed by XRD. However, with one exception, phases apart from calcite are not seen after 1 week of aging in parent solution. SM-$CaCO_3$ precipitates, on the other hand, show very interesting behaviour when left to age in parent solution. SM-$CaCO_3$ precipitates consistently show mixes of stable and metastable $CaCO_3$ poly(a)morph phases. These phases range in solubility, stability, and hydration. The ability to maintain similar mineralogical character for periods of weeks to months is especially telling, as it indicates that full crystallization to calcite has been almost entirely prohibited within the system.

Overall, the SM, which utilized the theories of isolation to stabilize the ACC phase was much more successful in preventing SM-ACC precipitate's eventual transformation to calcite. Furthermore, it proved a somewhat consistent method of producing monohydrocalcite in small amounts. While the AM did succeed in stabilizing ACC for short periods of time, any longer than 24 hours in the parent solution, and, interestingly, after 48 hours in air, eventual spontaneous transformation to calcite could not be avoided. Other factors could be used in conjunction with this method to lengthen the period in which ACC is the primary phase present in the precipitate, including a lower temperature, higher concentrations of NaOH, or possibly use of ethanol rather than water as the parent solution. However, use of more extreme manipulation to this system would even further separate it from systems seen in nature, and therefore, make it a less worthy candidate for studying ACC in a biomimetic manner. In this vein, the effect of vesicle diameter as well as the behaviour of ACC within different isolating mediums, such as liposomes, or perhaps even biologically produced vesicles could be a very interesting area of further study. As these isolating measures are seen in nature, they could make an excellent experimental system for studying how ACC might behave in vivo.

Smaller aging increments for both AM and SM-$CaCO_3$ precipitates in air and in solution could offer more specific information regarding the timescales over which these precipitation methods can stabilize ACC. The presence of less stable crystalline $CaCO_3$ poly(a)morphs within the precipitates may be present in larger percentages in the hours and days following initial precipitation and vacuum filtration. An in-depth study of the evolution of poly(a)morphic character over the first 24 hours following ACC precipitation and vacuum filtration could offer interesting insight into its crystallization mechanics. Another interesting vein of study would be to investigate methods which would assist in predictably producing monohydrocalcite without the accompanying calcite phase, perhaps by using an additional additive such as magnesium

which is thought to play a role in stabilizing monohydrocalcite, or use of a saline solution, which has also been used successfully in maintaining this hydrated polymorph of $CaCO_3$ (Kimura & Koga, 2011; Neumann & Epple, 2007). Furthermore, the presence of monohydrocalcite in SM-$CaCO_3$ precipitates may have relevance to biological systems, perhaps this hydrated crystalline phase is also utilized by $CaCO_3$ biomineralizers as a median step. However, there has been, to date, no studies indicating monohydrocalcite as a metastable step during ACC crystallization. Therefore, more research is necessary in understanding why and how monohydrocalcite forms in this system, and if there are biological parallels.

The methods discussed above were also used in conjunction with investigation into the $\delta^{18}O$ and $\delta^{13}C$ compositions of AM- and SM-ACC/$CaCO_3$ precipitates, parent solutions and re-equilibration solutions. This isotopic characterization, along with data regarding crystallization behaviour of AM- and SM-ACC/$CaCO_3$ precipitates discussed in this chapter, are used in conjunction in Chapter 3 to probe the isotopic composition of ACC precipitated by two different methods, as well as its isotopic evolution as it crystallizes in parent or re-equilibration solution.

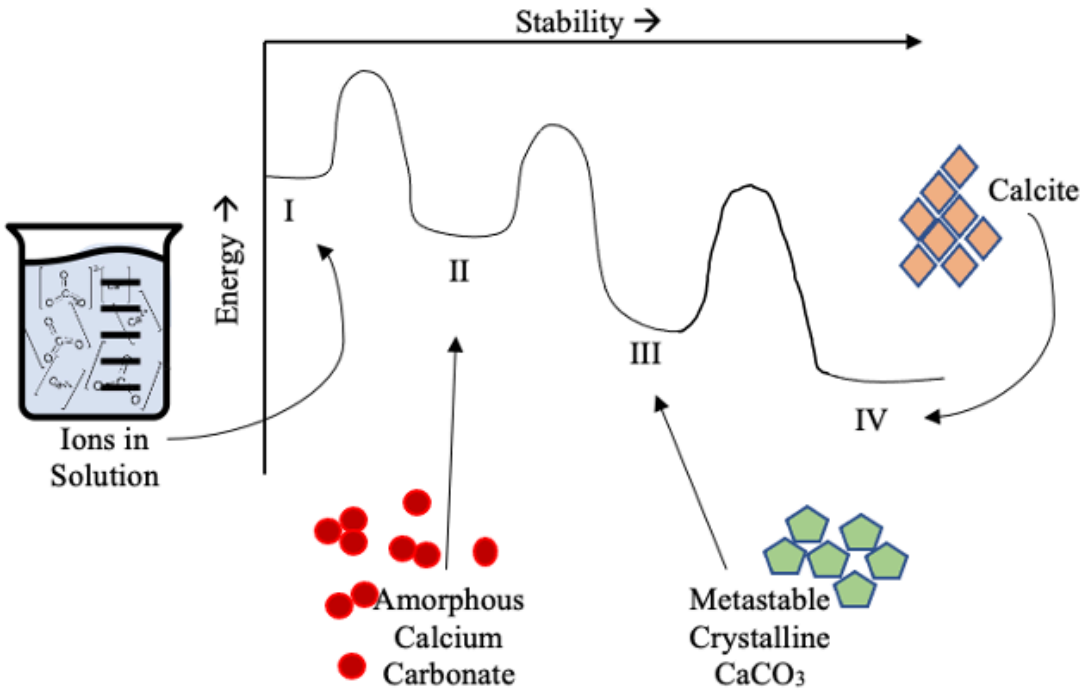

Figure 2.1. Basic schematic of the energy landscape of the stepwise crystallization of ions in solution to a final crystalline polymorph via higher energy metastable phases until the most stable/least soluble polymorph (i.e., calcite) precipitates.

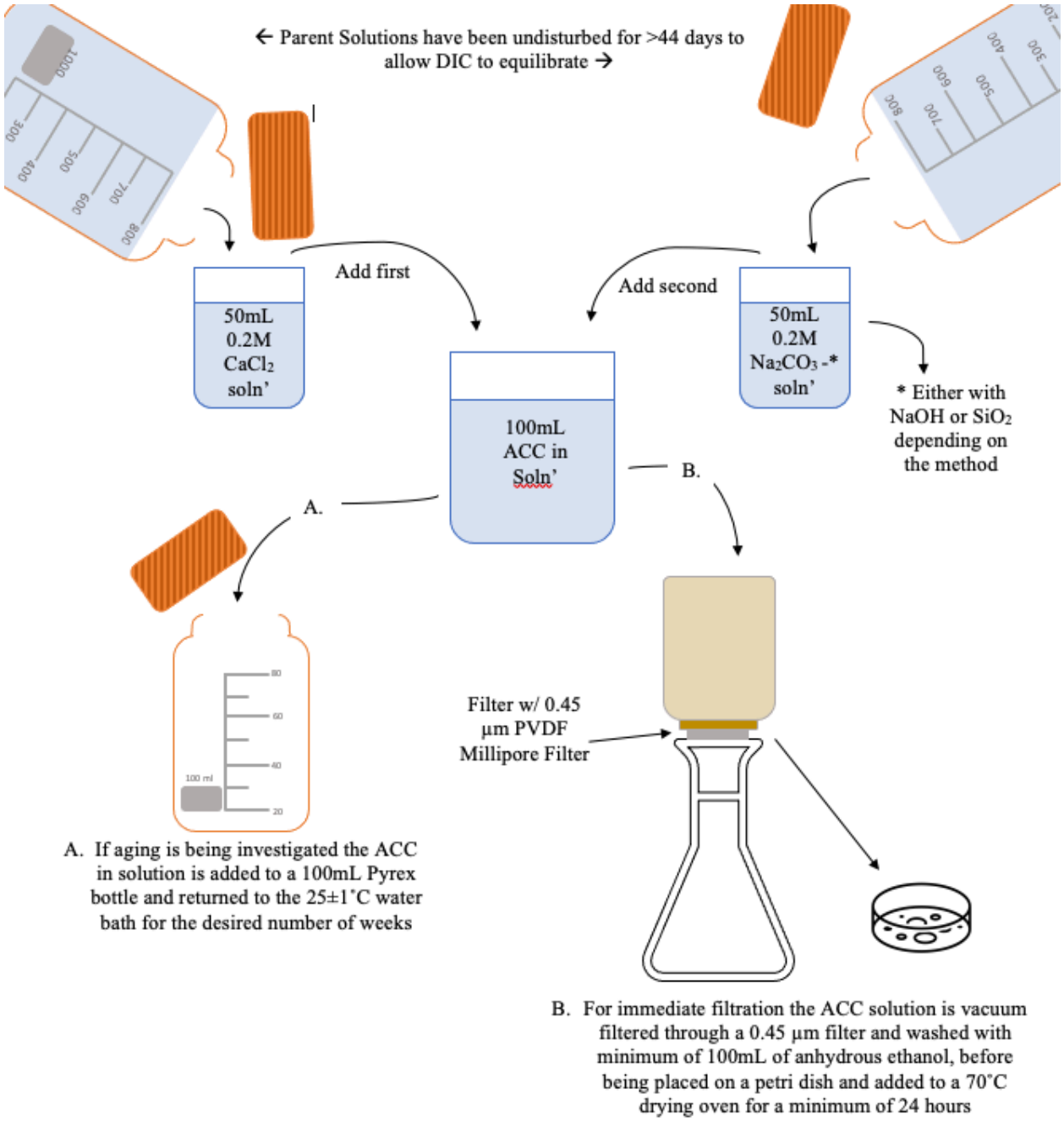

Figure 2.2. Schematic of ACC precipitation & vacuum filtration

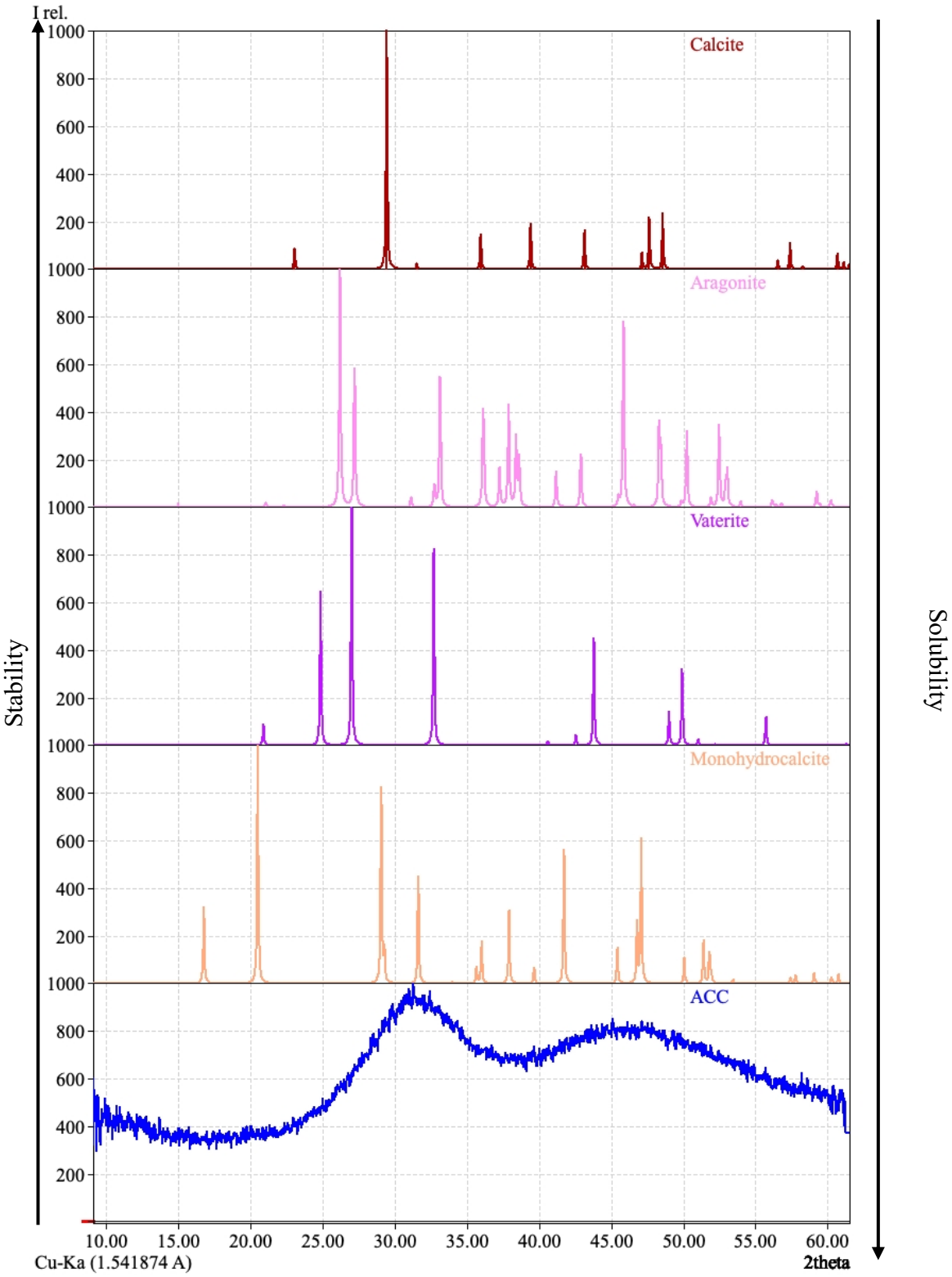

Figure 2.3. Typical XRD CuKα Spectrum of $CaCO_3$ poly(a)morphs, in order of decreasing stability. The calcite, aragonite, and vaterite spectra are taken from the ICDD PDF-4+ 2021 Diffraction Database, while the ACC spectra is an example from this study. Table 2.1 features the peaks specific to each poly(a)morph that are used in their identification. Peaks are measured in relative intensity versus 2θ

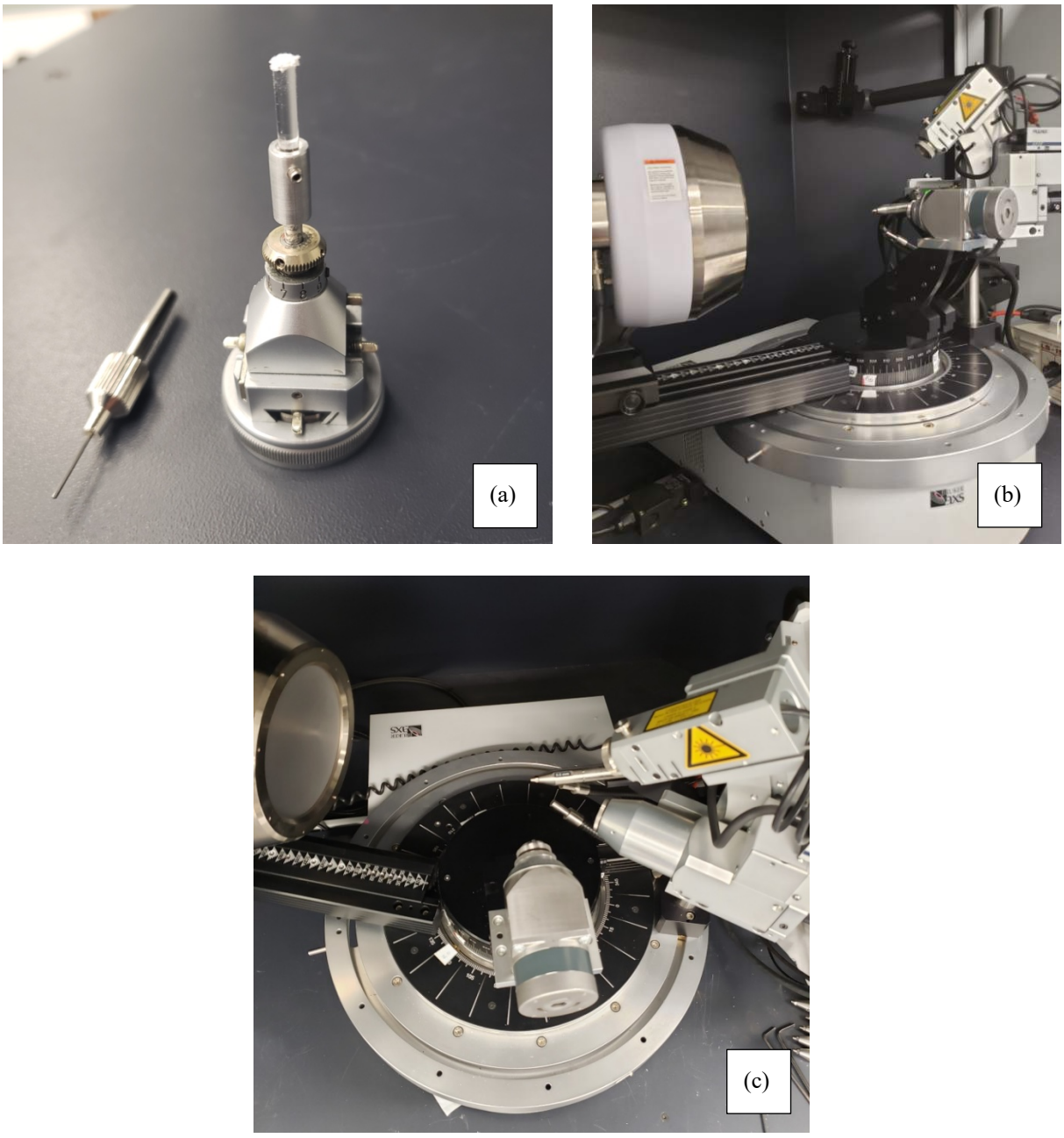

Figure 2.4. Images of (a) approximately 100 µg powdered precipitate mounted on the XRD sample mount which is then loaded into the (b)/(c) Bruker D8 DISCOVER diffractometer equipped with a Bruker Vantex600 area detector, and a CuKα sealed tube source for characterization.

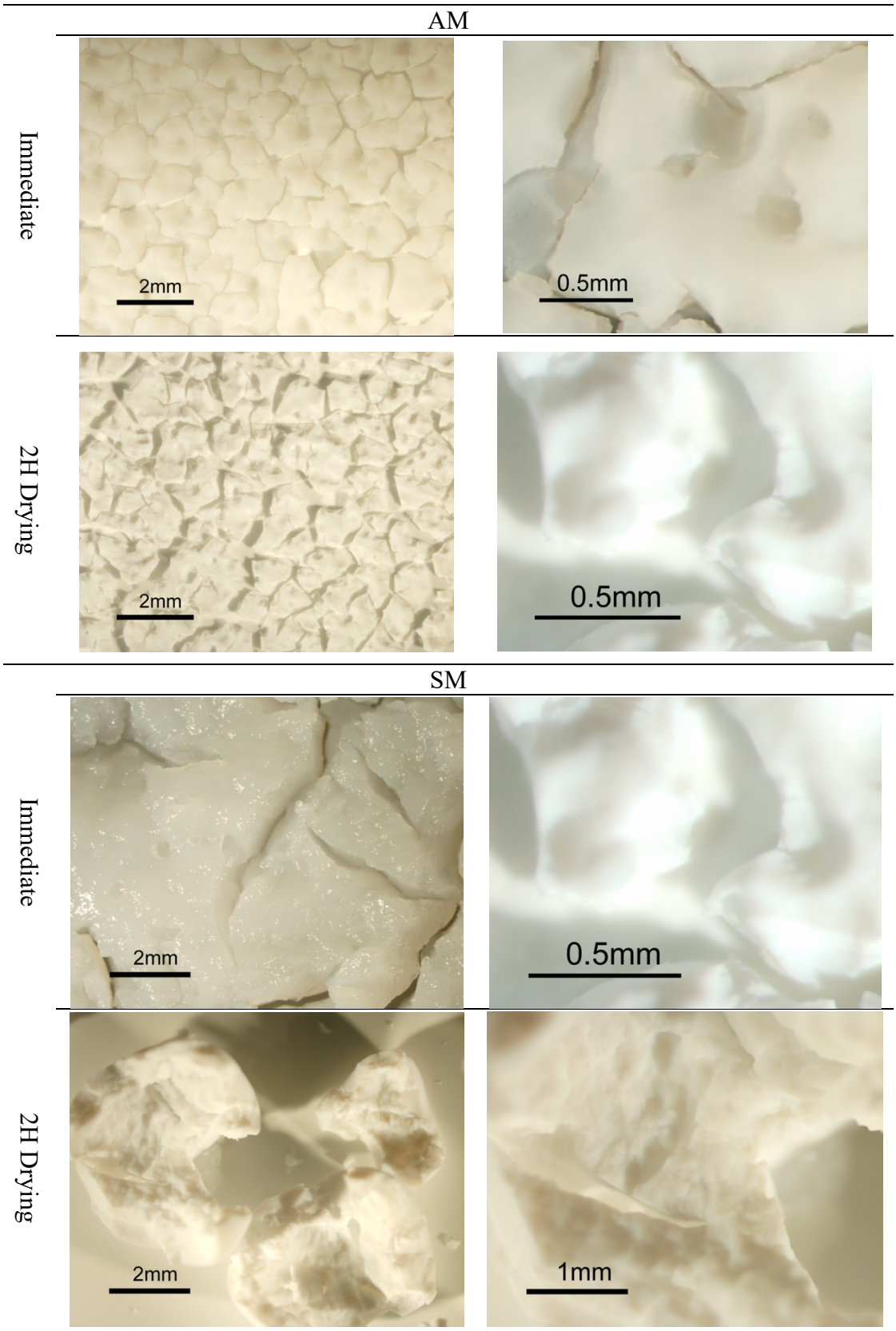

Figure 2.5. Microscopic images of AM & SM $CaCO_3$ precipitates immediately after precipitation, and following 2 hours in the 70 ± 0.3 ˚C drying oven. Taken using a Nikon Digital Camera DXM 1200F in conjunction with a Nikon SMZ 1000, and processed using ACT-1 software.

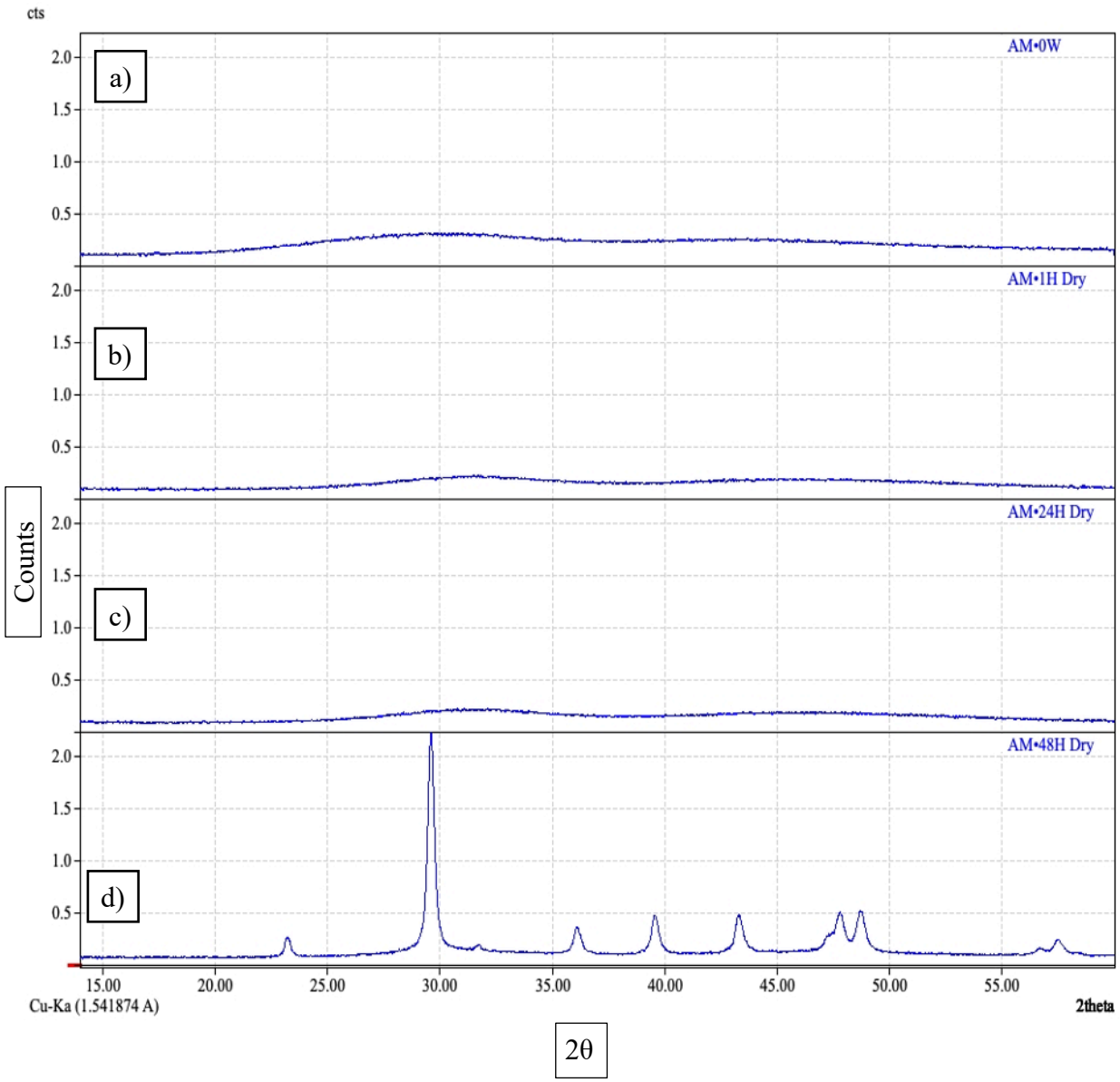

Figure 2.6. CuKα radiation XRD images of the same precipitate of AM-ACC at different times following precipitation in air. (a) immediately following precipitation, (b) 1 hour following precipitation and (c) 24 hours following precipitation. (d) 48 hours. Peaks are measured in counts versus 2θ.

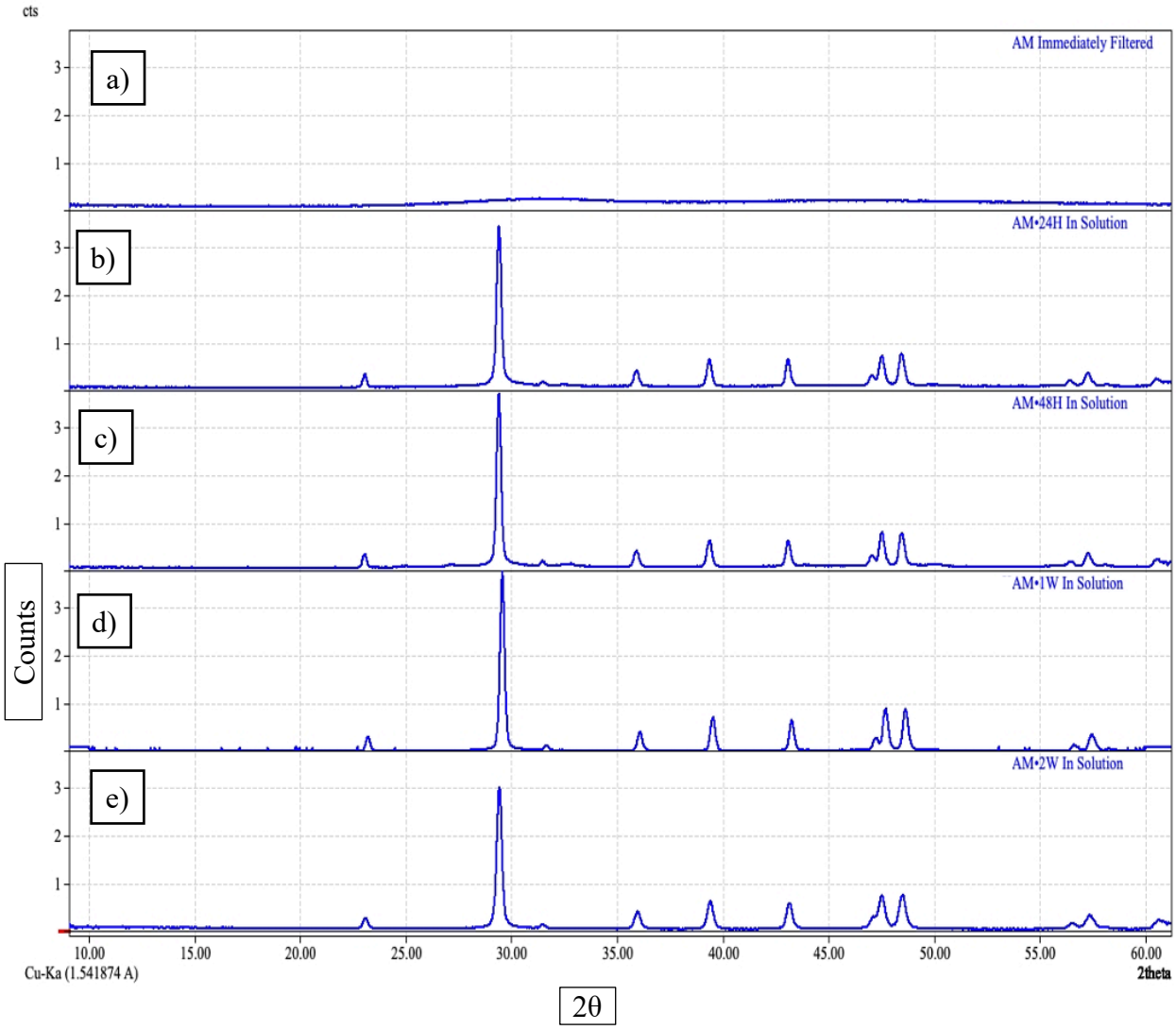

Figure 2.7. XRD spectra of AM-$CaCO_3$ precipitates, filtered following different periods of time crystallizing in parent solution. Peaks are measured in counts versus 2θ.

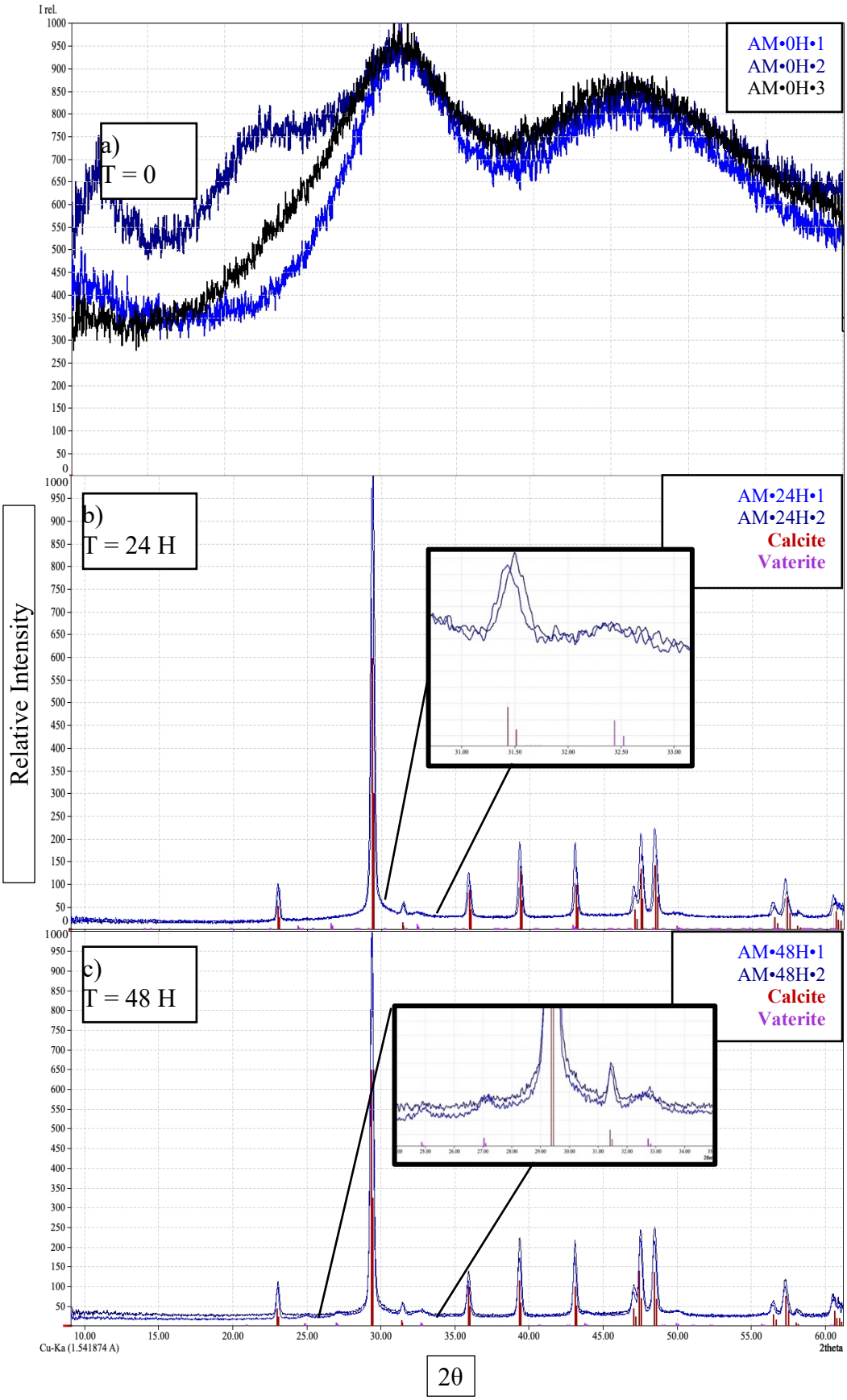
I rel.
a)
T = 0
AM•0H•1
AM•0H•2
AM•0H•3
b)
T = 24 H
AM•24H•1
AM•24H•2
Calcite
Vaterite
c)
T = 48 H
AM•48H•1
AM•48H•2
Calcite
Vaterite
Relative Intensity
Cu-Ka (1.541874 A)
2theta
2θ

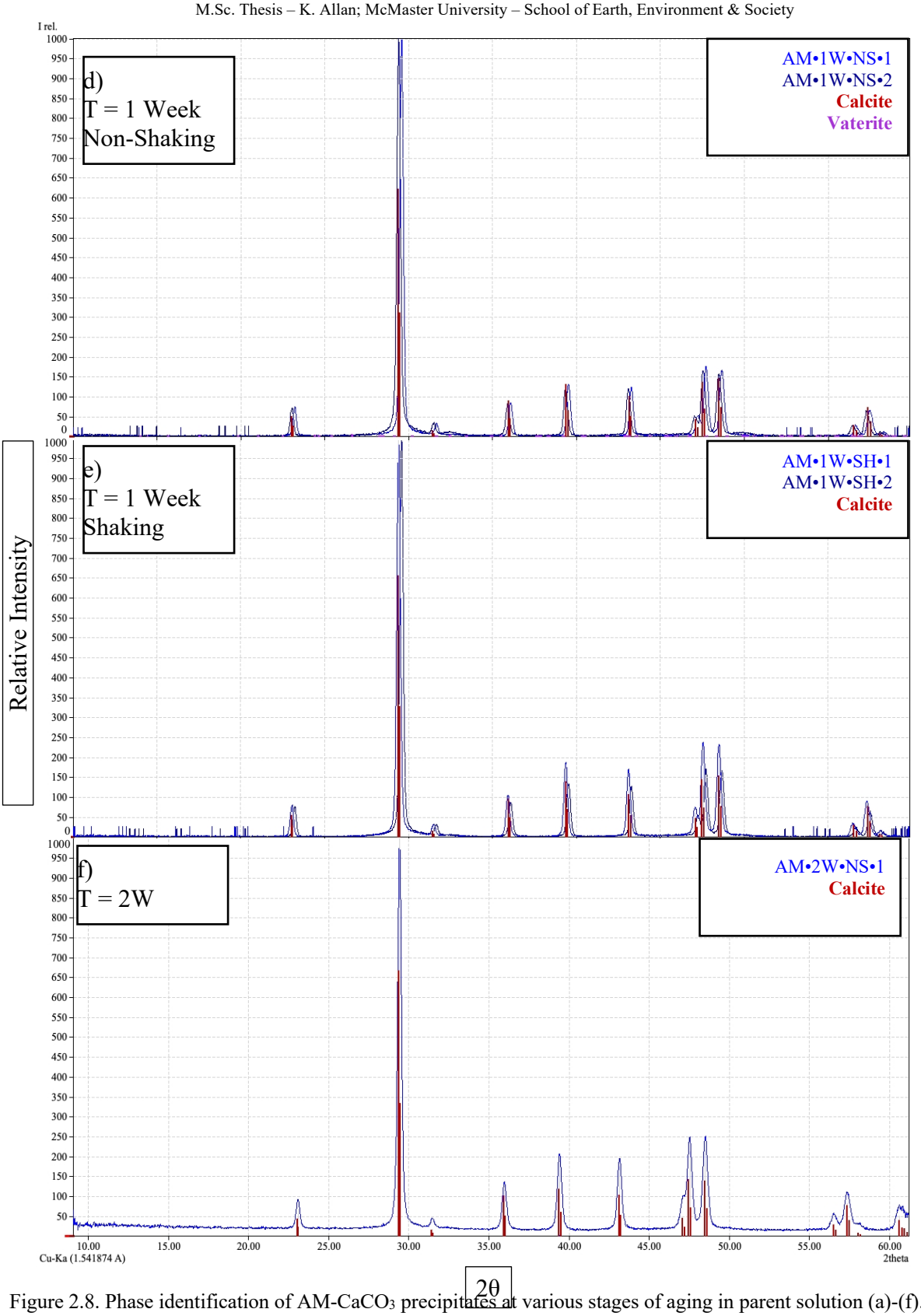

Figure 2.8. Phase identification of AM-$CaCO_3$ precipitates at various stages of aging in parent solution (a)-(f). Peaks are measured in relative intensity versus 2θ. Poly(a)morphic phases were identified using Match! Software in conjunction with Crystallography Open Database. Intensities were automatically normalized to assist in identifying mineral phases. Non-shaking indicated as NS, shaking as SH

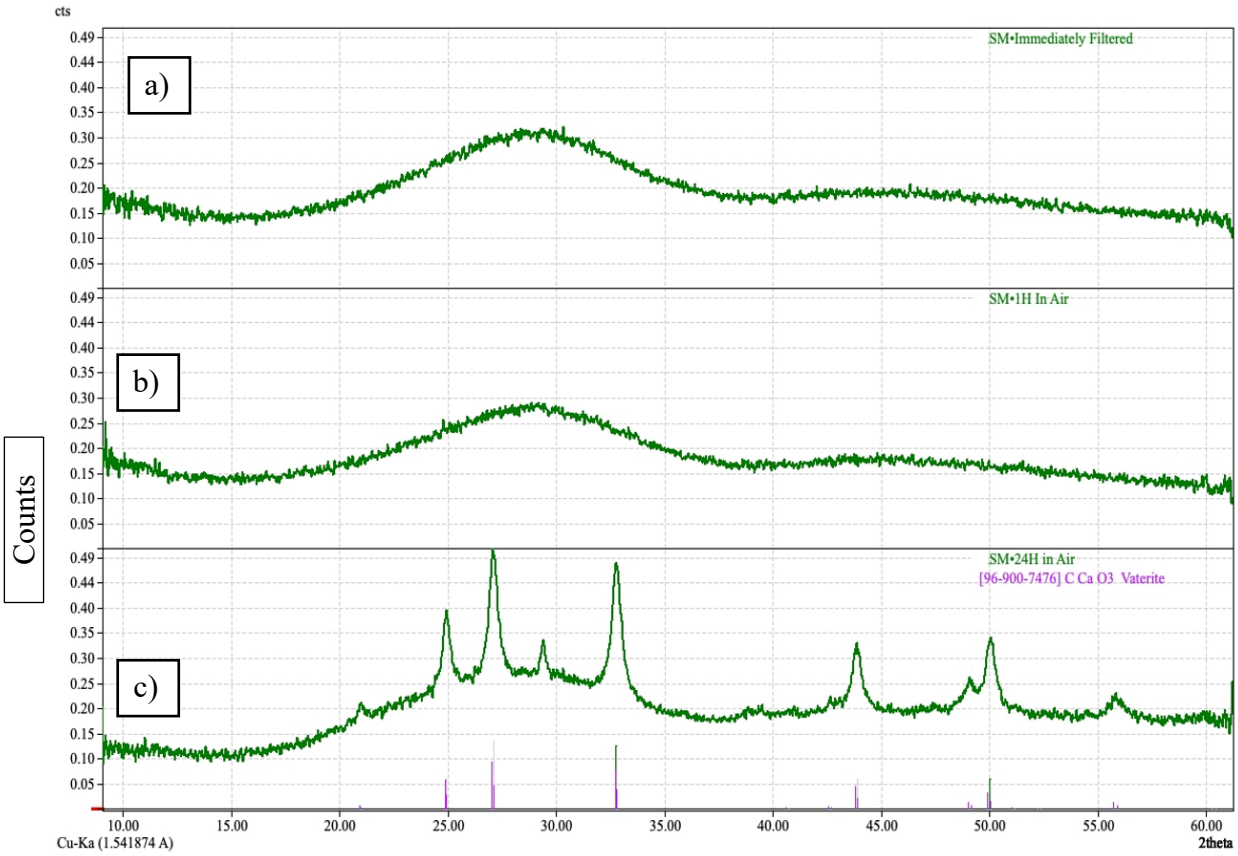

Figure 2.9. CuKα radiation XRD images of the same SM-ACC precipitate at different times following precipitation in air. (a) immediately following precipitation, (b) 1 hour following precipitation and (c) 24 hours following precipitation. Peaks are measured in counts versus 2θ.

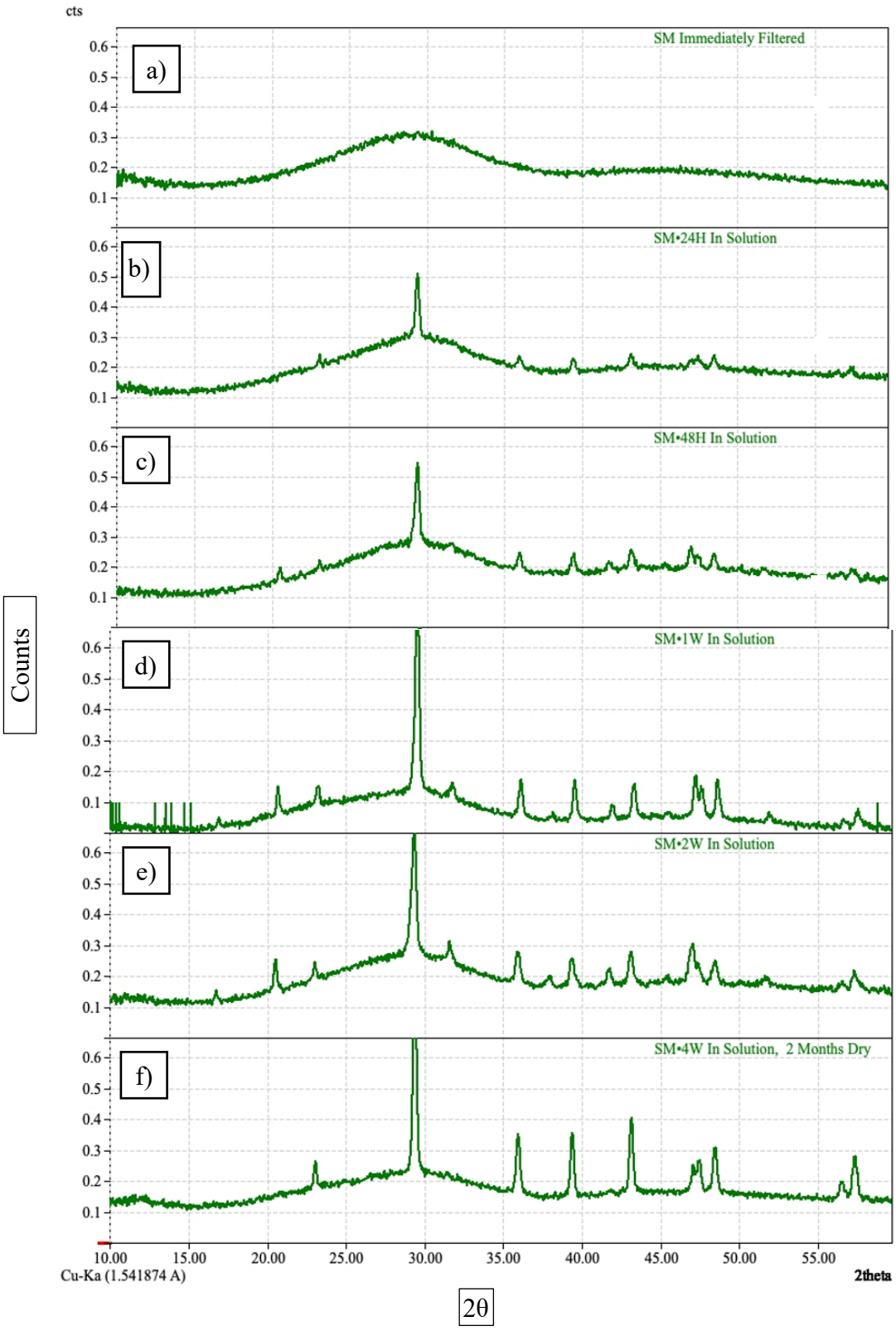

Figure 2.10. CuKα radiation XRD Spectra of SM-$CaCO_3$ precipitates, filtered following different periods of time crystallizing in parent solution. Peaks are measured in counts versus 2θ.

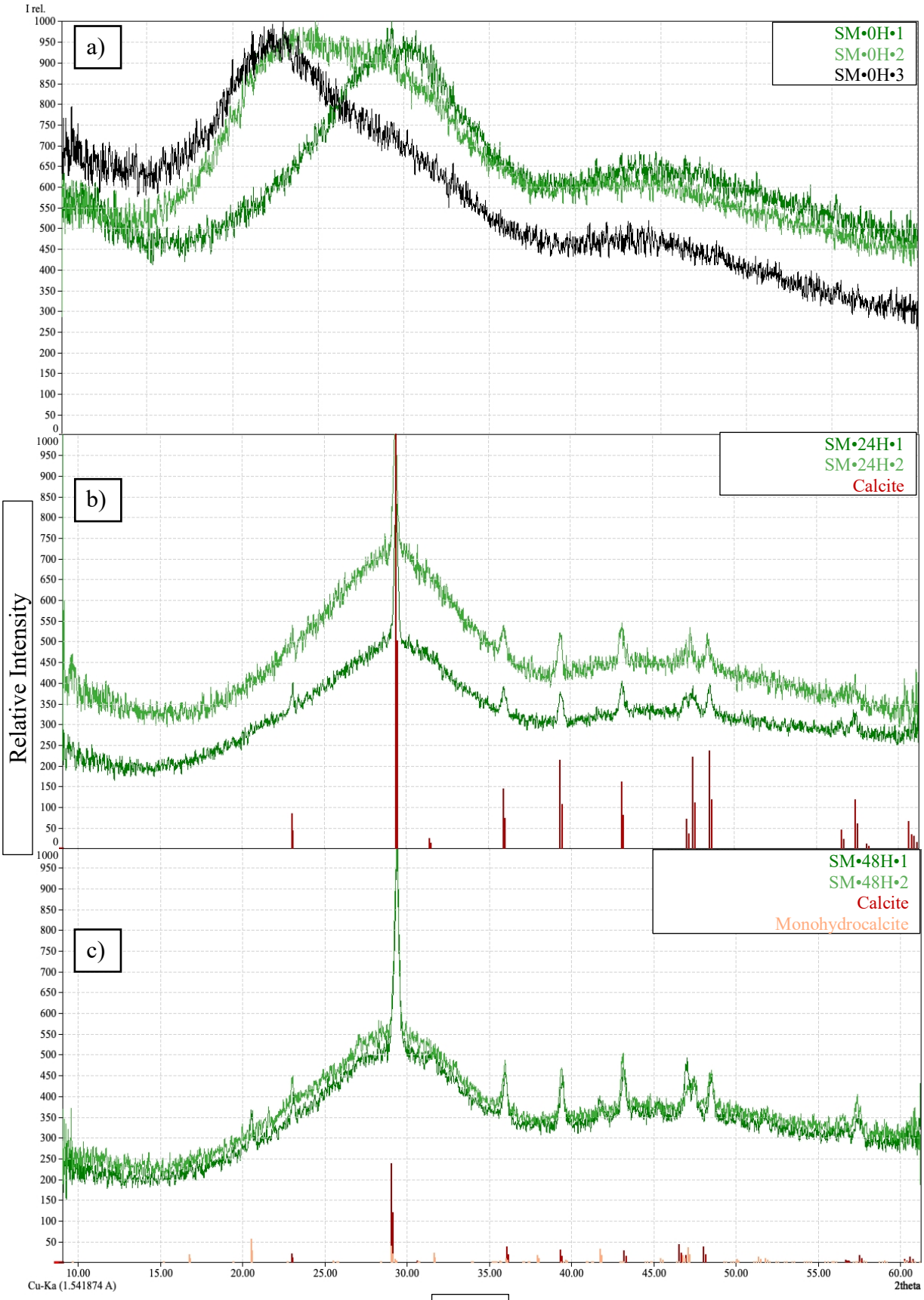
I rel.
a)
SM•0H•1
SM•0H•2
SM•0H•3
b)
SM•24H•1
SM•24H•2
Calcite
c)
SM•48H•1
SM•48H•2
Calcite
Monohydrocalcite
Relative Intensity
Cu-Ka (1.541874 A)
2theta
2θ

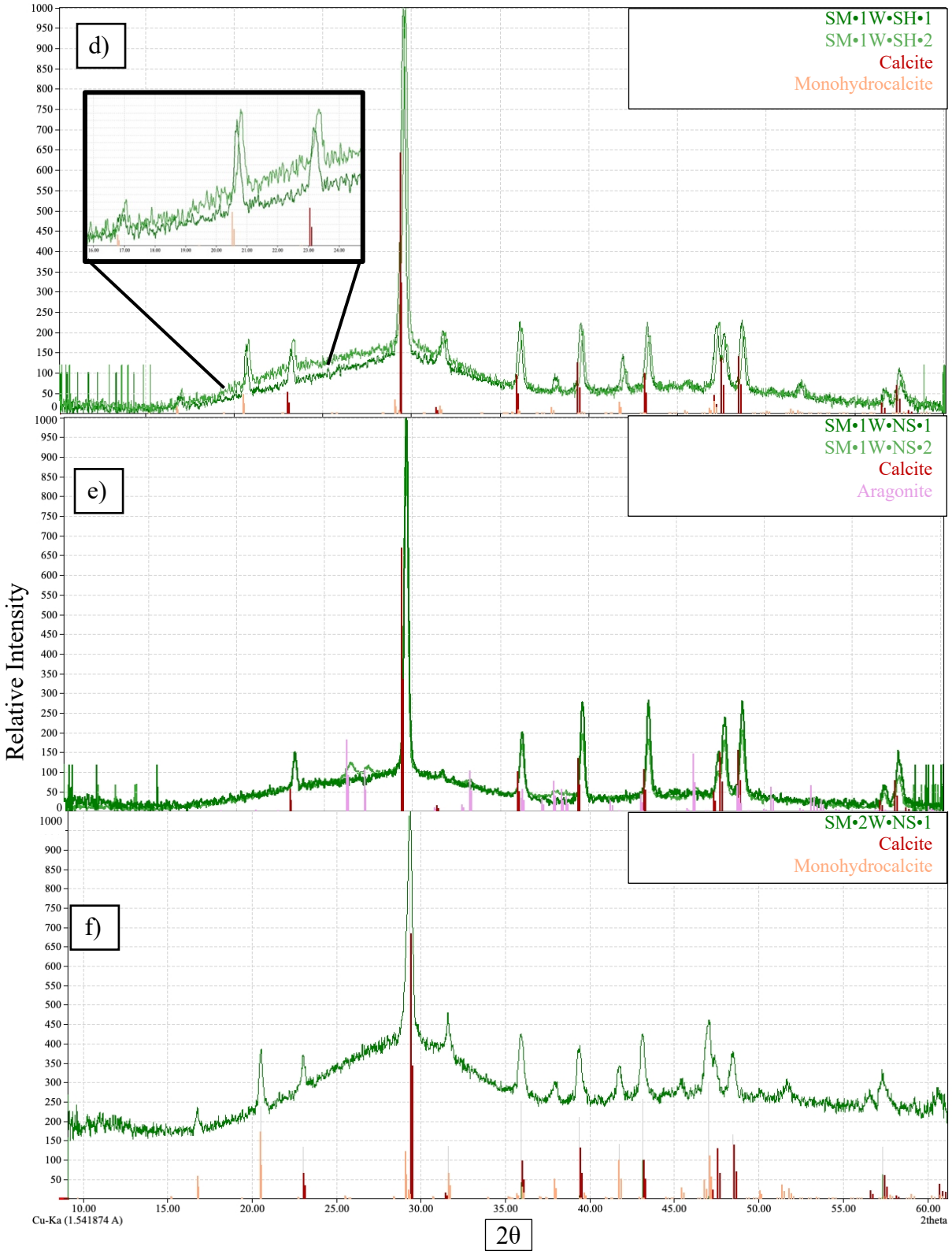

Figure 2.11. Phase identification of SM-$CaCO_3$ precipitates at various stages of aging in parent solution (a) – (f). Peaks are measured in relative intensity versus 2θ. Mineral phases were identified using Match! Software in conjunction with Crystallography Open Database. Intensities were automatically normalized to assist in identifying mineral phase

Calcium Carbonate Poly(a)morphs						
Decreasing Intensity (peak height)→	Decreasing Stability →					
	Calcite (rhombohedral)	Aragonite (orthorhombic)	Vaterite (hexagonal)	Monohydrocalcite (hexagonal, hydrated)	ACC (Amorphous)	
	2θ Maximum Peaks				2θ Areas of Broad Diffuse Maxima	
	29.42	26.24	25.27	20.52		25-38
	27.48	27.24	27.24	29.08		40-54
	33.30	33.18	27.48	47.1		
	33.10	36.16	33.30	41.74		
	21.33	37.94	33.10	31.64		
			21.33	16.78		

Table 2.1. Maximum peaks typical of different $CaCO_3$ poly(a)morphs when analyzed with Cu-Kα radiation. For ACC these are not peaks but broad diffuse maxima, also called "haloes," and a range is given rather than a specific wavelength.

Table 2.2. Experimental conditions of AM-/SM-$CaCO_3$ Precipitates. Ca^{2+} and AM/SM-CO_3^{2-}-donor parent solutions, were equilibrated with respect to DIC for 58 days prior to commencing precipitations. NS & SH are non-shaking or shaking trials which are conditions for the isotopic study and not relevant to this section. All experiments are done at a temperature of 25±0.1˚C. All precipitations were the result of vacuum filtration of 100 mL AM-/SM-$CaCO_3$ solutions.

Precipitate ID	Repeat	Precipitation Method	pH	Equilibration time in parent soln' (weeks)	Precipitate weight (mg)	Product Minerology (XRD Confirmed)
AM•0W•	1	AM*	12.70	IMMEDIATELY FILTERED	75.63	ACC
	2	AM	12.77		69.56	ACC
	3	AM	12.77		54.8	ACC
SM•0W•	1	SM*	10.37		151.28	ACC
	2	SM	10.37		143.98	ACC
	3	SM	10.40		141.65	ACC
AM•1W•NS•	1	AM	12.80	1	88.24	C*
	2	AM	12.78	1	85.24	C/V*
	3	AM	12.82	1	88.31	C
AM•1W•SH•	1	AM	12.82	1	79.97	C
	2	AM	12.82	1	73.76	C
	3	AM	12.82	1	64.46	C
SM•1W•NS•	1	SM	10.37	1	132.43	ACC/C/A*
	2	SM	10.42	1	236.47	ACC/C/A
	3	SM	10.40	1	134.72	ACC/C/A
SM•1W•SH•	1	SM	10.43	1	137.98	ACC/C/M*
	2	SM	10.43	1	153.5	ACC/C/M
	3	SM	10.43	1	124.75	ACC/C/M
AM•2W•NS•	1	AM	12.91	1	90.82	C
	2	AM	12.89	2	86.84	C
	3	AM	12.82	2	94.56	C
AM•2W•SH•	1	AM	12.80	2	89.26	C
	2	AM	12.82	2	72.95	C
	3	AM	12.82	2	88.35	C
SM•2W•NS•	1	SM	10.43	2	143.29	ACC/C/M
	2	SM	10.43	2	145.26	ACC/C/M
	3	SM	10.45	2	145.94	ACC/C/M
SM•2W•SH•	1	SM	10.46	2	194.24	ACC/C/M
	2	SM	10.46	2	131.25	ACC/C/M
	3	SM	10.46	2	161.98	ACC/C/M
AM•3W•NS•	1	AM	12.81	2	85.56	C
	2	AM	12.83	3	88.01	C
	3	AM	12.92	3	89.79	C
AM•3W•SH•	1	AM	12.83	3	88.36	C
	2	AM	12.84	3	79.83	C
	3	AM	12.86	3	87.86	C
SM•3W•NS•	1	SM	10.46	3	149.23	ACC/C
	2	SM	10.47	3	141.96	ACC/C
	3	SM	10.47	3	144.24	ACC/C
SM•3W•SH•	1	SM	10.51	3	128.74	ACC/C
	2	SM	10.52	3	107.22	ACC/C
	3	SM	10.52	3	133.1	ACC/C
AM•4W•NS•	1	AM	13.30	3	90.52	C
	2	AM	13.36	4	91.26	C
	3	AM	13.30	4	88.47	C
AM•4W•SH•	1	AM	13.34	4	71.58	C
	2	AM	13.32	4	81.79	C
	3	AM	13.34	4	82.62	C
SM•4W•NS•	1	SM	10.66	4	137.42	ACC/C
	2	SM	10.68	4	150.44	ACC/C
	3	SM	10.69	4	142.8	ACC/C
SM•4W•SH•	1	SM	10.76	4	147.63	ACC/C
	2	SM	10.74	4	109.67	ACC/C
	3	SM	10.74	4	121.22	ACC/C
AM•5W•NS•	1	AM	12.88	5	95.94	C
	2	AM	12.88	5	93.59	C
AM•5W•SH•	1	AM	12.87	5	76.56	C
	2	AM	12.92	5	106.44	C
SM•5W•NS•	1	SM	10.49	5	151.6	ACC/C
	2	SM	10.50	5	160.51	ACC/C
SM•5W•SH•	1	SM	10.52	5	134.12	ACC/C
	2	SM	10.51	5	155.03	ACC/C

AM: Alkaline method, SM: Silica method
ACC: Amorphous Calcium Carbonate, C: Calcite, V: Vaterite, A: Aragonite, M: Monohydrocalcite

References

Addadi, L., Raz, S., & Weiner, S. (2003). Taking Advantage of Disorder: Amorphous Calcium Carbonate and Its Roles in Biomineralization. *Advanced Materials*, *15*(12), 959–970. https://doi.org/10.1002/adma.200300381

Aizenberg, J. (1996). Stabilization of amorphous calcium carbonate by specialized macromolecules in biological and synthetic precipitates. *Advanced Materials*, *8*(3), 222–226. https://doi.org/10.1002/adma.19960080307

Aizenberg, J., Addadi, L., Weiner, S., & Lambert, G. (1996). Stabilization of amorphous calcium carbonate by specialized macromolecules in biological and synthetic precipitates. *Advanced Materials*, *8*(3), 222–226. https://doi.org/10.1002/adma.19960080307

Aizenberg, J., Lambert, G., Weiner, S., & Addadi, L. (2002). Factors Involved in the Formation of Amorphous and Crystalline Calcium Carbonate: A Study of an Ascidian Skeleton. *Journal of the American Chemical Society*, *124*(1), 32–39. https://doi.org/10.1021/ja016990l

Aizenberg, J., Weiner, S., & Addadi, L. (2003). Coexistence of amorphous and crystalline calcium carbonate in skeletal tissues. *Connective Tissue Research*, *44*(SUPPL. 1), 20–25. https://doi.org/10.1080/03008200390152034

Ajikumar, P. K., Ling, G. W., Subramanyam, G., Lakshminarayanan, R., & Valiyaveettil, S. (2005). Synthesis and characterization of monodispersed spheres of amorphous calcium carbonate and calcite spherules. *Crystal Growth and Design*, *5*(3), 1129–1134. https://doi.org/10.1021/cg049606f

Akiva-Tal, A., Kababya, S., Balazs, Y. S., Glazer, L., Berman, A., Sagi, A., & Schmidt, A. (2011). In situ molecular NMR picture of bioavailable calcium stabilized as amorphous CaCO 3 biomineral in crayfish gastroliths. *Proceedings of the National Academy of Sciences of the United States of America*, *108*(36), 14763–14768. https://doi.org/10.1073/pnas.1102608108

Al-Horani, F. A., Al-Moghrabi, S. M., & De Beer, D. (2003). The mechanism of calcification and its relation to photosynthesis and respiration in the scleractinian coral Galaxea fascicularis. *Marine Biology*, *142*(3), 419–426. https://doi.org/10.1007/S00227-002-0981-8/FIGURES/7

Albéric, M., Bertinetti, L., Zou, Z., Fratzl, P., Habraken, W., & Politi, Y. (2018). The Crystallization of Amorphous Calcium Carbonate is Kinetically Governed by Ion Impurities and Water. *Advanced Science*, *5*(5), 1701000. https://doi.org/10.1002/advs.201701000

Atkins, E. (1978). Elements of X-ray Diffraction. *Physics Bulletin*, *29*(12), 572–572. https://doi.org/10.1088/0031-9112/29/12/034

Beck, W. C., Grossman, E. L., & Morse, J. W. (2005). Experimental studies of oxygen isotope fractionation in the carbonic acid system at 15°, 25°, and 40°C. *Geochimica et Cosmochimica Acta*, *69*(14), 3493–3503. https://doi.org/10.1016/j.gca.2005.02.003

Becker, A., Bismayer, U., Epple, M., Fabritius, H., Hasse, B., Shi, J., & Ziegler, A. (2003). Structural characterisation of X-ray amorphous calcium carbonate (ACC) in sternal deposits of the crustacea Porcellio scaber. *Journal of the Chemical Society. Dalton Transactions*, *3*(4), 551–555. https://doi.org/10.1039/b210529b

Becker, A., Ziegler, A., & Epple, M. (2005). The mineral phase in the cuticles of two species of Crustacea consists of magnesium calcite, amorphous calcium carbonate, and amorphous calcium phosphate. *Dalton Transactions*, *10*, 1814. https://doi.org/10.1039/b412062k

Beniash, E., Addadi, L., & Weiner, S. (1999). Cellular Control Over Spicule Formation in Sea Urchin Embryos: A Structural Approach. *Journal of Structural Biology*, *125*(1), 50–62. https://doi.org/10.1006/jsbi.1998.4081

Beniash, E., Aizenberg, J., Addadi, L., & Weiner, S. (1997). Amorphous calcium carbonate transforms into calcite during sea urchin larval spicule growth. *Proceedings of the Royal Society of London. Series B: Biological Sciences*, *264*(1380), 461–465. https://doi.org/10.1098/rspb.1997.0066

Beniash, E., Metzler, R. A., Lam, R. S. K., & Gilbert, P. U. P. A. (2009). Transient amorphous calcium phosphate in forming enamel. *Journal of Structural Biology*, *166*(2), 133–143. https://doi.org/10.1016/j.jsb.2009.02.001

Bentov, S., Brownlee, C., & Erez, J. (2009). The role of seawater endocytosis in the biomineralization process in calcareous foraminifera. *Proceedings of the National Academy of Sciences of the United*

States of America, *106*(51), 21500–21504. https://doi.org/10.1073/pnas.0906636106

Bentov, S., Weil, S., Glazer, L., Sagi, A., & Berman, A. (2010). Stabilization of amorphous calcium carbonate by phosphate rich organic matrix proteins and by single phosphoamino acids. *Journal of Structural Biology*, *171*(2), 207–215. https://doi.org/10.1016/j.jsb.2010.04.007

Bergwerff, L., & van Paassen, L. A. (2021). Review and recalculation of growth and nucleation kinetics for calcite, vaterite and amorphous calcium carbonate. In *Crystals* (Vol. 11, Issue 11, p. 1318). Multidisciplinary Digital Publishing Institute. https://doi.org/10.3390/cryst11111318

Bewernitz, M. A., Gebauer, D., Long, J., Cölfen, H., & Gower, L. B. (2012). A metastable liquid precursor phase of calcium carbonate and its interactions with polyaspartate. *Faraday Discussions*, *159*, 291–312. https://doi.org/10.1039/c2fd20080e

Blue, C. R., Rimstidt, J. D., & Dove, P. M. (2013). A Mixed Flow Reactor Method to Synthesize Amorphous Calcium Carbonate Under Controlled Chemical Conditions. In *Methods in Enzymology* (Vol. 532, pp. 557–568). Academic Press Inc. https://doi.org/10.1016/B978-0-12-416617-2.00023-0

Brecevic, L., & Kralj, D. (2008). ChemInform Abstract: On Calcium Carbonates: From Fundamental Research to Application. *ChemInform*, *39*(5), 467–484. https://doi.org/10.1002/chin.200805226

Cai, G. Bin, Zhao, G. X., Wang, X. K., & Yu, S. H. (2010). Synthesis of polyacrylic acid stabilized amorphous calcium carbonate nanoparticles and their application for removal of toxic heavy metal ions in water. *Journal of Physical Chemistry C*, *114*(30), 12948–12954. https://doi.org/10.1021/jp103464p

Cartwright, J. H. E., Checa, A. G., Gale, J. D., Gebauer, D., & Sainz-Díaz, C. I. (2012). Calcium Carbonate Polyamorphism and Its Role in Biomineralization: How Many Amorphous Calcium Carbonates Are There? *Angewandte Chemie International Edition*, *51*(48), 11960–11970. https://doi.org/10.1002/anie.201203125

Chen, S. F., Cölfen, H., Antonietti, M., & Yu, S. H. (2013). Ethanol assisted synthesis of pure and stable amorphous calcium carbonate nanoparticles. *Chemical Communications*, *49*(83), 9564–9566. https://doi.org/10.1039/c3cc45427d

Cohn, M., & Urey, H. C. (1938). Oxygen Exchange Reactions of Organic Compounds and Water. *Journal of the American Chemical Society*, *60*(3), 679–687. https://doi.org/10.1021/ja01270a052

Cölfen, H. (2010). A crystal-clear view. In *Nature Materials* (Vol. 9, Issue 12, pp. 960–961). https://doi.org/10.1038/nmat2911

Coplen, T.B., & Schlanger, S. O. (1973). Oxygen and Carbon Isotope Studies of Carbonate Sediments from Site 167, Magellan Rise, Leg 17. In *Initial Reports of the Deep Sea Drilling Project, 17*. U.S. Government Printing Office. https://doi.org/10.2973/dsdp.proc.17.115.1973

Coplen, Tyler B. (2007). Calibration of the calcite-water oxygen-isotope geothermometer at Devils Hole, Nevada, a natural laboratory. *Geochimica et Cosmochimica Acta*, *71*(16), 3948–3957. https://doi.org/10.1016/j.gca.2007.05.028

Coronado, I., Fine, M., Bosellini, F. R., & Stolarski, J. (2019). Impact of ocean acidification on crystallographic vital effect of the coral skeleton. *Nature Communications*, *10*(1). https://doi.org/10.1038/s41467-019-10833-6

Costa, S. N., Freire, V. N., Caetano, E. W. S., Maia, F. F., Barboza, C. A., Fulco, U. L., & Albuquerque, E. L. (2016). DFT Calculations with van der Waals Interactions of Hydrated Calcium Carbonate Crystals CaCO3·(H2O, 6H2O): Structural, Electronic, Optical, and Vibrational Properties. *Journal of Physical Chemistry A*, *120*(28), 5752–5765. https://doi.org/10.1021/acs.jpca.6b05436

Cullity, B. D. (Bernard D. (2001). Elements of x-ray diffraction / B.D. Cullity, S.R. Stock. In *Book*. Prentice Hall,. https://discovery.mcmaster.ca/iii/encore/record/C__Rb1167916__SElements of x-ray diffraction__Orightresult__U__X6?lang=eng&suite=def

Darkins, R., Côté, A. S., Freeman, C. L., & Duffy, D. M. (2013). Crystallisation rates of calcite from an amorphous precursor in confinement. *Journal of Crystal Growth*, *367*, 110–114. https://doi.org/10.1016/j.jcrysgro.2012.12.027

De Nooijer, L. J., Toyofuku, T., & Kitazato, H. (2009). Foraminifera promote calcification by elevating their intracellular pH. *Proceedings of the National Academy of Sciences*, *106*(36), 15374–15378. https://doi.org/10.1073/PNAS.0904306106

De Yoreo, J. J., Gilbert, P. U. P. A., Sommerdijk, N. A. J. M., Penn, R. L., Whitelam, S., Joester, D., Zhang, H., Rimer, J. D., Navrotsky, A., Banfield, J. F., Wallace, A. F., Michel, F. M., Meldrum, F. C., Cölfen, H., & Dove, P. M. (2015). Crystallization by particle attachment in synthetic, biogenic, and geologic environments. In *Science* (Vol. 349, Issue 6247). https://doi.org/10.1126/science.aaa6760

Demény, A., Czuppon, G., Kern, Z., Leél-Őssy, S., Németh, A., Szabó, M., Tóth, M., Wu, C. C., Shen, C. C., Molnár, M., Németh, T., Németh, P., & Óvári, M. (2016). Recrystallization-induced oxygen isotope changes in inclusion-hosted water of speleothems – Paleoclimatological implications. *Quaternary International*, *415*, 25–32. https://doi.org/10.1016/j.quaint.2015.11.137

Demény, A., Németh, P., Czuppon, G., Leél-Ossy, S., Szabó, M., Judik, K., Németh, T., & Stieber, J. (2016). Formation of amorphous calcium carbonate in caves and its implications for speleothem research. *Scientific Reports*, *6*(1), 39602. https://doi.org/10.1038/srep39602

Devriendt, L. S., Watkins, J. M., & McGregor, H. V. (2017). Oxygen isotope fractionation in the CaCO3-DIC-H2O system. *Geochimica et Cosmochimica Acta*, *214*, 115–142. https://doi.org/10.1016/j.gca.2017.06.022

Dietzel, M., Purgstaller, B., Kluge, T., Leis, A., & Mavromatis, V. (2020). Oxygen and clumped isotope fractionation during the formation of Mg calcite via an amorphous precursor. *Geochimica et Cosmochimica Acta*, *276*, 258–273. https://doi.org/10.1016/j.gca.2020.02.032

DIFFRAC.EVA | Bruker. (n.d.). Retrieved December 3, 2021, from https://www.bruker.com/en/products-and-solutions/diffractometers-and-scattering-systems/x-ray-diffractometers/diffrac-suite-software/diffrac-eva.html

Douglas, R. C., & Savin, S. M. (1975). Oxygen and Carbon Isotope Analyses of Tertiary and Cretaceous Microfossils from Shatsky Rise and Other Sites in the North Pacific Ocean. In *Initial Reports of the Deep Sea Drilling Project, 32*. U.S. Government Printing Office. https://doi.org/10.2973/dsdp.proc.32.115.1975

Emiliani, C. (1966). Isotopic Paleotemperatures. *Science*, *154*(3751), 851–857.

https://doi.org/10.1126/science.154.3751.851

Epstein, S., & Mayeda, T. (1953). Variation of O18 content of waters from natural sources. *Geochimica et Cosmochimica Acta*, *4*(5), 213–224. https://doi.org/10.1016/0016-7037(53)90051-9

Epstein, Samuel, Buchsbaum, R., Lowenstam, H., & Urey, H. C. (1951). Carbonate-water isotopic temperature scale. *Bulletin of the Geological Society of America*, *62*(4), 417–426. https://doi.org/10.1130/0016-7606(1951)62[417:CITS]2.0.CO;2

Erez, J. (1978). *Vital Effect in Coral & Foram*.

Evans, D., Webb, P. B., Penkman, K., Kröger, R., & Allison, N. (2019). The Characteristics and Biological Relevance of Inorganic Amorphous Calcium Carbonate (ACC) Precipitated from Seawater. *Crystal Growth and Design*, *19*(8), 4300–4313. https://doi.org/10.1021/acs.cgd.9b00003

Fairchild, I. J., Smith, C. L., Baker, A., Fuller, L., Spötl, C., Mattey, D., & McDermott, F. (2006). Modification and preservation of environmental signals in speleothems. *Earth-Science Reviews*, *75*(1–4), 105–153. https://doi.org/10.1016/j.earscirev.2005.08.003

Farhadi Khouzani, M., Chevrier, D. M., Güttlein, P., Hauser, K., Zhang, P., Hedin, N., & Gebauer, D. (2015). Disordered amorphous calcium carbonate from direct precipitation. *CrystEngComm*, *17*(26), 4842–4849. https://doi.org/10.1039/c5ce00720h

Frisia, S., Borsato, A., Fairchild, I. J., McDermott, F., & Selmo, E. M. (2002). Aragonite-Calcite Relationships in Speleothems (Grotte De Clamouse, France): Environment, Fabrics, and Carbonate Geochemistry. *Journal of Sedimentary Research*, *72*(5), 687–699. https://doi.org/10.1306/020702720687

Gabitov, R. I., Watson, E. B., Sadekov, A., Watson, B. E., & Sadekov, A. (2012). Oxygen isotope fractionation between calcite and fluid as a function of growth rate and temperature: An in situ study. *Chemical Geology*, *306–307*, 92–102. https://doi.org/10.1016/j.chemgeo.2012.02.021

Gago-Duport, L., Briones, M. J. I., Rodríguez, J. B., & Covelo, B. (2008). Amorphous calcium carbonate biomineralization in the earthworm's calciferous gland: Pathways to the formation of crystalline phases. *Journal of Structural Biology*, *162*(3), 422–435. https://doi.org/10.1016/j.jsb.2008.02.007

Gal, A., Weiner, S., & Addadi, L. (2010). The stabilizing effect of silicate on biogenic and synthetic amorphous calcium carbonate. *Journal of the American Chemical Society*, *132*(38), 13208–13211. https://doi.org/10.1021/ja106883c

Gayathri, S., Lakshminarayanan, R., Weaver, J. C., Morse, D. E., Manjunatha Kini, R., & Valiyaveettil, S. (2007). In vitro study of magnesium-calcite biomineralization in the skeletal materials of the seastar Pisaster giganteus. *Chemistry - A European Journal*, *13*(11), 3262–3268. https://doi.org/10.1002/chem.200600825

Gebauer, D., Gunawidjaja, P. N., Ko, J. Y. P., Bacsik, Z., Aziz, B., Liu, L., Hu, Y., Bergström, L., Tai, C. W., Sham, T. K., Edén, M., & Hedin, N. (2010). Proto-calcite and proto-vaterite in amorphous calcium carbonates. *Angewandte Chemie - International Edition*, *49*(47), 8889–8891. https://doi.org/10.1002/anie.201003220

Gebauer, D., Völkel, A., & Cölfen, H. (2008). Stable prenucleation calcium carbonate clusters. *Science*, *322*(5909), 1819–1822. https://doi.org/10.1126/science.1164271

Ghosh, P., Adkins, J., Affek, H., Balta, B., Guo, W., Schauble, E. A., Schrag, D., & Eiler, J. M. (2006). 13C-18O bonds in carbonate minerals: A new kind of paleothermometer. *Geochimica et Cosmochimica Acta*, *70*(6), 1439–1456. https://doi.org/10.1016/j.gca.2005.11.014

Giuffre, A. J., Gagnon, A. C., De Yoreo, J. J., & Dove, P. M. (2015). Isotopic tracer evidence for the amorphous calcium carbonate to calcite transformation by dissolution-reprecipitation. *Geochimica et Cosmochimica Acta*, *165*, 407–417. https://doi.org/10.1016/j.gca.2015.06.002

Given, R. K., & Wilkinson, B. H. (1985). Kinetic control of morphology, composition, and mineralogy of abiotic sedimentary carbonates. *Journal of Sedimentary Petrology*, *55*(1), 109–119. https://doi.org/10.1306/212f862a-2b24-11d7-8648000102c1865d

Goldstein, J. I., Yakowitz, H., Newbury, D. E., Lifshin, E., Colby, J. W., & Coleman, J. R. (1975). Practical Scanning Electron Microscopy. In *Practical Scanning Electron Microscopy*. https://doi.org/10.1007/978-1-4613-4422-3

Gower, L. B. (2008). Biomimetic model systems for investigating the amorphous precursor pathway and

its role in biomineralization. *Chemical Reviews*, *108*(11), 4551–4627. https://doi.org/10.1021/cr800443h

Günther, C., Becker, A., Wolf, G., & Epple, M. (2005). In vitro Synthesis and Structural Characterization of Amorphous Calcium Carbonate. *Zeitschrift Für Anorganische Und Allgemeine Chemie*, *631*(13–14), 2830–2835. https://doi.org/10.1002/zaac.200500164

Hasse, B., Ehrenberg, H., Marxen, J. C., Becker, W., & Epple, M. (2000). Calcium carbonate modifications in the mineralized shell of the freshwater snail Biomphalaria glabrata. *Chemistry - A European Journal*, *6*(20), 3679–3685. https://doi.org/10.1002/1521-3765(20001016)6:20<3679::AID-CHEM3679>3.0.CO;2-#

Henini, M. (2000). Scanning electron microscopy: An introduction. *III-Vs Review*, *13*(4), 40–44. https://doi.org/10.1016/S0961-1290(00)80006-X

Hillaire-Marcel, C., Kim, S.-T., Landais, A., Ghosh, P., Assonov, S., Lécuyer, C., Blanchard, M., Meijer, H. A. J., & Steen-Larsen, H. C. (2021). A stable isotope toolbox for water and inorganic carbon cycle studies. *Nature Reviews Earth & Environment*, *2*(10), 699–719. https://doi.org/10.1038/s43017-021-00209-0

Hodson, M. E., Benning, L. G., Demarchi, B., Penkman, K. E. H., Rodriguez-Blanco, J. D., Schofield, P. F., & Versteegh, E. A. A. (2015). Biomineralisation by earthworms – an investigation into the stability and distribution of amorphous calcium carbonate. *Geochemical Transactions*, *16*(1), 4. https://doi.org/10.1186/s12932-015-0019-z

Huang, S. C., Naka, K., & Chujo, Y. (2007). A carbonate controlled-addition method for amorphous calcium carbonate spheres stabilized by poly(acrylic acid)s. *Langmuir*, *23*(24), 12086–12095. https://doi.org/10.1021/la701972n

ICDD. PDF-2+. (2002). *ICDD Database Search – ICDD*. International Centre for Diffraction Data, Newtown Square. https://www.icdd.com/pdfsearch/

Ihli, J., Kim, Y. Y., Noel, E. H., & Meldrum, F. C. (2013). The effect of additives on amorphous calcium carbonate (ACC): Janus behavior in solution and the solid state. *Advanced Functional Materials*,

23(12), 1575–1585. https://doi.org/10.1002/adfm.201201805

Ihli, J., Kulak, A. N., & Meldrum, F. C. (2013). Freeze-drying yields stable and pure amorphous calcium carbonate (ACC). *Chemical Communications*, *49*(30), 3134–3136. https://doi.org/10.1039/c3cc40807h

Immenhauser, A., Schöne, B. R., Hoffmann, R., & Niedermayr, A. (2016). Mollusc and brachiopod skeletal hard parts: Intricate archives of their marine environment. *Sedimentology*, *63*(1), 1–59. https://doi.org/10.1111/sed.12231

Jacob, D. E., Soldati, A. L., Wirth, R., Huth, J., Wehrmeister, U., & Hofmeister, W. (2008). Nanostructure, composition and mechanisms of bivalve shell growth. *Geochimica et Cosmochimica Acta*, *72*(22), 5401–5415. https://doi.org/10.1016/j.gca.2008.08.019

Jacob, D. E., Wirth, R., Soldati, A. L., Wehrmeister, U., & Schreiber, A. (2011). Amorphous calcium carbonate in the shells of adult Unionoida. *Journal of Structural Biology*, *173*(2), 241–249. https://doi.org/10.1016/j.jsb.2010.09.011

Jung, G. Y., Shin, E., Park, J. H., Choi, B. Y., Lee, S. W., & Kwak, S. K. (2019). Thermodynamic Control of Amorphous Precursor Phases for Calcium Carbonate via Additive Ions. *Chemistry of Materials*, *31*(18), 7547–7557. https://doi.org/10.1021/acs.chemmater.9b02346

Kellermeier, M., Melero-García, E., Glaab, F., Klein, R., Drechsler, M., Rachel, R., García-Ruiz, J. M., & Kunz, W. (2010). Stabilization of Amorphous Calcium Carbonate in Inorganic Silica-Rich Environments. *Journal of the American Chemical Society*, *132*(50), 17859–17866. https://doi.org/10.1021/ja106959p

Kim, S.-T., Coplen, T. B., & Horita, J. (2015). Normalization of stable isotope data for carbonate minerals: Implementation of IUPAC guidelines. *Geochimica et Cosmochimica Acta*, *158*, 276–289. https://doi.org/10.1016/j.gca.2015.02.011

Kim, S.-T., Hillaire-Marcel, C., & Mucci, A. (2006). Mechanisms of equilibrium and kinetic oxygen isotope effects in synthetic aragonite at 25 °C. *Geochimica et Cosmochimica Acta*, *70*(23 SPEC. ISS.), 5790–5801. https://doi.org/10.1016/j.gca.2006.08.003

Kim, S.-T., & O'Neil, J. R. (1997). Equilibrium and nonequilibrium oxygen isotope effects in synthetic carbonates. *Geochimica et Cosmochimica Acta*, *61*(16), 3461–3475. https://doi.org/10.1016/S0016-7037(97)00169-5

Kim, S. T., O'Neil, J. R., Hillaire-Marcel, C., & Mucci, A. (2007). Oxygen isotope fractionation between synthetic aragonite and water: Influence of temperature and Mg2+ concentration. *Geochimica et Cosmochimica Acta*, *71*(19), 4704–4715. https://doi.org/10.1016/j.gca.2007.04.019

Kimura, T., & Koga, N. (2011). Monohydrocalcite in comparison with hydrated amorphous calcium carbonate: Precipitation condition and thermal behavior. *Crystal Growth and Design*, *11*(9), 3877–3884. https://doi.org/10.1021/cg200412h

Kitano, Y., Okumura, M., & Idogaki, M. (1979). Behavior of dissolved silica in parent solution at the formation of calcium carbonate. *Geochemical Journal*, *13*(6), 253–260. https://doi.org/10.2343/geochemj.13.253

Koga, N., Nakagoe, Y., & Tanaka, H. (1998). Crystallization of amorphous calcium carbonate. *Thermochimica Acta*, *318*(1–2), 239–244. https://doi.org/10.1016/S0040-6031(98)00348-7

Koga, N., & Yamane, Y. (2008). Thermal behaviors of amorphous calcium carbonates prepared in aqueous and ethanol media. *Journal of Thermal Analysis and Calorimetry*, *94*(2), 379–387. https://doi.org/10.1007/s10973-008-9110-3

Köhler-Rink, S., & Kühl, M. (2007). The chemical microenvironment of the symbiotic planktonic foraminifer Orbulina universa. *Http://Dx.Doi.Org/10.1080/17451000510019015*, *1*(1), 68–78. https://doi.org/10.1080/17451000510019015

Kojima, Y., Sakama, K., Toyama, T., Yasue, T., & Arai, Y. (1994). Dehydration of the Water Molecule in Amorphous Calcium Phosphate. *Phosphorus Research Bulletin*, *4*, 47–52. https://doi.org/10.3363/prb1992.4.0_47

Konrad, F., Gallien, F., Gerard, D. E., & Dietzel, M. (2016). Transformation of Amorphous Calcium Carbonate in Air. *Crystal Growth and Design*, *16*(11), 6310–6317. https://doi.org/10.1021/acs.cgd.6b00906

Kontoyannis, C. G., & Vagenas, N. V. (2000). Calcium carbonate phase analysis using XRD and FT-Raman spectroscopy. *The Analyst*, *125*(2), 251–255. https://doi.org/10.1039/a908609i

Labuhn, I., Genty, D., Vonhof, H., Bourdin, C., Blamart, D., Douville, E., Ruan, J., Cheng, H., Edwards, R. L., Pons-Branchu, E., & Pierre, M. (2015). A high-resolution fluid inclusion δ18O record from a stalagmite in SW France: Modern calibration and comparison with multiple proxies. *Quaternary Science Reviews*, *110*, 152–165. https://doi.org/10.1016/j.quascirev.2014.12.021

Lachniet, M. S. (2009). Climatic and environmental controls on speleothem oxygen-isotope values. *Quaternary Science Reviews*, *28*(5–6), 412–432. https://doi.org/10.1016/j.quascirev.2008.10.021

Lam, R. S. K., Charnock, J. M., Lennie, A., & Meldrum, F. C. (2007). Synthesis-dependant structural variations in amorphous calcium carbonate. *CrystEngComm*, *9*(12), 1226–1236. https://doi.org/10.1039/b710895h

Lee, H. S., Ha, T. H., & Kim, K. (2005). Fabrication of unusually stable amorphous calcium carbonate in an ethanol medium. *Materials Chemistry and Physics*, *93*(2–3), 376–382. https://doi.org/10.1016/j.matchemphys.2005.03.037

Lee, M. R., Hodson, M. E., & Langworthy, G. N. (2008). Crystallization of calcite from amorphous calcium carbonate: earthworms show the way. *Mineralogical Magazine*, *72*(1), 257–261. https://doi.org/10.1180/minmag.2008.072.1.257

Levi-Kalisman, Y., Raz, S., Weiner, S., Addadi, L., & Sagi, I. (2002). Structural differences between biogenic amorphous calcium carbonate phases using X-ray absorption spectroscopy. *Advanced Functional Materials*, *12*(1), 43–48. https://doi.org/10.1002/1616-3028(20020101)12:1<43::AID-ADFM43>3.0.CO;2-C

Levi-Kalisman, Yael, Raz, S., Weiner, S., Addadi, L., & Sagi, I. (2000). X-Ray absorption spectroscopy studies on the structure of a biogenic "amorphous" calcium carbonate phase †. *Journal of the Chemical Society, Dalton Transactions*, *21*, 3977–3982. https://doi.org/10.1039/b003242p

Lewis, I. R., & Edwards, H. (2001). Handbook of Raman Spectroscopy. *Handbook of Raman Spectroscopy*. https://doi.org/10.1201/9781420029253

Li, J., Chen, Z., Wang, R. J., & Proserpio, D. M. (1999). Low temperature route towards new materials: solvothermal synthesis of metal chalcogenides in ethylenediamine. *Coordination Chemistry Reviews*, *190–192*, 707–735. https://doi.org/10.1016/S0010-8545(99)00107-1

Lowenstam, H. A, & Epstein, S. (1954). Paleotemperatures of the Post-Aptian Cretaceous as Determined by the Oxygen Isotope Method. *The Journal of Geology*, *62*(3), 207–248. https://doi.org/10.1086/626160

Lowenstam, Heinz A. (1972). Phosphatic hard tissues of marine invertebrates: Their nature and mechanical function, and some fossil implications. *Chemical Geology*, *9*(1–4), 153–166. https://doi.org/10.1016/0009-2541(72)90053-8

Mass, T., Giuffre, A. J., Sun, C. Y., Stifler, C. A., Frazier, M. J., Neder, M., Tamura, N., Stan, C. V., Marcus, M. A., & Gilbert, P. U. P. A. (2017). Amorphous calcium carbonate particles form coral skeletons. *Proceedings of the National Academy of Sciences of the United States of America*, *114*(37), E7670–E7678. https://doi.org/10.1073/pnas.1707890114

Mavromatis, V., Purgstaller, B., Dietzel, M., Buhl, D., Immenhauser, A., & Schott, J. (2017). Impact of amorphous precursor phases on magnesium isotope signatures of Mg-calcite. *Earth and Planetary Science Letters*, *464*, 227–236. https://doi.org/10.1016/j.epsl.2017.01.031

McConnaughey, T. (1989a). 13C and 18O isotopic disequilibrium in biological carbonates: I. Patterns. *Geochimica et Cosmochimica Acta*, *53*(1), 151–162. https://doi.org/10.1016/0016-7037(89)90282-2

McConnaughey, T. (1989b). 13C and 18O isotopic disequilibrium in biological carbonates: II. In vitro simulation of kinetic isotope effects. *Geochimica et Cosmochimica Acta*, *53*(1), 163–171. https://doi.org/10.1016/0016-7037(89)90283-4

McCrea, J. M. (1950). On the Isotopic Chemistry of Carbonates and a Paleotemperature Scale. *The Journal of Chemical Physics*, *18*(6), 849–857. https://doi.org/10.1063/1.1747785

McDermott, F. (2004). Palaeo-climate reconstruction from stable isotope variations in speleothems: A review. *Quaternary Science Reviews*, *23*(7–8), 901–918. https://doi.org/10.1016/j.quascirev.2003.06.021

Meldrum, F. C. (2003). Calcium carbonate in biomineralisation and biomimetic chemistry. In *International Materials Reviews* (Vol. 48, Issue 3, pp. 187–224). https://doi.org/10.1179/095066003225005836

Meldrum, F. C., & O'Shaughnessy, C. (2020). Crystallization in Confinement. In *Advanced Materials* (Vol. 32, Issue 31, p. 2001068). John Wiley & Sons, Ltd. https://doi.org/10.1002/adma.202001068

Michel, F. M., MacDonald, J., Feng, J., Phillips, B. L., Ehm, L., Tarabrella, C., Parise, J. B., & Reeder, R. J. (2008). Structural characteristics of synthetic amorphous calcium carbonate. *Chemistry of Materials*, *20*(14), 4720–4728. https://doi.org/10.1021/cm800324v

Nakashima, Y., Takai, C., Razavi-Khosroshahi, H., Suthabanditpong, W., & Fuji, M. (2018). Synthesis of ultra-small hollow silica nanoparticles using the prepared amorphous calcium carbonate in one-pot process. *Advanced Powder Technology*, *29*(4), 904–908. https://doi.org/10.1016/j.apt.2018.01.006

Navrotsky, A. (2004). Energetic clues to pathways to biomineralization: Precursors, clusters, and nanoparticles. *Proceedings of the National Academy of Sciences of the United States of America*, *101*(33), 12096–12101. https://doi.org/10.1073/pnas.0404778101

Neumann, M., & Epple, M. (2007). Monohydrocalcite and its relationship to hydrated amorphous calcium carbonate in biominerals. *European Journal of Inorganic Chemistry*, *2007*(14), 1953–1957. https://doi.org/10.1002/ejic.200601033

Njegić-Džakula, B., Brečević, L., Falini, G., & Kralj, D. (2011). Kinetic Approach to Biomineralization: Interactions of Synthetic Polypeptides with Calcium Carbonate Polymorphs. *Croatica Chemica Acta*, *84*(2), 301–314. https://doi.org/10.5562/cca1809

Northrop, D. A., & Clayton, R. N. (1966). Oxygen-Isotope Fractionations in Systems Containing Dolomite. *The Journal of Geology*, *74*(2), 174–196. https://doi.org/10.1086/627153

O'Day, P. A., Rehr, J. J., Zabinsky, S. I., & Brown, G. E. (1994). Extended X-ray Absorption Fine Structure (EXAFS) Analysis of Disorder and Multiple-Scattering in Complex Crystalline Solids. *Journal of the American Chemical Society*, *116*(7), 2938–2949. https://doi.org/10.1021/ja00086a026

Ogino, T., Suzuki, T., & Sawada, K. (1987). The formation and transformation mechanism of calcium

carbonate in water. *Geochimica et Cosmochimica Acta*, *51*(10), 2757–2767. https://doi.org/10.1016/0016-7037(87)90155-4

Ostwald, W. (1901). Reviews-On the assumed isomerism between red and yellow mercuric oxide and on the surface-tension of solids. *The Journal of Physical Chemistry*, *5*(1), 75–75. https://doi.org/10.1021/j150028a603

Paquin, F., Rivnay, J., Salleo, A., Stingelin, N., & Silva, C. (2015). Multi-phase semicrystalline microstructures drive exciton dissociation in neat plastic semiconductors. *J. Mater. Chem. C*, *3*, 10715–10722. https://doi.org/10.1039/b000000x

Pérez-Huerta, A., & C. Fred, T. A. (2010). Vital effects in the context of biomineralization. *Seminarios de La Sociedad Española de Mineralogía*, *7*, 35–45.

Ping, H., Xie, H., Wan, Y., Zhang, Z., Zhang, J., Xiang, M., Xie, J., Wang, H., Wang, W., & Fu, Z. (2016). Confinement controlled mineralization of calcium carbonate within collagen fibrils. *Journal of Materials Chemistry B*, *4*(5), 880–886. https://doi.org/10.1039/C5TB01990G

Politi, Y., Batchelor, D. R., Zaslansky, P., Chmelka, B. F., Weaver, J. C., Sagi, I., Weiner, S., & Addadi, L. (2010). Role of Magnesium Ion in the Stabilization of Biogenic Amorphous Calcium Carbonate: A Structure−Function Investigation. *Chemistry of Materials*, *22*(1), 161–166. https://doi.org/10.1021/cm902674h

Politi, Y., Levi-Kalisman, Y., Raz, S., Wilt, F., Addadi, L., Weiner, S., & Sagi, I. (2006). Structural Characterization of the Transient Amorphous Calcium Carbonate Precursor Phase in Sea Urchin Embryos. *Advanced Functional Materials*, *16*(10), 1289–1298. https://doi.org/10.1002/adfm.200600134

Purgstaller, B., Mavromatis, V., Immenhauser, A., & Dietzel, M. (2016). Transformation of Mg-bearing amorphous calcium carbonate to Mg-calcite - In situ monitoring. *Geochimica et Cosmochimica Acta*, *174*, 180–195. https://doi.org/10.1016/j.gca.2015.10.030

Radha, A. V., Forbes, T. Z., Killian, C. E., Gilbert, P. U. P. A., & Navrotsky, A. (2010). Transformation and crystallization energetics of synthetic and biogenic amorphous calcium carbonate. *Proceedings*

of the National Academy of Sciences, *107*(38), 16438–16443. https://doi.org/10.1073/pnas.1009959107

Rao, A., Vásquez-Quitral, P., Fernández, M. S., Berg, J. K., Sánchez, M., Drechsler, M., Neira-Carrillo, A., Arias, J. L., Gebauer, D., & Cölfen, H. (2016). PH-Dependent Schemes of Calcium Carbonate Formation in the Presence of Alginates. *Crystal Growth and Design*, *16*(3), 1349–1359. https://doi.org/10.1021/acs.cgd.5b01488

Raz, S., Hamilton, P. C., Wilt, F. H., Weiner, S., & Addadi, L. (2003). The Transient Phase of Amorphous Calcium Carbonate in Sea Urchin Larval Spicules: The Involvement of Proteins and Magnesium Ions in Its Formation and Stabilization. *Advanced Functional Materials*, *13*(6), 480–486. https://doi.org/10.1002/adfm.200304285

Raz, S., Testeniere, O., Hecker, A., Weiner, S., & Luquet, G. (2002). Stable amorphous calcium carbonate is the main component of the calcium storage structures of the crustacean Orchestia cavimana. *Biological Bulletin*, *203*(3), 269–274. https://doi.org/10.2307/1543569

Rodriguez-Blanco, J. D., Shaw, S., Bots, P., Roncal-Herrero, T., & Benning, L. G. (2012). The role of pH and Mg on the stability and crystallization of amorphous calcium carbonate. *Journal of Alloys and Compounds*, *536*(SUPPL.1), S477–S479. https://doi.org/10.1016/j.jallcom.2011.11.057

Rodriguez-Blanco, Juan Diego, Shaw, S., & Benning, L. G. (2011). The kinetics and mechanisms of amorphous calcium carbonate (ACC) crystallization to calcite, viavaterite. *Nanoscale*, *3*(1), 265–271. https://doi.org/10.1039/C0NR00589D

Rodriguez-Navarro, C., Kudłacz, K., Cizer, Ö., & Ruiz-Agudo, E. (2015). Formation of amorphous calcium carbonate and its transformation into mesostructured calcite. *CrystEngComm*, *17*(1), 58–72. https://doi.org/10.1039/c4ce01562b

Ross, E. E., Mok, S. W., & Bugni, S. R. (2011). Assembly of lipid bilayers on silica and modified silica colloids by reconstitution of dried lipid films. *Langmuir*, *27*(14), 8634–8644. https://doi.org/10.1021/la200952c

Roy, R. N., Roy, L. N., Vogel, K. M., Porter-Moore, C., Pearson, T., Good, C. E., Millero, F. J., &

Campbell, D. M. (1993). The dissociation constants of carbonic acid in seawater at salinities 5 to 45 and temperatures 0 to 45°C. *Marine Chemistry*, *44*(2–4), 249–267. https://doi.org/10.1016/0304-4203(93)90207-5

Saenger, C., & Wang, Z. (2014). Magnesium isotope fractionation in biogenic and abiogenic carbonates: Implications for paleoenvironmental proxies. In *Quaternary Science Reviews* (Vol. 90, pp. 1–21). Elsevier Ltd. https://doi.org/10.1016/j.quascirev.2014.01.014

Savin, S. M. (1977). The History of the Earth's Surface Temperature During the Past 100 Million Years. *Annual Review of Earth and Planetary Sciences*, *5*(1), 319–355. https://doi.org/10.1146/annurev.ea.05.050177.001535

Schmidt, M., Xeflide, S., Botz, R., & Mann, S. (2005). Oxygen isotope fractionation during synthesis of CaMg-carbonate and implications for sedimentary dolomite formation. *Geochimica et Cosmochimica Acta*, *69*(19), 4665–4674. https://doi.org/10.1016/j.gca.2005.06.025

Schwartz, A. M. (2002). Handbook of Industrial Crystallization - Chapter 01 - Solutions and solution properties. *Handbook of Industrial Crystallization*, *7*, 1–31. http://www.sciencedirect.com/science/article/pii/B9780750670128500033

Seo, K. S., Han, C., Wee, J. H., Park, J. K., & Ahn, J. W. (2005). Synthesis of calcium carbonate in a pure ethanol and aqueous ethanol solution as the solvent. *Journal of Crystal Growth*, *276*(3–4), 680–687. https://doi.org/10.1016/j.jcrysgro.2004.11.416

Setoguchi, H. (1989). Origin, Evolution, and Modern Aspects of Biomineralization in Plants and Animals. *Origin, Evolution, and Modern Aspects of Biomineralization in Plants and Animals*, *December*. https://doi.org/10.1007/978-1-4757-6114-6

Simkiss, K. (1991). Amorphous Minerals and Theories of Biomineralization. In *Mechanisms and Phylogeny of Mineralization in Biological Systems* (pp. 375–382). Springer Japan. https://doi.org/10.1007/978-4-431-68132-8_60

Smith, B. C. (2011). Fundamentals of fourier transform infrared spectroscopy, second edition. In *Fundamentals of Fourier Transform Infrared Spectroscopy, Second Edition*.

Stephens, C. J., Ladden, S. F., Meldrum, F. C., & Christenson, H. K. (2010). Amorphous calcium carbonate is stabilized in confinement. *Advanced Functional Materials*, *20*(13), 2108–2115. https://doi.org/10.1002/adfm.201000248

Swart, P. K. (2015). The geochemistry of carbonate diagenesis: The past, present and future. *Sedimentology*, *62*(5), 1233–1304. https://doi.org/10.1111/sed.12205

Taylor, M. G., Simkiss, K., Greaves, G. N., Okazaki, M., & Mann, S. (1993). An X-ray absorption spectroscopy study of the structure and transformation of amorphous calcium carbonate from plant cystoliths. *Proceedings of the Royal Society B: Biological Sciences*, *252*(1333), 75–80. https://doi.org/10.1098/rspb.1993.0048

Tester, C. C., Brock, R. E., Wu, C.-H., Krejci, M. R., Weigand, S., & Joester, D. (2011). In vitro synthesis and stabilization of amorphous calcium carbonate (ACC) nanoparticles within liposomes. *CrystEngComm*, *13*(12), 3975. https://doi.org/10.1039/c1ce05153a

Tester, C. C., Whittaker, M. L., & Joester, D. (2014). Controlling nucleation in giant liposomes. *Chemical Communications*, *50*(42), 5619–5622. https://doi.org/10.1039/c4cc01457j

Tobler, D. J., Rodriguez-Blanco, J. D., Sørensen, H. O., Stipp, S. L. S., & Dideriksen, K. (2016). Effect of pH on Amorphous Calcium Carbonate Structure and Transformation. *Crystal Growth and Design*, *16*(8), 4500–4508. https://doi.org/10.1021/acs.cgd.6b00630

Tompa, A. S., & Watabe, N. (1977). Calcified arteries in a gastropod. *Calcified Tissue Research*, *22*(1), 159–172. https://doi.org/10.1007/BF02010355

Townsend, D., Lahankar, S. A., Lee, S. K., Chambreau, S. D., Suits, A. G., Zhang, X., Rheinecker, J., Harding, L. B., & Bowman, J. M. (2004). The Roaming Atom: Straying from the Reaction Path in Formaldehyde Decomposition. *Science*, *306*(5699), 1158–1161. https://doi.org/10.1126/science.1104386

Travis, D. F. (2006). Structural features of mineralization from tissue to macromolecular levels of organization in the decapod crustacea. *Annals of the New York Academy of Sciences*, *109*(1), 177–245. https://doi.org/10.1111/j.1749-6632.1963.tb13467.x

Venn, A., Tambutté, E., Holcomb, M., Allemand, D., & Tambutté, S. (2011). Live tissue imaging shows reef corals elevate pH under their calcifying tissue relative to seawater. *PLoS ONE*, *6*(5). https://doi.org/10.1371/JOURNAL.PONE.0020013

Versteegh, E. A. A., Black, S., & Hodson, M. E. (2017). Carbon isotope fractionation between amorphous calcium carbonate and calcite in earthworm-produced calcium carbonate. *Applied Geochemistry*, *78*, 351–356. https://doi.org/10.1016/j.apgeochem.2017.01.017

Vinogradov, A. P. (1953). *The elementary chemical composition of marine organisms / A.P. Vinogradov.* https://discovery.mcmaster.ca/iii/encore/record/C__Rb2252090__SVinogradov, A. P. The Elementary Chemical Composition of Marine Organisms__Orightresult__U__X2?lang=eng&suite=def

Voorhees, P. W. (1985). The theory of Ostwald ripening. *Journal of Statistical Physics*, *38*(1–2), 231–252. https://doi.org/10.1007/BF01017860

Wang, S. S., & Xu, A. W. (2013). Amorphous calcium carbonate stabilized by a flexible biomimetic polymer inspired by marine mussels. *Crystal Growth and Design*, *13*(5), 1937–1942. https://doi.org/10.1021/cg301759t

Wang, Y., Zeng, M., Meldrum, F. C., & Christenson, H. K. (2017). Using confinement to study the crystallization pathway of calcium carbonate. *Crystal Growth and Design*, *17*(12), 6787–6792. https://doi.org/10.1021/acs.cgd.7b01359

Wang, Z. L., & Lee, J. L. (2008). Electron Microscopy Techniques for Imaging and Analysis of Nanoparticles. In *Developments in Surface Contamination and Cleaning: Second Edition* (Vol. 1, pp. 395–443). William Andrew Publishing. https://doi.org/10.1016/B978-0-323-29960-2.00009-5

Weiner, S. (2003). An Overview of Biomineralization Processes and the Problem of the Vital Effect. *Reviews in Mineralogy and Geochemistry*, *54*(1), 1–29. https://doi.org/10.2113/0540001

Weiner, S., Levi-Kalisman, Y., Raz, S., & Addadi, L. (2003). Biologically Formed Amorphous Calcium Carbonate. *Connective Tissue Research*, *44*(1), 214–218. https://doi.org/10.1080/03008200390181681

Weiss, I. M., Tuross, N., Addadi, L., & Weiner, S. (2002). Mollusc larval shell formation: amorphous calcium carbonate is a precursor phase for aragonite. *Journal of Experimental Zoology*, *293*(5), 478–491. https://doi.org/10.1002/jez.90004

Whittaker, M. L., Dove, P. M., & Joester, D. (2016). Nucleation on surfaces and in confinement. *MRS Bulletin*, *41*(5), 388–392. https://doi.org/10.1557/mrs.2016.90

Wombacher, F., Eisenhauer, A., Böhm, F., Gussone, N., Regenberg, M., Dullo, W. C., & Rüggeberg, A. (2011). Magnesium stable isotope fractionation in marine biogenic calcite and aragonite. *Geochimica et Cosmochimica Acta*, *75*(19), 5797–5818. https://doi.org/10.1016/j.gca.2011.07.017

Xto, J. M., Borca, C. N., van Bokhoven, J. A., & Huthwelker, T. (2019). Aerosol-based synthesis of pure and stable amorphous calcium carbonate. *Chemical Communications*, *55*(72), 10725–10728. https://doi.org/10.1039/c9cc03749g

Xu, N., Li, Y., Zheng, L., Gao, Y., Yin, H., Zhao, J., Chen, Z., Chen, J., & Chen, M. (2014). Synthesis and application of magnesium amorphous calcium carbonate for removal of high concentration of phosphate. *Chemical Engineering Journal*, *251*, 102–110. https://doi.org/10.1016/j.cej.2014.04.037

Xu, X. R., Cai, A. H., Liu, R., Pan, H. H., Tang, R. K., & Cho, K. (2008). The roles of water and polyelectrolytes in the phase transformation of amorphous calcium carbonate. *Journal of Crystal Growth*, *310*(16), 3779–3787. https://doi.org/10.1016/j.jcrysgro.2008.05.034

Zeebe, R. E. (1999). An explanation of the effect of seawater carbonate concentration on foraminiferal oxygen isotopes. *Geochimica et Cosmochimica Acta*, *63*(13–14), 2001–2007. https://doi.org/10.1016/S0016-7037(99)00091-5

Zeebe, R. E., & Wolf-Gladrow, D. A. (2001). CO2 in Seawater: Equilibrium, Kinetics, Isotopes. In *Elsevier*. https://linkinghub.elsevier.com/retrieve/pii/S0924796302001793

Zeebe, R. E., Wolf-Gladrow, D. A., & Jansen, H. (1999). On the time required to establish chemical and isotopic equilibrium in the carbon dioxide system in seawater. *Marine Chemistry*, *65*, 135–153.

Zhang, H., Cai, Y., Tan, L., Qin, S., & An, Z. (2014). Stable isotope composition alteration produced by the aragonite-to-calcite transformation in speleothems and implications for paleoclimate

reconstructions. *Sedimentary Geology*, *309*, 1–14. https://doi.org/10.1016/j.sedgeo.2014.05.007

Zhang, M., Li, J., Zhao, J., Cui, Y., & Luo, X. (2020). Comparison of CH4and CO2Adsorptions onto Calcite(10.4), Aragonite(011)Ca, and Vaterite(010)CO3Surfaces: An MD and DFT Investigation. *ACS Omega*, *5*(20), 11369–11377. https://doi.org/10.1021/acsomega.0c00345

Ziveri, P., Stoll, H., Probert, I., Klaas, C., Geisen, M., Ganssen, G., & Young, J. (2003). Stable isotope "vital effects" in coccolith calcite. *Earth and Planetary Science Letters*, *210*(1–2), 137–149. https://doi.org/10.1016/S0012-821X(03)00101-8

Zou, Z., Bertinetti, L., Politi, Y., Jensen, A. C. S., Weiner, S., Addadi, L., Fratzl, P., & Habraken, W. J. E. M. (2015). Supplementary - Opposite Particle Size Effect on Amorphous Calcium Carbonate Crystallization in Water and during Heating in Air. *Chemistry of Materials*, *27*(12), 4237–4246. https://doi.org/10.1021/acs.chemmater.5b00145

CHAPTER 3

Stable Isotope Effects in Amorphous Calcium Carbonate (ACC) during its Crystallization

Katherine Allan[a]

allank2@mcmcaster.ca

&

Sang-Tae Kim[a]

sangtae@mcmaster.ca

School of Earth, Environment & Society, McMaster University, 1280 Main Street West, Hamilton, ON, L8S 4K1, Canada

To be submitted to *Geochimica et Cosmochimica Acta*

Abstract

The role of Amorphous Calcium Carbonate (ACC) as a precursor to calcite, and other crystalline $CaCO_3$ polymorphs has been recognized for several decades and has important implications for the proper understanding of the classic oxygen isotope carbonate-water paleothermometry as it relies on the formation calcium carbonate minerals. In this study, ACC was precipitated using two different precipitation methods – the alkaline method (AM) which stabilizes ACC through high pH solution, and the silica method (SM), which surrounds and isolates ACC in silica envelopes to prevent its crystallization. This ACC was then subjected to a variety of experiments, including aging parent solution for periods of 1 to 5, and aging in an ^{18}O-enriched re-equilibration solution for a period of 1 to 2 weeks. Both of these aging experiments were performed in conjunction with immediately filtered ACC precipitates by both methods, for the purpose of establishing a baseline.

Our results indicated that the oxygen isotope composition and its subsequent evolution during ACC crystallization is dependent upon the used precipitation method. The AM produced ACC precipitates with lower $\delta^{18}O$ values relative to that of corresponding SM produced ACC precipitates, equilibrium CO_3^{2-} and equilibrium calcite, and these values did not vary with ACC crystallization. These low $\delta^{18}O$ values for ACC were confirmed to be a result of ACC precipitation from CO_3^2 dominant parent solutions that had not yet reached DIC-water oxygen isotope equilibrium. Notably, the $\delta^{18}O$ values for ACC precipitated using the SM, while much more variable following ACC crystallization, started with the expected equilibrium $\delta^{18}O$ value for calcite. The ACC precipitates prepared using SM were also able to exchange readily with the ^{18}O-enriched solution.

This study shed light on the role of ACC stabilization and the associated oxygen isotope effects in ACC and during its transformation to polymorphs of crystalline $CaCO_3$. The question then shifts from – is ACC responsible for the vital effect – to – under what stabilizing scenarios is ACC responsible for the vital effect.

CHAPTER 3: STABLE ISOTOPE EFFECTS IN AMORPHOUS CALCIUM CARBONATE (ACC) DURING ITS CRYSTALLIZATION

3.1 Introduction

Amorphous calcium carbonate (ACC) has been found in many biomineralizing organisms in nature, including molluscs (Hasse et al., 2000; Jacob et al., 2008; Raz et al., 2002; Tompa & Watabe, 1977), sea urchins (Beniash et al., 1997, 1999; Radha et al., 2010; Raz et al., 2003; Townsend et al., 2004), certain plants (Gal et al., 2010; Taylor et al., 1993), and a number of crustaceans (Raz et al., 2002; Travis, 2006; Vinogradov, 1953). In particular, the importance of ACC as a precursor phase in the biomineralization process of these organisms has been acknowledged numerous times in the literature (Addadi et al., 2003; De Yoreo et al., 2015; Politi et al., 2006; Weiner et al., 2003). However, a proper understanding of the stable isotope properties of ACC has been impeded by the difficulties of ACC synthesis under laboratory conditions because ACC, a poly*a*morph of calcium carbonate ($CaCO_3$), spontaneously transforms to crystalline $CaCO_3$ polymorphs due to its high solubility and tendency to spontaneously crystallize. This physicochemical property of ACC could inhibit isotopic equilibrium between ACC and its parent (or surrounding) solution, and thus may cause a problem in determining an accurate oxygen isotope fractionation between ACC and water, as well as any isotope effects during ACC transformation to a crystalline $CaCO_3$ polymorph. Nevertheless, this information is important to our complete understanding of the classic oxygen isotope carbonate-water paleothermometry (Samuel Epstein et al., 1951; Kim & O'Neil, 1997; McCrea, 1950), which has been extensively used as a tool for reconstructing Earth's climate history since the middle of the last century (e.g., Coplen & Schlanger, 1973; Douglas & Savin, 1975; Emiliani, 1966; Lowenstam & Epstein, 1954; Savin, 1977).

Theoretically, the classic paleothermometry relies mostly on the temperature-dependent oxygen isotope fractionation between a carbonate mineral and parent water; however, this ideal situation can be complicated by several other factors, such as parent water chemistry and the nature of carbonate formation. Most notably, many biogenic carbonates are known to be associated with kinetic isotope effects when they form (e.g., Coronado et al., 2019; Devriendt et al., 2017; Lécuyer & O'Neil, 1994; Ziveri et al., 2003). These nonequilibrium isotope effects of biological origin have been referred to the "vital effect," (Pérez-Huerta & Fred, 2010) and an understanding of this overriding of the environmental signal in biogenic carbonates is vital to the proper use of the oxygen isotope carbonate-water palaeothermometry, especially for biogenic carbonates (Coronado et al., 2019; McConnaughey, 1989b, 1989a; Weiner, 2003). There are a number of possible culprits that have been proposed as the source for the vital effect, such as organism-specific metabolism or physiology during $CaCO_3$ biomineralization (Coronado et al., 2019; Pérez-Huerta & Fred, 2010; Ziveri et al., 2003). One mechanism that has been repeatedly proposed to account for the vital effect is the formation of biogenic $CaCO_3$ mineral parts via an ACC precursor phase (Addadi et al., 2003; Weiner, 2003). In some biomineralizing organisms, ACC is produced and stored in specialized vesicles or organs as a readily available reservoir of Ca^{2+} ions. It is later transformed to a polymorph of $CaCO_3$, most frequently calcite, whenever needed, allowing both poly*a*morphs (ACC) and polymorphs of $CaCO_3$ (calcite, aragonite, vaterite) to co-exist within one organism – henceforth, poly(a)morphs. This could mean that ACC is precipitated and stabilized for days or weeks prior to its transformation into a final $CaCO_3$ mineral form (Coronado et al., 2019; Raz et al., 2002). Furthermore, ACC is thought to be transformed into a crystalline $CaCO_3$ via a dissolution-reprecipitation pathway, rather than a solid-state transformation (Addadi et al., 2003; Giuffre et al., 2015; Versteegh et al., 2017).

Researchers have investigated the precipitation of stable ACC both in organisms, such as bivalves and foraminifera (Jacob et al., 2011; Weiss et al., 2002) and in the laboratory using various additives and experimental conditions that suppress its transformation to more stable crystalline polymorphs of $CaCO_3$ (e.g., Blue et al., 2013; Kellermeier et al., 2010; Koga et al., 1998; Ross et al., 2011; Tobler et al., 2016). However, very little is understood about the stable isotope properties of ACC. Currently, the oxygen isotope fractionation between ACC and water has not been characterized, and it is unclear whether ACC can establish an isotopic equilibrium with its parent water. Schmidt et al. (2005), for the first time, investigated the effect of a magnesium-rich amorphous calcium carbonate (Mg-ACC) precursor on the oxygen isotope composition of the resultant carbonate. They found that precipitated Mg-ACC is isotopically light initially but becomes more ^{18}O enriched as it transforms into dolomite. Subsequently, Giuffre et al. (2015) synthesized Mg-ACC where the Mg^{2+} ions act as a stabilizer; however, they aimed to elucidate the ACC to calcite transformation pathway (i.e., solid-state transformation vs. dissolution reprecipitation) using solutions spiked with ^{43}C and ^{25}Mg, rather than to investigate the isotopic fractionation itself. Versteegh et al. (2017) examined the carbon isotope composition of $CaCO_3$ that was precipitated via an ACC precursor in vivo by earthworms and observed a ^{13}C depletion in the primary precipitate (either milky ACC-fluid, ACC-calcite granules, or calcite granules). They determined a carbon isotope fractionation of -1.20 ± 0.52 ‰ between initial ACC-milky fluid and internally deposited calcite-ACC granules and a secondary carbon isotope fractionation of -0.46 ± 0.45 ‰ when the internal granules are fully transformed into calcite and deposited in the wake of the moving worm, implying that this biogenic ACC was transforming to calcite via a dissolution-reprecipitation pathway. Mavromatis et al. (2017) examined the magnesium isotope fractionation between parent solutions and magnesium-rich calcites (Mg-

calcites) that were either transformed from Mg-ACC or directly precipitated (without an Mg-ACC precursor). The authors found that the initial magnesium isotope composition of the Mg-ACC is not maintained during its transformation to Mg-calcite because the associated dissolution-reprecipitation reaction involves a magnesium isotope re-equilibration, which does not occur with direct Mg-calcite precipitation. Recently, Dietzel et al. (2020) studied oxygen ($\delta^{18}O$) and clumped (Δ_{47}) isotope fractionations when Mg-calcite forms via an Mg-ACC precursor. They noted a rapid oxygen isotope exchange upon Mg-ACC precipitation, and a subsequent expeditious re-equilibration between Mg-ACC and the parent solution during its transformation to Mg-calcite, providing yet another confirmation of crystallization via a dissolution-reprecipitation pathway. Furthermore, it was found that the use of an Mg-ACC precursor had no effect on the clumped isotope composition of the final Mg-calcite.

Although Schmidt et al. (2005) and Dietzel et al. (2020) examined the oxygen isotope systematics of Mg-ACC, there has yet to be any study that investigate the oxygen isotope systematics of non-Mg-ACC, including ACC. This study aims to examine the oxygen isotope evolution during ACC transformation into crystalline $CaCO_3$ polymorphs (or ACC crystallization) via an ACC precursor phase in the $CaCO_3$-H_2O system by using two ACC precipitation methods (the Alkaline Method vs the Silica Method) and two post ACC treatments (Aging vs Re-equilibration). This study is unique, compared to the previous studies, in three distinct ways: (1) We investigated the transformation of ACC into crystalline $CaCO_3$ polymorphs, which has direct implication to the classic oxygen isotope carbonate-water paleothermometry, as opposed to the Mg-ACC transformation to Mg-rich calcite or dolomite. (2) We utilized available information regarding the correlation between pH and isotope exchange to try and ensure that oxygen isotope equilibrium between DIC (Dissolved Inorganic Carbon) and

all the ACC-forming parent solutions was established prior to any precipitations to identify the initial oxygen isotope composition of DIC species in the parent solutions. (3) We monitored the oxygen isotope evolution during ACC to $CaCO_3$ transformation to examine whether ACC can reach oxygen isotope equilibrium with its parent water and the geochemical significance of an ACC-precursor to the classic oxygen isotope carbonate-water paleothermometry. An over-arching view of the experimental goals of this study can be viewed in Figure 3.1.

3.2 Experimental & Analytical Methods

3.2.1: Preparation of Parent Solutions

Several sets of constituent ion-donating parent solutions were prepared to facilitate the precipitation of ACC that was stabilized in two different ways. The Alkaline Method (or the AM) utilizes a highly alkaline solution of pH (>12) to discourage crystallization of the precipitated ACC, and it employed Koga (1988)'s method except that anhydrous ethanol was used instead of acetone during filtration (see 3.2.2. for details). In contrast, the Silica Method (or the SM) mitigates or entirely prevents ACC crystallization by enveloping the precipitating ACC in a sort of silica envelope with a high silica concentration (31 mmolal).

All parent solutions for ACC precipitation were prepared and kept in Pyrex® media bottles at 25 ± 0.1 °C. The media bottles were cleaned in an acid bath containing ~5% hydrochloric acid (HCl) for a minimum of 2 days, and up to a week. They were then removed, rinsed thrice with tap water, twice with reverse osmosis water, and once with de-ionized 18 MΩ water before being placed in a drying oven for a minimum of 24 hours. All solid chemicals were ACS grade and weighed out using a Sartorious® scale, and their chemical identities and lot numbers were also carefully recorded. Deionized (DI) water (κ = ~ 0.6 μS cm-1 or ~18 MΩ) was

used for all the parent solution preparations and vacuum filtrations, and it was kept in a high density polyethylene (HDPE) carboy, which was labelled using the following convention: KW-(Day, Month, Year made). The oxygen isotope composition of the DI water in the carboy was regularly checked, especially when the carboy was refilled with new DI water. These isotopic compositions were used to determine the oxygen isotope fractionation ($1000\ln\alpha_{CaCO3\text{-}H2O}$) between the precipitated ACC or $CaCO_3$ and can be viewed in Tables 3.2 and 3.3.

For both the AM and SM, 20 mmolal $CaCl_2$ solutions were prepared by dissolving $CaCl_2$ into 1L KW-15Mar21 water and they are referred to as 'Ca^{2+}-donor parent solutions' hereafter. For the AM, a solution of 20 mmolal Na_2CO_3 and 200 mmolal NaOH was prepared by dissolving anhydrous Na_2CO_3 powder and NaOH pellets into 1L KW-15Mar21 water. For the SM, a solution of 20 mmolal Na_2CO_3 and 31 mmolal SiO_2 was prepared by first dissolving anhydrous Na_2CO_3 into 1L KW-15Mar21 water, to which several millilitres of reagent grade sodium metasilicate solution with 26.8 wt % as SiO_2 was later added. These two Na_2CO_3-containing parent solutions are henceforth referred to as 'AM- or SM-CO_3^{2-}-donor parent solution'. All the parent solutions were then stored in tightly capped media bottles, wrapped with Parafilm® to avoid evaporation, and placed in a 25 ± 0.1°C water bath. It must be noted that two Na_2CO_3 chemicals of a distinct isotopic composition were used for the CO_3^{2-}-donor parent solutions, due to the exhaustion of the firstly used Na_2CO_3 chemical. More specifically, Na_2CO_3-A ($\delta^{13}C$ = –2.34 ‰, $\delta^{18}O$ = 14.15 ‰) was used for one of the two post ACC treatments (Aging) and Na_2CO_3-B ($\delta^{13}C$ = –21.52 ‰, $\delta^{18}O$ = 8.18 ‰) was used for the other post ACC treatment (Re-equilibration) (see Table 3.1)

A minimum of 44 days was estimated by extrapolating available data from Beck et al. (2005) and was allowed in this study to establish the oxygen isotope equilibrium between DIC and the parent solutions at 25 °C based on their pH values.

3.2.2. Precipitation of Amorphous Calcium Carbonate (via AM vs SM)

The AM and the SM took advantage of the scientific observation that ACC is stabilized either in high pH environments (Koga & Yamane, 2008; Koga et al., 1998) or spatially confined precipitation environments (Kellermeier et al., 2010; Stephens et al., 2010; Tester et al., 2011, 2014), respectively. Therefore, the two ACC precipitation methods utilized in this study allowed us to examine the effect of different ACC stabilization mechanisms on the oxygen isotope composition of ACC and its resultant crystalline $CaCO_3$ polymorphs. In addition, various alcohols were used in previous ACC synthesis studies to stabilize ACC during filtration (e.g., Ihli et al., 2013; Paquin et al., 2015; Wombacher et al., 2011) and tests were hence performed in this study to gauge the efficacy of several alcohols (methanol, 95% ethanol, anhydrous ethanol, acetone) as a stabilizing washing solution during vacuum filtration. Our XRD analysis indicated that anhydrous ethanol is the most effective in maintaining ACC as the primary phase in the $CaCO_3$ precipitate and anhydrous ethanol was therefore used in both the AM and SM. Lastly, a rapid mixing of the Ca^{2+}-donor and AM/SM-CO_3^{2-}-donor parent solutions was also employed in both the AM and SM methods to promote the precipitation of stable ACC, as a slow mixing is associated with larger precipitating particle sizes and increased likelihood of nucleation (Simkiss, 1991).

For the AM, a volumetric flask and a pipette were used to measure 50 mL of Ca^{2+}-donor or AM-CO_3^{2-}-donor parent solution, and each donor parent solution was then decanted into a

glass beaker. Subsequently, the Ca^{2+}-donor parent solution was rapidly dumped into the AM-CO_3^{2-}-donor parent solution (Figure 3.2). This rapidly mixed parent solution was found to yield ACC based on our X-Ray Diffraction (XRD) analysis and was referred to as the AM-ACC solution hereafter. It was then vigorously shaken, and its pH was monitored with an Oakton® pH electrode. The pH electrode was calibrated prior to each use, using a set of three pH standard solutions (pH = 4, 7, and 10). The vacuum-filtered precipitates from the AM-ACC solution (or AM-ACC precipitates, hereafter) were subsequently treated in two different ways: either by aging in the same solution in which they initially precipitated, called the parent solution (PS) ($\delta^{18}O_{PS}$ = –6.45 ‰) or aging in a ^{18}O-enriched solution, also called re-equilibration solution (RS) ($\delta^{18}O_{RS}$ = 9.67 ‰). Several precipitates, alongside these post-ACC-treatments, were filtered immediately, without any aging in either a parent or ^{18}O-enriched solution, to provide baseline values for the post-ACC-treatment experiments. See Figure 3.1 as well as Sections 3.2.3 and 3.2.4 for more details. For the SM, a rapid mixing of the two donor parent solutions and subsequent vacuum filtration with anhydrous ethanol were performed in an identical manner to those of the AM, to produce SM-ACC precipitates from SM-ACC solution, with the same naming convention used in the SM. Figure 3.3 shows a more detailed summary of our naming conventions & definitions.

3.2.3 Post-ACC-treatments

3.2.3.1 Aging in parent solution

A series of aging experiments were performed to probe the isotopic evolution of transforming ACC and resultant crystalline $CaCO_3$ polymorphs in the PS. Following initial ACC precipitation after rapidly mixing Ca^{2+}- and AM/SM-CO_3^{2-}-donor parent solutions in PS by

either the AM or the SM, the resultant ACC-solution was decanted into a sealed 100 mL Pyrex media bottle, wrapped in Parafilm®, and then stored at 25 ± 0.1 °C water bath by increments of 1 week for 5 weeks (1W-5W) (Figure 3.2). These 100 mL media bottles were either left undisturbed (NS: Non-Shaking) or shaken vigorously (SH: Shaking) for at least 1 minute once per week, and each of these two experimental groups was prepared in triplicate (1-3). Upon aging, there was evidence of ACC crystallization in the mixed PS within 24 hours in some cases, as confirmed by XRD (see 3.3), and these precipitates were referred to as 'AM-$CaCO_3$ precipitates' or 'SM-$CaCO_3$ precipitates' because they were one or a mixture of ACC, calcite, aragonite, vaterite, and monohydrocalcite. This mixed PS were also called either 'AM-$CaCO_3$-solutions' or 'SM-$CaCO_3$-solutions' because of the variable poly(a)morphic nature of the precipitates it contains. The exact experimental treatments each of the AM-/SM-$CaCO_3$-solutions underwent are enumerated in Table 3.2.

At the appropriate time, either 1, 2, 3, 4 or 5 weeks, the AM-/SM-$CaCO_3$-solution of interest was taken from the water bath at 25 ± 0.1 °C and measured for its pH using an Oakton® pH electrode. Subsequently, this solution was shaken, and vacuum filtered through a 0.47 µm polyvinylidene difluoride (PVDF) membrane disk filter, and the solid $CaCO_3$ precipitate was subsequently washed with at least 50 mL of anhydrous ethanol. The emptied media bottle was also washed several times with anhydrous ethanol and was then again added to the vacuum filtration apparatus to ensure maximum sample retrieval. Small amounts of the resultant precipitates were immediately taken to the McMaster Analytical X-Ray Diffraction facility, and they were tested for XRD using a Bruker D8 DISCOVER diffractometer equipped with a Bruker Vantex600 area detector, and a CuKα sealed tube source. The remainder of the AM/SM-$CaCO_3$ precipitates not reserved for XRD analysis were dried at 70 ± 0.3 °C for at least 24 hours,

weighed and ground before being transferred in glass carbonate storage vial and stored in a desiccator until isotopic analysis was performed.

3.2.3.2 Aging in ^{18}O-enriched solution or Re-Equilibration

A series of aging experiments were also performed using an ^{18}O enriched water ($\delta^{18}O_{RS}$ = 9.67 ‰) as the RS for two types of precipitates (AM- and SM-ACC precipitates vs AM- and SM-$CaCO_3$ precipitates) so that ACC or $CaCO_3$ transformation into more stable crystalline $CaCO_3$ polymorphs occurs in an isotopically distinct solution with respect to the PS. This re-equilibration experiment was to mimic a natural system in which ACC is precipitated and stored in one environment, transforms to a crystalline polymorph of $CaCO_3$ in another (e.g., Darkins et al., 2013; Politi et al., 2006; Wang & Xu, 2013). For instance, some organisms store ACC in an isolated area of their body for long periods of time before releasing it to crystallize, in a controlled manner, to a $CaCO_3$ mineral shell part (Becker et al., 2005; Beniash et al., 1999; Travis, 2006).

For the first type of precipitates, where ACC is the starting material, freshly precipitated AM- or SM-ACC precipitates were immediately added to 50 mL RS within a sealed 100 mL Pyrex media bottle and then aged at 25 ± 0.1 °C for 1 week (RE-AM•1W•RS•1-3/RE-SM•1W•RS•1-3) or 2 weeks (RE-AM•2W•RS•1-3/RE-SM•2W•RS•1-3) to investigate the isotopic evolution while the freshly prepared ACC transformed to crystalline polymorphs of $CaCO_3$. Small fractions of these re-equilibrated AM- and SM-ACC precipitates were tested by XRD, and they were found to have transformed to AM- and SM-$CaCO_3$ precipitates, respectively, meaning they were no longer fully amorphous. The remaining re-equilibrated AM- and SM-$CaCO_3$ precipitates, initially AM- and SM-ACC precipitates, were dried in a 70 ± 0.3 °C

oven for ≥ 24 hours, ground, and stored in glass carbonate storage vials for stable isotopic analysis.

For the second precipitate type, where $CaCO_3$ that had crystallized from ACC was used as the starting material, AM- and SM-$CaCO_3$ precipitates were used from the beginning for the re-equilibration experiment. They had been initially precipitated as ACC, but since were transformed to either a complete crystalline polymorph of $CaCO_3$ in PS, in the case of AM-$CaCO_3$ precipitates (see Figure 3.4-(d)), or almost complete crystalline $CaCO_3$ polymorph in PS for SM-$CaCO_3$ precipitates (see Figure 3.5-(c)). These precipitates were referred to as 'post-ACC-carbonates' (or P-ACC-C, hereafter) and included AM•4W•NS•2, AM•4W•NS•3, SM•4W•NS•2, and SM•4W•NS•3. They had previously been ground, weighed, isotopically characterized, and stored within glass vials in a desiccator for ~2 months. Upon re-equilibration, they were partially renamed to reflect their new experimental conditions by keeping their original ID within square brackets such that AM•4W•NS•2 becomes RE-[AM•4W•NS•2]•RS•2W•1. About 60 or 120 mg of P-ACC-C, which was a typical weight of ACC precipitated from a 50 mL parent solution by the AM or SM, was added to 50 mL RS within a sealed 100 mL media bottle and then aged for 2 weeks at 25 ± 0.1 °C. After 1 or 2 weeks of re-equilibration, AM- or SM-$CaCO_3$ precipitates were collected as usual and small fractions of each type of precipitate were isolated in glass vials for XRD analysis. The remaining precipitates were dried for 24 hours in a 70 ± 0.3 °C drying oven, ground, weighed, and stored in glass carbonate storage vials for isotopic analysis. See Table 3.3 and Figure 3.6 for detailed information.

3.2.3.3 Immediate Filtration for Baseline Condition

Several AM- and SM-ACC precipitates were subjected to immediate filtration, without aging in either PS or RS in order to quantify a baseline condition. For each aging or re-equilibration post ACC treatment, immediate filtration samples were prepared in triplicate from both AM and SM. The precipitates AM•0W•1-3 and SM•0W•1-3 were the immediate (i.e., 0W) filtration samples for the aging experiment (Table 3.2) while RE•AM•0W•1-3 and RE•SM•0W•1-3 were the equivalent samples for the re-equilibration experiment (Table 3.3). Following immediate filtration, the corresponding AM-/SM-ACC-solutions were measured for pH and small amounts of each AM-/SM-ACC precipitate was taken for XRD analysis. The remaining ACC was dried for 24 hours at 70 ± 0.3 °C prior to grinding and weighing, and then stored in a glass carbonate storage vial. Additionally, AM•0W•86dEQT•1, AM•0W•144dEQT•1, and AM•0W•144dEQT•2 were prepared by using the same Ca^{2+}- and AM-CO_3^{2-}-donor parent solutions as the other re-equilibrated precipitate samples, but with increased DIC-H_2O equilibration time (86 or 144 days) to check the isotopic compositions of the AM-ACC-precipitates with different DIC-H_2O equilibration time.

3.2.4: Isotopic ($\delta^{18}O$ & $\delta^{13}C$) analysis of precipitates

All $\delta^{18}O_{carb}$ and $\delta^{13}C_{carb}$ values of AM-/SM-ACC/$CaCO_3$ precipitates as well as Na_2CO_3 chemicals were measured using a Thermo Finnigan Delta plus XP Continuous-Flow Isotope Ratio Mass Spectrometer (CF-IRMS) equipped with a Gas Bench II headspace autosampler. Firstly, small amounts of each dried and ground precipitate (~ 150 µg) were weighed out using a Mettler Toledo analytical balance and transferred to 12 mL septum-capped Labco Exetainer® glass vials (Labco Ltd, Lampeter, UK), along with a suite of 50 µg to 250 µg reference materials, including NBS 18 ($\delta^{18}O$ = 7.20 ‰ and $\delta^{13}C$ = –5.01 ‰), NBS 19 ($\delta^{18}O$ = 28.65 ‰ and $\delta^{13}C$ =

1.95 ‰), and IAEA-603 ($\delta^{18}O$ = 28.47 ‰ and $\delta^{13}C$ = 2.46 ‰). Secondly, the sample- or reference material-containing Labco vials were loaded into the Gas Bench II sample block at 25 ± 0.1 °C and each vial was flushed and filled using 99.999% helium gas to remove any ambient air. Thirdly, 6-7 drops of 105 % phosphoric acid (H_3PO_4) were injected into each Labco vial. About 24 hours was allowed at 25 ± 0.1 °C for the reaction between each carbonate sample/reference material and the phosphoric acid to liberated carbon dioxide (CO_2) before the acid-liberated CO_2 gas samples were measured for their stable isotope compositions.

An acid fractionation factor of calcite at 25 °C (or $\alpha_{CO2(ACID)\text{-}calcite}$ = 1.01025) was used in this study for all the ACC and $CaCO_3$ precipitates, regardless of their mineralogy (Kim et al., 2015). Note that the acid fractionation factor for ACC was assumed to be identical to that of calcite because there is no reported acid fractionation factor for ACC. In addition, our XRD analyses (i.e., ~ 30 % of total samples) indicated that $CaCO_3$ precipitates were mostly crystallized to calcite by the time the stable isotope analysis was performed. The raw $\delta^{18}O_{Carb}$ and $\delta^{13}C_{Carb}$ values were normalized using NBS 18 and NBS 19 based on the recommendations by Kim et al. (2015) and reported on the VSMOW and VPDB-LSVEC scale, respectively. Results of $\delta^{18}O$ and $\delta^{13}C$ measurements were determined to have an analytical precision of < 0.1 ‰. The permil fractionation ($1000\ln\alpha_{ACC/CaCO3\text{-}water}$) is used to show the degree of oxygen isotope equilibrium between ACC or $CaCO_3$ precipitates and their parent solutions, with respect to that of calcite/CO_3^{2-}/HCO_3^-.

3.2.5: Isotopic ($\delta^{18}O$) analysis of solutions

Samples of both DI carboy water, used for PS preparation and precipitate washing, and RS, were all stored in triplicate for stable isotope analysis. Using the classic CO_2-H_2O

equilibration method (Cohn & Urey, 1938), oxygen isotope compositions of these waters were measured using a Thermo Finnigan Delta plus XP isotope ratio mass spectrometer with a Gas Bench II headspace autosampler.

Empty, septum-capped 12 mL Labco Exetainer® glass vials were placed in the Gas Bench II sample block at 25 ± 0.1 °C and were initially flushed and filled with a 0.3 % CO_2 and 99.8 % He mixture with a double needle and a flow of 100 mL/min. A 1 mL syringe was used to inject 0.2 mL of the desired water sample thereafter. After a CO_2-H_2O equilibration time of at least 24 hours at 25 ± 0.1 °C, the headspace CO_2 gas, which had isotopically equilibrated with each water sample within the Labco vial, was analyzed for its $\delta^{18}O$ value (Figure 3.7). Two inter-laboratory water standards called MRSI-STD-W1 and MRSI-STD-W2 were analyzed along with water samples. These standards had been previously calibrated against both VSMOW and VSLAP and have the $\delta^{18}O$ values of –0.58 ‰ and –28.08 ‰ respectively. An overall analytical precision of $\delta^{18}O_{H2O}$ measurement was determined to be < 0.1 ‰ and $\delta^{18}O_{H2O}$ values were reported on the VSMOW scale in this study.

The $\delta^{13}C$ values of DIC in AM/SM-CO_3^{2-}-donor parent solutions, and AM or SM-ACC/$CaCO_3$-solutions were not directly measured, but they were instead estimated by using the $\delta^{13}C$ values of the carbon source, namely, the Na_2CO_3 chemicals used for the preparation of the solutions. This was because the highly alkaline pH of the AM/SM-CO_3^{2-}-donor parent solutions and the resultant AM- or SM-ACC/$CaCO_3$-solutions caused the adsorption of all acid-liberated CO_2 gas, resulting in negligible or complete lack of sample peaks for isotopic measurements. $\Delta^{13}C_{DIC}$ values of the Na_2CO_3 chemicals used are reported in Table 3.1.

3.3 Results

3.3.1: Aging in parent solution

3.3.1.1: Alkaline Method (AM)

Table 3.2 shows the pH, sample weight (mg), mineralogy as well as the isotopic composition (‰) of AM-$CaCO_3$ precipitates. The pH values of PSs for AM-$CaCO_3$ precipitates ranged from 12.70 to 13.36 and remained consistently very alkaline with an average value of 12.93 ± 0.21, regardless of aging time in PS (Table 3.2a: "Time in Soln' (weeks)"). The AM-$CaCO_3$ precipitates ranged from 54.80 to 106.44 mg and ~ 30% of them were reserved for XRD analysis to identify their mineralogy. All the XRD-tested unaged (i.e., immediate filtration after precipitation) AM-$CaCO_3$ precipitates (i.e., AM•0W•1, AM•0W•2, AM•0W•3) were identified to be completely amorphous based on XRD analysis (Figure 3.4a). Of the AM-$CaCO_3$ precipitates that had aged 1 week in PS, the majority of those taken for XRD analysis were found to have crystallized to calcite (i.e., AM•1W•NS•1, AM•1W•SH•1/2, see Figure 3.4b) with one exception of AM•1W•NS•2, which was found to be a mix of calcite with a small amount of vaterite (~ 1%) (see Figure 3.4-(c)). Our XRD data also showed that AM-$CaCO_3$ precipitates that had spent two or 4 weeks in PS were entirely calcite (i.e., AM•2W•NS•1, AM•4W•NS•1, see Figure 3.4-(d)). It is assumed that all the AM-$CaCO_3$ precipitates, not characterized with XRD, shared this mineralogical nature.

The oxygen isotope fractionation between AM-$CaCO_3$ and PS, or $1000\ln\alpha_{CaCO3\text{-}water}$, ranged from 21.66 ‰ to 22.91 ‰ and averaged 21.91 ± 0.15 ‰ for all 34 AM-$CaCO_3$ precipitates at 25 ± 0.1 °C, showing little change with weeks of aging time in PS (see Figure 3.8. In the case of the AM-$CaCO_3$ precipitates, no correlation was also observed between their $1000\ln\alpha_{CaCO3\text{-}water}$ values and pH, or sample weight (mg) (Figures 3.9. 3.10).

3.3.1.2: Silica Method (SM)

Table 3.2 shows the pH, sample weight (mg), mineralogy as well as the $\delta^{13}C$ and $\delta^{18}O$ values (‰) of all SM-$CaCO_3$ precipitates. Solution pH, measured prior to filtration, ranged from 10.37 to 10.76 with an average of 10.50 ± 0.11, and did not appear to be correlated with aging time. The sample weights of all the SM-$CaCO_3$ precipitates ranged from 107.22 to 194.24 mg, while the corresponding weights for the AM-$CaCO_3$ precipitates were only between 55 and 100 mg. This discrepancy was due to the presence of silica in the SM-$CaCO_3$ precipitates. In this study, about 30 % of the total number of SM-$CaCO_3$ precipitates were analyzed for XRD at each stage of the aging experiments. All the unaged SM-$CaCO_3$ precipitates (i.e., SM•0W•1, SM•0W•2, SM•0W•3) were found to be fully amorphous (see Figure 3.5-(a)). After 1 week of aging in PS, SM-$CaCO_3$ precipitates featured more mixed poly(a)morphic character. For example, most precipitates (i.e., SM•1W•SH•1, SM•1W•SH•2, SM•2W•NS•1) showed evidence of a mixture of calcite and monohydrocalcite with some ACC (see Figure 3.5-(b), 3.5-(d)) while SM•1W•NS•2 showed a mix of calcite, ACC, and traces (~ 6.4 %) of aragonite (see Figure 3.5-(c)) and SM•1W•NS•1 showed evidence of ACC and calcite (Figure 3.5-(d)).

The $1000\ln\alpha_{CaCO3\text{-}water}$ values of the SM-$CaCO_3$ precipitates were highly variable both within the same and different experimental condition groups. For example, SM•1W•NS•2, which had a $1000\ln\alpha_{CaCO3\text{-}water}$ value of 28.95 ‰, and SM•1W•NS•3, which yielded a $1000\ln\alpha_{CaCO3\text{-}water}$ value of 27.08 ‰, were precipitated under the exact same conditions, but their $1000\ln\alpha_{CaCO3\text{-}water}$ values were different from each other by 1.87 ‰. Regarding the different experimental condition groups, for example, SM•1W•NS•2, the non-shaking precipitate that had aged 1 week in PS, showed a $1000\ln\alpha_{CaCO3\text{-}water}$ value of 28.95 ‰, while SM•4W•SH•1, the shaken precipitate that had aged 4 weeks in PS, had a $1000\ln\alpha_{CaCO3\text{-}water}$ value of 26.5 ‰, corresponding with a

difference of 2.3 ‰. In contrast, SM•0W•1, SM•0W•2, and SM•0W•3, the unaged SM-$CaCO_3$ precipitates, showed similar $1000\ln\alpha_{CaCO3\text{-}water}$ values, ranging from 27.52 ‰ to 27.90 ‰. The oxygen isotope fractionation between all SM-$CaCO_3$ precipitates for the aging experiments and PS (or $1000\ln\alpha_{CaCO3\text{-}water}$) varied from 25.81 ‰ to 28.95 ‰ with an average of 27.22 ± 0.79 ‰ (Figure 3.8, Table 3.2).

3.3.2: Re-Equilibration

3.3.2.1: Alkaline Method (AM)

Detailed information regarding time in solution (days), experimental conditions, pH, sample weight (mg), mineralogy and isotopic composition (‰) of re-equilibration AM-$CaCO_3$ precipitates is listed in Table 3.3. When AM-ACC precipitate was filtered immediately following precipitation (i.e., the first precipitation type), AM-ACC-solution pH ranged from 12.70 to 13.20 and these AM-ACC precipitates (i.e., RE-AM•0W•1, RE-AM•0W•2, RE-AM•0W•3), weigh from 62.45 to 64.41 mg, had $1000\ln\alpha_{CaCO3\text{-}water}$ values from 18.36 ‰ to 18.64 ‰ with an average value of 18.50 ± 0.14 ‰. Based on XRD analysis, they were found to be amorphous (Figure 3.11a). Upon re-equilibration of AM-ACC precipitates for 1 or 2 weeks, there was a consistent drop in AM-$CaCO_3$ (initially AM-ACC)-solution pH from an average of 12.96 ± 0.13 to 11.35 ± 0.08. These re-equilibrated AM-$CaCO_3$ precipitates (initially AM-ACC precipitates) weighed from 36.76 to 55.25 mg and were believed to be calcite based on the XRD analysis of RE-AM•1W•RS•3, RE-AM•2W•RS•3, and RE-[AM•4W•NS•2]•RS•2W•1 (Figure 3.11-(b), 3.11-(c)). They yielded relatively consistent $1000\ln\alpha_{CaCO3\text{-}water}$ values (17.97 ‰ - 18.26 ‰) with an average of 18.14 ± 0.1 ‰. In addition, two previously prepared AM-$CaCO_3$ precipitates (AM•4W•NS•2 and AM•4W•NS•3) were used for the re-equilibration experiment as a second

precipitate type referred to as P-ACC-C. AM•4W•NS•2 was initially found to have a pH of 13.36, a weight of 91.26 mg, and a $1000\ln\alpha_{CaCO3\text{-}water}$ value of 21.73 ‰ whileAM•4W•NS•3 had a pH of 13.30, a weight of 88.47 mg, and a $1000\ln\alpha_{CaCO3\text{-}water}$ value of 21.89 ‰. Following a 2-week re-equilibration (now renamed as RE-[AM•4W•NS•2]•RS•2W•1 and RE-[AM•4W•NS•3]•RS•2W•2), their $1000\ln\alpha_{CaCO3\text{-}water}$ values became 21.86 ‰ and 22.16 ‰, representing small increases of 0.13 ‰ and 0.27 ‰ respectively.

One sample was left in PS for 2 weeks (RE-AM•2W•1) as a control to test the consistency between aged and re-equilibrated AM-$CaCO_3$ precipitates. This sample had a pH of 17.95, a weight of 54.03 mg and was confirmed to be calcite.

3.3.2.2: Silica Method (SM)

In general, re-equilibrated SM-$CaCO_3$ precipitates were treated identically to the corresponding AM-$CaCO_3$ precipitates. When immediately filtered SM-ACC precipitates (the first precipitation type) and SM-P-ACC-C precipitates (the second precipitation type) were transferred to 50 mL of RS ($\delta^{18}O$ = 9.67 ‰), there was a small pH drop of –0.21 ± 0.14 in newly mixed SM- P-ACC-C solutions as well as SM-P-ACC-C solutions. Re-equilibrated SM-ACC precipitates also yielded smaller weights on average, ranging from 74.97 - 94.17 mg after 1 or 2-week re-equilibration, as compared to their initial weights of 103.47 - 130.93 mg. This decrease in sample weight can be attributed to silica loss due to dissolution in water, as well as sample loss due to double filtration. Immediately filtered baseline SM-ACC precipitates for the first precipitate type, RE-SM•0W•1, RE-SM•0W•2, and RE-SM•0W•3, were confirmed to be fully amorphous upon XRD analysis (Figure 3.12-(a)). After 1 week in RS, RE-SM•1W•RS•3 was found to be a mix of ACC, calcite and monohydrocalcite (Figure 3.12-(b)). At 2 weeks in either

PS (applicable only to one precipitate used as a baseline, i.e., RE-SM•2W•1), or RS (i.e., RE-SM•2W•RS•1-3), SM-$CaCO_3$ precipitates were all found to be a mix of calcite and monohydrocalcite (Figure 3.12-(b)). The initial $1000\ln\alpha_{CaCO3\text{-}water}$ values of the SM-ACC precipitates ranged from 27.15 ‰ to 27.27 ‰ with an average value of 27.29 ± 0.15 ‰. However, they (now mostly crystalline SM-$CaCO_3$ precipitates; Figure 3.12-(b)) ranged from 28.93 ‰ to 29.15 ‰ with an average of 29.06 ± 0.12 ‰ or from 29.92 ‰ to 32.43 ‰ with an average of 30.91 ± 1.34 ‰ after 1- or 2-week re-equilibration, respectively (see Figure 3.13).

Concurrently, SM•4W•NS•2 and SM•4W•NS•3 were examined as the second precipitation type (P-ACC-C precipitates) and were found to be calcite with some amorphous character by XRD analysis both before and after re-equilibration (Figure 3.12-(c)). They initially had pH values of 10.68 and 10.69, sample weights of 150.44 mg and 142.80 mg, and $1000\ln\alpha_{CaCO3\text{-}water}$ values of 26.70 ‰ and 27.14 ‰. After 2 weeks of re-equilibration, they, renamed RE-[SM•4W•NS•2]•RS•2W•1 and RE-[SM•4W•NS•3]•RS•2W•2, showed $1000\ln\alpha_{CaCO3\text{-}water}$ values of 28.30 ‰ and 27.95 ‰ respectively (Table 3.3). Comparatively, the one precipitate left in PS for a period of 2 weeks for the purpose of comparison, (RE-SM•2W•1) had a $1000\ln\alpha_{CaCO3\text{-}water}$ value of 27.04 ‰.

3.4 Discussion

3.4.1: Effect of Precipitation Method on $1000\ln\alpha_{CaCO_3-H_2O}$

The AM and the SM yield stable ACC precipitates (i.e., AM- or SM-ACC precipitates) with a distinct $\delta^{18}O$ range (Figure 3.8). When the aging time is zero, AM-ACC precipitates (circle symbols) show a clear oxygen isotope disequilibrium with respect to calcite (a long-dotted line) from Kim & O'Neil, (1997), but are rather isotopically closer, although not

particularly so, to the equilibrium CO_3^2 (a dashed-dotted line) determined by Kim et al. (2006). Indeed, their $\delta^{18}O$ values are about 1.52 ‰ to 2.05 ‰ lower than the equilibrium $\delta^{18}O$ value of CO_3^2 (or $1000\ln\alpha_{CO_3^{2-}-water} = 23.71$ ‰; Kim et. Al, 2006). This suggests that the AM-CO_3^{2-}-donor parent solution had yet to achieve oxygen isotope equilibrium between DIC and water upon AM-ACC precipitation, as well as possible kinetic isotope effects resulting from rapid AM-ACC precipitation.

On the contrary, the $\delta^{18}O$ values of the SM-ACC precipitates are similar to the equilibrium $\delta^{18}O$ value for calcite ($1000\ln\alpha_{CaCO3\text{-}water} = 28.05$ ‰; Hillaire-Marcel et al., 2021; Kim & O'Neil, 1997), but they are much different from the equilibrium $\delta^{18}O$ value for CO_3^{2-} ($1000\ln\alpha_{CO_3^{2-}-water} = 23.71$ ‰; Kim et. Al, 2006). This is interesting because one would expect the isotopic signature of CO_3^{2-} from the immediately filtered SM-ACC, as well as AM-ACC, precipitates because CO_3^{2-} is the most dominant DIC species in the CO_3^{2-}-donor PS (e.g., 99.77 % CO_3^{2-} when pH = 11.75 at 25 °C) (Roy et al., 1993; Zeebe & Wolf-Gladrow, 2001). Note that the term "immediately filtered" in this study refers to three processes, including mixing of Ca^{2+}- and CO_3^{2-}-donor PS (~ 0.5 minutes), pH monitoring (~5 minutes), and vacuum filtration (~ 40 minutes for the SM and ~20 minutes for the AM). Therefore, our isotopic data from the SM-ACC precipitates hints a rapid oxygen isotope exchange between SM-ACC precipitates and the mixed PS during this ~45.5-minute period until SM-ACC precipitates are separated from the mixed PS. First, the slightly lower parent solution pH of the SM (11.75 ± 0.12 and 10.50 ±0.11 before and after mixing) than the AM (13.97 ± 0.03 and 12.93 ± 0.21 before and after mixing, respectively) would support a faster oxygen isotope exchange for the SM-ACC precipitates, as the SM-ACC precipitates would be more soluble and reactive. Second, growing ACC particles are volumetrically constrained by silica envelopes in the SM and this isolation is known to both

reduce the growth rate and particle size of precipitating ACC. As a result, this would result in an increase in the surface area of ACC particles exposed to solution and would expedite the oxygen isotope exchange between precipitating ACC and PS. Therefore, these physicochemical conditions that are specific to each ACC precipitation method are important to dictate $\delta^{18}O$ value of AM-/SM-ACC precipitates. Dietzel et al. (2020) also reported that Mg-ACC underwent quick oxygen isotope exchange with its parent solution and began to approach the expected oxygen isotope equilibrium within 100 minutes in solution. However, they studied Mg-ACC, instead of ACC, and used solutions of pH = 8.30 ± 0.03.

3.4.2: Effect of Aging Time in Parent Solution on $1000ln\,\alpha_{CaCO_3-H_2O}$

AM-/SM-ACC precipitates were aged for 1 to 5 weeks in PS while they transformed to AM-/SM-$CaCO_3$ precipitates (Figure 3.8). For AM-ACC/$CaCO_3$ precipitates, this aging time in PS had no effect on the oxygen isotope fractionation between AM-$CaCO_3$ precipitates and PS, or the $1000ln\alpha_{CaCO3\text{-}water}$ value. In other words, $\delta^{18}O$ values of the AM-$CaCO_3$ precipitates, inherited from the AM-ACC precipitates, did not change much for the 5 weeks. They were consistently lower than the equilibrium $\delta^{18}O$ value for CO_3^{2-} as well as that for calcite. In general, ACC crystallization and the associated isotopic re-equilibration in the DIC-$CaCO_3$-H_2O system could shift the isotopic composition of the resultant AM-$CaCO_3$ precipitates. Several studies (e.g., Giuffre et al., 2015; Schmidt et al., 2005; Versteegh et al., 2017; Zhang et al., 2014) have demonstrated that ACC transforms to calcite (or ACC crystallization) via a dissolution-reprecipitation reaction (Figure 3.15). This reaction differs from a solid-state transformation pathway such that ACC dissolves completely to constituent ions and then re-precipitates as calcite, promoting more drastic isotopic shift in the resultant $CaCO_3$ precipitates via isotopic

exchanges between ACC/$CaCO_3$ precipitates and PS. If, instead of dissolution-reprecipitation, the ACC was transforming by solid-state transformation, in which each ACC particle individually transforms to crystalline $CaCO_3$, this drastic isotopic shift would not be seen (Giuffre et al., 2015; Rodriguez-Navarro et al., 2015). Therefore, considering the lack of change in $\delta^{18}O$ values of the AM-ACC/$CaCO_3$ precipitates during ACC crystallization, it could be posited that the AM-ACC is crystallizing via solid-state transformation rather dissolution-reprecipitation. As increased pH is inversely correlated with solubility, it could be that neither AM-ACC nor AM-$CaCO_3$ are dissolving in PS, and hence, ACC transforms via a solid-state transformation. This would explain the lack of isotopic change despite time in PS and crystallization. Alternatively, the dissolution-reprecipitation reaction could indeed be occurring; however, the high pH of the AM-ACC/$CaCO_3$ solutions (pH = 12.93 ± 0.21 on average) might have not allowed detectable oxygen isotope exchange among DIC species and PS because of the short 5 weeks of aging time for this pH (Beck et al., 2005; Devriendt et al., 2017). There is a large body of research that indicates that ACC transforms via dissolution-reprecipitation (Mavromatis et al., 2017; Rodriguez-Blanco et al., 2012; Schmidt et al., 2005; Versteegh et al., 2017) however, these results indicate that above a given pH threshold the energy barrier to dissolution may be too high, and the ACC transforms via solid-state transformation instead.

Conversely, SM-ACC/$CaCO_3$ precipitates did not follow the same isotopic evolution. They vary from 25.81 ‰ to 28.95 ‰ in $1000\ln\alpha_{CaCO3\text{-}water}$ during the 5-week aging time. The SM-ACC precipitates (i.e., SM•0W•1, SM•0W•2 & SM•0W•3) are more or less consistent in their $\delta^{18}O$ values ($1000\ln\alpha_{CaCO3\text{-}water}$ = 27.67 ± 0.20 ‰) whereas the SM-$CaCO_3$ precipitates, even produced by the identical method, are not as isotopically homogeneous ($1000\ln\alpha_{CaCO3\text{-}water}$ = 27.22 ± 0.79 ‰). Most interestingly, SM-ACC/$CaCO_3$ precipitates hover around the expected

equilibrium oxygen isotope composition for calcite (Kim & O'Neil, 1997), but slowly decrease with aging time, though not in a significant manner. Despite this lack of consistency, SM-ACC/$CaCO_3$ precipitates do appear to group together depending on time in PS as illustrated in Figure 3.8. It is unclear why these groupings occur, possibly these variations are associated with another process, such as the level of crystallization each SM-$CaCO_3$ precipitate has achieved, their mineralogy, see section 3.4.5 for further explanation. It is also possible that these groupings are a product of precipitation methodology, however, as all SM-$CaCO_3$ solutions were made at the same time, and in the same manner, this is unlikely.

3.4.3.: Effect of DIC-H_2O equilibration time on 1000ln $\alpha_{CaCO_3-H_2O}$

Upon comparison of the 1000ln$\alpha_{CaCO3\text{-}water}$ values of aged AM-ACC/$CaCO_3$ precipitates (Figure 3.8) with re-equilibrated AM-ACC/$CaCO_3$ precipitates (Figure 3.14), there was an obvious difference in 1000ln$\alpha_{CaCO3\text{-}water}$ values, with aged AM-ACC/$CaCO_3$ precipitates yielding average 1000ln$\alpha_{CaCO3\text{-}water}$ values of 21.91 ± 0.15 ‰, as compared to the average of 18.14 ± 0.1 ‰ for re-equilibration AM-ACC/$CaCO_3$ precipitates (excluding AM-P-ACC-C precipitates).

To examine the observed difference, a test was performed to check the validity of the estimated DIC-H_2O equilibration time of 44 days (Section 3.2.1). Three new AM-ACC precipitates were prepared using the same AM-CO_3^{2-}-donor parent solution as the one for the earlier re-equilibrated AM-ACC/$CaCO_3$ precipitates except that the AM-CO_3^{2-}-donor parent solution was equilibrated for 86 days (AM•0W•86dEQT•1) or 144 days (AM•0W•144dEQT•1, AM•0W•144dEQT•1), as opposed to 75 days for earlier samples. Experimental data and results for these precipitates are denoted by the triangle symbol in Table 3.3. Figure 3.14 shows that the 1000ln$\alpha_{CaCO3\text{-}water}$ values of AM-ACC precipitates increases with the DIC-H_2O equilibration

times, but it is unclear with the current data whether this increasing trend in $1000\ln\alpha_{CaCO3\text{-}water}$ towards the equilibrium CO_3^2 value represents disequilibrium in the DIC-H_2O system possibly in combination with the kinetic isotope effect of rapid and/or non-quantitative precipitation of AM-ACC precipitates. In addition, it should be also considered that a Na_2CO_3 chemical with a distinct oxygen isotope composition was used to prepare an AM-CO_3^{2-}-donor parent solution for each aging or re-equilibration experiments. Though the mole fraction of oxygen contributed by the Na_2CO_3 chemical should have been negligible as compared to the water, the slow rate of DIC-water oxygen isotope exchange meant that a significant portion of oxygen in the CO_3^{2-} still bore the oxygen isotope signature of the original Na_2CO_3 chemical upon ACC precipitation in the AM.

3.4.4: Effect of pH & precipitate weight on $1000\ln\alpha_{CaCO_3-H_2O}$

The $1000\ln\alpha_{CaCO3\text{-}water}$ values of AM-ACC/$CaCO_3$ precipitates were unaffected by variation in the pH of their antecedent AM-ACC/$CaCO_3$-solutions (Figure 3.9). The variation in the $1000\ln\alpha_{CaCO3\text{-}water}$ values of SM-ACC/$CaCO_3$ precipitates did not seem to correspond in a significant manner with SM-ACC/$CaCO_3$-solution pH. There is slight evidence, contributed by approximately 6 samples, that higher pH of SM-ACC/$CaCO_3$-solutions could cause lower $1000\ln\alpha_{CaCO3\text{-}water}$ values of SM-ACC/$CaCO_3$ precipitates as compared to ones precipitated from lower pH SM-ACC/$CaCO_3$ solutions. However, similar $1000\ln\alpha_{CaCO3\text{-}water}$ values are yielded by SM-ACC/$CaCO_3$ precipitates filtered from lower pH SM-ACC/$CaCO_3$-solutions. Therefore, more data is required to confirm this correlation. However, this would fit well with the data from corresponding AM-ACC/$CaCO_3$ precipitates (see section 3.4.3) whereby the high pH of the AM solutions prevented isotope exchange.

Furthermore, the $1000\ln\alpha_{CaCO3\text{-}water}$ values of AM-ACC/$CaCO_3$ precipitates were not apparently correlated with the precipitate weight yielded following drying and grinding (Figure 3.10). The $1000\ln\alpha_{CaCO3\text{-}water}$ values of SM-ACC/$CaCO_3$ precipitates were also not obviously correlated with their respective precipitate weights (mg), as shown in Figure 3.10. The reported range of precipitate weights of both AM- and SM-ACC/$CaCO_3$ precipitates is most likely due to sample loss during grinding and weighing owing to the lightweight and fluffy nature of the precipitates, meaning they were easily disturbed. In the case of SM-ACC/$CaCO_3$ precipitates, which were heavier than corresponding AM-ACC/$CaCO_3$ precipitates because of the presence of silica, the larger range of precipitate weights was also resulted from partial silica dissolution and loss during filtration, as crystallization of SM-ACC to SM-$CaCO_3$ would disrupt the interactions between silica and ACC, leading to their dissolution in surrounding solution.

3.4.5: Effect of mineralogy on $1000\ln\alpha_{CaCO_3-H_2O}$

Both the AM- and SM-$CaCO_3$ precipitates started to crystallize from preceding AM- and SM-ACC within 1 week of aging in PS (Figures 3.4 & 3.5). Transformation to crystalline $CaCO_3$ polymorphs had no apparent effect on the isotopic composition of AM-$CaCO_3$ precipitates, and this is thought to be a result of rapid transformation to a single mineral, calcite, as well as the effect of high pH AM-ACC/$CaCO_3$ solutions that significantly slow down the exchange of oxygen isotopes between AM precipitates and solutions. See Sections 3.4.2 and 3.4.3 for clarification and details. Conversely, SM-$CaCO_3$ precipitates, which transformed from SM-ACC in PS or RS, did vary in their $\delta^{18}O$ value or $1000\ln\alpha_{CaCO3\text{-}water}$, a variance that may be linked to the mixed mineralogical character (either calcite and ACC; calcite, aragonite and ACC; or calcite, monohydrocalcite and ACC; see Figure 3.5 and Figure 3.12) of the SM-$CaCO_3$

precipitates upon crystallization from SM-ACC. Following 2 weeks in PS or RS, SM-$CaCO_3$ precipitates were mostly calcite with evidence of ACC (Figure 3.5, Figure 3.12). Therefore, it is possible that the differences in $1000\ln\alpha_{CaCO3\text{-}water}$ of SM-$CaCO_3$ precipitates are correlated to the degree to which these precipitates have crystallized and their respective mineralogy. Notably, when SM-ACC precipitates are freshly precipitated, and immediately vacuum filtered, they possess the most consistent $1000\ln\alpha_{CaCO3\text{-}water}$ values (27.67 ± 0.20 ‰ for aging SM-ACC, 27.29 ± 0.15 ‰ for re-equilibration SM-ACC) and this may be linked to the fact that these SM-ACC precipitates are entirely ACC, as opposed to a mix of $CaCO_3$ poly(a)morphs. Furthermore, the SM stabilizes ACC via isolation of ACC particles in silica envelopes upon precipitation. With time in PS or RS, and subsequent filtration, the SM-ACC precipitates within these envelopes will be released and crystallize to differing extents. This may also account for the larger degree of mineral variability in SM-$CaCO_3$ precipitates.

XRD characterization further illustrated the difference in crystallization speed between SM-ACC and AM-ACC precipitates. Specifically, SM precipitates took much longer to crystallize in solution (either PS or RS). This comparatively slow crystallization to SM-$CaCO_3$ precipitates via SM-ACC precipitates– exemplified by the lower intensity of crystalline peaks at earlier stages of aging in PS or RS on the XRD patterns, as well as the lower solution pH in the SM - would have allowed longer oxygen isotope exchange reaction between SM-ACC/SM-$CaCO_3$ precipitates and PS during crystallization. This is further indicated by the results of the re-equilibration experiments (3.3.2). On the contrary, the rapidity with which AM-ACC precipitates transformed to AM-$CaCO_3$ precipitates in solution, paired with high solution pH, could account for the lack of isotopic variation with time in PS, by disfavouring the isotopic exchange (Figure 3.8).

Furthermore, SM-$CaCO_3$ precipitates displayed a positive correlation ($p < 0.5$) between $\delta^{13}C$ and their $1000\ln\alpha_{CaCO3\text{-}water}$ values (Figure 3.16), a correlation that was not shared by corresponding AM-$CaCO_3$ precipitates which did not vary in their $\delta^{18}O$ values. This correlation may correspond to the extent to which the individual SM-$CaCO_3$ precipitates had crystallized to that point, and the time since which they had been released from isolating silica vesicles.

3.4.6: Effect of crystallizing environment on $1000\ln \alpha_{CaCO_3-H_2O}$

The design of the re-equilibration experiments was meant to mimic conditions in which ACC is precipitated in one isotopic environment (i.e., $\delta^{18}O_{PS} = -6.45$ ‰) but crystallized in another (i.e., $\delta^{18}O_{RS} = 9.67$ ‰). This could have possible parallels to biological systems in which ACC is used as a readily accessible reservoir of constituent CO_3^{2-} and Ca^{2+} ions to be released at a time and in an environment that differs from its original precipitation site. ACC is, therefore, precipitated in PS but transferred to the ^{18}O-enriched RS where transformation to crystalline $CaCO_3$ occurs. As with earlier experiments, AM-$CaCO_3$ precipitates (Figure 3.13 - dotted circle symbols), which transformed from AM-ACC precipitates in RS, and AM-P-ACC-C precipitates (Figure 3.13 - upward-pointed dotted triangles) remained virtually unaffected by this new isotopic environment, when compared to the original isotopic composition of the AM-ACC precipitates (Figure 3.13 - open circle symbols; $1000\ln a = 18.50 \pm 0.14$‰) and AM-$CaCO_3$ precipitates used as P-ACC-C ($1000\ln\alpha_{CaCO3\text{-}water}$ AM•4W•NS•2 = 21.73 ‰, RE•[AM•4W•NS•2]•RS•2W = 21.86 ‰, AM•4W•NS•3 = 21.89 ‰, RE•[AM•4W•NS•3]•RS•2W = 22.16 ‰) (Figure 3.13). These results bolster earlier suppositions about AM-ACC/$CaCO_3$ precipitates' inability to re-equilibrate (see section 3.3.4 and 3.3.5). SM-$CaCO_3$ precipitates (dotted square symbols), which had crystallized from SM-ACC precipitates

in RS, however, showed a steady increase in $1000\ln\alpha_{CaCO3\text{-}water}$ values with time in RS (Figure 3.13), suggesting that the precipitates are undergoing oxygen isotope exchange with RS to achieve newer isotopic equilibrium with the ^{18}O-enriched RS solution. Although a longer experimental period would be required to confirm the establishment of new isotopic equilibrium, this indicates both the dynamic oxygen isotope exchange environment of the SM-ACC/$CaCO_3$-solution, as well as adding to the current body of research that indicates ACC crystallization occurs via a dissolution-reprecipitation pathway. If solid-state transformation, instead, was the crystallization pathway at play, one would expect to see no discernable change in the isotopic composition of the precipitates with time in RS. Furthermore, a slight increase in the $1000\ln\alpha_{CaCO3\text{-}water}$ values of SM-P-ACC-C (down-pointing dotted triangles) after 2 weeks in RS was also observed, though to a lesser extent (Figure 3.13). This smaller change was likely due to the almost complete crystallization of these P-ACC-C precipitates upon their addition to the RS, meaning significant isotopic re-equilibration was unlikely to occur.

3.5 Conclusions

This study represents the first investigation of oxygen isotope composition of ACC, upon initial precipitation by two separate precipitation methods, and as it transforms to crystalline forms of $CaCO_3$ in a number of different experimental conditions. Specifically, with time in parent solution (PS), and with time in ^{18}O-enriched re-equilibration solution (RS), both of which are compared to baseline, immediately filtered ACC. These two post-ACC-treatments were purposefully chosen to probe whether ACC can reach oxygen isotope equilibrium with parent water, as well as whether the final crystalline $CaCO_3$ precipitates from ACC will carry the isotopic signature of its precursor phase, or if the signature will be overwritten during

crystallization. Overall, the results of our experiments hint at answers to several of these questions and may be valuable in designing future research into the ACC- crystalline $CaCO_3$-H2O system.

When the AM was used, the precipitated and immediately filtered AM-ACC bore anomalously low $1000\ln\alpha_{CaCO3\text{-}water}$ values, lower even than the equilibrium oxygen isotope composition of CO_3^2 (or $1000\ln\alpha_{CO_3^{2-}-water} = 23.71$ ‰ from Kim et. al, 2006) This suggests an incomplete oxygen isotope equilibration between the primary DIC species in solution (i.e., CO_3^{2-}) and water prior to precipitation, in conjunction with possible kinetic effects due to non-quantitative precipitation of AM-ACC/$CaCO_3$. Furthermore, these values remained the same despite aging in PS or RS and concurrent transformation to resultant AM-$CaCO_3$. This could imply that this AM-ACC transformed via solid state transformation due to high solution pH.

Conversely, when the SM was used, the precipitated and immediately filtered SM-ACC were found to have much higher $1000\ln\alpha_{CaCO3\text{-}water}$ values that were much closer to that of equilibrium calcite. This is especially interesting because this can be considered evidence of rapid isotopic exchange between SM-ACC and parent solution during, as well as immediately following, precipitation. Typically, upon mixing and immediate filtration from the high pH (CO_3^{2-} dominant) solution, one would expect an SM-ACC precipitate to bear a $1000\ln\alpha_{CaCO3\text{-}water}$ value closer to that of equilibrium CO_3^{2-} as there has been so little time for the freshly precipitated mineral to interact with surrounding solution. This implies that achievement of oxygen isotope equilibrium between SM-ACC and PS is not only possible, but very rapid. Moreover, with aging in PS SM-$CaCO_3$ precipitates, which had transformed from SM-ACC precipitates, hovered around the expected equilibrium calcite value. This rapid isotopic exchange is thought to be some combination of the slower crystallization speed of the SM-ACC, the effect

of small SM-ACC particle size due to the isolating effect of the silica envelopes, and the lower pH relative to the AM, although these suppositions would require further study. Significantly, SM-ACC precipitates that were added to the ^{18}O-enriched RS underwent isotopic re-equilibration with aging time in RS and transformation to SM-$CaCO_3$, seemingly approaching oxygen isotope equilibrium with the new solution. This same re-equilibration was seen to a much lesser extent when SM-$CaCO_3$ precipitates that had already crystallized (SM-P-ACC-C) were added to the RS, indicating that the dynamic isotopic exchange the SM-ACC is capable of is lost upon crystallization.

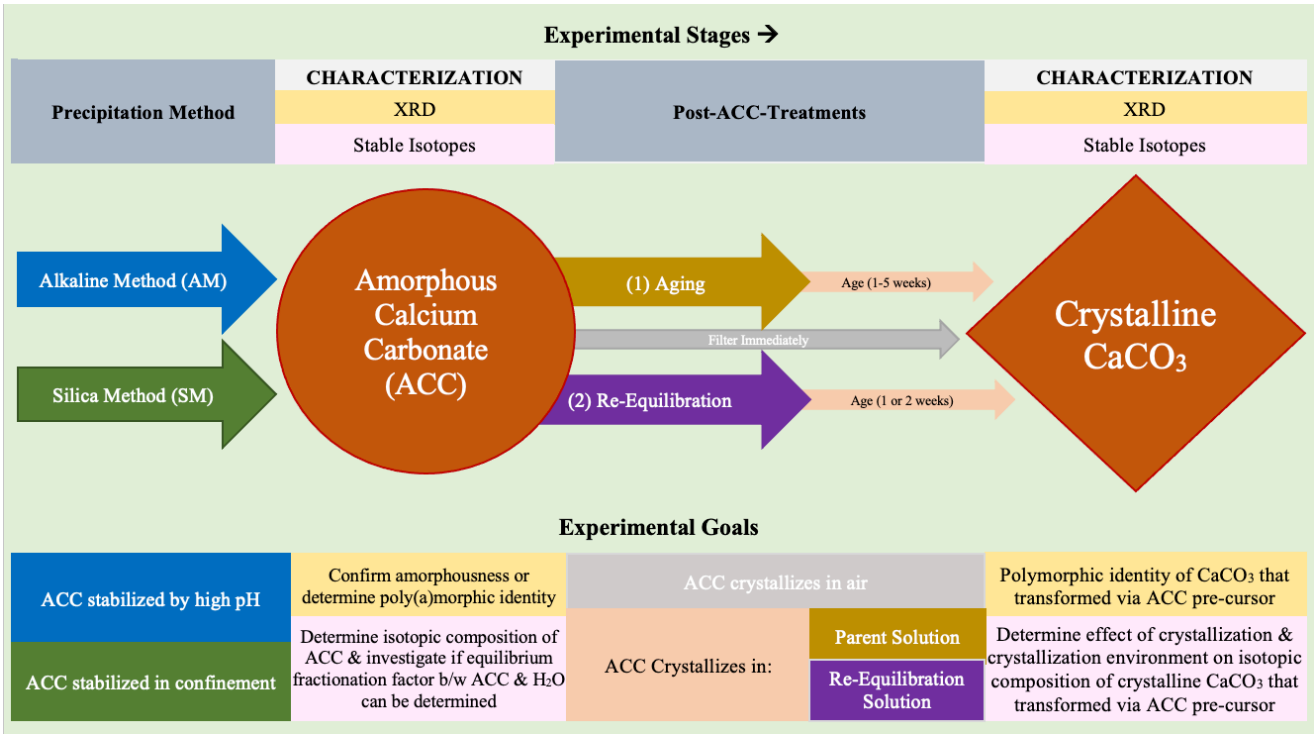

Figure 3.1: Experimental stages and goals

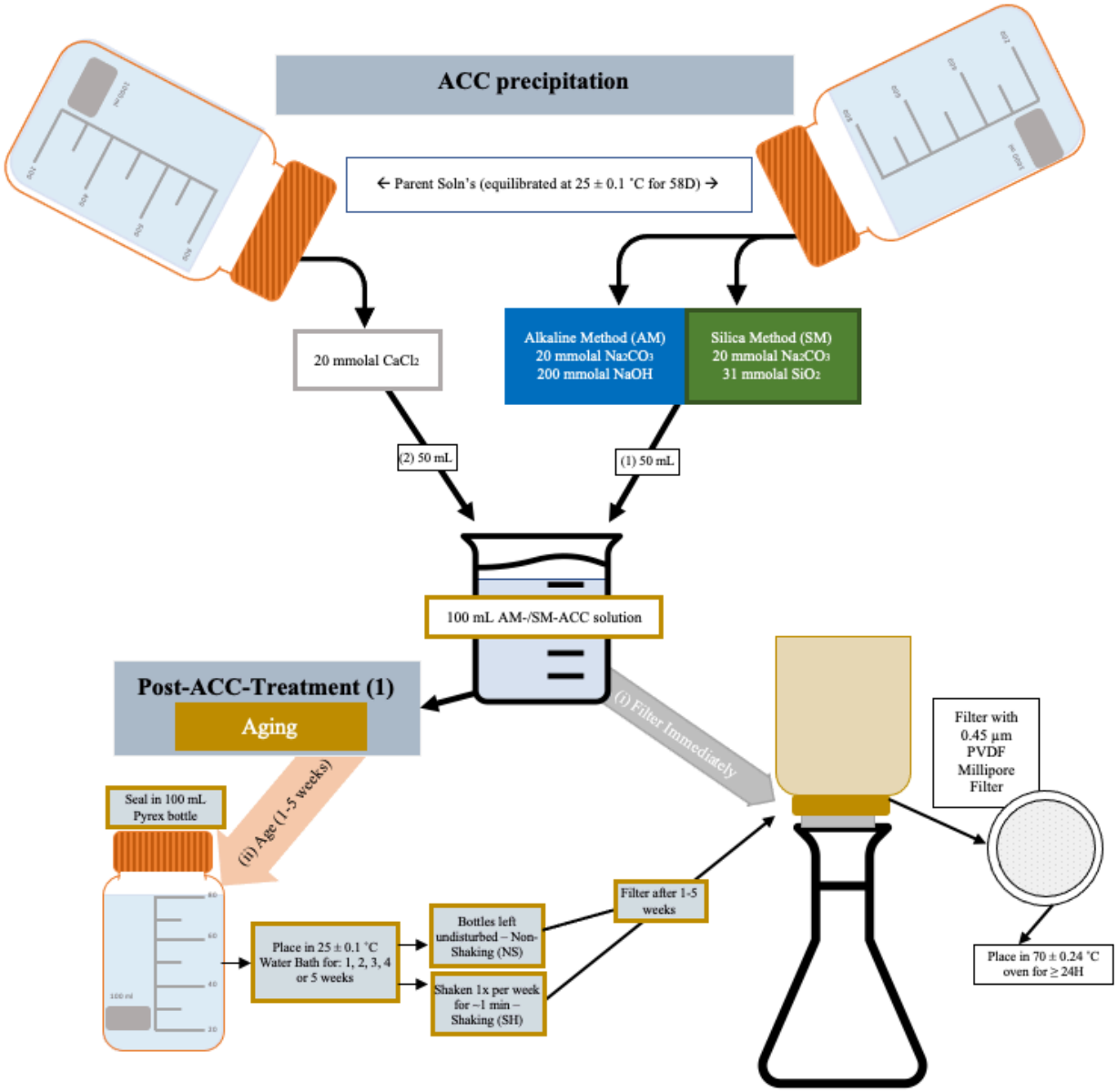

Figure 3.2: Schematic ACC precipitation, aging post-ACC-treatment and filtration.

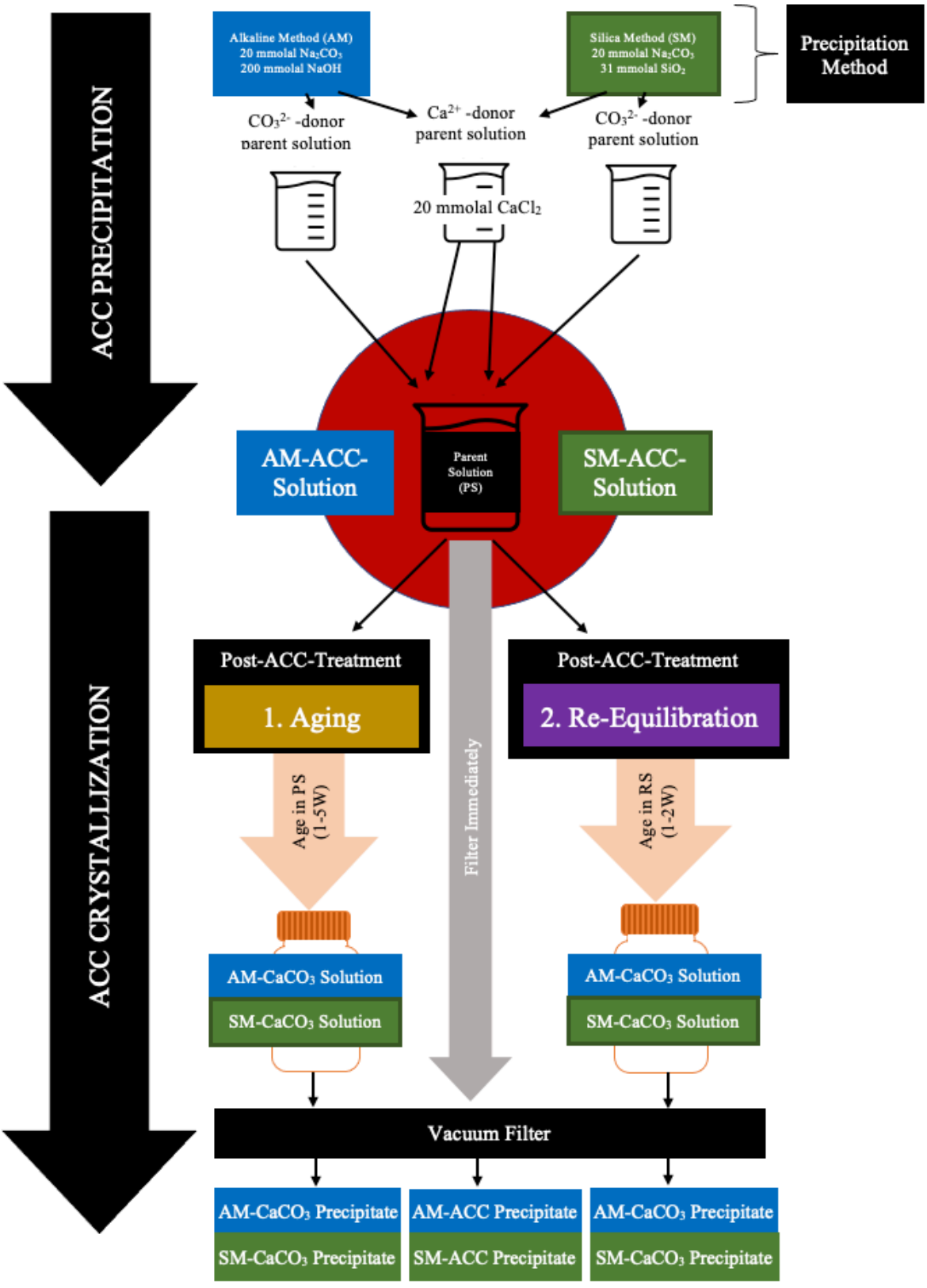

Figure 3.3: Flow chart indicating definitions of solutions, precipitates, and actions over the course of the study

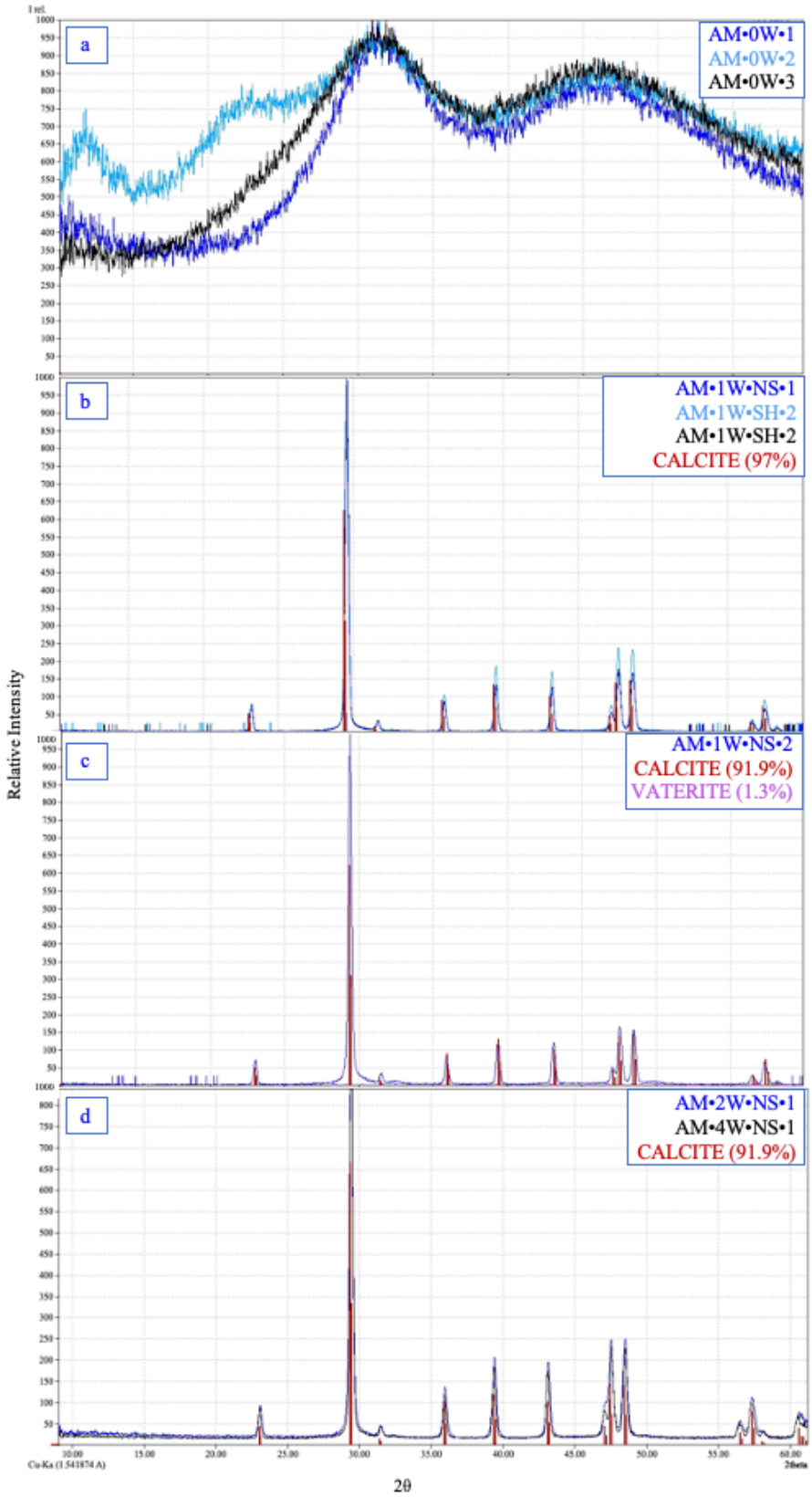

Figure 3.4: XRD spectra of aging AM-ACC and AM-$CaCO_3$ precipitates obtained using CuKα radiation and measured in relative intensity

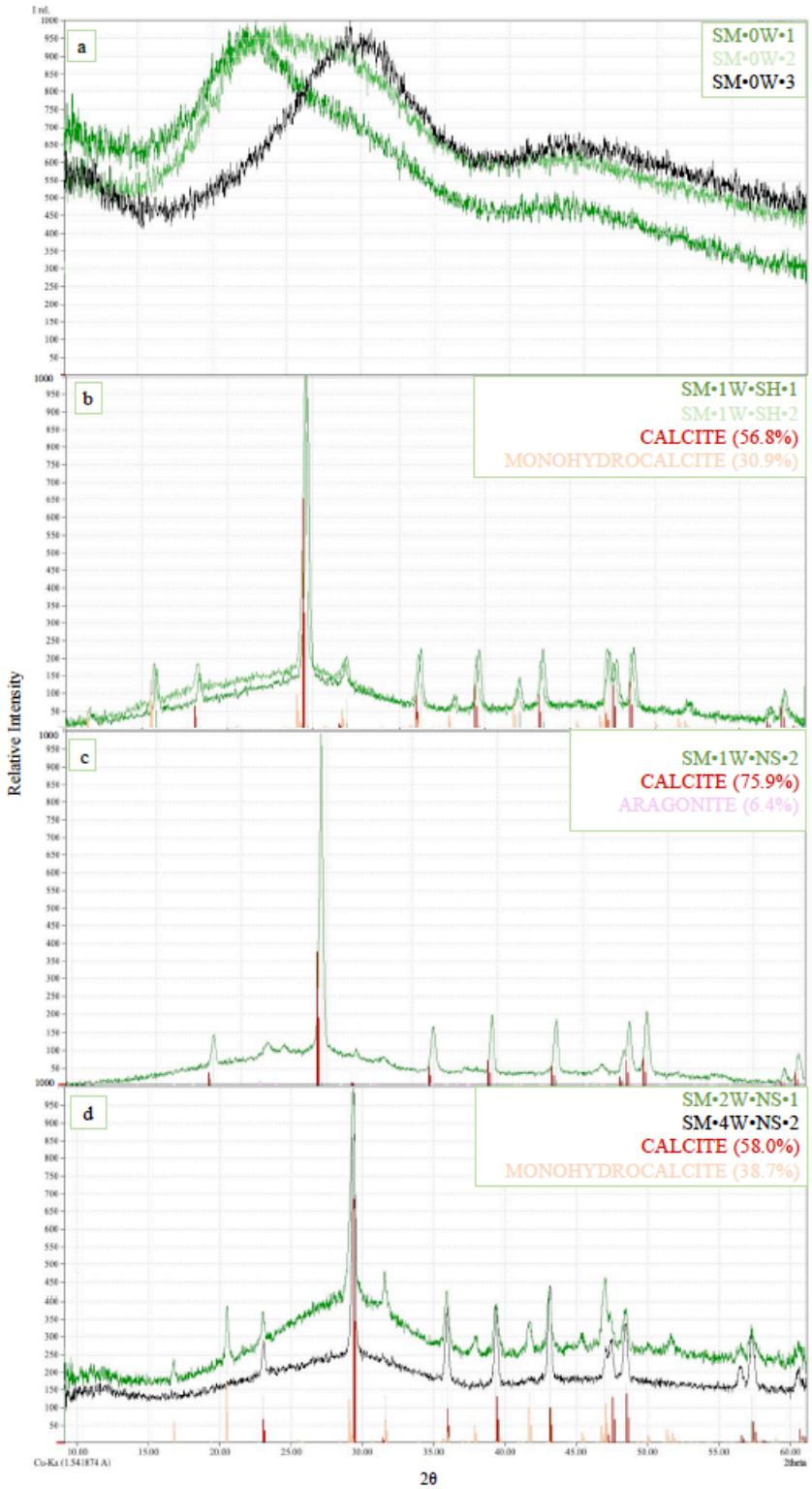

Figure 3.5: XRD spectra of aging SM-ACC and SM-$CaCO_3$ precipitates. Obtained using Cu Kα radiation and measured in relative intensity.

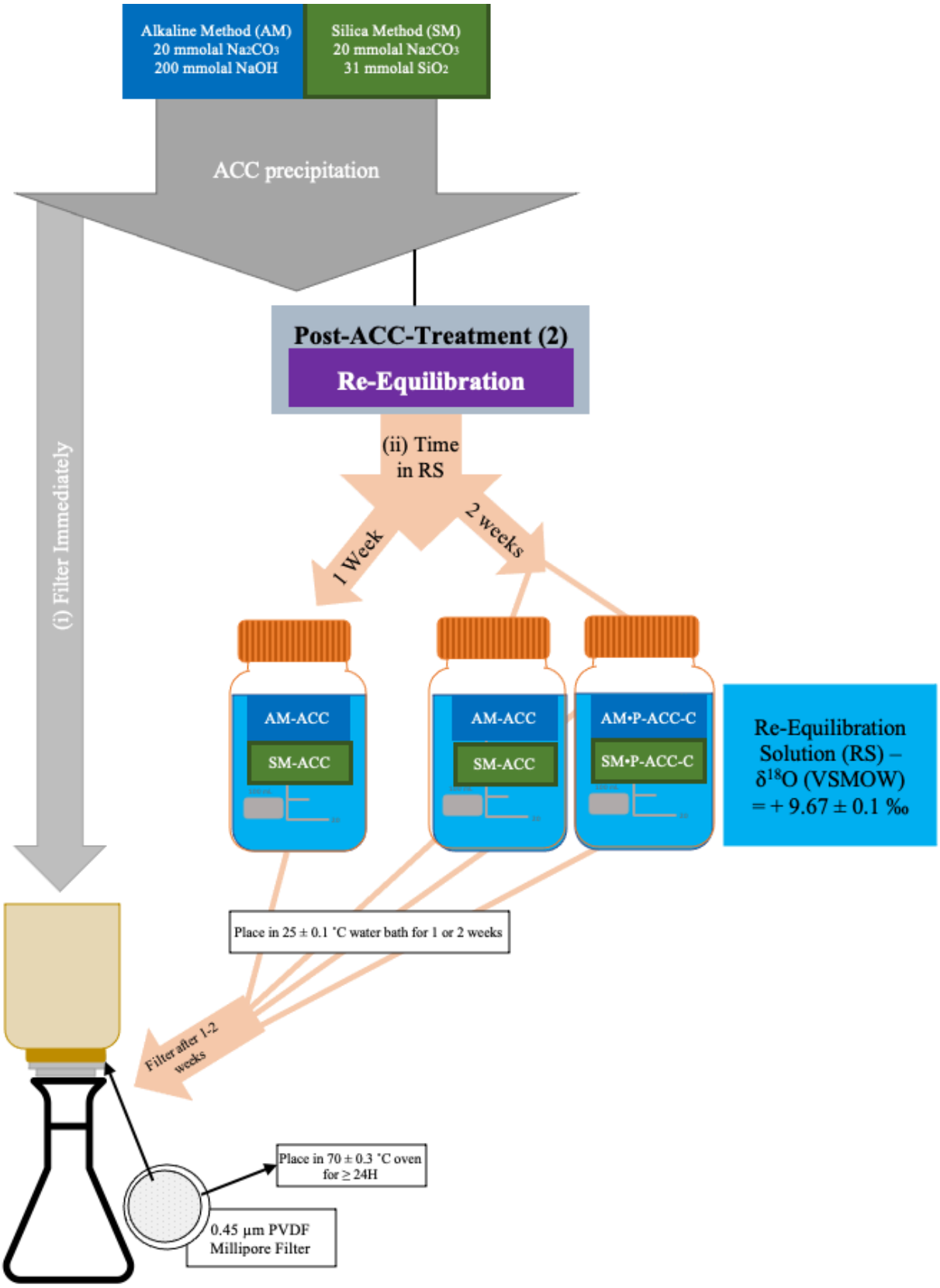

Figure 3.6: Schematic of re-equilibration post-ACC-treatment.

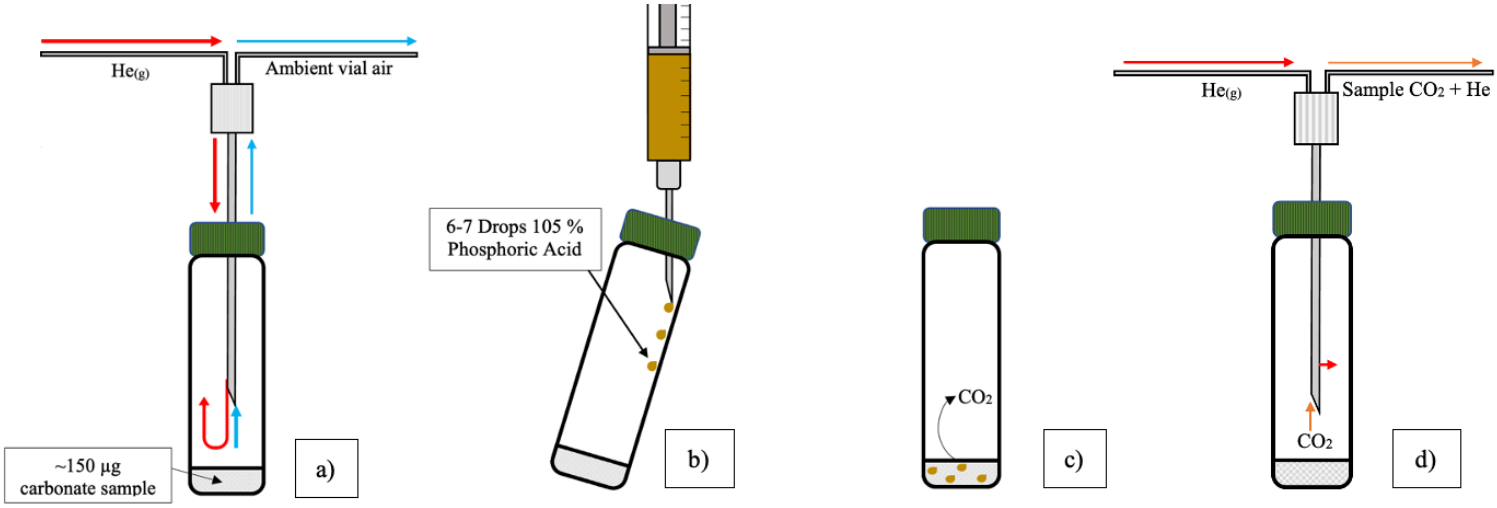

Figure 3.7: Process of analyzing headspace CO_2 with Gas Bench II system. (a) 12 mm Exetainer® vials preloaded with approximately 150 µg of carbonate samples, these Exetainer® vials are flushed and filled with He gas, eliminating ambient vial air. Following flushing and filling samples are (b) injected with 6-7 drops of 105 % phosphoric acid (H_3PO_4) that, once added, slide down the side of the Exetainer® vial, allowing them to reach the internal system temperature of 25 ± 0.1 °C. Once the acid has reached the carbonate sample (c) the acid reacts with the carbonate to produce CO_2 gas. Following ≥ 24 h of reaction time this CO_2 gas is (d) sampled by the Gas Bench II headspace autosampler and analyzed with respect to $\delta^{18}O$ and $\delta^{13}C$ isotope composition.

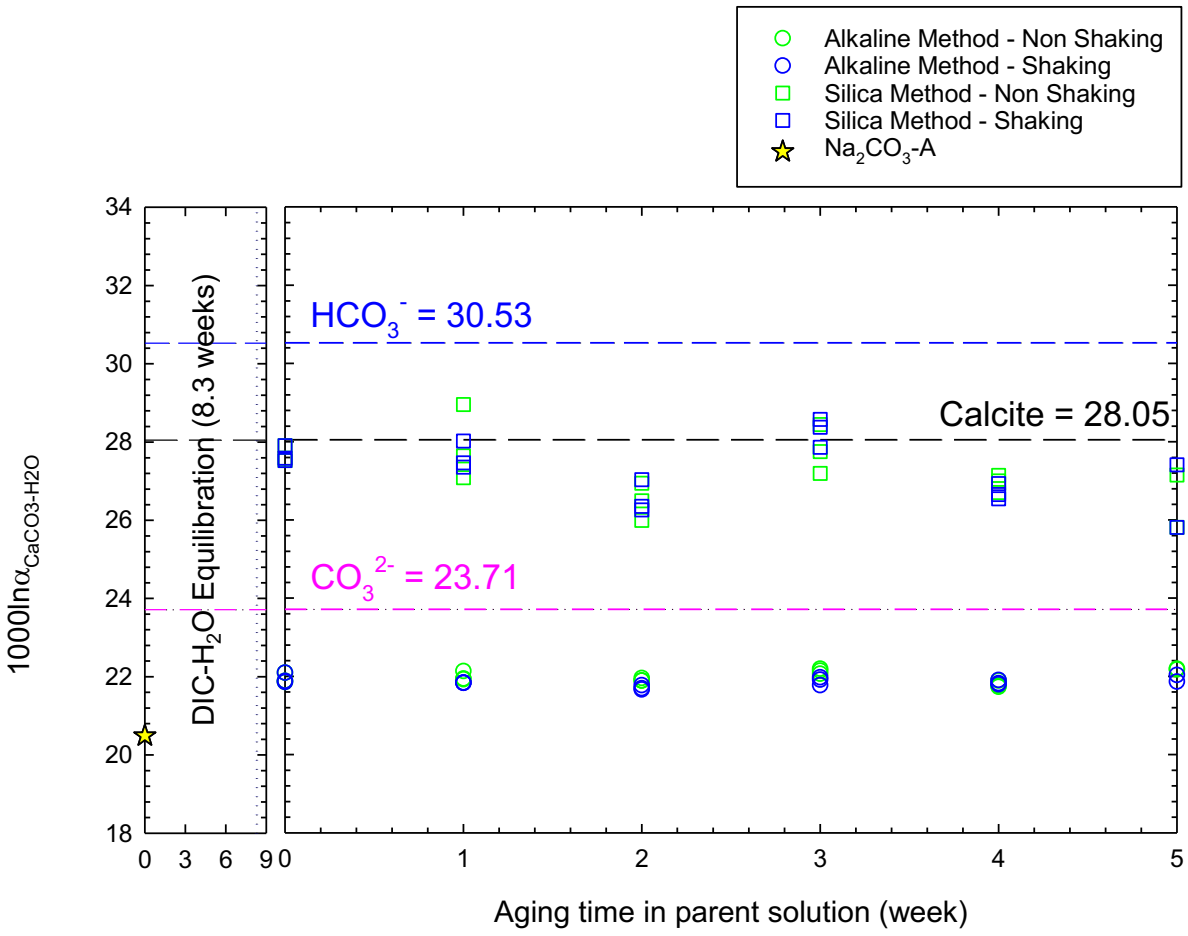

Figure 3.8: Comparison of $1000\ln\alpha_{CaCO3\text{-}water}$ values with time in parent solution (weeks) for AM-$CaCO_3$ and SM-$CaCO_3$ precipitates. DIC-water equilibration time for AM/SM-CO_3^{2-}-donor parent solution indicated in left-hand box.

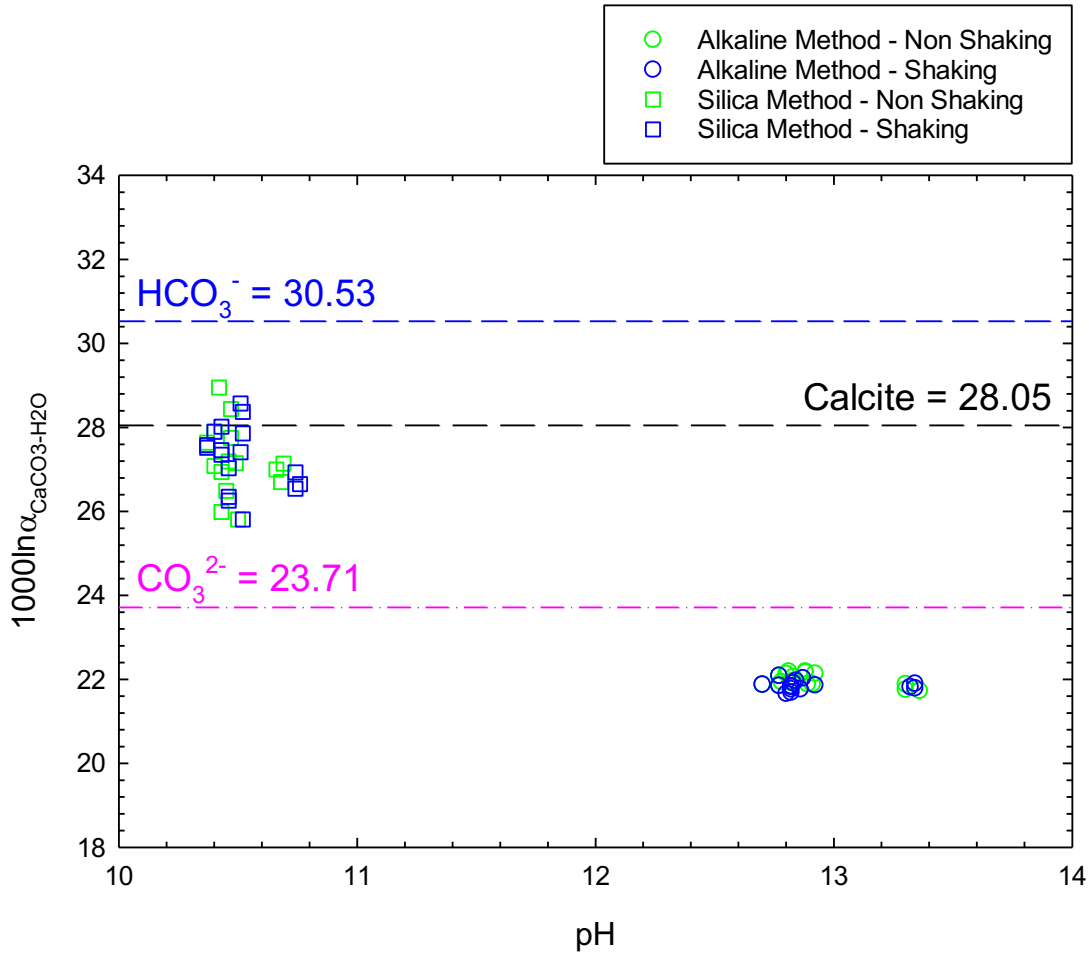

Figure 3.9: Comparison of $1000\ln\alpha_{CaCO3\text{-}water}$ values of AM-ACC/$CaCO_3$ and SM-ACC/$CaCO_3$ precipitates with AM-ACC/$CaCO_3$-solution and SM-ACC/$CaCO_3$-solution pH

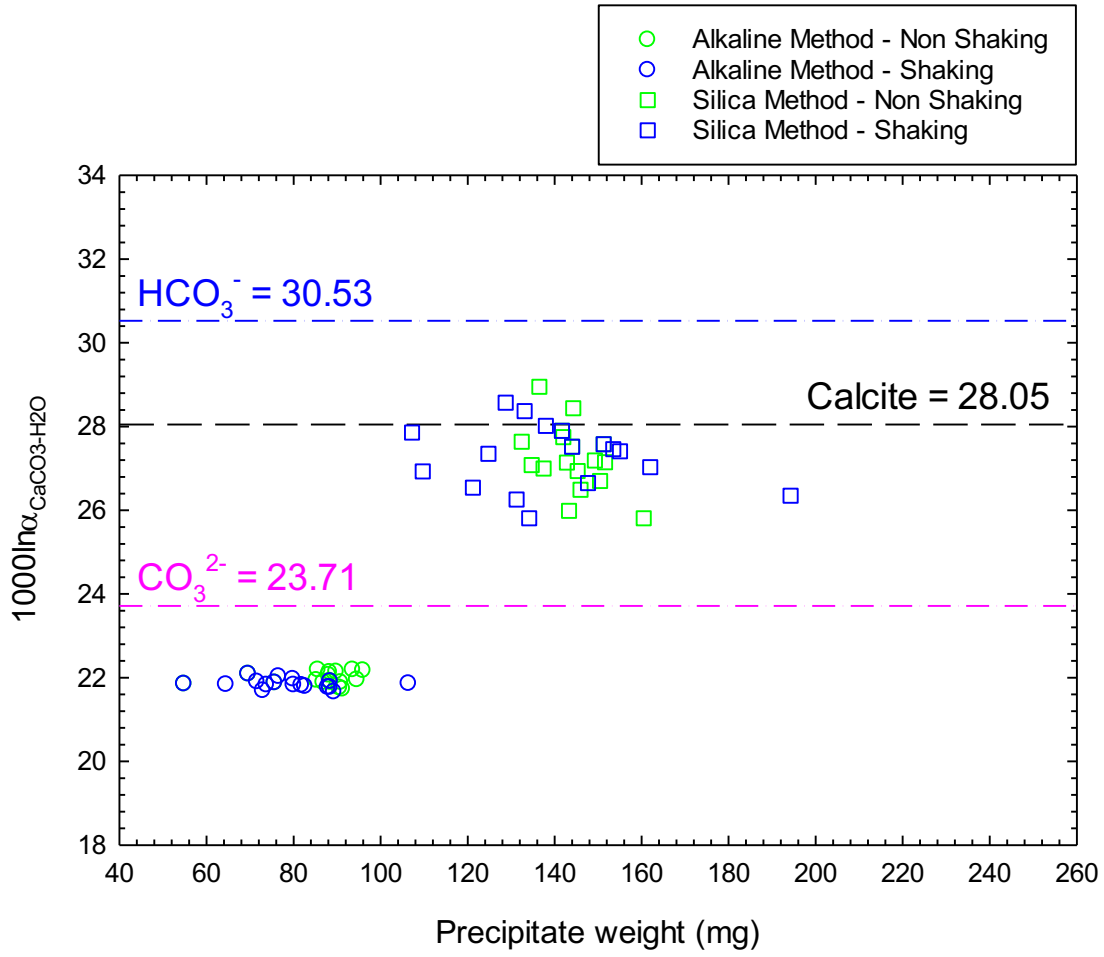

Figure 3.10: Comparison of $1000\ln\alpha_{CaCO3\text{-}water}$ values with yielded sample weight (mg) of AM-ACC/$CaCO_3$ and SM-ACC/$CaCO_3$ precipitates.

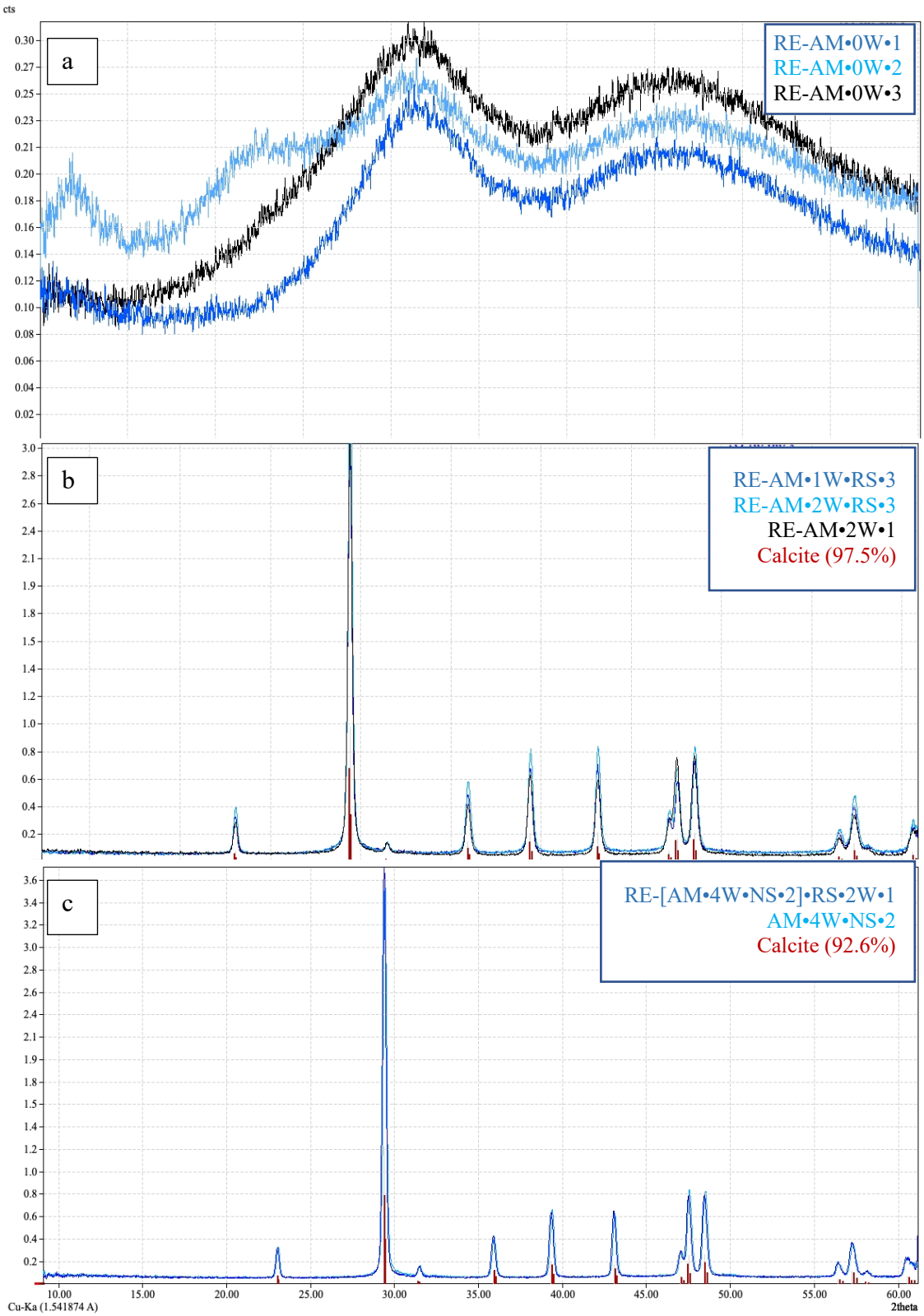

Figure 3.11: XRD spectra of re-equilibration AM-ACC and AM-$CaCO_3$ precipitates. Obtained using Cu Kα radiation and measured in counts.

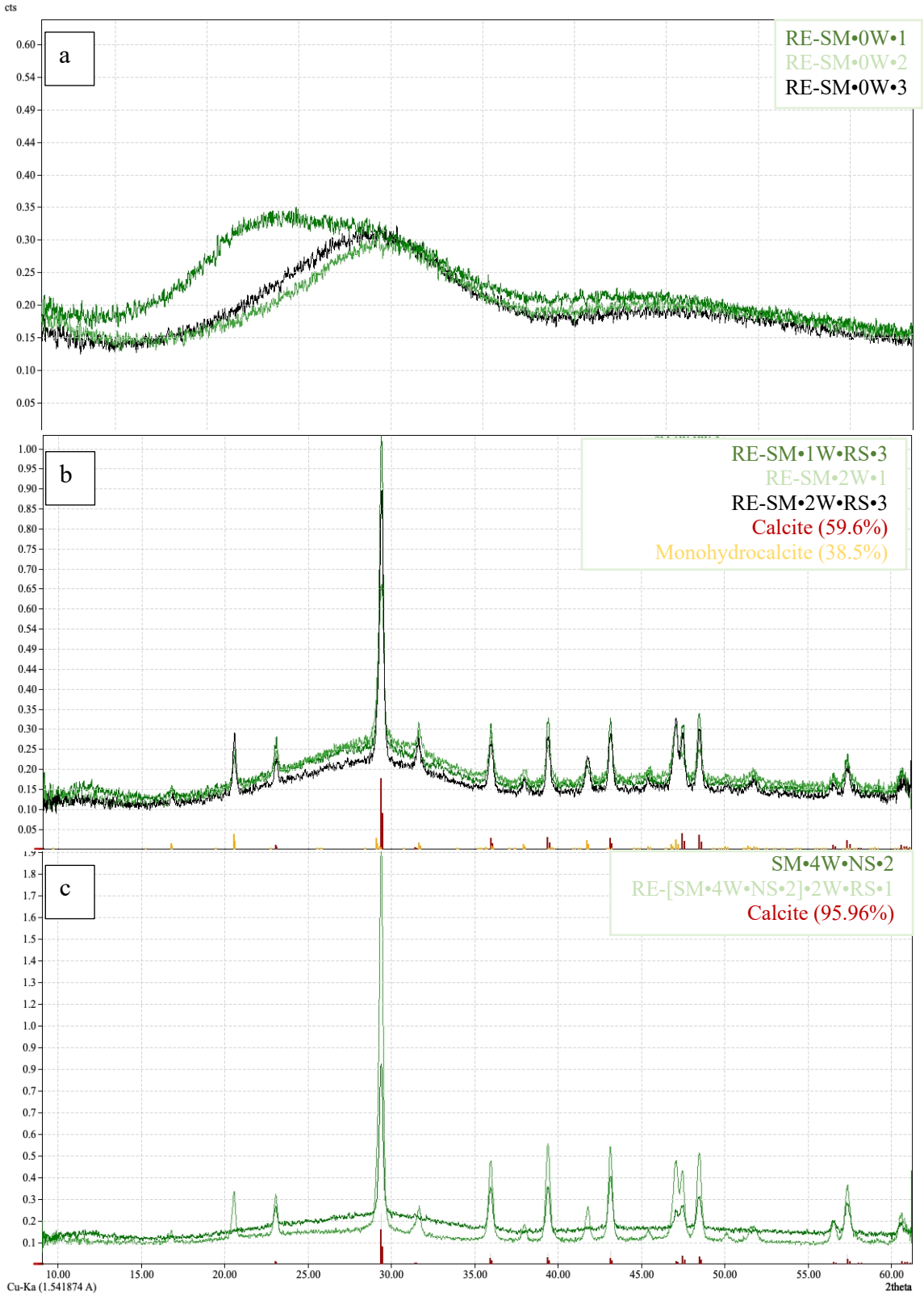

Figure 3.12: XRD spectra of re-equilibration SM-ACC and SM-$CaCO_3$ precipitates. Obtained using Cu Kα radiation and measured in counts.

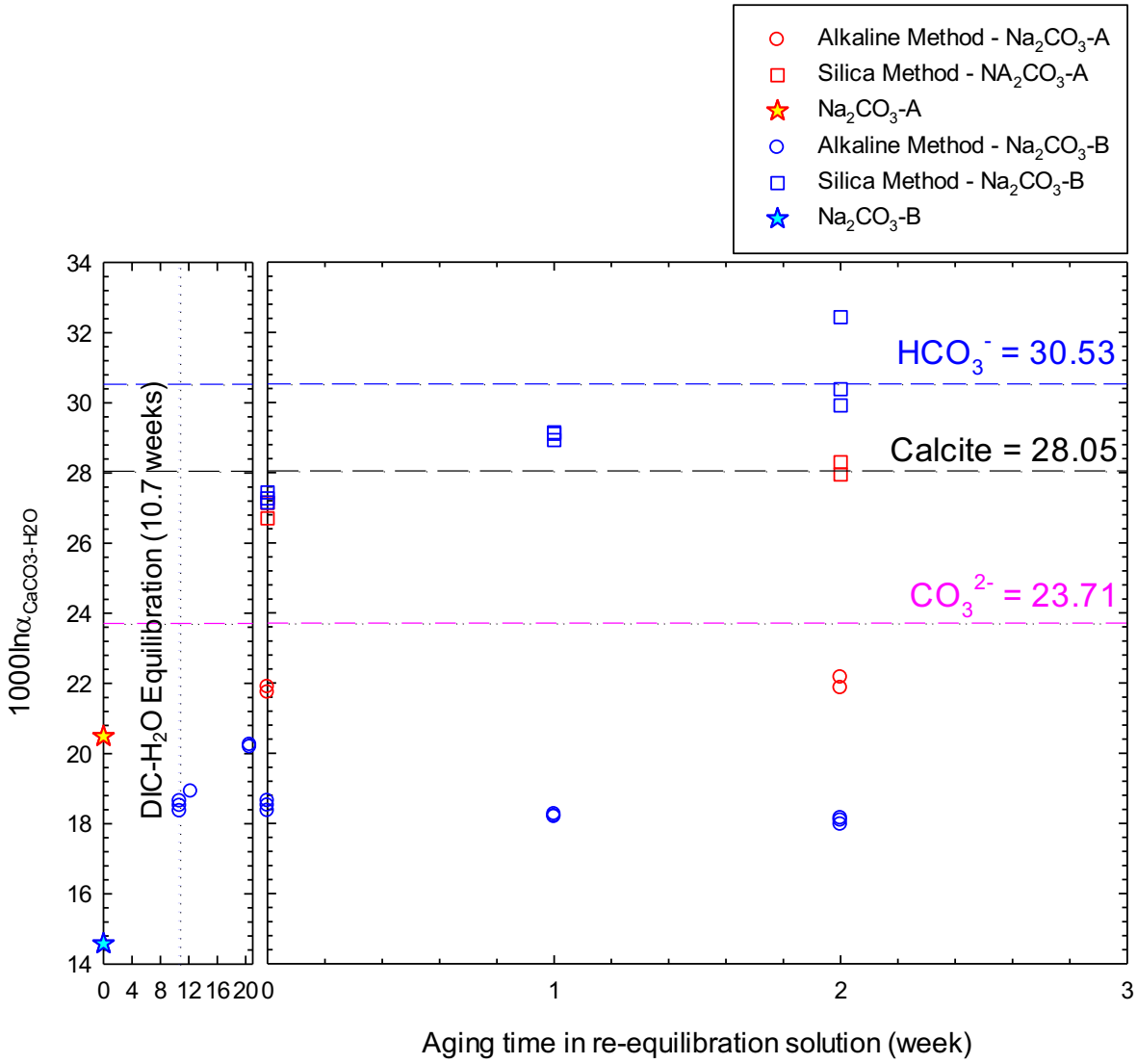

Figure 3.13: Comparison of $1000\ln\alpha_{CaCO3\text{-}water}$ values of AM-ACC/$CaCO_3$ and SM-ACC/$CaCO_3$ precipitates, with time in re-equilibration solution (days). Precipitates are visually differentiated by colour based on the parent Na_2CO_3 chemical used to prepare the AM/SM-CO_3^{2-}-donor parent solution and differentiated by shape based on precipitation method. The left-hand panel shows the DIC-water equilibration time of CO_3^{2-}-donor parent solutions.

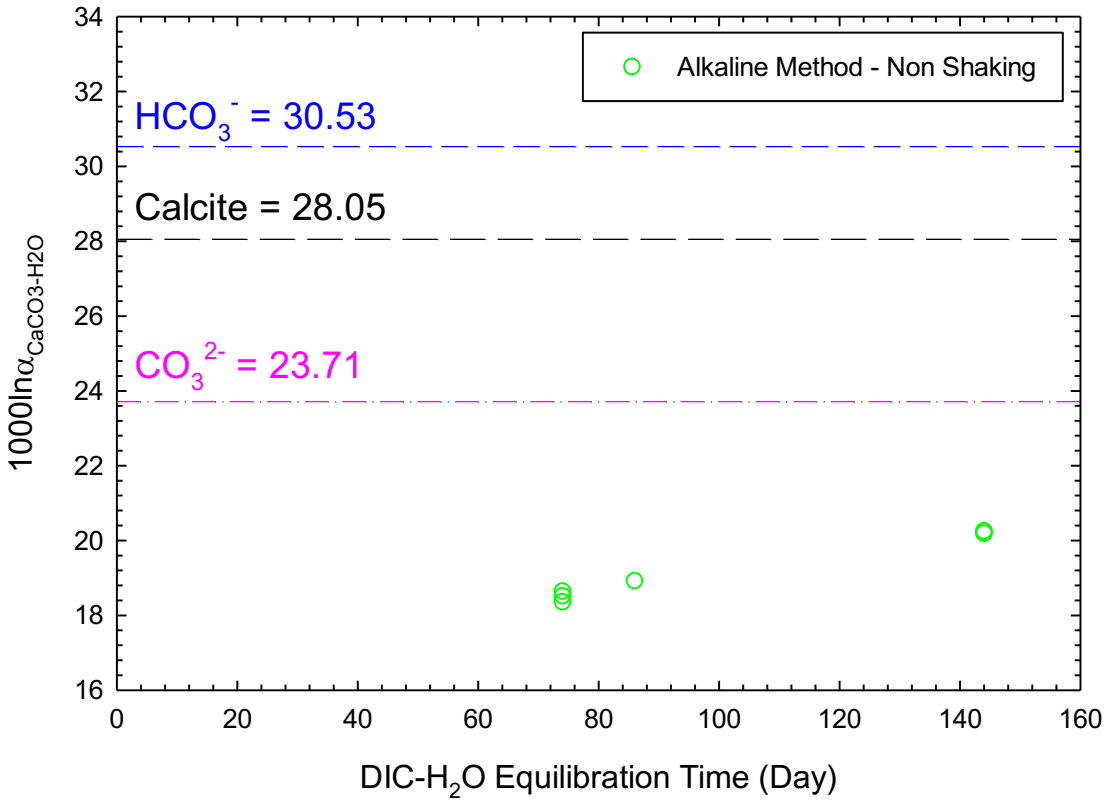

Figure 3.14: Comparison of $1000\ln\alpha_{CaCO3\text{-}water}$ values of AM-ACC precipitates with AM-CO_3^{2-}-donor parent solution DIC-H_2O equilibration time.

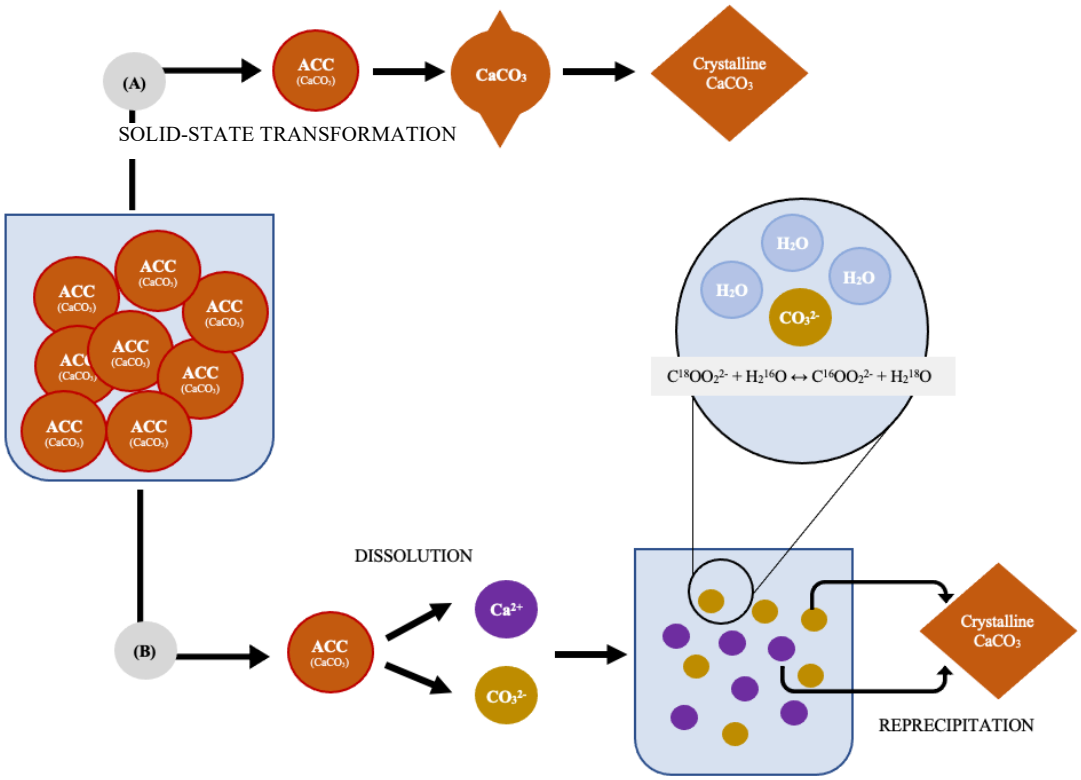

Figure 3.15: Comparison of crystallization via (A) solid-state transformation vs (B) dissolution-reprecipitation pathways

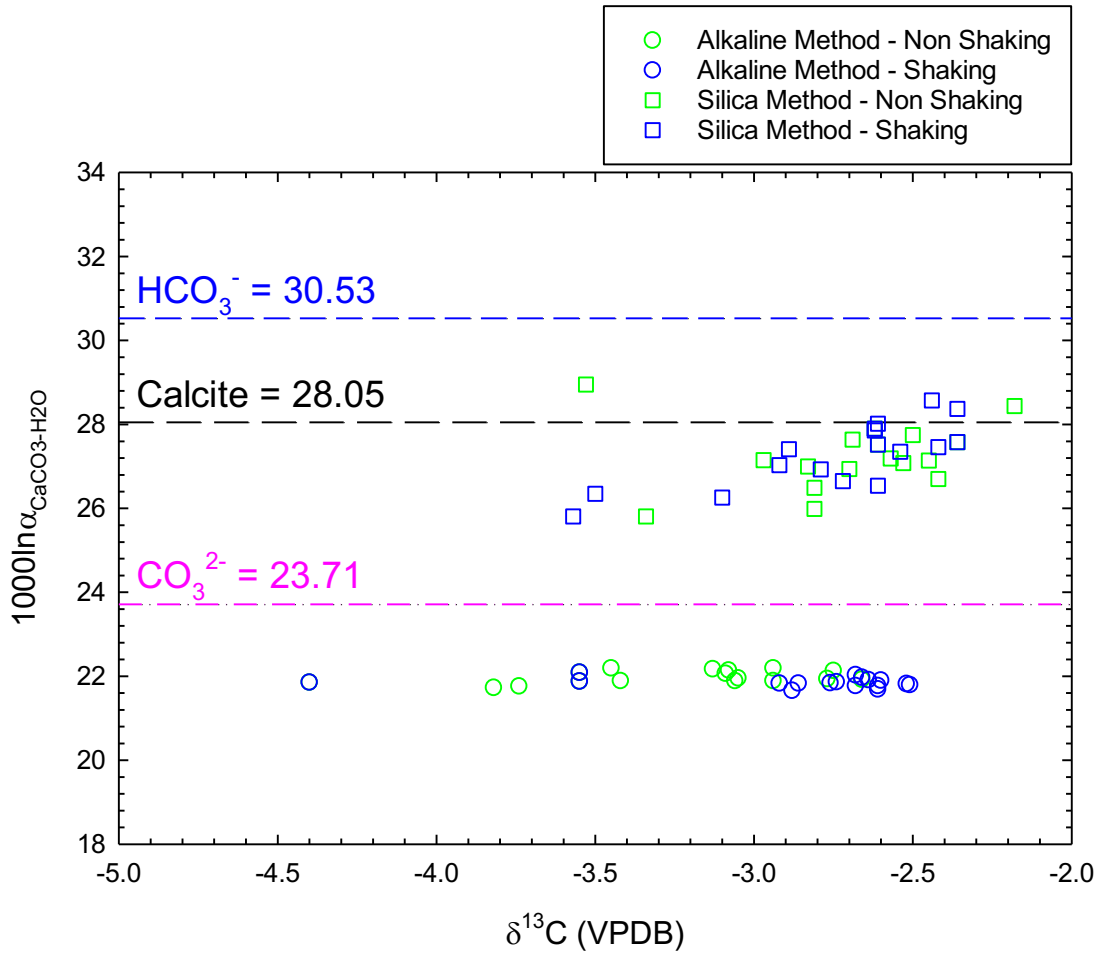

Figure 3.16: Comparison of $1000\ln\alpha_{CaCO3\text{-}water}$ values with $\delta^{13}C$ (VPDB) of AM-ACC/$CaCO_3$ and SM-ACC/$CaCO_3$ precipitates.

Table 3.1 Properties & Isotopic Compositions of Parent Solutions

Parent Solution ID	Na_2CO_3 Used (A/B)	Water ID	$\delta^{18}O_{water}$ (‰)	Date Made	Date Used	DIC Eq Time (days)
Na_2CO_3-NaOH-H_2O•I	A	KW•15Mar21	-6.41	2021-05-05	2021-07-02	58
Na_2CO_3-NaOH-H2O•II	A	KW•15Mar21	-6.41	2021-05-05	2021-07-02	58
Na_2CO_3-NaOH-H2O•III	B	KW•09Jul21	-6.45	2021-07-11	2021-09-24	75
Na_2CO_3-NaOH-H2O•IV	B	KW•16Jul21	-6.45	2021-07-11	2021-09-24	75
Na_2CO_3-SiO_2-H2O•I	A	KW•15Mar21	-6.41	2021-05-05	2021-07-02	58
Na_2CO_3-SiO_2-H2O•II	A	KW•15Mar21	-6.41	2021-05-05	2021-07-02	58
Na_2CO_3-SiO_2-H2O•III	B	KW•09Jul21	-6.45	2021-07-11	2021-09-24	75
Na_2CO_3-SiO_2-H2O•IV	B	KW•16Jul21	-6.45	2021-07-11	2021-09-24	75
$CaCl_2$-H_2O•I	N/A	KW•15Mar21	-6.41	2021-05-05	2021-07-02	58
$CaCl_2$-H_2O•II		KW•15Mar21	-6.41	2021-05-05	2021-07-02	58
$CaCl_2$-H_2O•III		KW•15Mar21	-6.41	2021-05-05	2021-07-02	58
$CaCl_2$-H_2O•IV		KW•15Mar21	-6.41	2021-05-05	2021-07-02	58
$CaCl_2$-H_2O•V		KW•09Jul21	-6.45	2021-07-11	2021-09-24	75
$CaCl_2$-H_2O•VI		KW•16Jul21	-6.45	2021-07-11	2021-09-24	75

Chemical	Inter-Lab ID	Chemical	Lot #	mmolal	$\delta^{13}C$ (‰)	$\delta^{18}O$ (‰)	$\delta^{18}O_{water}$ (‰)	Theoretical $1000\ln\alpha_{Na2CO3\text{-}H2O}$
Na_2CO_3	A	SC0395-1	81814	20	-2.34	14.15	-6.41	20.49
Na_2CO_3	B	S263-500	203030	20	-21.52	8.18	-6.41	14.58
NaOH		SX0590-1	B0414769	200				
SiO_2		MKCG-0528	338443	31				
$CaCl_2$		C77-500	61753	20				

Table 3.2: Detailed experimental conditions and isotopic results for all AM- and SM-$CaCO_3$ precipitates from the Aging Post-ACC-Treatment

Parent solutions were left to equilibrate for 58 days in a water bath at 25 ˚C ± 0.1 ˚C to establish DIC-H2O equilibrium, each precipitation yielded a 100 mL ACC-solution, all isotopic composition data represents an average of samples run in duplicate. Precipitates that were aged in parent solution were kept in a 25 ˚C ± 0.1 ˚C water bath. All parent solutions were made using the same Na_2CO_3 source (δ18O = 14.38 ‰, δ13C = -2.20 ‰)

Precipitation Method	Precipitate ID	Repeat	Time in Soln' (weeks)	Exp Condition	Na_2CO_3 Parent Soln ID	$CaCl_2$ Parent Soln' ID	pH	Sample weight (mg)	Mineralogy	Isotopic Compositions of Parent Materials (‰)			Isotopic composition of precipitates (‰)		$\alpha_{CaCO3-H2O}$	$1000\ln\alpha_{(CaCO3-H2O)}$
										$\delta^{13}C_{Carb Source}$	$\delta^{18}O_{Carb Source}$	$\delta^{18}O_{Parent soln'}$ (VSMOW)	$\delta^{13}C$ (VPDB)	$\delta^{18}O$ (VSMOW)		
Alkaline Method (AM)	AM•0W	1	0	N/A	Na_2CO_3/NaOH•I	$CaCl_2$•I	12.70	75.63	ACC	-2.34	14.15	-6.41	-3.55	15.57	1.02213	21.88
		2	0	N/A	Na_2CO_3/NaOH•I	$CaCl_2$•I	12.77	69.56	ACC	-2.34	14.15	-6.41	-3.55	15.78	1.02233	22.09
		3	0	N/A	Na_2CO_3/NaOH•I	$CaCl_2$•I	12.77	54.80	ACC	-2.34	14.15	-6.41	-4.40	15.54	1.02209	21.85
	AM•1W•NS	1	1	NS	Na_2CO_3/NaOH•I	$CaCl_2$•I	12.80	88.24	C*	-2.34	14.15	-6.41	-2.75	15.83	1.02238	22.13
		2	1	NS	Na_2CO_3/NaOH•I	$CaCl_2$•I	12.78	85.24	C/V*	-2.34	14.15	-6.41	-2.77	15.62	1.02218	21.94
		3	1	NS	Na_2CO_3/NaOH•I	$CaCl_2$•I	12.82	88.31	C	-2.34	14.15	-6.41	-2.66	15.61	1.02216	21.92
	AM•2W•NS	1	2	NS	Na_2CO_3/NaOH•I	$CaCl_2$•I	12.91	90.82	C	-2.34	14.15	-6.41	-3.06	15.58	1.02213	21.89
		2	2	NS	Na_2CO_3/NaOH•I	$CaCl_2$•I	12.89	86.84	C	-2.34	14.15	-6.41	-3.42	15.57	1.02213	21.89
		3	2	NS	Na_2CO_3/NaOH•I	$CaCl_2$•I	12.82	94.56	C	-2.34	14.15	-6.41	-3.05	15.64	1.02220	21.95
	AM•3W•NS	1	3	NS	Na_2CO_3/NaOH•I	$CaCl_2$•I	12.81	85.56	C	-2.34	14.15	-6.41	-2.94	15.88	1.02243	22.19
		2	3	NS	Na_2CO_3/NaOH•I	$CaCl_2$•I	12.83	88.01	C	-2.34	14.15	-6.41	-3.09	15.75	1.02230	22.06
		3	3	NS	Na_2CO_3/NaOH•I	$CaCl_2$•I	12.92	89.79	C	-2.34	14.15	-6.41	-3.08	15.83	1.02238	22.14
	AM•4W•NS	1	4	NS	Na_2CO_3/NaOH•I	$CaCl_2$•I	13.30	90.52	C	-2.34	14.15	-6.41	-3.74	15.44	1.02199	21.76
		2	4	NS	Na_2CO_3/NaOH•I	$CaCl_2$•I	13.36	91.26	C	-2.34	14.15	-6.41	-3.82	15.41	1.02197	21.73
		3	4	NS	Na_2CO_3/NaOH•I	$CaCl_2$•I	13.30	88.47	C	-2.34	14.15	-6.41	-2.94	15.58	1.02213	21.89
	AM•5W•NS	1	5	NS	Na_2CO_3/NaOH•I	$CaCl_2$•I	12.88	95.94	C	-2.34	14.15	-6.41	-3.13	15.86	1.02241	22.17
		2	5	NS	Na_2CO_3/NaOH•I	$CaCl_2$•1/2	12.88	93.59	C	-2.34	14.15	-6.41	-3.45	15.89	1.02244	22.19
	AM•0W	1	0	N/A	Na_2CO_3/NaOH•I	$CaCl_2$•I	12.70	75.63	ACC	-2.34	14.15	-6.41	-3.55	15.57	1.02213	21.88
		2	0	N/A	Na_2CO_3/NaOH•I	$CaCl_2$•I	12.77	69.56	ACC	-2.34	14.15	-6.41	-3.55	15.78	1.02233	22.09
		3	0	N/A	Na_2CO_3/NaOH•I	CaCl2•II	12.77	54.80	ACC	-2.34	14.15	-6.41	-4.40	15.54	1.02209	21.85
	AM•1W•SH	1	1	SH	Na_2CO_3/NaOH•I	CaCl2•II	12.82	79.97	C	-2.34	14.15	-6.41	-2.86	15.51	1.02207	21.83
		2	1	SH	Na_2CO_3/NaOH•I/	CaCl2•II/III	12.82	73.76	C	-2.34	14.15	-6.41	-2.92	15.52	1.02207	21.83
		3	1	SH	Na_2CO_3/NaOH•II	$CaCl_2$•III	12.82	64.46	C	-2.34	14.15	-6.41	-2.76	15.53	1.02208	21.84
	AM•2W•SH	1	2	SH	Na_2CO_3/NaOH•II	$CaCl_2$•III	12.80	89.26	C	-2.34	14.15	-6.41	-2.88	15.35	1.02190	21.66
		2	2	SH	Na_2CO_3/NaOH•II	$CaCl_2$•III	12.82	72.95	C	-2.34	14.15	-6.41	-2.61	15.37	1.02192	21.69
		3	2	SH	Na_2CO_3/NaOH•II	$CaCl_2$•III	12.82	88.35	C	-2.34	14.15	-6.41	-2.61	15.46	1.02201	21.77
	AM•3W•SH	1	3	SH	Na_2CO_3/NaOH•II	$CaCl_2$•III	12.83	88.36	C	-2.34	14.15	-6.41	-2.64	15.60	1.02215	21.91
		2	3	SH	Na_2CO_3/NaOH•II	$CaCl_2$•III	12.84	79.83	C	-2.34	14.15	-6.41	-2.66	15.65	1.02221	21.97
		3	3	SH	Na_2CO_3/NaOH•II	$CaCl_2$•III	12.86	87.86	C	-2.34	14.15	-6.41	-2.68	15.46	1.02201	21.77
	AM•4W•SH	1	4	SH	Na_2CO_3/NaOH•II	$CaCl_2$•III	13.34	71.58	C	-2.34	14.15	-6.41	-2.60	15.59	1.02214	21.90
		2	4	SH	Na_2CO_3/NaOH•II	$CaCl_2$•III	13.32	81.79	C	-2.34	14.15	-6.41	-2.52	15.51	1.02206	21.82
		3	4	SH	Na_2CO_3/NaOH•II	$CaCl_2$•III	13.34	82.62	C	-2.34	14.15	-6.41	-2.51	15.48	1.02203	21.79
	AM•5W•SH	1	5	SH	Na_2CO_3/NaOH•II	$CaCl_2$•III	12.87	76.56	C	-2.34	14.15	-6.41	-2.68	15.72	1.02227	22.03
		2	5	SH	Na_2CO_3/NaOH•II	$CaCl_2$•III	12.92	106.44	C	-2.34	14.15	-6.41	-2.74	15.54	1.02210	21.86

Silica Method (SM)	SM•0W	1	0	N/A	Na_2CO_3/SiO_2•I	$CaCl_2$•I	10.37	151.28	ACC	-2.34	14.15	-6.41	-2.36	21.38	1.02797	27.58
		2	0	N/A	Na_2CO_3/SiO_2•I	$CaCl_2$•I	10.37	143.98	ACC	-2.34	14.15	-6.41	-2.61	21.31	1.02790	27.52
		3	0	N/A	Na_2CO_3/SiO_2•I	$CaCl_2$•I	10.40	141.65	ACC	-2.34	14.15	-6.41	-2.62	21.70	1.02829	27.90
	SM•1W•NS	1	1	NS	Na_2CO_3/SiO_2•I	CaCl2•II	10.37	132.43	ACC/C/A*	-2.34	14.15	-6.41	-2.69	21.44	1.02803	27.64
		2	1	NS	Na_2CO_3/SiO_2•I	CaCl2•II	10.42	136.47	ACC/C/A	-2.34	14.15	-6.41	-3.53	22.77	1.02937	28.95
		3	1	NS	Na_2CO_3/SiO_2•I	CaCl2•II	10.40	134.72	ACC/C/A	-2.34	14.15	-6.41	-2.53	20.86	1.02745	27.08
	SM•2W•NS	1	2	NS	Na_2CO_3/SiO_2•I	CaCl2•II	10.43	143.29	ACC/C/M	-2.34	14.15	-6.41	-2.81	19.75	1.02633	25.99
		2	2	NS	Na_2CO_3/SiO_2•I	CaCl2•II	10.43	145.26	ACC/C/M	-2.34	14.15	-6.41	-2.70	20.72	1.02731	26.94
		3	2	NS	Na_2CO_3/SiO_2•I	CaCl2•II	10.45	145.94	ACC/C/M	-2.34	14.15	-6.41	-2.81	20.26	1.02685	26.49
	SM•3W•NS	1	3	NS	Na_2CO_3/SiO_2•I	CaCl2•II	10.46	149.23	ACC/C	-2.34	14.15	-6.41	-2.57	20.97	1.02756	27.19
		2	3	NS	Na_2CO_3/SiO_2•I	CaCl2•II	10.47	141.96	ACC/C	-2.34	14.15	-6.41	-2.50	21.54	1.02814	27.75
		3	3	NS	Na_2CO_3/SiO_2•I	CaCl2•II	10.47	144.24	ACC/C	-2.34	14.15	-6.41	-2.18	22.25	1.02885	28.44
	SM•4W•NS	1	4	NS	Na_2CO_3/SiO_2•I	CaCl2•II	10.66	137.42	ACC/C	-2.34	14.15	-6.41	-2.83	20.78	1.02737	27.00
		2	4	NS	Na_2CO_3/SiO_2•I	CaCl2•II	10.68	150.44	ACC/C	-2.34	14.15	-6.41	-2.42	20.47	1.02706	26.70
		3	4	NS	Na_2CO_3/SiO_2•I	CaCl2•II	10.69	142.80	ACC/C	-2.34	14.15	-6.41	-2.45	20.93	1.02751	27.14
	SM•5W•NS	1	5	NS	Na_2CO_3/SiO_2•I	CaCl2•II	10.49	151.60	ACC/C	-2.34	14.15	-6.41	-2.97	20.93	1.02752	27.15
		2	5	NS	Na_2CO_3/SiO_2•I	CaCl2•II	10.50	160.51	ACC/C	-2.34	14.15	-6.41	-3.34	19.57	1.02615	25.81
	SM•0W	1	0	N/A	Na_2CO_3/SiO_2•I	$CaCl_2$•I	10.37	151.28	ACC	-2.34	14.15	-6.41	-2.36	21.38	1.02797	27.58
		2	0	N/A	Na_2CO_3/SiO_2•I	$CaCl_2$•I	10.37	143.98	ACC	-2.34	14.15	-6.41	-2.61	21.31	1.02790	27.52
		3	0	N/A	Na_2CO_3/SiO_2•I	$CaCl_2$•I	10.40	141.65	ACC	-2.34	14.15	-6.41	-2.62	21.70	1.02829	27.90
	SM•1W•SH	1	1	SH	Na_2CO_3/SiO_2•I	$CaCl_2$•III	10.43	137.98	ACC/C/M*	-2.34	14.15	-6.41	-2.61	21.82	1.02842	28.02
		2	1	SH	Na_2CO_3/SiO_2•I/II	$CaCl_2$•III	10.43	153.50	ACC/C/M	-2.34	14.15	-6.41	-2.42	21.25	1.02784	27.46
		3	1	SH	Na_2CO_3/SiO_2•II	$CaCl_2$•III	10.43	124.75	ACC/C/M	-2.34	14.15	-6.41	-2.54	21.13	1.02772	27.35
	SM•2W•SH	1	2	SH	Na_2CO_3/SiO_2•II	$CaCl_2$•III	10.46	194.24	ACC/C/M	-2.34	14.15	-6.41	-3.50	20.11	1.02670	26.35
		2	2	SH	Na_2CO_3/SiO_2•II	$CaCl_2$•III	10.46	131.25	ACC/C/M	-2.34	14.15	-6.41	-3.10	20.03	1.02661	26.26
		3	2	SH	Na_2CO_3/SiO_2•II	CaCl2•III/IV	10.46	161.98	ACC/C/M	-2.34	14.15	-6.41	-2.92	20.81	1.02740	27.03
	SM•3W•SH	1	3	SH	Na_2CO_3/SiO_2•II	CaCl2•III/IV	10.51	128.74	ACC/C	-2.34	14.15	-6.41	-2.44	22.38	1.02898	28.57
		2	3	SH	Na_2CO_3/SiO_2•II	CaCl2•III/IV	10.52	107.22	ACC/C	-2.34	14.15	-6.41	-2.62	21.65	1.02825	27.86
		3	3	SH	Na_2CO_3/SiO_2•II	CaCl2•III/IV	10.52	133.10	ACC/C	-2.34	14.15	-6.41	-2.36	22.18	1.02878	28.37
	SM•4W•SH	1	4	SH	Na_2CO_3/SiO_2•II	CaCl2•III/IV	10.76	147.63	ACC/C	-2.34	14.15	-6.41	-2.72	20.43	1.02701	26.65
		2	4	SH	Na_2CO_3/SiO_2•II	CaCl2•IV	10.74	109.67	ACC/C	-2.34	14.15	-6.41	-2.79	20.71	1.02730	26.93
		3	4	SH	Na_2CO_3/SiO_2•II	CaCl2•IV	10.74	121.22	ACC/C	-2.34	14.15	-6.41	-2.61	20.32	1.02690	26.54
	SM•5W•SH	1	5	SH	Na_2CO_3/SiO_2•II	CaCl2•IV	10.52	134.12	ACC/C	-2.34	14.15	-6.41	-3.57	19.56	1.02614	25.81
		2	5	SH	Na_2CO_3/SiO_2•II	CaCl2•IV	10.51	155.03	ACC/C	-2.34	14.15	-6.41	-2.89	21.20	1.02779	27.41

* (NS) Non-Shaking, (SH) Shaking, 0 – ACC that is filtered immediately after precipitation, (ACC) Amorphous Calcium Carbonate, (C) Calcite, (V) Vaterite, (A) Aragonite, (M) Monohydrocalcite

Table 3.3: Detailed experimental conditions and isotopic results for all AM/SM-ACC/$CaCO_3$ precipitates for the Re-Equilibration Post-ACC-Treatment

Ca^{2+}- and CO_3^{2-}-donor parent solutions were left to equilibrate for 74 days (with exception of red text) in a water bath at 25 °C ± 0.1 °C to establish DIC-H2O equilibrium, each precipitation yielded a 50 mL ACC-solution, all isotopic composition data represents an average of precipitates run in duplicate. Precipitates that remained in solution were kept in a 25 °C ± 0.1 °C water bath and left undistrubed (non-shaking) for the duration. All re-equilibration $CaCO_3$ precipitates were made using same Na_2CO_3 - isotopic composition indicated in chart.

Precipitation Method	Precipitate ID	Repeat	DIC Equilibration Time (Days)	Time in Soln' (days)	Exp Condition	Na_2CO_3 Parent Soln ID	$CaCl_2$ Parent Soln' ID	Initial pH (in PS)	Final pH (in RS)	Sample Weight (mg)	Mineralogy	Isotopic Compositions of Parent Materials (‰)				Isotopic composition of precipitates (‰)		$\alpha_{CaCO3\text{-}H2O}$	$1000ln\alpha_{(CaCO3\text{-}H2O)}$
												$\delta^{13}C_{CarbSource}$	$\delta^{18}O_{CarbSource}$	$\delta18O_{PS}$ (VSMOW)	$\delta18O_{RS}$ (VSMOW)	$\delta^{13}C$ (VPDB)	$\delta^{18}O$ (VSMOW)		
Alkaline Method (AM)	RE-AM•0W	1	74	0	NRE	Na_2CO_3/NaOH•II	$CaCl_2$•V	12.70	N/A	63.62	ACC	-21.15	8.18	-6.45	N/A	-18.72	11.96	1.01853	18.36
		2	74	0	NRE	Na_2CO_3/NaOH•II	$CaCl_2$•V	12.77	N/A	64.41	ACC	-21.15	8.18	-6.45	N/A	-18.90	12.11	1.01868	18.51
		3	74	0	NRE	Na_2CO_3/NaOH•II	$CaCl_2$•V	12.77	N/A	62.45	ACC	-21.15	8.18	-6.45	N/A	-18.64	12.24	1.01882	18.64
	AM•0W•86dEQT	1▲	86	0	NRE	Na_2CO_3/NaOH•III	$CaCl_2$•VI	13.12	N/A	64.44	ACC	-21.15	8.18	-6.45	N/A	-19.00	12.52	1.01910	18.92
	AM•0W•144dEQT	1▲	144	0	NRE	Na_2CO_3/NaOH•III	$CaCl_2$•VI	13.32	N/A	64.24	ACC	-21.15	8.18	-6.45	N/A	-19.40	13.87	1.02045	20.25
		2▲	144	0	NRE	Na_2CO_3/NaOH•III	$CaCl_2$•VI	13.39	N/A	59.84	ACC	-21.15	8.18	-6.45	N/A	-19.14	13.81	1.02040	20.19
	RE-AM•2W	1	74	14	NRE	Na_2CO_3/NaOH•II	$CaCl_2$•V	12.97	13.30	54.03	C	-21.15	8.18	-6.45	9.670	-19.72	11.54	1.01811	17.95
	RE-AM•1W•RS	1	74	7	RE	Na_2CO_3/NaOH•II	$CaCl_2$•V	12.97	11.29	40.17	C	-21.15	8.18	-6.45	9.670	-20.33	11.78	1.01836	18.19
		2	74	7	RE	Na_2CO_3/NaOH•II	$CaCl_2$•V	12.95	11.27	41.79	C	-21.15	8.18	-6.45	9.670	-20.49	11.85	1.01842	18.26
		3	74	7	RE	Na_2CO_3/NaOH•II	$CaCl_2$•V	13.20	11.27	43.6	C	-21.15	8.18	-6.45	9.670	-20.21	11.80	1.01837	18.21
	RE-AM•2W•RS	1	74	14	RE	Na_2CO_3/NaOH•II	$CaCl_2$•V	12.86	11.37	39.36	C	-21.15	8.18	-6.45	9.670	-19.92	11.75	1.01832	18.15
		2	74	14	RE	Na_2CO_3/NaOH•II	$CaCl_2$•V	12.91	11.42	36.76	C	-21.15	8.18	-6.45	9.670	-20.20	11.56	1.01813	17.97
		3	74	14	RE	Na_2CO_3/NaOH•II	$CaCl_2$•V	12.84	11.46	36.89	C	-21.15	8.18	-6.45	9.670	-20.67	11.67	1.01824	18.08
	RE-[AM•4W•NS•2]•RS•2W	1*	74	14	RE	Na_2CO_3/NaOH•I	$CaCl_2$•I	13.36	10.42	54.18	C	-2.34	14.15	-6.45	N/A	-3.52	15.51	1.02211	21.86
		2**	74	14	RE	Na_2CO_3/NaOH•I	$CaCl_2$•I	13.30	10.47	55.25	C	-2.34	14.15	-6.45	9.670	-2.80	15.81	1.02240	22.16
	▲Refers to ACC prepared from parent solution that has been equilibrated for 86 or 144 days to determine if DIC-H2O equilibrium has been reached.																		
Silica Method (SM)	RE-SM•0W	1	74	0	NRE	Na_2CO_3/SiO_2•II	$CaCl_2$•V	10.37	N/A	130.93	ACC	-21.15	8.18	-6.45	N/A	-17.88	21.19	1.02782	27.44
		2	74	0	NRE	Na_2CO_3/SiO_2•II	$CaCl_2$•V	10.37	N/A	126.74	ACC	-21.15	8.18	-6.45	N/A	-18.82	20.89	1.02752	27.15
		3	74	0	NRE	Na_2CO_3/SiO_2•II	$CaCl_2$•V	10.40	N/A	125.08	ACC	-21.15	8.18	-6.41	N/A	-18.63	21.06	1.02764	27.27
	RE-SM•2W	1	74	14	NRE	Na_2CO_3/SiO_2•II	$CaCl_2$•V	10.61	10.67	103.47	ACC/C/M	-21.15	8.18	-6.45	9.670	-3.12	20.78	1.02741	27.04
	RE-SM•1W•RS	1	74	7	RE	Na_2CO_3/SiO_2•II	$CaCl_2$•V	10.61	10.63	89.6	ACC/C/M	-21.15	8.18	-6.45	9.670	-20.43	22.89	1.02954	29.11
		2	74	7	RE	Na_2CO_3/SiO_2•II	$CaCl_2$•V	10.49	10.61	94.17	ACC/C/M	-21.15	8.18	-6.45	9.670	-20.42	22.94	1.02958	29.15
		3	74	7	RE	Na_2CO_3/SiO_2•II	$CaCl_2$•V	10.50	10.63	87.34	ACC/C/M	-21.15	8.18	-6.45	9.670	-20.31	22.71	1.02936	28.93
	RE-SM•2W•RS	1	74	14	RE	Na_2CO_3/SiO_2•II	$CaCl_2$•V	10.49	10.71	87.34	ACC/C/M	-21.15	8.18	-6.45	9.670	-19.87	23.72	1.03037	29.92
		2	74	14	RE	Na_2CO_3/SiO_2•II	$CaCl_2$•V	10.50	10.77	87.95	ACC/C/M	-21.15	8.18	-6.45	9.670	-19.33	24.19	1.03084	30.38
		3	74	14	RE	Na_2CO_3/SiO_2•II	$CaCl_2$•V	10.49	10.70	74.97	ACC/C/M	-21.15	8.18	-6.45	9.670	-18.54	26.29	1.03296	32.43
	RE-[SM•4W•NS•2]•RS•2W	1*	74	14	RE	Na_2CO_3/SiO_2•I	$CaCl_2$•II	10.68	10.30	93.91	ACC/C	-2.34	14.15	-6.45	N/A	-19.75	22.07	1.02871	28.30
		2**	74	14	RE	Na_2CO_3/SiO_2•I	$CaCl_2$•II	10.69	10.27	91.86	ACC/C	-2.34	14.15	-6.45	9.670	-3.18	21.71	1.02835	27.95

*Original AM- and SM-$CaCO_3$ precipitates used for P•ACC•C

	Re-Equilibration Precipitate ID	Repeat	Original Sample ID	Weight added to RS (mg)	Original $\delta^{13}C$	Original $\delta^{18}O$	Original $\alpha_{CaCO3\text{-}H2O}$	Original $1000ln\alpha_{(CaCO3\text{-}H2O)}$
AM	RE-[AM•4W•NS•2]•RS•2W	1*	AM•4W•NS•2	62.70	-3.82	15.41	1.02197	21.73
		2**	AM•4W•NS•3	66.00	-2.94	15.58	1.02213	21.89
SM	RE-[SM•4W•NS•2]•RS•2W	1*	SM•4W•NS•2	123.57	-2.42	20.47	1.02706	26.70
		2**	SM•4W•NS•3	124.11	-2.45	20.93	1.02751	27.14

0 – Refers to ACC that is filtered immediately following precipitation, (NRE) – Non-Re-Equilibration, ACC is not added to ^{18}O enriched RS, (RE) –Re-Equilibration, ACC is added to ^{18}O enriched RS

(ACC) Amorphous Calcium Carbonate, (C) Calcite, (M) Monohydrocalcite

N/A: Not applicable

PS: Parent Solution, RS: Re-Equilibration Solution

References

Addadi, L., Raz, S., & Weiner, S. (2003). Taking Advantage of Disorder: Amorphous Calcium Carbonate and Its Roles in Biomineralization. *Advanced Materials*, *15*(12), 959–970. https://doi.org/10.1002/adma.200300381

Aizenberg, J. (1996). Stabilization of amorphous calcium carbonate by specialized macromolecules in biological and synthetic precipitates. *Advanced Materials*, *8*(3), 222–226. https://doi.org/10.1002/adma.19960080307

Aizenberg, J., Addadi, L., Weiner, S., & Lambert, G. (1996). Stabilization of amorphous calcium carbonate by specialized macromolecules in biological and synthetic precipitates. *Advanced Materials*, *8*(3), 222–226. https://doi.org/10.1002/adma.19960080307

Aizenberg, J., Lambert, G., Weiner, S., & Addadi, L. (2002). Factors Involved in the Formation of Amorphous and Crystalline Calcium Carbonate: A Study of an Ascidian Skeleton. *Journal of the American Chemical Society*, *124*(1), 32–39. https://doi.org/10.1021/ja016990l

Aizenberg, J., Weiner, S., & Addadi, L. (2003). Coexistence of amorphous and crystalline calcium carbonate in skeletal tissues. *Connective Tissue Research*, *44*(SUPPL. 1), 20–25. https://doi.org/10.1080/03008200390152034

Ajikumar, P. K., Ling, G. W., Subramanyam, G., Lakshminarayanan, R., & Valiyaveettil, S. (2005). Synthesis and characterization of monodispersed spheres of amorphous calcium carbonate and calcite spherules. *Crystal Growth and Design*, *5*(3), 1129–1134. https://doi.org/10.1021/cg049606f

Akiva-Tal, A., Kababya, S., Balazs, Y. S., Glazer, L., Berman, A., Sagi, A., & Schmidt, A. (2011). In situ molecular NMR picture of bioavailable calcium stabilized as amorphous CaCO 3 biomineral in crayfish gastroliths. *Proceedings of the National Academy of Sciences of the United States of America*, *108*(36), 14763–14768. https://doi.org/10.1073/pnas.1102608108

Al-Horani, F. A., Al-Moghrabi, S. M., & De Beer, D. (2003). The mechanism of calcification and its relation to photosynthesis and respiration in the scleractinian coral Galaxea fascicularis. *Marine Biology*, *142*(3), 419–426. https://doi.org/10.1007/S00227-002-0981-8/FIGURES/7

Albéric, M., Bertinetti, L., Zou, Z., Fratzl, P., Habraken, W., & Politi, Y. (2018). The Crystallization of Amorphous Calcium Carbonate is Kinetically Governed by Ion Impurities and Water. *Advanced Science*, *5*(5), 1701000. https://doi.org/10.1002/advs.201701000

Atkins, E. (1978). Elements of X-ray Diffraction. *Physics Bulletin*, *29*(12), 572–572. https://doi.org/10.1088/0031-9112/29/12/034

Beck, W. C., Grossman, E. L., & Morse, J. W. (2005). Experimental studies of oxygen isotope fractionation in the carbonic acid system at 15°, 25°, and 40°C. *Geochimica et Cosmochimica Acta*, *69*(14), 3493–3503. https://doi.org/10.1016/j.gca.2005.02.003

Becker, A., Bismayer, U., Epple, M., Fabritius, H., Hasse, B., Shi, J., & Ziegler, A. (2003). Structural characterisation of X-ray amorphous calcium carbonate (ACC) in sternal deposits of the crustacea Porcellio scaber. *Journal of the Chemical Society. Dalton Transactions*, *3*(4), 551–555. https://doi.org/10.1039/b210529b

Becker, A., Ziegler, A., & Epple, M. (2005). The mineral phase in the cuticles of two species of Crustacea consists of magnesium calcite, amorphous calcium carbonate, and amorphous calcium phosphate. *Dalton Transactions*, *10*, 1814. https://doi.org/10.1039/b412062k

Beniash, E., Addadi, L., & Weiner, S. (1999). Cellular Control Over Spicule Formation in Sea Urchin Embryos: A Structural Approach. *Journal of Structural Biology*, *125*(1), 50–62. https://doi.org/10.1006/jsbi.1998.4081

Beniash, E., Aizenberg, J., Addadi, L., & Weiner, S. (1997). Amorphous calcium carbonate transforms into calcite during sea urchin larval spicule growth. *Proceedings of the Royal Society of London. Series B: Biological Sciences*, *264*(1380), 461–465. https://doi.org/10.1098/rspb.1997.0066

Beniash, E., Metzler, R. A., Lam, R. S. K., & Gilbert, P. U. P. A. (2009). Transient amorphous calcium phosphate in forming enamel. *Journal of Structural Biology*, *166*(2), 133–143. https://doi.org/10.1016/j.jsb.2009.02.001

Bentov, S., Brownlee, C., & Erez, J. (2009). The role of seawater endocytosis in the biomineralization process in calcareous foraminifera. *Proceedings of the National Academy of Sciences of the United*

States of America, *106*(51), 21500–21504. https://doi.org/10.1073/pnas.0906636106

Bentov, S., Weil, S., Glazer, L., Sagi, A., & Berman, A. (2010). Stabilization of amorphous calcium carbonate by phosphate rich organic matrix proteins and by single phosphoamino acids. *Journal of Structural Biology*, *171*(2), 207–215. https://doi.org/10.1016/j.jsb.2010.04.007

Bergwerff, L., & van Paassen, L. A. (2021). Review and recalculation of growth and nucleation kinetics for calcite, vaterite and amorphous calcium carbonate. In *Crystals* (Vol. 11, Issue 11, p. 1318). Multidisciplinary Digital Publishing Institute. https://doi.org/10.3390/cryst11111318

Bewernitz, M. A., Gebauer, D., Long, J., Cölfen, H., & Gower, L. B. (2012). A metastable liquid precursor phase of calcium carbonate and its interactions with polyaspartate. *Faraday Discussions*, *159*, 291–312. https://doi.org/10.1039/c2fd20080e

Blue, C. R., Rimstidt, J. D., & Dove, P. M. (2013). A Mixed Flow Reactor Method to Synthesize Amorphous Calcium Carbonate Under Controlled Chemical Conditions. In *Methods in Enzymology* (Vol. 532, pp. 557–568). Academic Press Inc. https://doi.org/10.1016/B978-0-12-416617-2.00023-0

Brecevic, L., & Kralj, D. (2008). ChemInform Abstract: On Calcium Carbonates: From Fundamental Research to Application. *ChemInform*, *39*(5), 467–484. https://doi.org/10.1002/chin.200805226

Cai, G. Bin, Zhao, G. X., Wang, X. K., & Yu, S. H. (2010). Synthesis of polyacrylic acid stabilized amorphous calcium carbonate nanoparticles and their application for removal of toxic heavy metal ions in water. *Journal of Physical Chemistry C*, *114*(30), 12948–12954. https://doi.org/10.1021/jp103464p

Cartwright, J. H. E., Checa, A. G., Gale, J. D., Gebauer, D., & Sainz-Díaz, C. I. (2012). Calcium Carbonate Polyamorphism and Its Role in Biomineralization: How Many Amorphous Calcium Carbonates Are There? *Angewandte Chemie International Edition*, *51*(48), 11960–11970. https://doi.org/10.1002/anie.201203125

Chen, S. F., Cölfen, H., Antonietti, M., & Yu, S. H. (2013). Ethanol assisted synthesis of pure and stable amorphous calcium carbonate nanoparticles. *Chemical Communications*, *49*(83), 9564–9566. https://doi.org/10.1039/c3cc45427d

Cohn, M., & Urey, H. C. (1938). Oxygen Exchange Reactions of Organic Compounds and Water. *Journal of the American Chemical Society*, *60*(3), 679–687. https://doi.org/10.1021/ja01270a052

Cölfen, H. (2010). A crystal-clear view. In *Nature Materials* (Vol. 9, Issue 12, pp. 960–961). https://doi.org/10.1038/nmat2911

Coplen, T.B., & Schlanger, S. O. (1973). Oxygen and Carbon Isotope Studies of Carbonate Sediments from Site 167, Magellan Rise, Leg 17. In *Initial Reports of the Deep Sea Drilling Project, 17*. U.S. Government Printing Office. https://doi.org/10.2973/dsdp.proc.17.115.1973

Coplen, Tyler B. (2007). Calibration of the calcite-water oxygen-isotope geothermometer at Devils Hole, Nevada, a natural laboratory. *Geochimica et Cosmochimica Acta*, *71*(16), 3948–3957. https://doi.org/10.1016/j.gca.2007.05.028

Coronado, I., Fine, M., Bosellini, F. R., & Stolarski, J. (2019). Impact of ocean acidification on crystallographic vital effect of the coral skeleton. *Nature Communications*, *10*(1). https://doi.org/10.1038/s41467-019-10833-6

Costa, S. N., Freire, V. N., Caetano, E. W. S., Maia, F. F., Barboza, C. A., Fulco, U. L., & Albuquerque, E. L. (2016). DFT Calculations with van der Waals Interactions of Hydrated Calcium Carbonate Crystals CaCO3·(H2O, 6H2O): Structural, Electronic, Optical, and Vibrational Properties. *Journal of Physical Chemistry A*, *120*(28), 5752–5765. https://doi.org/10.1021/acs.jpca.6b05436

Cullity, B. D. (Bernard D. (2001). Elements of x-ray diffraction / B.D. Cullity, S.R. Stock. In *Book*. Prentice Hall,. https://discovery.mcmaster.ca/iii/encore/record/C__Rb1167916__SElements of x-ray diffraction__Orightresult__U__X6?lang=eng&suite=def

Darkins, R., Côté, A. S., Freeman, C. L., & Duffy, D. M. (2013). Crystallisation rates of calcite from an amorphous precursor in confinement. *Journal of Crystal Growth*, *367*, 110–114. https://doi.org/10.1016/j.jcrysgro.2012.12.027

De Nooijer, L. J., Toyofuku, T., & Kitazato, H. (2009). Foraminifera promote calcification by elevating their intracellular pH. *Proceedings of the National Academy of Sciences*, *106*(36), 15374–15378. https://doi.org/10.1073/PNAS.0904306106

De Yoreo, J. J., Gilbert, P. U. P. A., Sommerdijk, N. A. J. M., Penn, R. L., Whitelam, S., Joester, D., Zhang, H., Rimer, J. D., Navrotsky, A., Banfield, J. F., Wallace, A. F., Michel, F. M., Meldrum, F. C., Cölfen, H., & Dove, P. M. (2015). Crystallization by particle attachment in synthetic, biogenic, and geologic environments. In *Science* (Vol. 349, Issue 6247). https://doi.org/10.1126/science.aaa6760

Demény, A., Czuppon, G., Kern, Z., Leél-Őssy, S., Németh, A., Szabó, M., Tóth, M., Wu, C. C., Shen, C. C., Molnár, M., Németh, T., Németh, P., & Óvári, M. (2016). Recrystallization-induced oxygen isotope changes in inclusion-hosted water of speleothems – Paleoclimatological implications. *Quaternary International*, *415*, 25–32. https://doi.org/10.1016/j.quaint.2015.11.137

Demény, A., Németh, P., Czuppon, G., Leél-Ossy, S., Szabó, M., Judik, K., Németh, T., & Stieber, J. (2016). Formation of amorphous calcium carbonate in caves and its implications for speleothem research. *Scientific Reports*, *6*(1), 39602. https://doi.org/10.1038/srep39602

Devriendt, L. S., Watkins, J. M., & McGregor, H. V. (2017). Oxygen isotope fractionation in the CaCO3-DIC-H2O system. *Geochimica et Cosmochimica Acta*, *214*, 115–142. https://doi.org/10.1016/j.gca.2017.06.022

Dietzel, M., Purgstaller, B., Kluge, T., Leis, A., & Mavromatis, V. (2020). Oxygen and clumped isotope fractionation during the formation of Mg calcite via an amorphous precursor. *Geochimica et Cosmochimica Acta*, *276*, 258–273. https://doi.org/10.1016/j.gca.2020.02.032

DIFFRAC.EVA | Bruker. (n.d.). Retrieved December 3, 2021, from https://www.bruker.com/en/products-and-solutions/diffractometers-and-scattering-systems/x-ray-diffractometers/diffrac-suite-software/diffrac-eva.html

Douglas, R. C., & Savin, S. M. (1975). Oxygen and Carbon Isotope Analyses of Tertiary and Cretaceous Microfossils from Shatsky Rise and Other Sites in the North Pacific Ocean. In *Initial Reports of the Deep Sea Drilling Project, 32*. U.S. Government Printing Office. https://doi.org/10.2973/dsdp.proc.32.115.1975

Emiliani, C. (1966). Isotopic Paleotemperatures. *Science*, *154*(3751), 851–857.

https://doi.org/10.1126/science.154.3751.851

Epstein, S., & Mayeda, T. (1953). Variation of O18 content of waters from natural sources. *Geochimica et Cosmochimica Acta*, *4*(5), 213–224. https://doi.org/10.1016/0016-7037(53)90051-9

Epstein, Samuel, Buchsbaum, R., Lowenstam, H., & Urey, H. C. (1951). Carbonate-water isotopic temperature scale. *Bulletin of the Geological Society of America*, *62*(4), 417–426. https://doi.org/10.1130/0016-7606(1951)62[417:CITS]2.0.CO;2

Erez, J. (1978). *Vital Effect in Coral & Foram*.

Evans, D., Webb, P. B., Penkman, K., Kröger, R., & Allison, N. (2019). The Characteristics and Biological Relevance of Inorganic Amorphous Calcium Carbonate (ACC) Precipitated from Seawater. *Crystal Growth and Design*, *19*(8), 4300–4313. https://doi.org/10.1021/acs.cgd.9b00003

Fairchild, I. J., Smith, C. L., Baker, A., Fuller, L., Spötl, C., Mattey, D., & McDermott, F. (2006). Modification and preservation of environmental signals in speleothems. *Earth-Science Reviews*, *75*(1–4), 105–153. https://doi.org/10.1016/j.earscirev.2005.08.003

Farhadi Khouzani, M., Chevrier, D. M., Güttlein, P., Hauser, K., Zhang, P., Hedin, N., & Gebauer, D. (2015). Disordered amorphous calcium carbonate from direct precipitation. *CrystEngComm*, *17*(26), 4842–4849. https://doi.org/10.1039/c5ce00720h

Frisia, S., Borsato, A., Fairchild, I. J., McDermott, F., & Selmo, E. M. (2002). Aragonite-Calcite Relationships in Speleothems (Grotte De Clamouse, France): Environment, Fabrics, and Carbonate Geochemistry. *Journal of Sedimentary Research*, *72*(5), 687–699. https://doi.org/10.1306/020702720687

Gabitov, R. I., Watson, E. B., Sadekov, A., Watson, B. E., & Sadekov, A. (2012). Oxygen isotope fractionation between calcite and fluid as a function of growth rate and temperature: An in situ study. *Chemical Geology*, *306–307*, 92–102. https://doi.org/10.1016/j.chemgeo.2012.02.021

Gago-Duport, L., Briones, M. J. I., Rodríguez, J. B., & Covelo, B. (2008). Amorphous calcium carbonate biomineralization in the earthworm's calciferous gland: Pathways to the formation of crystalline phases. *Journal of Structural Biology*, *162*(3), 422–435. https://doi.org/10.1016/j.jsb.2008.02.007

Gal, A., Weiner, S., & Addadi, L. (2010). The stabilizing effect of silicate on biogenic and synthetic amorphous calcium carbonate. *Journal of the American Chemical Society*, *132*(38), 13208–13211. https://doi.org/10.1021/ja106883c

Gayathri, S., Lakshminarayanan, R., Weaver, J. C., Morse, D. E., Manjunatha Kini, R., & Valiyaveettil, S. (2007). In vitro study of magnesium-calcite biomineralization in the skeletal materials of the seastar Pisaster giganteus. *Chemistry - A European Journal*, *13*(11), 3262–3268. https://doi.org/10.1002/chem.200600825

Gebauer, D., Gunawidjaja, P. N., Ko, J. Y. P., Bacsik, Z., Aziz, B., Liu, L., Hu, Y., Bergström, L., Tai, C. W., Sham, T. K., Edén, M., & Hedin, N. (2010). Proto-calcite and proto-vaterite in amorphous calcium carbonates. *Angewandte Chemie - International Edition*, *49*(47), 8889–8891. https://doi.org/10.1002/anie.201003220

Gebauer, D., Völkel, A., & Cölfen, H. (2008). Stable prenucleation calcium carbonate clusters. *Science*, *322*(5909), 1819–1822. https://doi.org/10.1126/science.1164271

Ghosh, P., Adkins, J., Affek, H., Balta, B., Guo, W., Schauble, E. A., Schrag, D., & Eiler, J. M. (2006). 13C-18O bonds in carbonate minerals: A new kind of paleothermometer. *Geochimica et Cosmochimica Acta*, *70*(6), 1439–1456. https://doi.org/10.1016/j.gca.2005.11.014

Giuffre, A. J., Gagnon, A. C., De Yoreo, J. J., & Dove, P. M. (2015). Isotopic tracer evidence for the amorphous calcium carbonate to calcite transformation by dissolution-reprecipitation. *Geochimica et Cosmochimica Acta*, *165*, 407–417. https://doi.org/10.1016/j.gca.2015.06.002

Given, R. K., & Wilkinson, B. H. (1985). Kinetic control of morphology, composition, and mineralogy of abiotic sedimentary carbonates. *Journal of Sedimentary Petrology*, *55*(1), 109–119. https://doi.org/10.1306/212f862a-2b24-11d7-8648000102c1865d

Goldstein, J. I., Yakowitz, H., Newbury, D. E., Lifshin, E., Colby, J. W., & Coleman, J. R. (1975). Practical Scanning Electron Microscopy. In *Practical Scanning Electron Microscopy*. https://doi.org/10.1007/978-1-4613-4422-3

Gower, L. B. (2008). Biomimetic model systems for investigating the amorphous precursor pathway and

its role in biomineralization. *Chemical Reviews*, *108*(11), 4551–4627. https://doi.org/10.1021/cr800443h

Günther, C., Becker, A., Wolf, G., & Epple, M. (2005). In vitro Synthesis and Structural Characterization of Amorphous Calcium Carbonate. *Zeitschrift Für Anorganische Und Allgemeine Chemie*, *631*(13–14), 2830–2835. https://doi.org/10.1002/zaac.200500164

Hasse, B., Ehrenberg, H., Marxen, J. C., Becker, W., & Epple, M. (2000). Calcium carbonate modifications in the mineralized shell of the freshwater snail Biomphalaria glabrata. *Chemistry - A European Journal*, *6*(20), 3679–3685. https://doi.org/10.1002/1521-3765(20001016)6:20<3679::AID-CHEM3679>3.0.CO;2-#

Henini, M. (2000). Scanning electron microscopy: An introduction. *III-Vs Review*, *13*(4), 40–44. https://doi.org/10.1016/S0961-1290(00)80006-X

Hillaire-Marcel, C., Kim, S.-T., Landais, A., Ghosh, P., Assonov, S., Lécuyer, C., Blanchard, M., Meijer, H. A. J., & Steen-Larsen, H. C. (2021). A stable isotope toolbox for water and inorganic carbon cycle studies. *Nature Reviews Earth & Environment*, *2*(10), 699–719. https://doi.org/10.1038/s43017-021-00209-0

Hodson, M. E., Benning, L. G., Demarchi, B., Penkman, K. E. H., Rodriguez-Blanco, J. D., Schofield, P. F., & Versteegh, E. A. A. (2015). Biomineralisation by earthworms – an investigation into the stability and distribution of amorphous calcium carbonate. *Geochemical Transactions*, *16*(1), 4. https://doi.org/10.1186/s12932-015-0019-z

Huang, S. C., Naka, K., & Chujo, Y. (2007). A carbonate controlled-addition method for amorphous calcium carbonate spheres stabilized by poly(acrylic acid)s. *Langmuir*, *23*(24), 12086–12095. https://doi.org/10.1021/la701972n

ICDD. PDF-2+. (2002). *ICDD Database Search – ICDD*. International Centre for Diffraction Data, Newtown Square. https://www.icdd.com/pdfsearch/

Ihli, J., Kim, Y. Y., Noel, E. H., & Meldrum, F. C. (2013). The effect of additives on amorphous calcium carbonate (ACC): Janus behavior in solution and the solid state. *Advanced Functional Materials*,

23(12), 1575–1585. https://doi.org/10.1002/adfm.201201805

Ihli, J., Kulak, A. N., & Meldrum, F. C. (2013). Freeze-drying yields stable and pure amorphous calcium carbonate (ACC). *Chemical Communications*, *49*(30), 3134–3136. https://doi.org/10.1039/c3cc40807h

Immenhauser, A., Schöne, B. R., Hoffmann, R., & Niedermayr, A. (2016). Mollusc and brachiopod skeletal hard parts: Intricate archives of their marine environment. *Sedimentology*, *63*(1), 1–59. https://doi.org/10.1111/sed.12231

Jacob, D. E., Soldati, A. L., Wirth, R., Huth, J., Wehrmeister, U., & Hofmeister, W. (2008). Nanostructure, composition and mechanisms of bivalve shell growth. *Geochimica et Cosmochimica Acta*, *72*(22), 5401–5415. https://doi.org/10.1016/j.gca.2008.08.019

Jacob, D. E., Wirth, R., Soldati, A. L., Wehrmeister, U., & Schreiber, A. (2011). Amorphous calcium carbonate in the shells of adult Unionoida. *Journal of Structural Biology*, *173*(2), 241–249. https://doi.org/10.1016/j.jsb.2010.09.011

Jung, G. Y., Shin, E., Park, J. H., Choi, B. Y., Lee, S. W., & Kwak, S. K. (2019). Thermodynamic Control of Amorphous Precursor Phases for Calcium Carbonate via Additive Ions. *Chemistry of Materials*, *31*(18), 7547–7557. https://doi.org/10.1021/acs.chemmater.9b02346

Kellermeier, M., Melero-García, E., Glaab, F., Klein, R., Drechsler, M., Rachel, R., García-Ruiz, J. M., & Kunz, W. (2010). Stabilization of Amorphous Calcium Carbonate in Inorganic Silica-Rich Environments. *Journal of the American Chemical Society*, *132*(50), 17859–17866. https://doi.org/10.1021/ja106959p

Kim, S.-T., Coplen, T. B., & Horita, J. (2015). Normalization of stable isotope data for carbonate minerals: Implementation of IUPAC guidelines. *Geochimica et Cosmochimica Acta*, *158*, 276–289. https://doi.org/10.1016/j.gca.2015.02.011

Kim, S.-T., Hillaire-Marcel, C., & Mucci, A. (2006). Mechanisms of equilibrium and kinetic oxygen isotope effects in synthetic aragonite at 25 °C. *Geochimica et Cosmochimica Acta*, *70*(23 SPEC. ISS.), 5790–5801. https://doi.org/10.1016/j.gca.2006.08.003

Kim, S.-T., & O'Neil, J. R. (1997). Equilibrium and nonequilibrium oxygen isotope effects in synthetic carbonates. *Geochimica et Cosmochimica Acta*, *61*(16), 3461–3475. https://doi.org/10.1016/S0016-7037(97)00169-5

Kim, S. T., O'Neil, J. R., Hillaire-Marcel, C., & Mucci, A. (2007). Oxygen isotope fractionation between synthetic aragonite and water: Influence of temperature and Mg2+ concentration. *Geochimica et Cosmochimica Acta*, *71*(19), 4704–4715. https://doi.org/10.1016/j.gca.2007.04.019

Kimura, T., & Koga, N. (2011). Monohydrocalcite in comparison with hydrated amorphous calcium carbonate: Precipitation condition and thermal behavior. *Crystal Growth and Design*, *11*(9), 3877–3884. https://doi.org/10.1021/cg200412h

Kitano, Y., Okumura, M., & Idogaki, M. (1979). Behavior of dissolved silica in parent solution at the formation of calcium carbonate. *Geochemical Journal*, *13*(6), 253–260. https://doi.org/10.2343/geochemj.13.253

Koga, N., Nakagoe, Y., & Tanaka, H. (1998). Crystallization of amorphous calcium carbonate. *Thermochimica Acta*, *318*(1–2), 239–244. https://doi.org/10.1016/S0040-6031(98)00348-7

Koga, N., & Yamane, Y. (2008). Thermal behaviors of amorphous calcium carbonates prepared in aqueous and ethanol media. *Journal of Thermal Analysis and Calorimetry*, *94*(2), 379–387. https://doi.org/10.1007/s10973-008-9110-3

Köhler-Rink, S., & Kühl, M. (2007). The chemical microenvironment of the symbiotic planktonic foraminifer Orbulina universa. *Http://Dx.Doi.Org/10.1080/17451000510019015*, *1*(1), 68–78. https://doi.org/10.1080/17451000510019015

Kojima, Y., Sakama, K., Toyama, T., Yasue, T., & Arai, Y. (1994). Dehydration of the Water Molecule in Amorphous Calcium Phosphate. *Phosphorus Research Bulletin*, *4*, 47–52. https://doi.org/10.3363/prb1992.4.0_47

Konrad, F., Gallien, F., Gerard, D. E., & Dietzel, M. (2016). Transformation of Amorphous Calcium Carbonate in Air. *Crystal Growth and Design*, *16*(11), 6310–6317. https://doi.org/10.1021/acs.cgd.6b00906

Kontoyannis, C. G., & Vagenas, N. V. (2000). Calcium carbonate phase analysis using XRD and FT-Raman spectroscopy. *The Analyst*, *125*(2), 251–255. https://doi.org/10.1039/a908609i

Labuhn, I., Genty, D., Vonhof, H., Bourdin, C., Blamart, D., Douville, E., Ruan, J., Cheng, H., Edwards, R. L., Pons-Branchu, E., & Pierre, M. (2015). A high-resolution fluid inclusion δ18O record from a stalagmite in SW France: Modern calibration and comparison with multiple proxies. *Quaternary Science Reviews*, *110*, 152–165. https://doi.org/10.1016/j.quascirev.2014.12.021

Lachniet, M. S. (2009). Climatic and environmental controls on speleothem oxygen-isotope values. *Quaternary Science Reviews*, *28*(5–6), 412–432. https://doi.org/10.1016/j.quascirev.2008.10.021

Lam, R. S. K., Charnock, J. M., Lennie, A., & Meldrum, F. C. (2007). Synthesis-dependant structural variations in amorphous calcium carbonate. *CrystEngComm*, *9*(12), 1226–1236. https://doi.org/10.1039/b710895h

Lee, H. S., Ha, T. H., & Kim, K. (2005). Fabrication of unusually stable amorphous calcium carbonate in an ethanol medium. *Materials Chemistry and Physics*, *93*(2–3), 376–382. https://doi.org/10.1016/j.matchemphys.2005.03.037

Lee, M. R., Hodson, M. E., & Langworthy, G. N. (2008). Crystallization of calcite from amorphous calcium carbonate: earthworms show the way. *Mineralogical Magazine*, *72*(1), 257–261. https://doi.org/10.1180/minmag.2008.072.1.257

Levi-Kalisman, Y., Raz, S., Weiner, S., Addadi, L., & Sagi, I. (2002). Structural differences between biogenic amorphous calcium carbonate phases using X-ray absorption spectroscopy. *Advanced Functional Materials*, *12*(1), 43–48. https://doi.org/10.1002/1616-3028(20020101)12:1<43::AID-ADFM43>3.0.CO;2-C

Levi-Kalisman, Yael, Raz, S., Weiner, S., Addadi, L., & Sagi, I. (2000). X-Ray absorption spectroscopy studies on the structure of a biogenic "amorphous" calcium carbonate phase †. *Journal of the Chemical Society, Dalton Transactions*, *21*, 3977–3982. https://doi.org/10.1039/b003242p

Lewis, I. R., & Edwards, H. (2001). Handbook of Raman Spectroscopy. *Handbook of Raman Spectroscopy*. https://doi.org/10.1201/9781420029253

Li, J., Chen, Z., Wang, R. J., & Proserpio, D. M. (1999). Low temperature route towards new materials: solvothermal synthesis of metal chalcogenides in ethylenediamine. *Coordination Chemistry Reviews*, *190–192*, 707–735. https://doi.org/10.1016/S0010-8545(99)00107-1

Lowenstam, H. A, & Epstein, S. (1954). Paleotemperatures of the Post-Aptian Cretaceous as Determined by the Oxygen Isotope Method. *The Journal of Geology*, *62*(3), 207–248. https://doi.org/10.1086/626160

Lowenstam, Heinz A. (1972). Phosphatic hard tissues of marine invertebrates: Their nature and mechanical function, and some fossil implications. *Chemical Geology*, *9*(1–4), 153–166. https://doi.org/10.1016/0009-2541(72)90053-8

Mass, T., Giuffre, A. J., Sun, C. Y., Stifler, C. A., Frazier, M. J., Neder, M., Tamura, N., Stan, C. V., Marcus, M. A., & Gilbert, P. U. P. A. (2017). Amorphous calcium carbonate particles form coral skeletons. *Proceedings of the National Academy of Sciences of the United States of America*, *114*(37), E7670–E7678. https://doi.org/10.1073/pnas.1707890114

Mavromatis, V., Purgstaller, B., Dietzel, M., Buhl, D., Immenhauser, A., & Schott, J. (2017). Impact of amorphous precursor phases on magnesium isotope signatures of Mg-calcite. *Earth and Planetary Science Letters*, *464*, 227–236. https://doi.org/10.1016/j.epsl.2017.01.031

McConnaughey, T. (1989a). 13C and 18O isotopic disequilibrium in biological carbonates: I. Patterns. *Geochimica et Cosmochimica Acta*, *53*(1), 151–162. https://doi.org/10.1016/0016-7037(89)90282-2

McConnaughey, T. (1989b). 13C and 18O isotopic disequilibrium in biological carbonates: II. In vitro simulation of kinetic isotope effects. *Geochimica et Cosmochimica Acta*, *53*(1), 163–171. https://doi.org/10.1016/0016-7037(89)90283-4

McCrea, J. M. (1950). On the Isotopic Chemistry of Carbonates and a Paleotemperature Scale. *The Journal of Chemical Physics*, *18*(6), 849–857. https://doi.org/10.1063/1.1747785

McDermott, F. (2004). Palaeo-climate reconstruction from stable isotope variations in speleothems: A review. *Quaternary Science Reviews*, *23*(7–8), 901–918. https://doi.org/10.1016/j.quascirev.2003.06.021

Meldrum, F. C. (2003). Calcium carbonate in biomineralisation and biomimetic chemistry. In *International Materials Reviews* (Vol. 48, Issue 3, pp. 187–224). https://doi.org/10.1179/095066003225005836

Meldrum, F. C., & O'Shaughnessy, C. (2020). Crystallization in Confinement. In *Advanced Materials* (Vol. 32, Issue 31, p. 2001068). John Wiley & Sons, Ltd. https://doi.org/10.1002/adma.202001068

Michel, F. M., MacDonald, J., Feng, J., Phillips, B. L., Ehm, L., Tarabrella, C., Parise, J. B., & Reeder, R. J. (2008). Structural characteristics of synthetic amorphous calcium carbonate. *Chemistry of Materials*, *20*(14), 4720–4728. https://doi.org/10.1021/cm800324v

Nakashima, Y., Takai, C., Razavi-Khosroshahi, H., Suthabanditpong, W., & Fuji, M. (2018). Synthesis of ultra-small hollow silica nanoparticles using the prepared amorphous calcium carbonate in one-pot process. *Advanced Powder Technology*, *29*(4), 904–908. https://doi.org/10.1016/j.apt.2018.01.006

Navrotsky, A. (2004). Energetic clues to pathways to biomineralization: Precursors, clusters, and nanoparticles. *Proceedings of the National Academy of Sciences of the United States of America*, *101*(33), 12096–12101. https://doi.org/10.1073/pnas.0404778101

Neumann, M., & Epple, M. (2007). Monohydrocalcite and its relationship to hydrated amorphous calcium carbonate in biominerals. *European Journal of Inorganic Chemistry*, *2007*(14), 1953–1957. https://doi.org/10.1002/ejic.200601033

Njegić-Džakula, B., Brečević, L., Falini, G., & Kralj, D. (2011). Kinetic Approach to Biomineralization: Interactions of Synthetic Polypeptides with Calcium Carbonate Polymorphs. *Croatica Chemica Acta*, *84*(2), 301–314. https://doi.org/10.5562/cca1809

Northrop, D. A., & Clayton, R. N. (1966). Oxygen-Isotope Fractionations in Systems Containing Dolomite. *The Journal of Geology*, *74*(2), 174–196. https://doi.org/10.1086/627153

O'Day, P. A., Rehr, J. J., Zabinsky, S. I., & Brown, G. E. (1994). Extended X-ray Absorption Fine Structure (EXAFS) Analysis of Disorder and Multiple-Scattering in Complex Crystalline Solids. *Journal of the American Chemical Society*, *116*(7), 2938–2949. https://doi.org/10.1021/ja00086a026

Ogino, T., Suzuki, T., & Sawada, K. (1987). The formation and transformation mechanism of calcium

carbonate in water. *Geochimica et Cosmochimica Acta*, *51*(10), 2757–2767. https://doi.org/10.1016/0016-7037(87)90155-4

Ostwald, W. (1901). Reviews-On the assumed isomerism between red and yellow mercuric oxide and on the surface-tension of solids. *The Journal of Physical Chemistry*, *5*(1), 75–75. https://doi.org/10.1021/j150028a603

Paquin, F., Rivnay, J., Salleo, A., Stingelin, N., & Silva, C. (2015). Multi-phase semicrystalline microstructures drive exciton dissociation in neat plastic semiconductors. *J. Mater. Chem. C*, *3*, 10715–10722. https://doi.org/10.1039/b000000x

Pérez-Huerta, A., & C. Fred, T. A. (2010). Vital effects in the context of biomineralization. *Seminarios de La Sociedad Española de Mineralogía*, *7*, 35–45.

Ping, H., Xie, H., Wan, Y., Zhang, Z., Zhang, J., Xiang, M., Xie, J., Wang, H., Wang, W., & Fu, Z. (2016). Confinement controlled mineralization of calcium carbonate within collagen fibrils. *Journal of Materials Chemistry B*, *4*(5), 880–886. https://doi.org/10.1039/C5TB01990G

Politi, Y., Batchelor, D. R., Zaslansky, P., Chmelka, B. F., Weaver, J. C., Sagi, I., Weiner, S., & Addadi, L. (2010). Role of Magnesium Ion in the Stabilization of Biogenic Amorphous Calcium Carbonate: A Structure−Function Investigation. *Chemistry of Materials*, *22*(1), 161–166. https://doi.org/10.1021/cm902674h

Politi, Y., Levi-Kalisman, Y., Raz, S., Wilt, F., Addadi, L., Weiner, S., & Sagi, I. (2006). Structural Characterization of the Transient Amorphous Calcium Carbonate Precursor Phase in Sea Urchin Embryos. *Advanced Functional Materials*, *16*(10), 1289–1298. https://doi.org/10.1002/adfm.200600134

Purgstaller, B., Mavromatis, V., Immenhauser, A., & Dietzel, M. (2016). Transformation of Mg-bearing amorphous calcium carbonate to Mg-calcite - In situ monitoring. *Geochimica et Cosmochimica Acta*, *174*, 180–195. https://doi.org/10.1016/j.gca.2015.10.030

Radha, A. V., Forbes, T. Z., Killian, C. E., Gilbert, P. U. P. A., & Navrotsky, A. (2010). Transformation and crystallization energetics of synthetic and biogenic amorphous calcium carbonate. *Proceedings*

of the National Academy of Sciences, *107*(38), 16438–16443. https://doi.org/10.1073/pnas.1009959107

Rao, A., Vásquez-Quitral, P., Fernández, M. S., Berg, J. K., Sánchez, M., Drechsler, M., Neira-Carrillo, A., Arias, J. L., Gebauer, D., & Cölfen, H. (2016). PH-Dependent Schemes of Calcium Carbonate Formation in the Presence of Alginates. *Crystal Growth and Design*, *16*(3), 1349–1359. https://doi.org/10.1021/acs.cgd.5b01488

Raz, S., Hamilton, P. C., Wilt, F. H., Weiner, S., & Addadi, L. (2003). The Transient Phase of Amorphous Calcium Carbonate in Sea Urchin Larval Spicules: The Involvement of Proteins and Magnesium Ions in Its Formation and Stabilization. *Advanced Functional Materials*, *13*(6), 480–486. https://doi.org/10.1002/adfm.200304285

Raz, S., Testeniere, O., Hecker, A., Weiner, S., & Luquet, G. (2002). Stable amorphous calcium carbonate is the main component of the calcium storage structures of the crustacean Orchestia cavimana. *Biological Bulletin*, *203*(3), 269–274. https://doi.org/10.2307/1543569

Rodriguez-Blanco, J. D., Shaw, S., Bots, P., Roncal-Herrero, T., & Benning, L. G. (2012). The role of pH and Mg on the stability and crystallization of amorphous calcium carbonate. *Journal of Alloys and Compounds*, *536*(SUPPL.1), S477–S479. https://doi.org/10.1016/j.jallcom.2011.11.057

Rodriguez-Blanco, Juan Diego, Shaw, S., & Benning, L. G. (2011). The kinetics and mechanisms of amorphous calcium carbonate (ACC) crystallization to calcite, viavaterite. *Nanoscale*, *3*(1), 265–271. https://doi.org/10.1039/C0NR00589D

Rodriguez-Navarro, C., Kudłacz, K., Cizer, Ö., & Ruiz-Agudo, E. (2015). Formation of amorphous calcium carbonate and its transformation into mesostructured calcite. *CrystEngComm*, *17*(1), 58–72. https://doi.org/10.1039/c4ce01562b

Ross, E. E., Mok, S. W., & Bugni, S. R. (2011). Assembly of lipid bilayers on silica and modified silica colloids by reconstitution of dried lipid films. *Langmuir*, *27*(14), 8634–8644. https://doi.org/10.1021/la200952c

Roy, R. N., Roy, L. N., Vogel, K. M., Porter-Moore, C., Pearson, T., Good, C. E., Millero, F. J., &

Campbell, D. M. (1993). The dissociation constants of carbonic acid in seawater at salinities 5 to 45 and temperatures 0 to 45°C. *Marine Chemistry*, *44*(2–4), 249–267. https://doi.org/10.1016/0304-4203(93)90207-5

Saenger, C., & Wang, Z. (2014). Magnesium isotope fractionation in biogenic and abiogenic carbonates: Implications for paleoenvironmental proxies. In *Quaternary Science Reviews* (Vol. 90, pp. 1–21). Elsevier Ltd. https://doi.org/10.1016/j.quascirev.2014.01.014

Savin, S. M. (1977). The History of the Earth's Surface Temperature During the Past 100 Million Years. *Annual Review of Earth and Planetary Sciences*, *5*(1), 319–355. https://doi.org/10.1146/annurev.ea.05.050177.001535

Schmidt, M., Xeflide, S., Botz, R., & Mann, S. (2005). Oxygen isotope fractionation during synthesis of CaMg-carbonate and implications for sedimentary dolomite formation. *Geochimica et Cosmochimica Acta*, *69*(19), 4665–4674. https://doi.org/10.1016/j.gca.2005.06.025

Schwartz, A. M. (2002). Handbook of Industrial Crystallization - Chapter 01 - Solutions and solution properties. *Handbook of Industrial Crystallization*, *7*, 1–31. http://www.sciencedirect.com/science/article/pii/B9780750670128500033

Seo, K. S., Han, C., Wee, J. H., Park, J. K., & Ahn, J. W. (2005). Synthesis of calcium carbonate in a pure ethanol and aqueous ethanol solution as the solvent. *Journal of Crystal Growth*, *276*(3–4), 680–687. https://doi.org/10.1016/j.jcrysgro.2004.11.416

Setoguchi, H. (1989). Origin, Evolution, and Modern Aspects of Biomineralization in Plants and Animals. *Origin, Evolution, and Modern Aspects of Biomineralization in Plants and Animals*, *December*. https://doi.org/10.1007/978-1-4757-6114-6

Simkiss, K. (1991). Amorphous Minerals and Theories of Biomineralization. In *Mechanisms and Phylogeny of Mineralization in Biological Systems* (pp. 375–382). Springer Japan. https://doi.org/10.1007/978-4-431-68132-8_60

Smith, B. C. (2011). Fundamentals of fourier transform infrared spectroscopy, second edition. In *Fundamentals of Fourier Transform Infrared Spectroscopy, Second Edition*.

Stephens, C. J., Ladden, S. F., Meldrum, F. C., & Christenson, H. K. (2010). Amorphous calcium carbonate is stabilized in confinement. *Advanced Functional Materials*, *20*(13), 2108–2115. https://doi.org/10.1002/adfm.201000248

Swart, P. K. (2015). The geochemistry of carbonate diagenesis: The past, present and future. *Sedimentology*, *62*(5), 1233–1304. https://doi.org/10.1111/sed.12205

Taylor, M. G., Simkiss, K., Greaves, G. N., Okazaki, M., & Mann, S. (1993). An X-ray absorption spectroscopy study of the structure and transformation of amorphous calcium carbonate from plant cystoliths. *Proceedings of the Royal Society B: Biological Sciences*, *252*(1333), 75–80. https://doi.org/10.1098/rspb.1993.0048

Tester, C. C., Brock, R. E., Wu, C.-H., Krejci, M. R., Weigand, S., & Joester, D. (2011). In vitro synthesis and stabilization of amorphous calcium carbonate (ACC) nanoparticles within liposomes. *CrystEngComm*, *13*(12), 3975. https://doi.org/10.1039/c1ce05153a

Tester, C. C., Whittaker, M. L., & Joester, D. (2014). Controlling nucleation in giant liposomes. *Chemical Communications*, *50*(42), 5619–5622. https://doi.org/10.1039/c4cc01457j

Tobler, D. J., Rodriguez-Blanco, J. D., Sørensen, H. O., Stipp, S. L. S., & Dideriksen, K. (2016). Effect of pH on Amorphous Calcium Carbonate Structure and Transformation. *Crystal Growth and Design*, *16*(8), 4500–4508. https://doi.org/10.1021/acs.cgd.6b00630

Tompa, A. S., & Watabe, N. (1977). Calcified arteries in a gastropod. *Calcified Tissue Research*, *22*(1), 159–172. https://doi.org/10.1007/BF02010355

Townsend, D., Lahankar, S. A., Lee, S. K., Chambreau, S. D., Suits, A. G., Zhang, X., Rheinecker, J., Harding, L. B., & Bowman, J. M. (2004). The Roaming Atom: Straying from the Reaction Path in Formaldehyde Decomposition. *Science*, *306*(5699), 1158–1161. https://doi.org/10.1126/science.1104386

Travis, D. F. (2006). Structural features of mineralization from tissue to macromolecular levels of organization in the decapod crustacea. *Annals of the New York Academy of Sciences*, *109*(1), 177–245. https://doi.org/10.1111/j.1749-6632.1963.tb13467.x

Venn, A., Tambutté, E., Holcomb, M., Allemand, D., & Tambutté, S. (2011). Live tissue imaging shows reef corals elevate pH under their calcifying tissue relative to seawater. *PLoS ONE*, *6*(5). https://doi.org/10.1371/JOURNAL.PONE.0020013

Versteegh, E. A. A., Black, S., & Hodson, M. E. (2017). Carbon isotope fractionation between amorphous calcium carbonate and calcite in earthworm-produced calcium carbonate. *Applied Geochemistry*, *78*, 351–356. https://doi.org/10.1016/j.apgeochem.2017.01.017

Vinogradov, A. P. (1953). *The elementary chemical composition of marine organisms / A.P. Vinogradov.* https://discovery.mcmaster.ca/iii/encore/record/C__Rb2252090__SVinogradov, A. P. The Elementary Chemical Composition of Marine Organisms__Orightresult__U__X2?lang=eng&suite=def

Voorhees, P. W. (1985). The theory of Ostwald ripening. *Journal of Statistical Physics*, *38*(1–2), 231–252. https://doi.org/10.1007/BF01017860

Wang, S. S., & Xu, A. W. (2013). Amorphous calcium carbonate stabilized by a flexible biomimetic polymer inspired by marine mussels. *Crystal Growth and Design*, *13*(5), 1937–1942. https://doi.org/10.1021/cg301759t

Wang, Y., Zeng, M., Meldrum, F. C., & Christenson, H. K. (2017). Using confinement to study the crystallization pathway of calcium carbonate. *Crystal Growth and Design*, *17*(12), 6787–6792. https://doi.org/10.1021/acs.cgd.7b01359

Wang, Z. L., & Lee, J. L. (2008). Electron Microscopy Techniques for Imaging and Analysis of Nanoparticles. In *Developments in Surface Contamination and Cleaning: Second Edition* (Vol. 1, pp. 395–443). William Andrew Publishing. https://doi.org/10.1016/B978-0-323-29960-2.00009-5

Weiner, S. (2003). An Overview of Biomineralization Processes and the Problem of the Vital Effect. *Reviews in Mineralogy and Geochemistry*, *54*(1), 1–29. https://doi.org/10.2113/0540001

Weiner, S., Levi-Kalisman, Y., Raz, S., & Addadi, L. (2003). Biologically Formed Amorphous Calcium Carbonate. *Connective Tissue Research*, *44*(1), 214–218. https://doi.org/10.1080/03008200390181681

Weiss, I. M., Tuross, N., Addadi, L., & Weiner, S. (2002). Mollusc larval shell formation: amorphous calcium carbonate is a precursor phase for aragonite. *Journal of Experimental Zoology*, *293*(5), 478–491. https://doi.org/10.1002/jez.90004

Whittaker, M. L., Dove, P. M., & Joester, D. (2016). Nucleation on surfaces and in confinement. *MRS Bulletin*, *41*(5), 388–392. https://doi.org/10.1557/mrs.2016.90

Wombacher, F., Eisenhauer, A., Böhm, F., Gussone, N., Regenberg, M., Dullo, W. C., & Rüggeberg, A. (2011). Magnesium stable isotope fractionation in marine biogenic calcite and aragonite. *Geochimica et Cosmochimica Acta*, *75*(19), 5797–5818. https://doi.org/10.1016/j.gca.2011.07.017

Xto, J. M., Borca, C. N., van Bokhoven, J. A., & Huthwelker, T. (2019). Aerosol-based synthesis of pure and stable amorphous calcium carbonate. *Chemical Communications*, *55*(72), 10725–10728. https://doi.org/10.1039/c9cc03749g

Xu, N., Li, Y., Zheng, L., Gao, Y., Yin, H., Zhao, J., Chen, Z., Chen, J., & Chen, M. (2014). Synthesis and application of magnesium amorphous calcium carbonate for removal of high concentration of phosphate. *Chemical Engineering Journal*, *251*, 102–110. https://doi.org/10.1016/j.cej.2014.04.037

Xu, X. R., Cai, A. H., Liu, R., Pan, H. H., Tang, R. K., & Cho, K. (2008). The roles of water and polyelectrolytes in the phase transformation of amorphous calcium carbonate. *Journal of Crystal Growth*, *310*(16), 3779–3787. https://doi.org/10.1016/j.jcrysgro.2008.05.034

Zeebe, R. E. (1999). An explanation of the effect of seawater carbonate concentration on foraminiferal oxygen isotopes. *Geochimica et Cosmochimica Acta*, *63*(13–14), 2001–2007. https://doi.org/10.1016/S0016-7037(99)00091-5

Zeebe, R. E., & Wolf-Gladrow, D. A. (2001). CO2 in Seawater: Equilibrium, Kinetics, Isotopes. In *Elsevier*. https://linkinghub.elsevier.com/retrieve/pii/S0924796302001793

Zeebe, R. E., Wolf-Gladrow, D. A., & Jansen, H. (1999). On the time required to establish chemical and isotopic equilibrium in the carbon dioxide system in seawater. *Marine Chemistry*, *65*, 135–153.

Zhang, H., Cai, Y., Tan, L., Qin, S., & An, Z. (2014). Stable isotope composition alteration produced by the aragonite-to-calcite transformation in speleothems and implications for paleoclimate

reconstructions. *Sedimentary Geology*, *309*, 1–14. https://doi.org/10.1016/j.sedgeo.2014.05.007

Zhang, M., Li, J., Zhao, J., Cui, Y., & Luo, X. (2020). Comparison of CH4and CO2Adsorptions onto Calcite(10.4), Aragonite(011)Ca, and Vaterite(010)CO3Surfaces: An MD and DFT Investigation. *ACS Omega*, *5*(20), 11369–11377. https://doi.org/10.1021/acsomega.0c00345

Ziveri, P., Stoll, H., Probert, I., Klaas, C., Geisen, M., Ganssen, G., & Young, J. (2003). Stable isotope "vital effects" in coccolith calcite. *Earth and Planetary Science Letters*, *210*(1–2), 137–149. https://doi.org/10.1016/S0012-821X(03)00101-8

Zou, Z., Bertinetti, L., Politi, Y., Jensen, A. C. S., Weiner, S., Addadi, L., Fratzl, P., & Habraken, W. J. E. M. (2015). Supplementary - Opposite Particle Size Effect on Amorphous Calcium Carbonate Crystallization in Water and during Heating in Air. *Chemistry of Materials*, *27*(12), 4237–4246. https://doi.org/10.1021/acs.chemmater.5b00145

APPENDICES

Figures

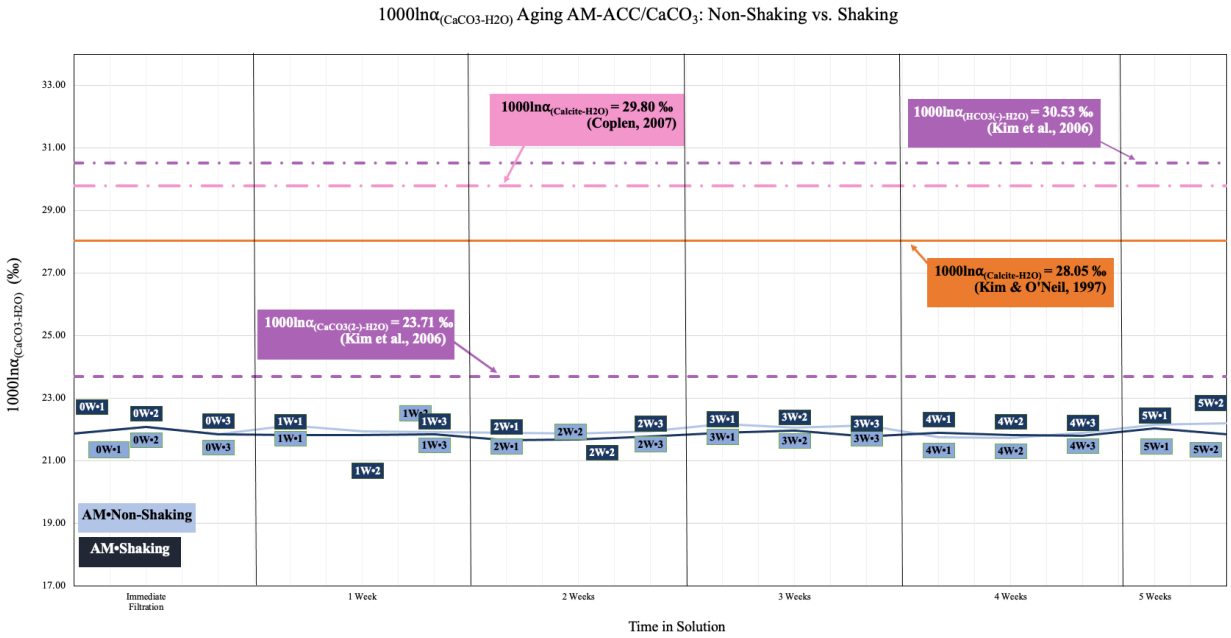

Figure 3.A1. Comparison of $1000\ln\alpha_{CaCO3\text{-}H2O}$ of AM-ACC/$CaCO_3$ precipitates from the aging post-ACC-treatment experiment

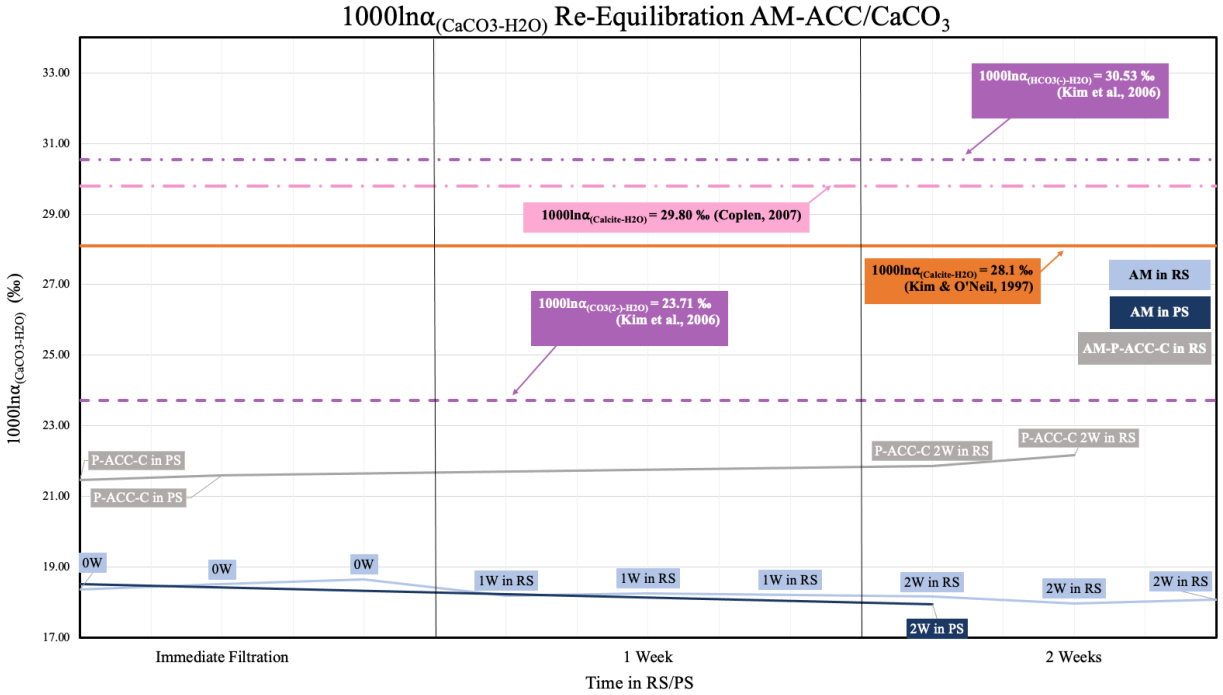

Figure 3.A2. Comparison of $1000\ln\alpha_{CaCO3\text{-}H2O}$ of AM-ACC/$CaCO_3$/P-ACC-C precipitates from the re-equilibration post-ACC-treatment experiment

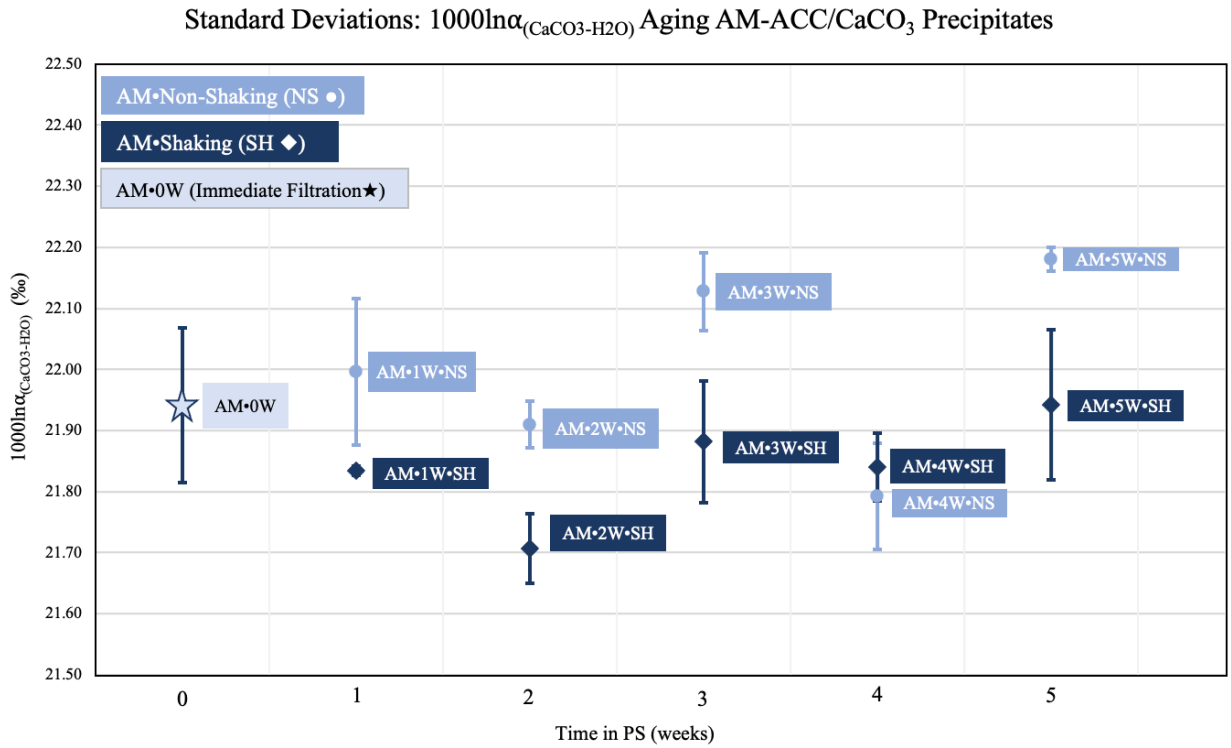

Figure 3.A3. Average $1000\ln\alpha_{CaCO3\text{-}H2O}$ values and standard deviations for AM-ACC/$CaCO_3$ precipitates from the aging post-ACC-treatment experiment

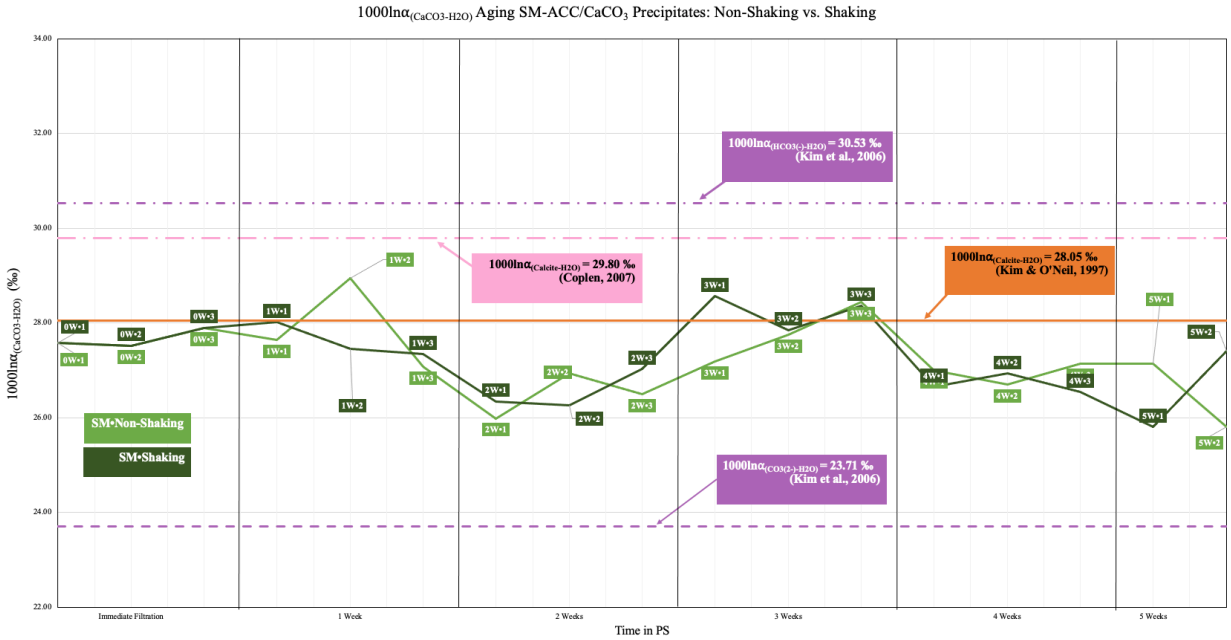

Figure 3.A4. Comparison of $1000\ln\alpha_{CaCO3\text{-}H2O}$ of SM-ACC/$CaCO_3$ precipitates from the aging post-ACC-treatment experiment

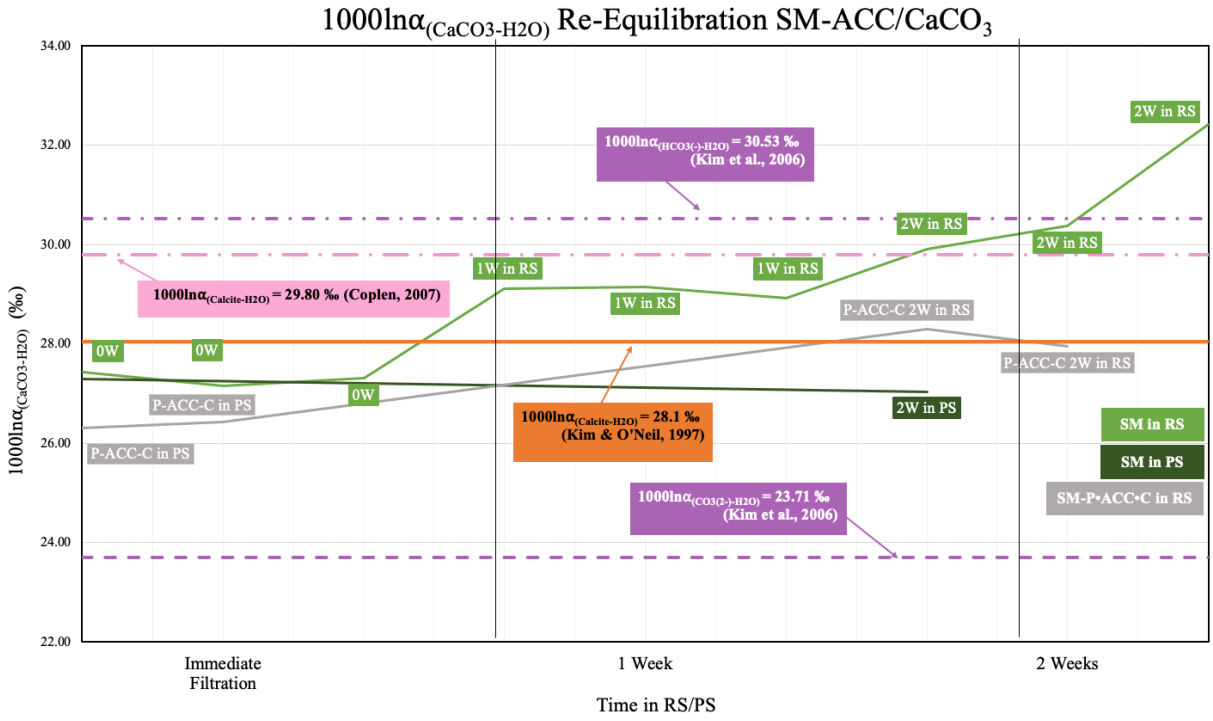

Figure 3.A5. Comparison of $1000\ln\alpha_{CaCO3\text{-}H2O}$ of SM-ACC/$CaCO_3$/P-ACC-C precipitates from the re-equilibration post-ACC-treatment experiment

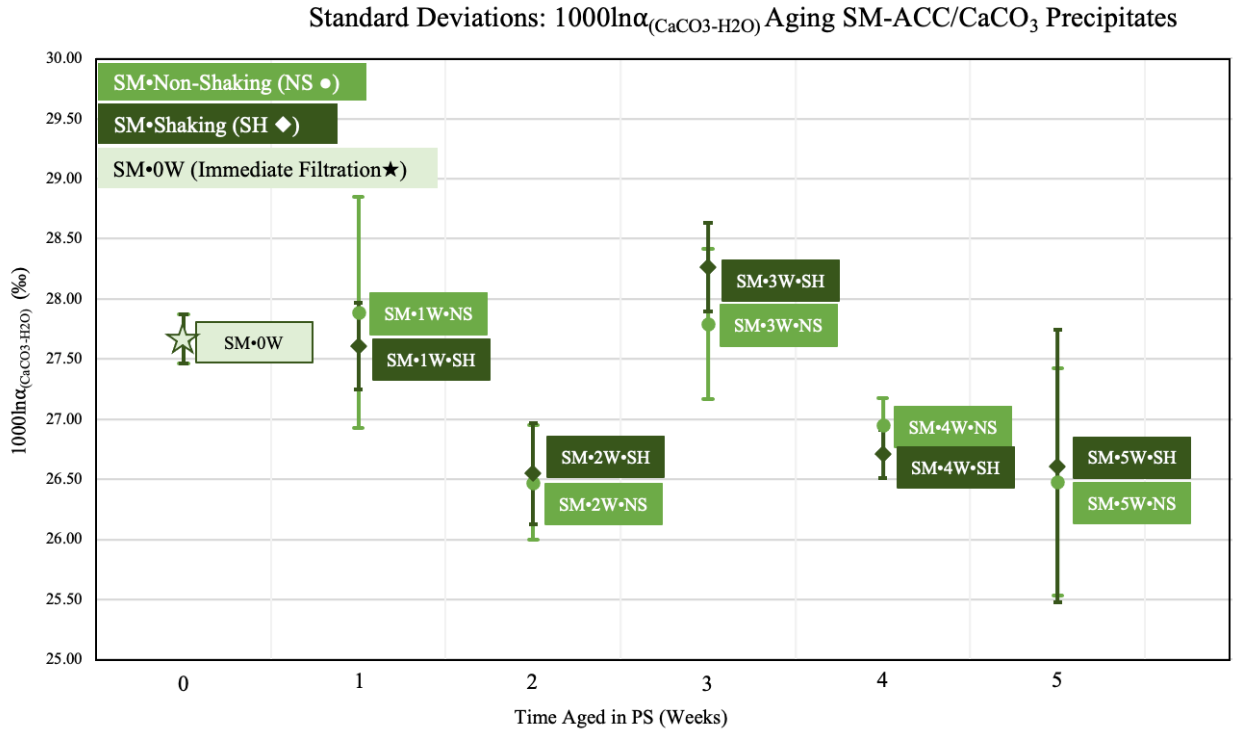

Figure 3.A6. Average $1000\ln\alpha_{CaCO3\text{-}H2O}$ values and standard deviations for SM-ACC/$CaCO_3$ precipitates from the aging post-ACC-treatment experiment

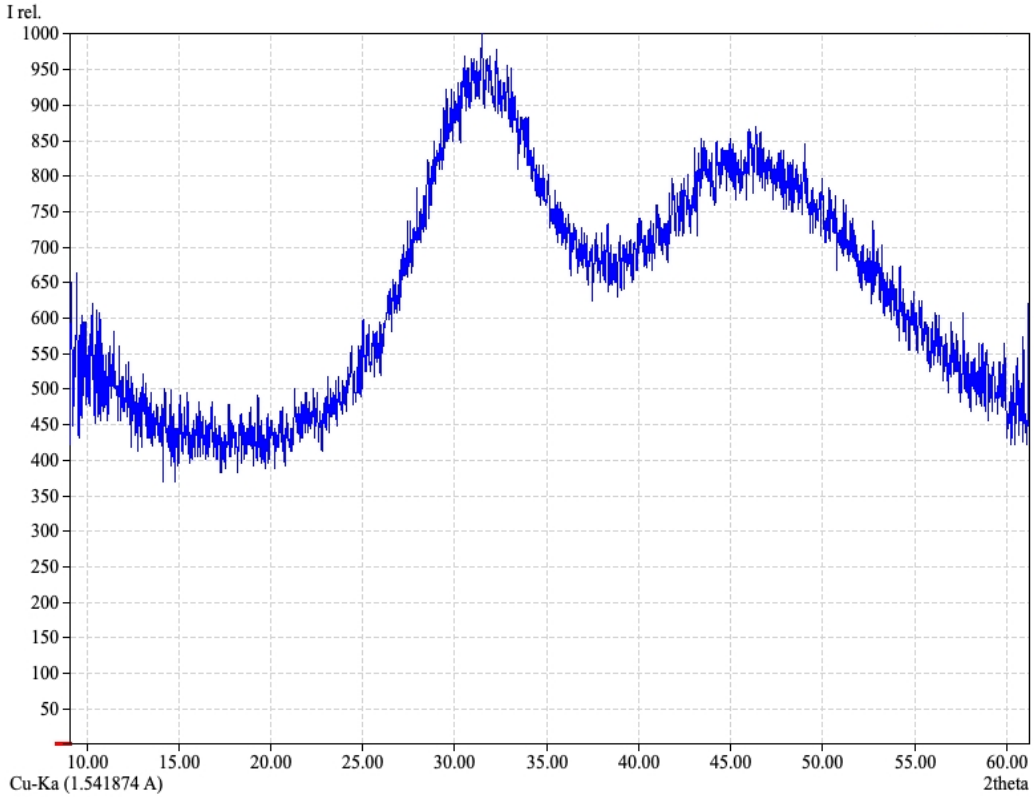

Figure 3.A7. XRD pattern for precipitate AM•0W•1, obtained with CuKα radiation.

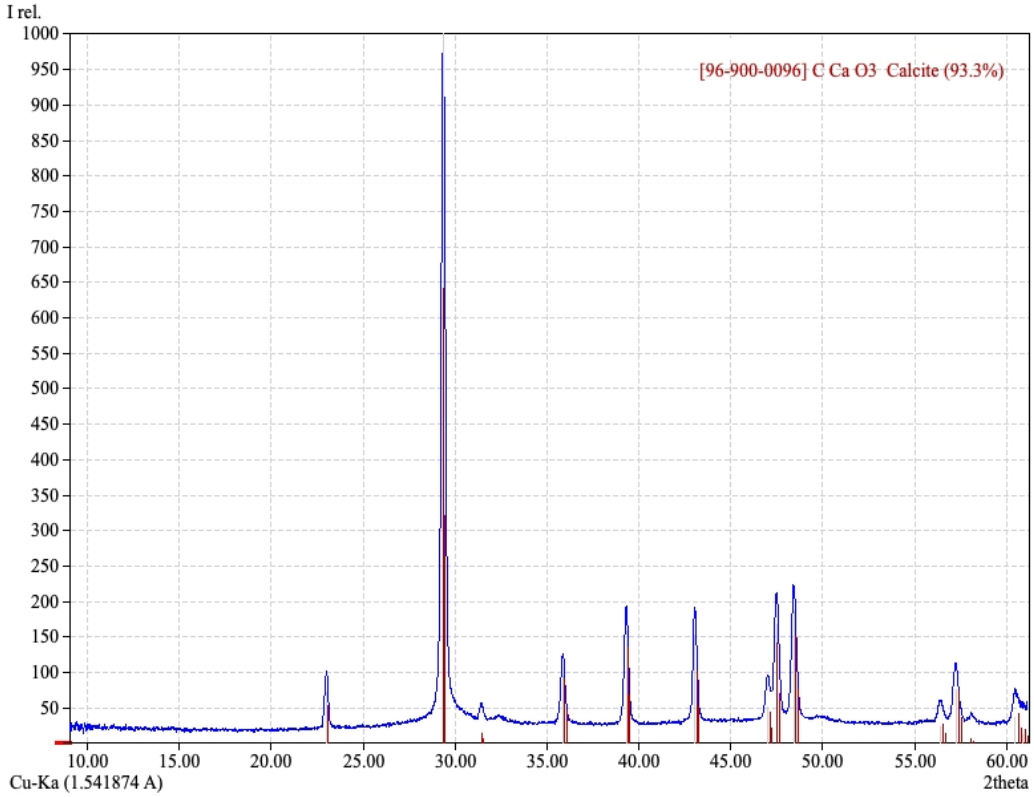

Figure 3.A8. XRD pattern and phase ID for precipitate AM•24H•1, obtained with CuKα radiation.

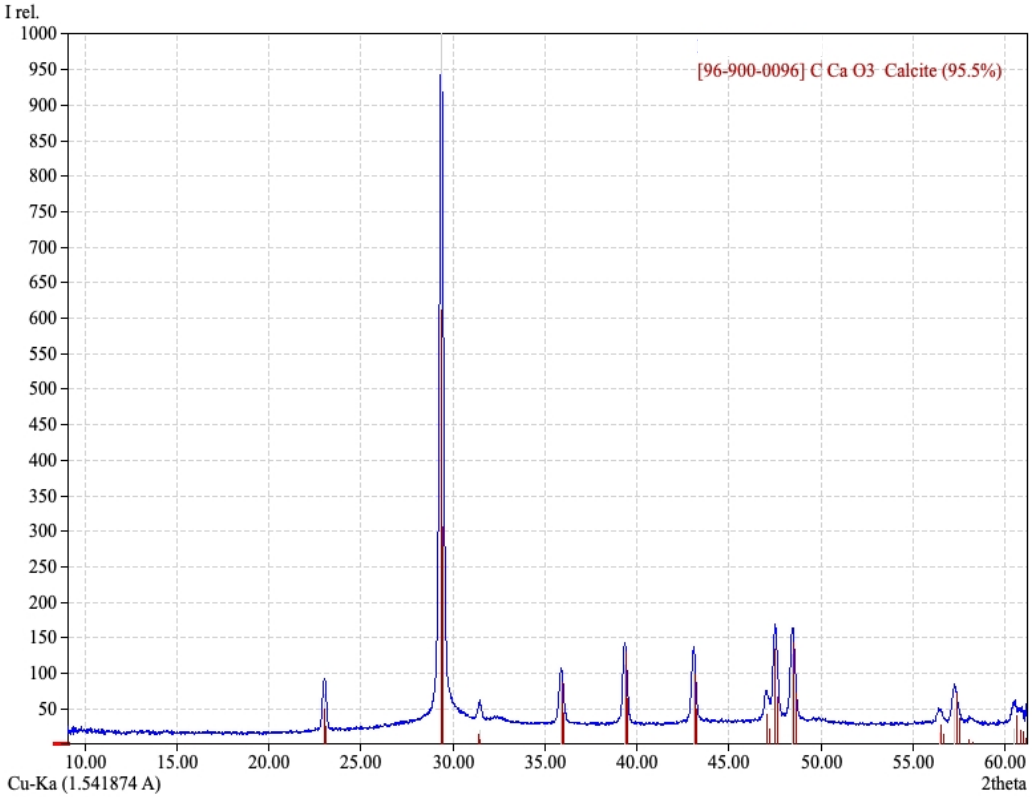

Figure 3.A9. XRD pattern and phase ID for precipitate AM•24H•2, obtained with CuKα radiation.

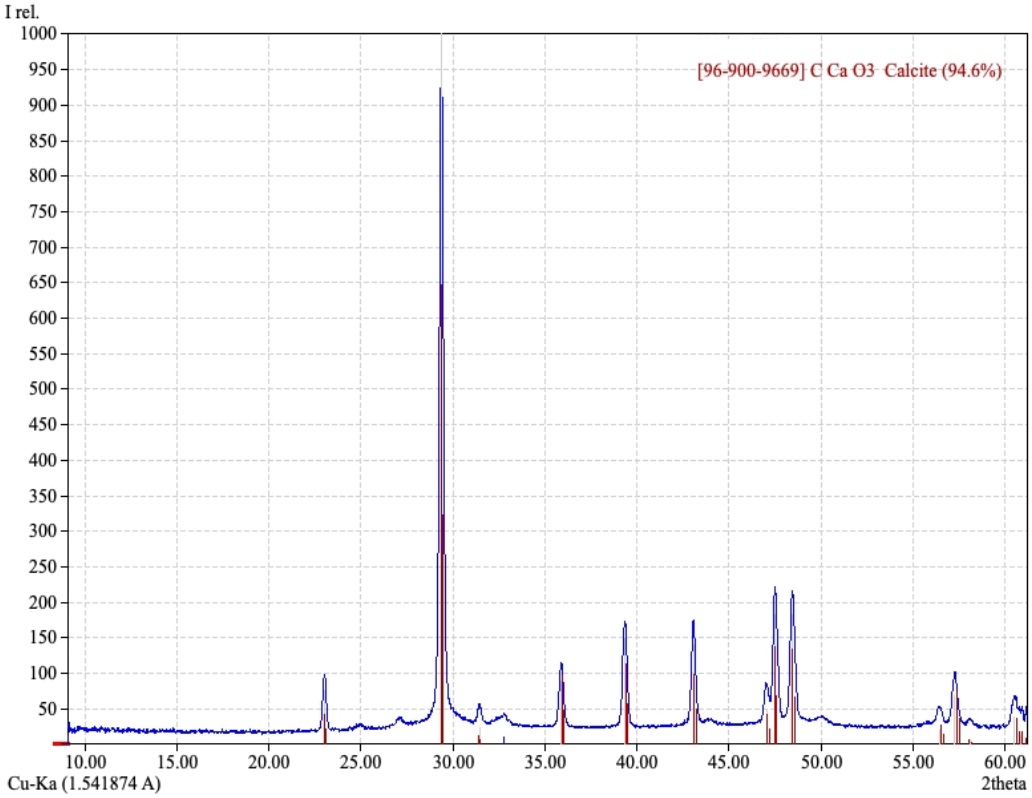

Figure 3.A10. XRD pattern and phase ID for precipitate AM•48H•1, obtained with CuKα radiation.

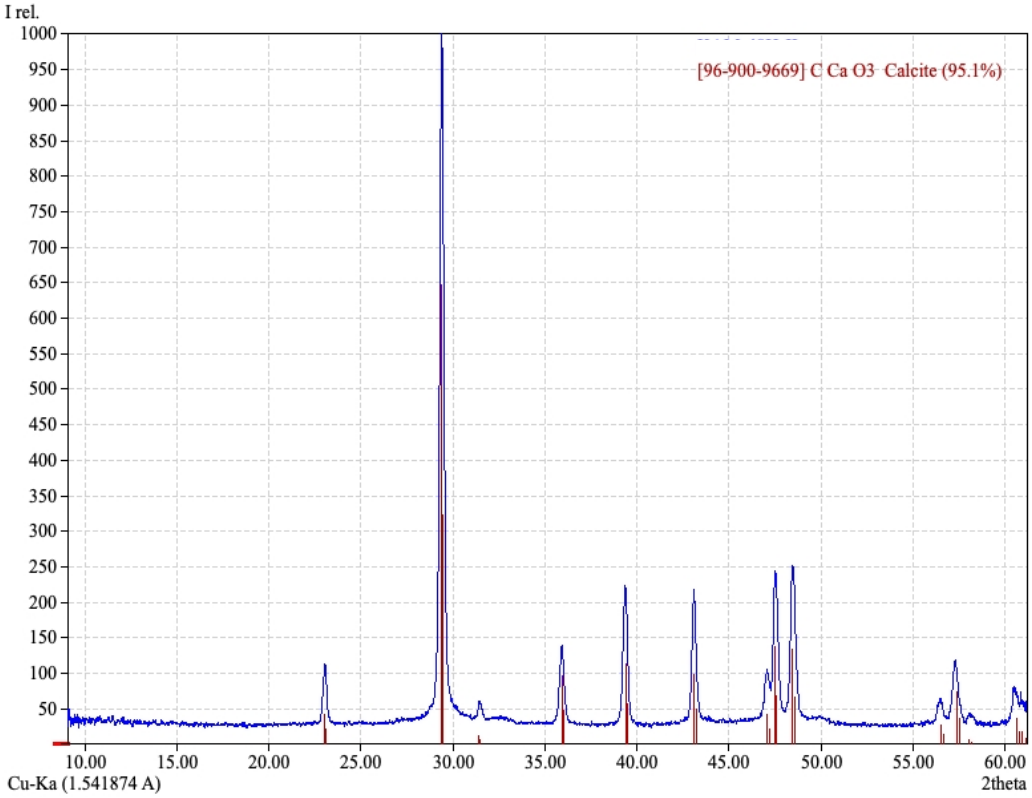

Figure 3.A11. XRD pattern and phase ID for precipitate AM•48H•2, obtained with CuKα radiation.

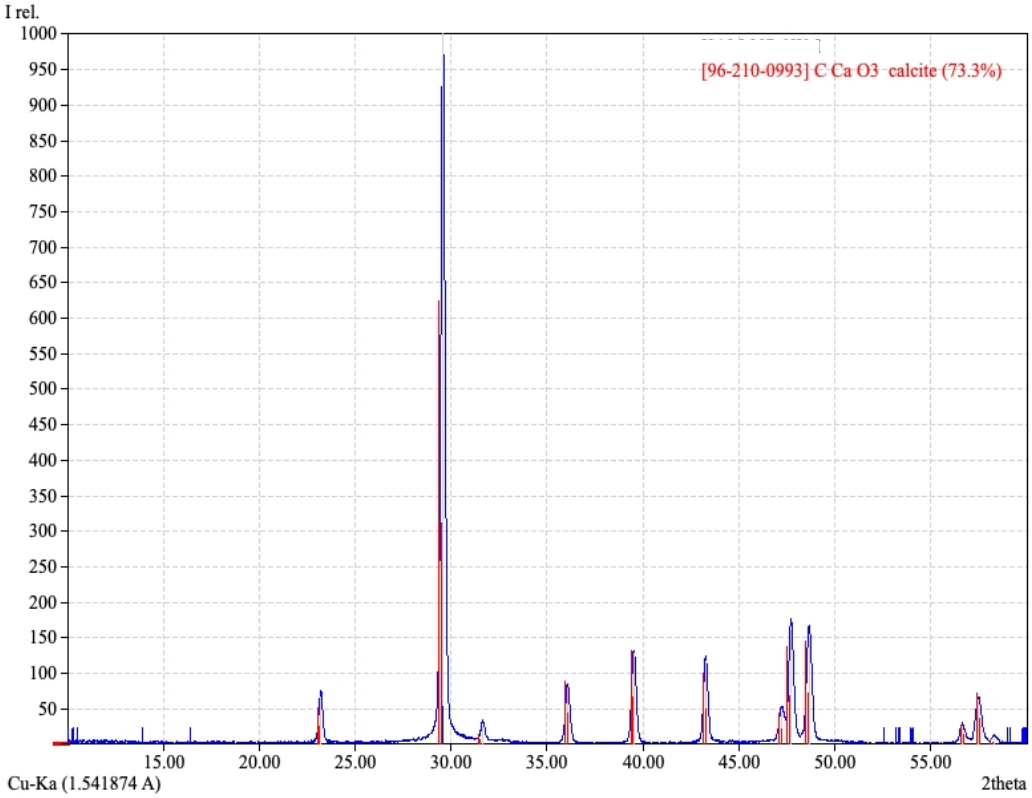

Figure 3.A12. XRD pattern and phase ID for precipitate AM•NS•1W•1, obtained with CuKα radiation.

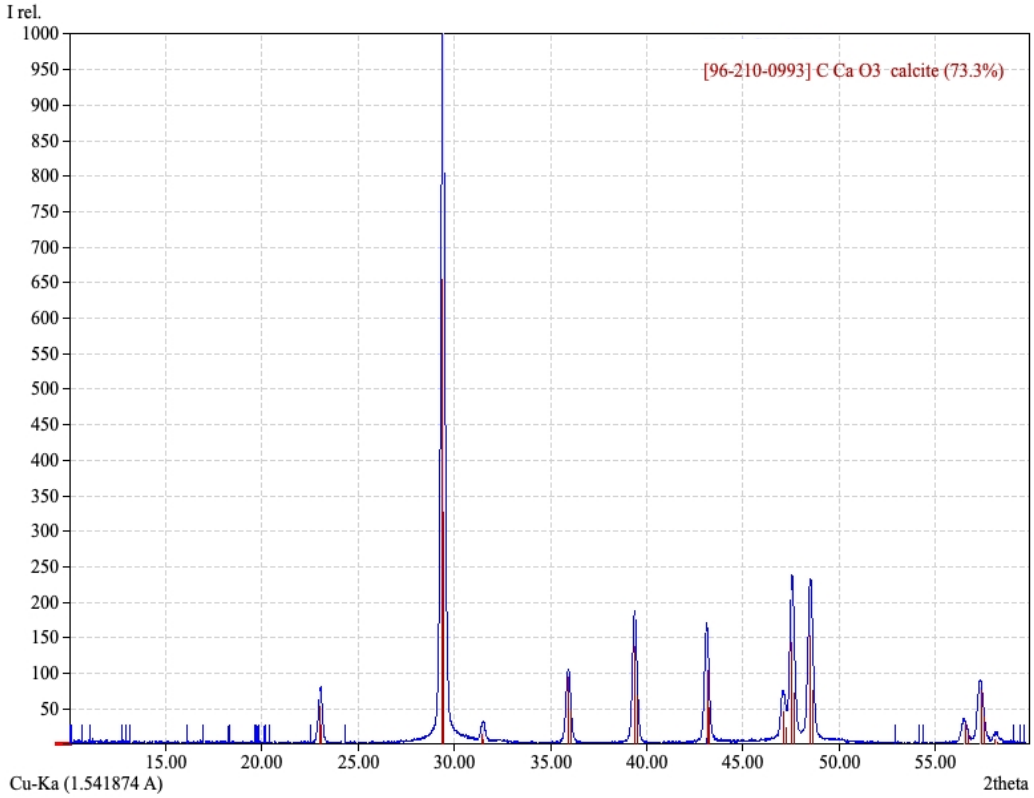

Figure 3.A13. XRD pattern and phase ID for precipitate AM•SH•1W•1, obtained with CuKα radiation.

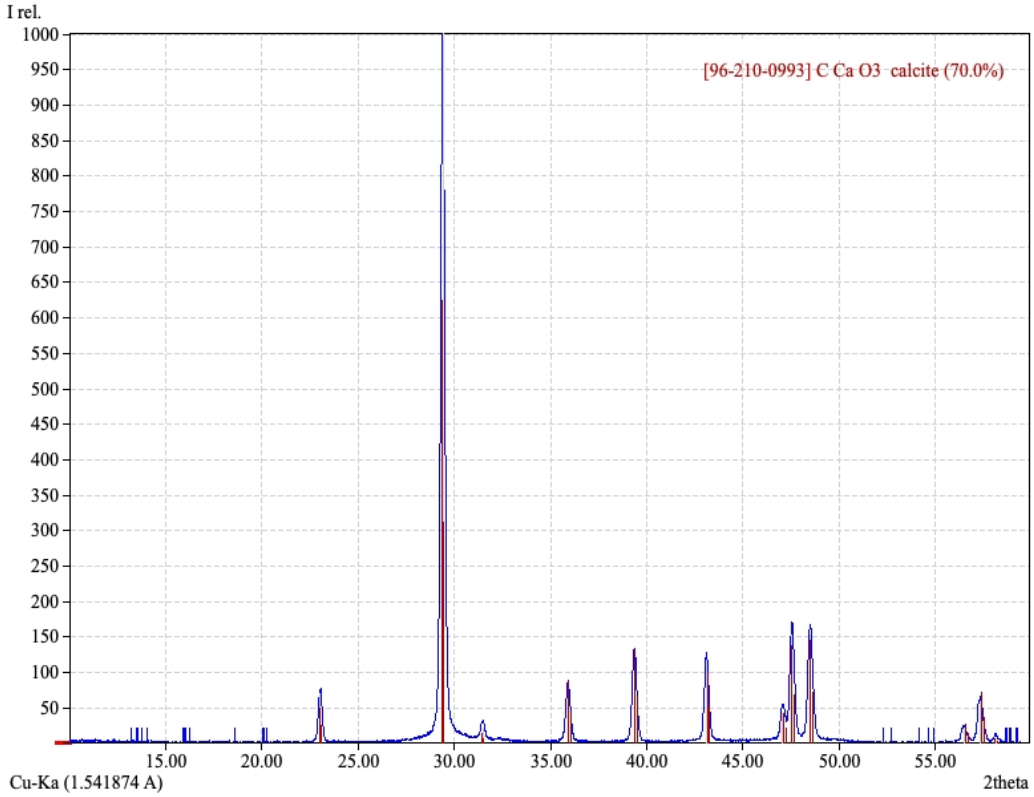

Figure 3.A14. XRD pattern and phase ID for precipitate AM•SH•1W•2, obtained with CuKα radiation.

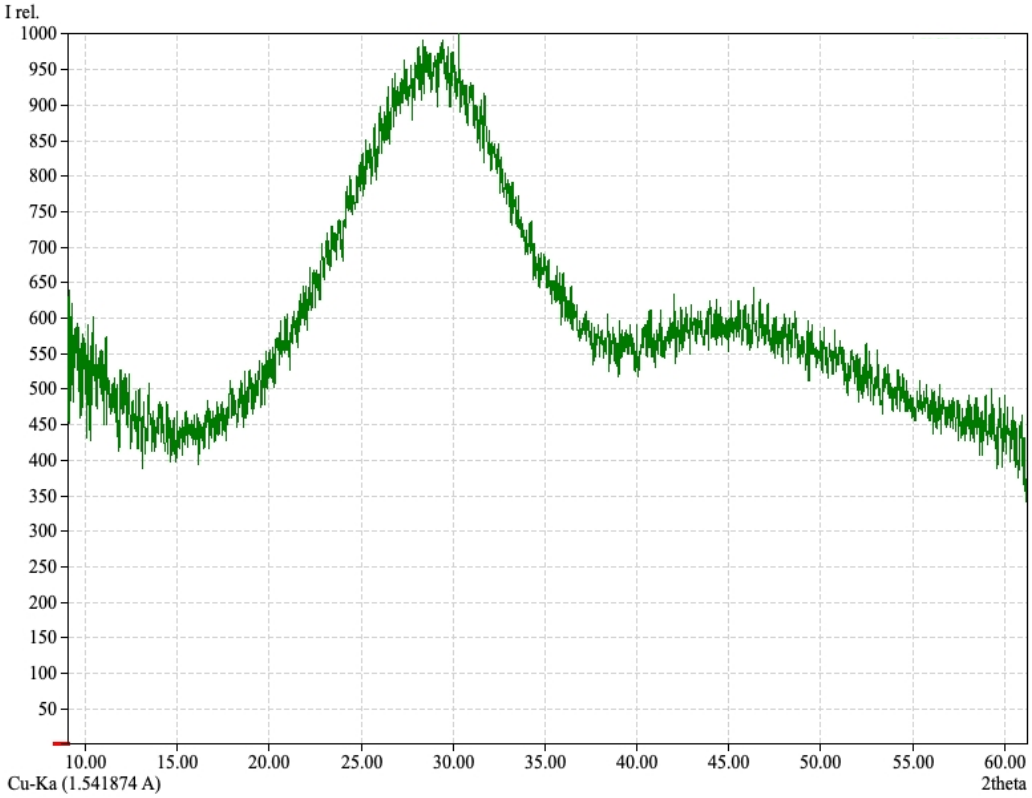

Figure 3.A15. XRD pattern for precipitate SM•0W•1, obtained with CuKα radiation.

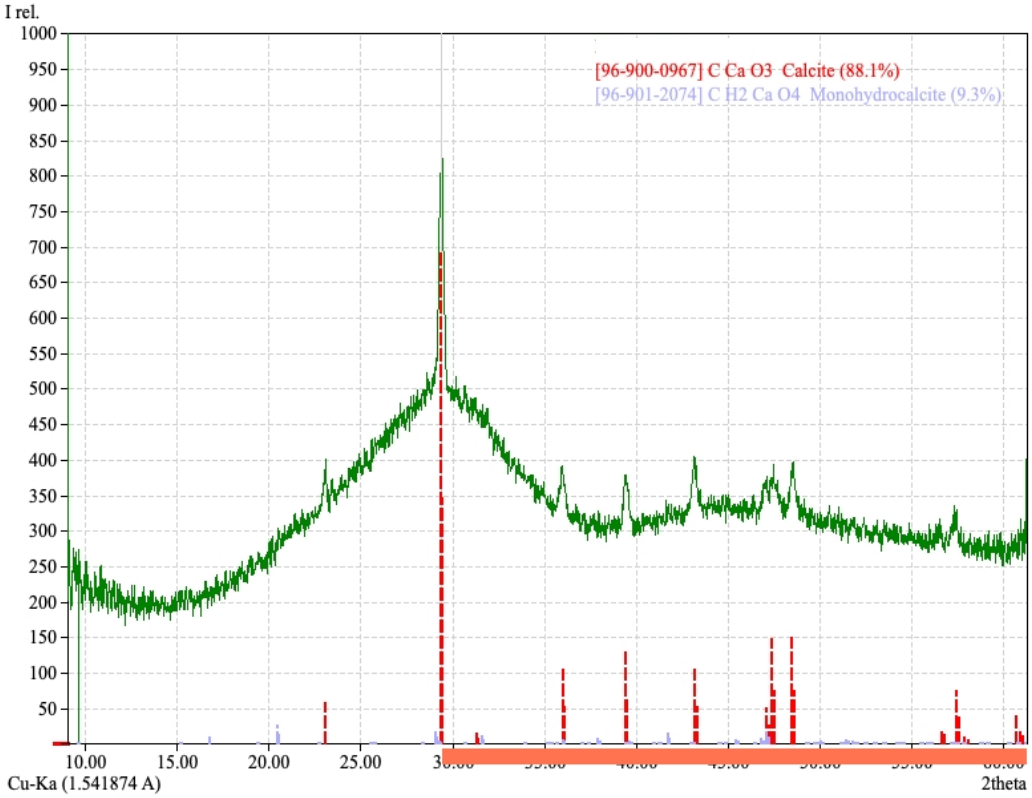

Figure 3.A16. XRD pattern and phase ID for precipitate SM•24H•1, obtained with CuKα radiation.

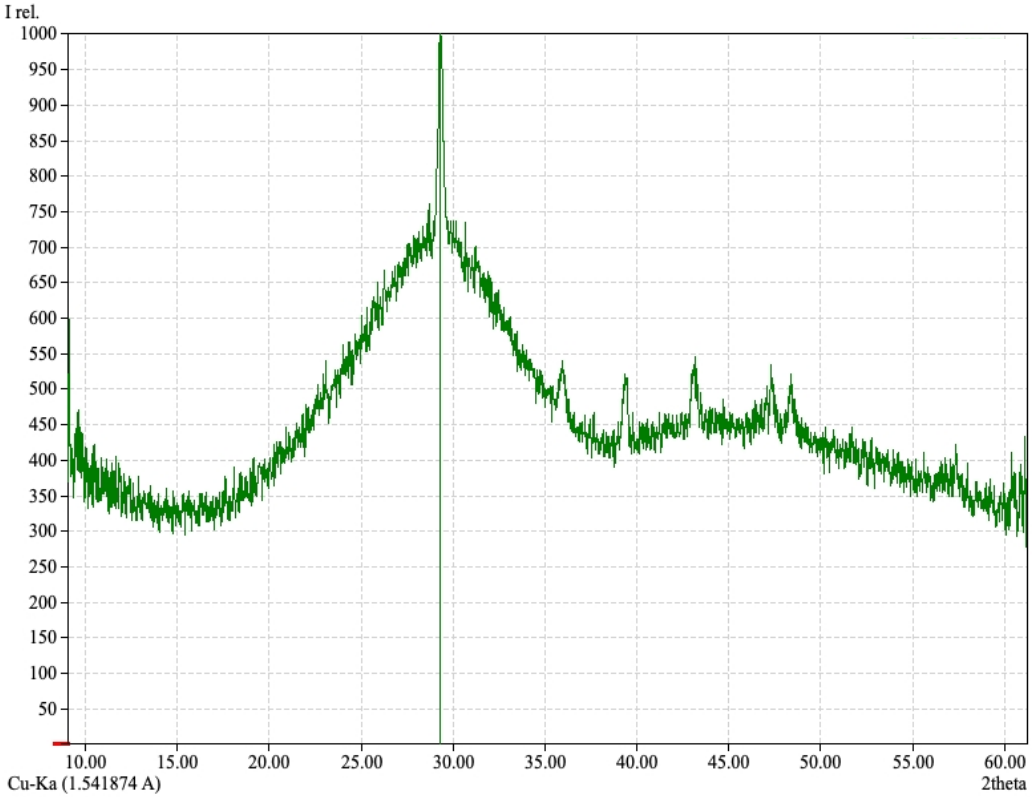

Figure 3.A17. XRD pattern and phase ID for precipitate SM•24H•2, obtained with CuKα radiation.

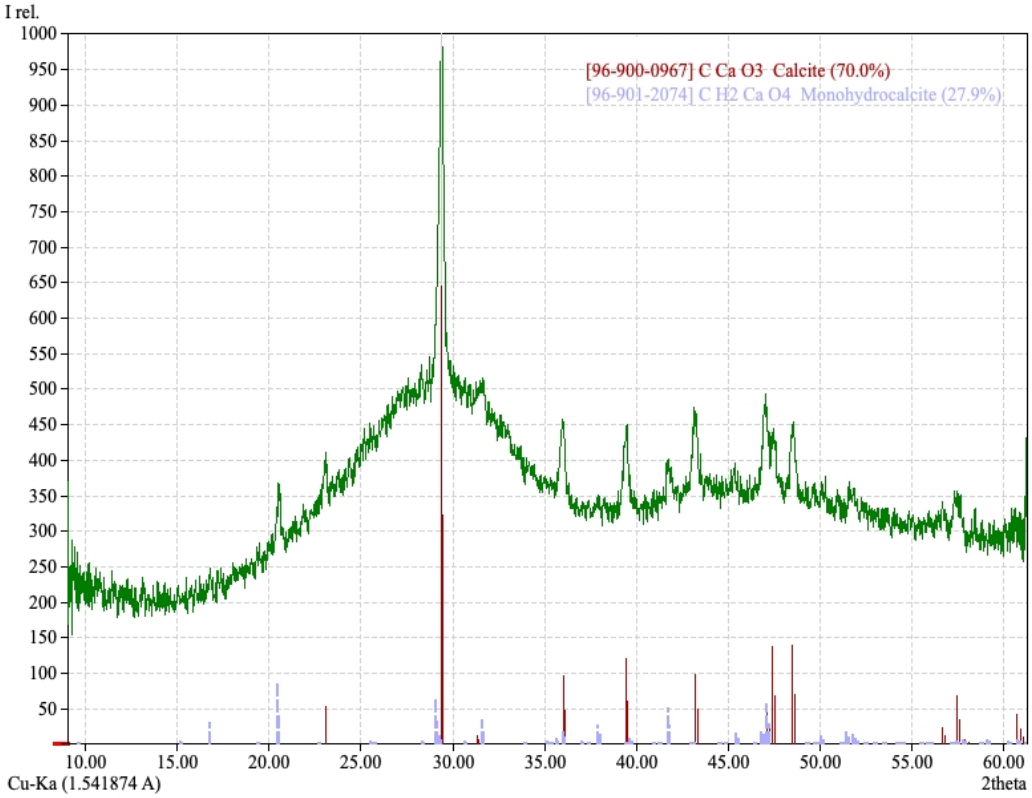

Figure 3.A18. XRD pattern and phase ID for precipitate SM•48H•1, obtained with CuKα radiation.

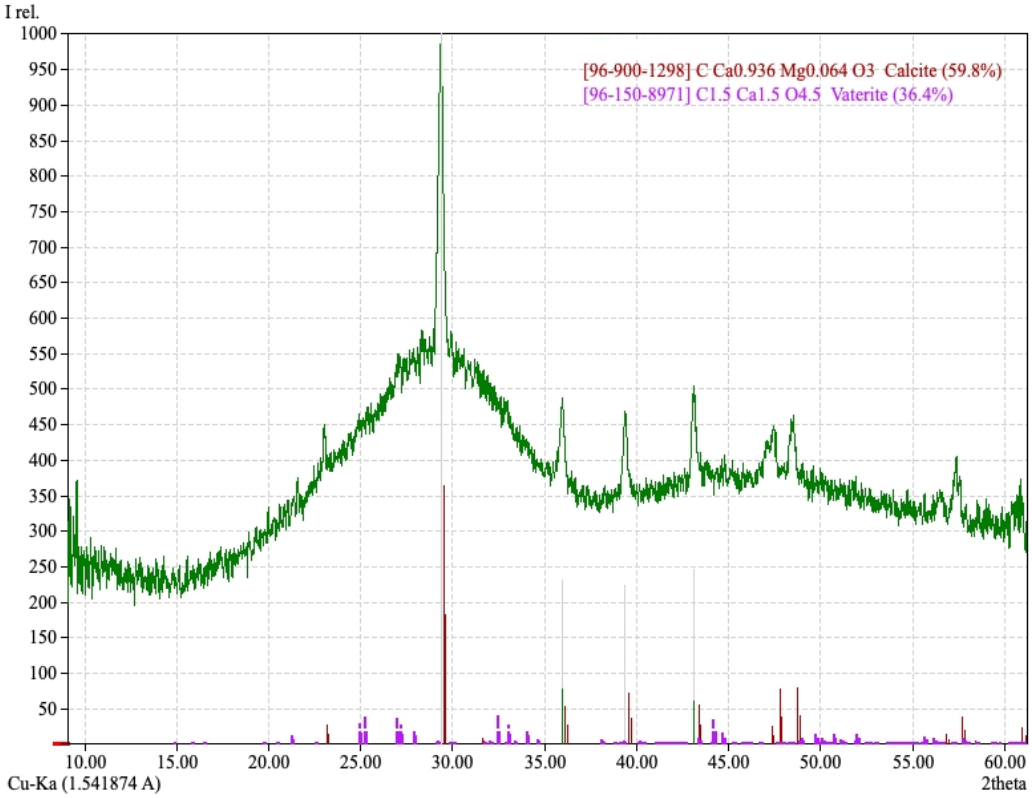

Figure 3.A19. XRD pattern and phase ID for precipitate SM•48H•2, obtained with CuKα radiation.

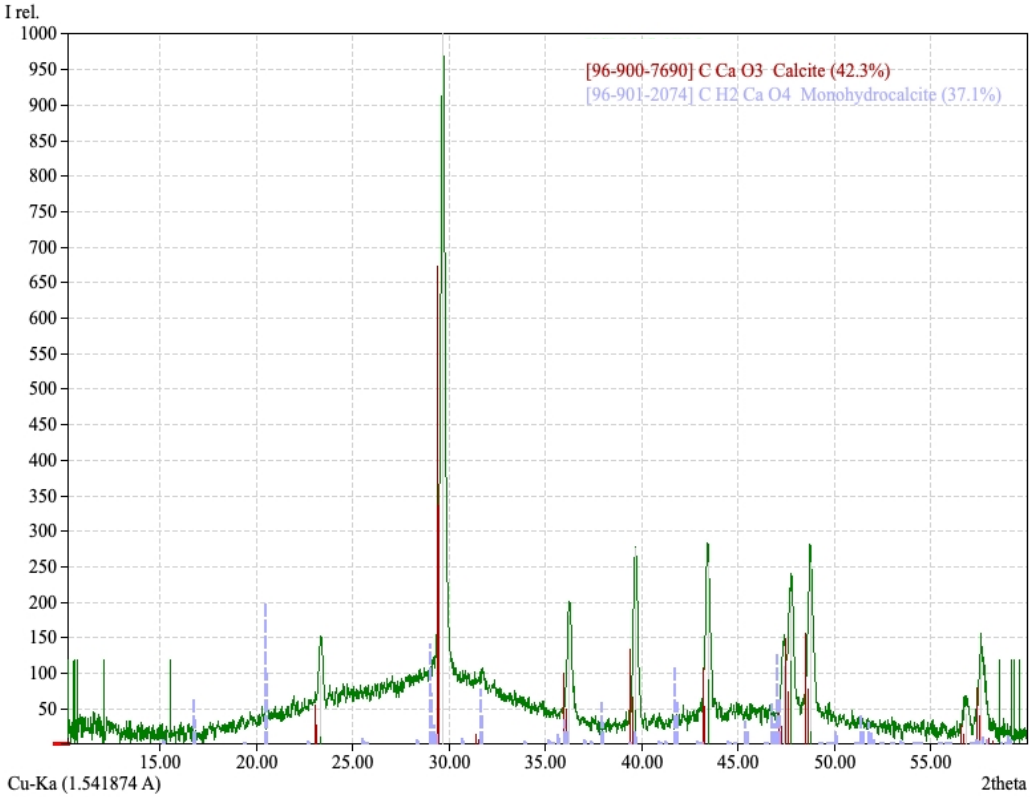

Figure 3.A20. XRD pattern and phase ID for precipitate SM•1W•NS•1, obtained with CuKα radiation.

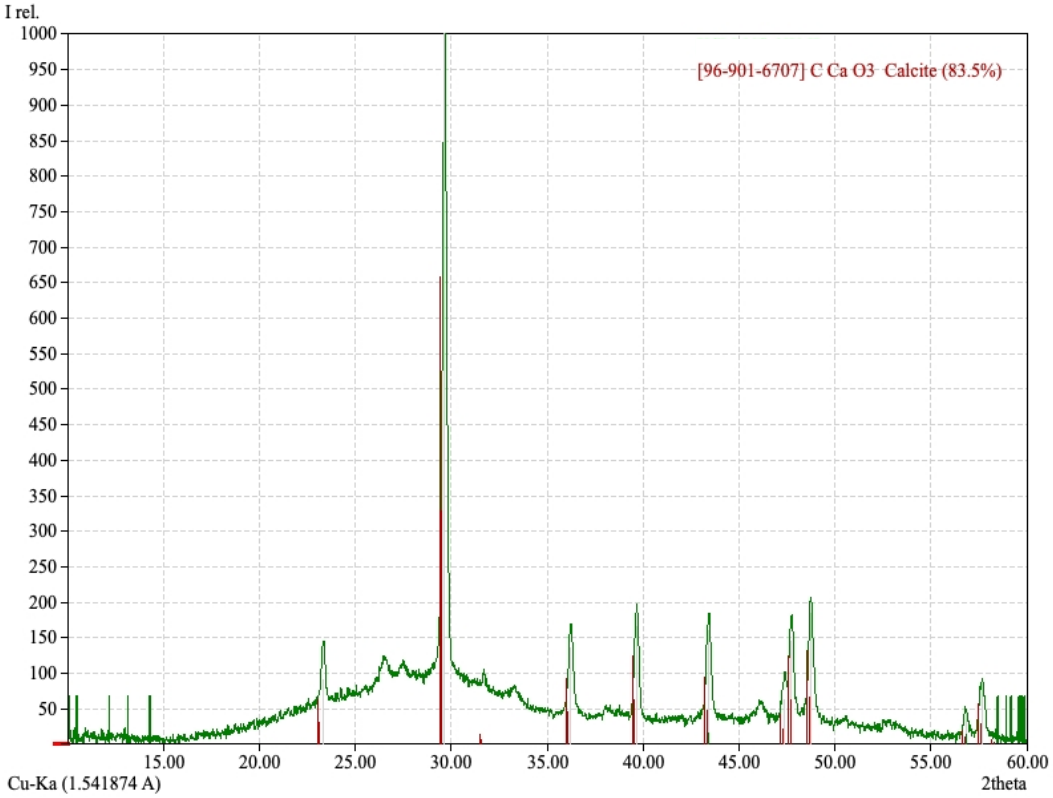

Figure 3.A21. XRD pattern and phase ID for precipitate SM•1W•NS•2, obtained with CuKα radiation.

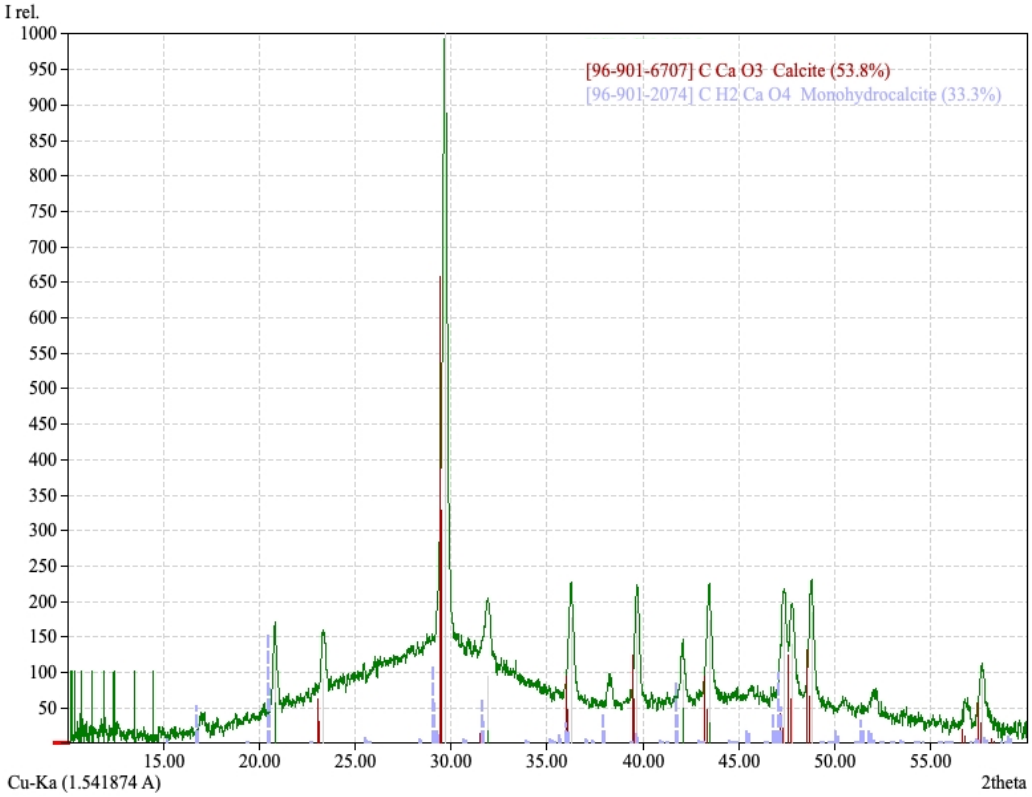

Figure 3.A22. XRD pattern and phase ID for precipitate SM•1W•SH•1, obtained with CuKα radiation.

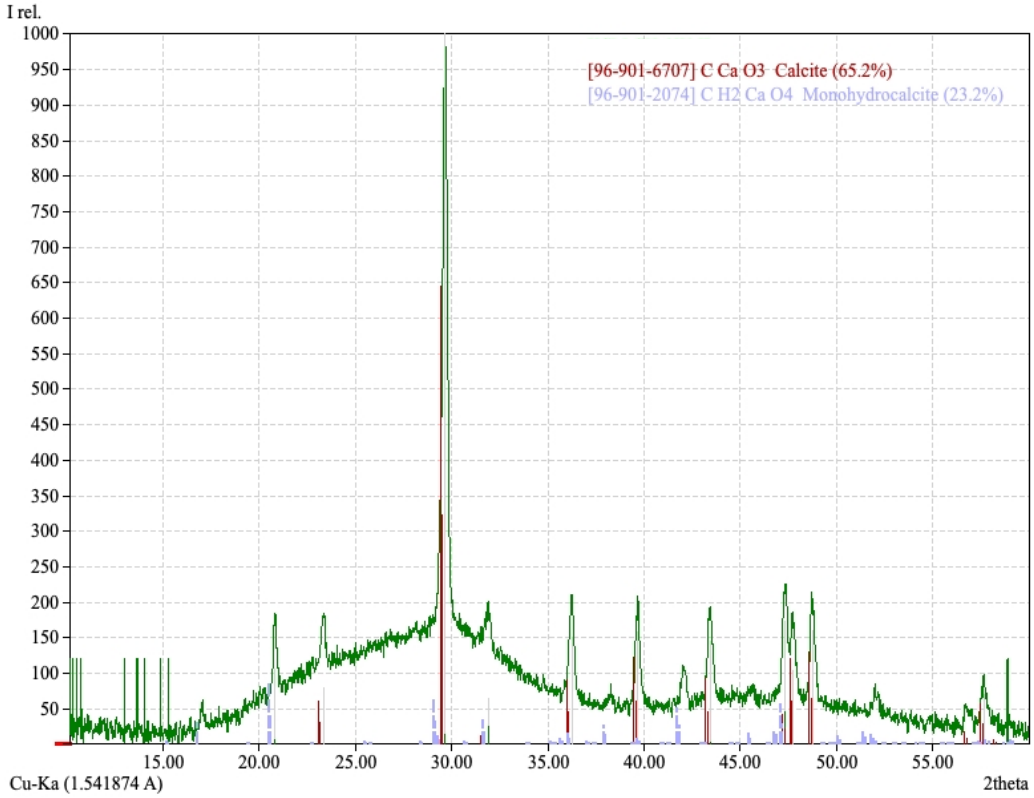

Figure 3.A23. XRD pattern and phase ID for precipitate SM•1W•SH•2, obtained with CuKα radiation.

CHAPTER 4: CONCLUSIONS AND FUTURE RESEARCH

CHAPTER 4: CONCLUSIONS AND FUTURE RESEARCH

4.1: Principal Findings

This study represents, to the best of our knowledge, the first direct comparison of ACC-precipitation methods in their ability to stabilize ACC, their effect on crystallization, and their effect on oxygen isotope composition and evolution. Two methods, the Alkaline Method (AM) and Silica Method (SM), were used to precipitate ACC. These precipitation methods were both intended to stabilize ACC and prevent its transformation to crystalline $CaCO_3$. While the AM used high concentrations of NaOH in the AM-CO_3^{2-}-donor parent solution to raise the pH of the precipitating solution, the SM stabilized ACC by surrounding ACC particles with an isolating layer of silica as they precipitated. The AM was less effective at maintaining ACC in parent solution, and AM-ACC predictably transformed to calcite within days. The SM was more effective in stabilizing ACC in solution and even upon crystallization typically resulted in less stable polymorphs of $CaCO_3$, often with some ACC still present after 2 weeks. Interestingly, when immediately filtered AM- and SM-ACC-precipitates were allowed to crystallize in air, the AM-ACC precipitates remained fully amorphous for longer than the SM-ACC precipitates, although these same AM-ACC precipitates transformed completely to calcite before the SM-ACC precipitates.

AM- and SM-ACC also differed significantly in terms of their oxygen isotope fractionation with their respective parent solution, or $1000\ln\alpha_{CaCO3\text{-}water}$, both immediately following precipitation and filtration, and with time aging in PS and concurrent crystallization. AM-ACC precipitates and subsequent AM-$CaCO_3$ precipitates maintained smaller $1000\ln\alpha_{CaCO3\text{-}water}$ values than that for equilibrium CO_3^{2-}, that hardly varied with time in PS or RS, indicating both incomplete DIC-water equilibration in the AM-CO_3^{2-}-donor parent solution, as well as

possible kinetic isotope effects from non-quantitative AM-ACC/$CaCO_3$ precipitation. This also indicates possible crystallization of AM-ACC via solid-state transformation. Addition of freshly precipitated AM-ACC precipitates to ^{18}O-enriched RS yielded similar results, and the resultant AM-$CaCO_3$ precipitates underwent no apparent oxygen isotope exchange with the RS. Subsequent investigation was performed to determine whether these low $1000ln\alpha_{CaCO3\text{-}water}$ values were due to non-quantitative precipitation of AM-ACC precipitates, or disequilibrium in the DIC-H_2O system. It was found that the latter was the main reason for the low $1000ln\alpha_{CaCO3\text{-}water}$ values of the AM-ACC/AM-$CaCO_3$ precipitates during ACC crystallization. The initial estimate of 44 days as sufficient for oxygen isotope DIC-H_2O equilibration, as extrapolated from Beck et al. (2005), was likely not applicable to the very high pH of the AM-CO_3^{2-}-donor parent solution.

SM-ACC/$CaCO_3$ precipitates yielded significantly different $1000ln\alpha_{CaCO3\text{-}water}$ values, despite being treated identically to corresponding AM-ACC/$CaCO_3$ precipitates. Upon immediate precipitation and filtration, SM-ACC precipitates were consistently found to have $1000ln\alpha_{CaCO3\text{-}water}$ values at or near the expected equilibrium oxygen isotope fractionation factor for calcite and water at 25 ˚C, as published by Kim & O'Neil, (1997). With time aging in PS SM-$CaCO_3$ precipitates, which had transformed from antecedent SM-ACC precipitates, bore $1000ln\alpha_{CaCO3\text{-}water}$ values that, though quite variable, remained close to this value. Furthermore, when freshly precipitated SM-ACC was added to ^{18}O-enriched RS, there was a clear oxygen isotope re-equilibration with the RS as the SM-ACC transformed to SM-$CaCO_3$. This re-equilibration during ACC crystallization occurred to a much smaller degree with SM-P-ACC-C samples, which had mostly crystallized upon being introduced to RS.

These results are significant in several ways. First, the high initial $1000\ln\alpha_{CaCO3\text{-}water}$ values of SM-ACC precipitates indicates the possibility that oxygen isotope exchange between SM-ACC and parent solution was very rapid. Upon immediate precipitation and filtration, one would expect $1000\ln\alpha_{CaCO3\text{-}water}$ values that reflect oxygen isotope equilibrium between the primary DIC species in parent solution, in this case CO_3^{2-}, and water. However, the data clearly indicates that SM-ACC precipitates and parent solution underwent a rapid oxygen isotope exchange in the short time between the point of actually precipitation and complete isolation from PS by vacuum filtration. Second, SM-ACC precipitates were far more capable of undergoing oxygen isotope re-equilibration with RS than SM-P-ACC-C precipitates.

4.2: Candidate's contribution to the field

The candidate carried out the majority of all experimental procedures and analyses outlined in this study. These include preparation of all parent solutions, as well as the performance of all precipitations and filtrations. Initial XRD analyses were performed by the candidate with assistance by experts, however, due to COVID-19 restrictions, the majority of later XRD characterizations were carried out either by Victoria Jarvis, Maureen Fitzpatrick, or Jim Britten of the McMaster Analytical X-Ray Diffraction (MAX) facility. All subsequent XRD pattern analyses were conducted by the candidate. All carbonate and water sample preparations and analyses via CF-IRMS were carried out by the candidate in McMaster Research Group of Stable Isotopologues (MRIS) at McMaster University, as well as subsequent data correction and analyses. The candidate wrote the entirety of this thesis with the invaluable guidance and editorial assistance of the candidate's supervisor, Dr. Sang-Tae Kim.

There has been a great deal of interest in ACC as a precursor phase in biomineralization, and furthermore, how it effects the isotopic composition of the final biomineral it transforms into (Addadi et al., 2003; Pérez-Huerta & Fred, 2010; Weiner et al., 2003). Knowledge regarding how an ACC precursor phase effects the isotopic composition of a resultant biomineral can denote whether these calcium carbonate deposits can be used as accurate proxies of their precipitation environments (Aizenberg et al., 2003; Mass et al., 2017; Pérez-Huerta & C. Fred, 2010). Furthermore, ACC precursor phases have often been cited as possible culprits for the vital effect (e.g., Devriendt et al., 2017; Erez, 1978; Saenger & Wang, 2014), a kinetic isotope signature of biological original which obscures any proxy data a biogenic carbonate may have offered (Erez, 1978; Simkiss, 1991; Ziveri et al., 2003). It is, therefore, important to determine whether ACC precipitation as a precursor phase can indeed impart these kinetic isotope signatures, or if the source of the vital effect lies elsewhere.

The results of this thesis research may shed light upon both of these long-standing questions in geochemistry. First, this study offers additional proof that ACC transforms to crystalline $CaCO_3$ via a dissolution-reprecipitation reaction. Overall, this indicates that if biomineralizing organisms precipitate ACC as a precursor phase, given certain precipitation conditions, this ACC can re-equilibrate with surrounding water as it dissolves to constituent ions prior to re-precipitation as a crystalline $CaCO_3$ biomineral. Therefore, $CaCO_3$ biominerals produced by organisms known to precipitate ACC precursors cannot be dismissed out of hand as feasible sources of paleoclimatic proxies. Furthermore, this study indicates that, under certain precipitation conditions, ACC equilibration with water may be far more rapid than crystalline $CaCO_3$ and water. Therefore, rather than marking subsequent biominerals with a kinetic isotope

signature, biogenic $CaCO_3$ that has transformed from an ACC precursor may be more likely to precipitate in isotopic equilibrium with surrounding water.

Another long-standing question regarding the ACC to $CaCO_3$ crystallization system is whether the final crystalline $CaCO_3$ would reflect the isotopic environment in which ACC precipitated, or the isotopic environment in which ACC crystallized (e.g., Dietzel et al., 2020; Mavromatis et al., 2017; Purgstaller et al., 2016; Schmidt et al., 2005). The results of the re-equilibration treatment indicate that, when ACC is precipitated by the SM in PS, and subsequently added to RS, oxygen isotope exchange occurred and resulted in SM-$CaCO_3$ precipitates that appeared to be approaching oxygen isotope with their new environment (i.e., the RS from the PS). Conversely, when SM-$CaCO_3$ precipitates which had already mostly crystallized (i.e., SM-P-ACC-C) were added to the RS, isotopic re-equilibration occurred to a much smaller extent. Parallels may be drawn between these two scenarios and biomineralizing pathways. Specifically, the isotopic composition of the ACC precursor can be overwritten during ACC transformation to crystalline $CaCO_3$. However, once the ACC has crystallized, further isotopic exchange is much slower. Isotope fractionation similar in direction and magnitude to vital effects were seen in this study with AM-ACC/$CaCO_3$ precipitates, however, these were seemingly also a result of high pH precipitation and crystallization environments of the AM-ACC/$CaCO_3$-solutions

Therefore, given sufficiently low pH and in the absence of other mitigating factors, the final isotopic composition of a $CaCO_3$ precipitate that transforms via an ACC phase seems to be dependent upon the isotopic conditions of the crystallization environment, rather than the ACC-precipitation environment. However, above this threshold the precipitated ACC and subsequent crystalline $CaCO_3$ will bear low isotopic signatures as a result of the high solution pH

significantly reducing solubility of the precipitated ACC/$CaCO_3$ phase to the point that very little isotopic exchange occurs, and crystallization proceeds via solid state transformation rather than dissolution-reprecipitation. These results indicate that the ACC precursor phase may, depending on the precipitation method, account for the low stable isotope compositions, or vital effects, noted in some biogenic $CaCO_3$.

4.3: Areas for Future Research

Although this study offered a great deal of insight into the crystallization and isotopic dynamics of the ACC-parent solution system, there is still a great deal of work necessary. First and foremost, shorter timescales following ACC-precipitation are required. Aging in PS for minutes and hours following ACC-precipitation, rather than weeks, may offer a better understanding into whether ACC can reach isotope equilibrium with its surrounding solution. These shorter periods may also provide further evidence regarding the rapid ACC-water equilibration indicated by data from this study. Conversely, longer periods in re-equilibration solution are called for to determine whether full re-equilibration with the ^{18}O enriched solution is possible. The study by Giuffre et al. (2015) found that an increased ratio of solution to Mg-ACC mitigated the precursor's isotopic effect on the final Mg-calcite. In this vein, altering the relative fractions of ACC to PS or RS may also be important to a more robust understanding of the isotopic dynamics, and have connotations for biological systems that biomineralize $CaCO_3$ via an ACC precursor.

The AM was revealed by this study to be a poor candidate for stable isotope research, as the high pH environment of precipitation and crystallization seemed to allow negligible isotopic exchange between AM-ACC/$CaCO_3$ precipitates and water. Therefore, the use of alternative

ACC precipitation methods could instead be used in conjunction with the SM to compare their effects on the isotopic composition of precipitated ACC, ACC's ability to achieve isotopic equilibrium with surrounding water, and ACC's isotopic evolution as it transforms to a crystalline polymorph of $CaCO_3$. However, the results yielded by AM-ACC/$CaCO_3$ precipitates do hint at an extreme dependence of isotopic composition and re-equilibration upon solution pH. Several species of coral (e.g., Al-Horani et al., 2003; Venn et al., 2011), and foraminifera (De Nooijer et al., 2009; Köhler-Rink & Kühl, 2007), are known to promote calcification by elevating pH at the site of precipitation relative to seawater, some of which share similar isotope signatures to AM-$CaCO_3$ precipitates (Devriendt et al., 2017). This may offer some avenues of study into how the precipitation of ACC precursor phases may contribute to vital effects found in marine sediments.

The SM proved more successful as a candidate for studying the stable isotope composition and evolution of ACC, however, refinements upon SM methodology may offer a clearer picture. First, washing SM precipitates more thoroughly with DI water to remove all silica may allow for more complete and predictable crystallization, which may reduce the isotopic variability seen among SM $CaCO_3$ precipitates. Moreover, it may be beneficial to assess the effect of silica concentration upon the isotopic composition of ACC and the crystalline $CaCO_3$ it transforms into. The effect of temperature upon SM-ACC/$CaCO_3$ precipitates is also a worthy candidate for further study. Moreover, increasing the pH of the parent solution could shed further light on whether SM-ACC/$CaCO_3$ precipitates were able to re-equilibrate due only to lower pH, or by some combination of lower pH and the isolating silica vesicles.

Along with these research possibilities, drawing direct parallels between synthetic ACC and $CaCO_3$ precipitates and similarly precipitated biogenic ACC and $CaCO_3$ is also an important

next step. While synthetic precipitations under rigorously controlled laboratory conditions are vital to our understanding of the rules underlying stable isotope exchange, it is just as important to investigate how these isotope exchange dynamics manifest themselves in existing biological systems. For example, ACC and $CaCO_3$ precipitated via the SM might be compared to biogenic ACC precipitated in certain angiosperms known to precipitate ACC stabilized by silica in small calcified bodies called Cystoliths (Gal et al., 2010). Moreover, the use of macromolecules, proteins, and additives from biogenic ACC producers could be used in vitro to study the isotopic evolution of the resultant ACC and $CaCO_3$ precipitates.

References

Addadi, L., Raz, S., & Weiner, S. (2003). Taking Advantage of Disorder: Amorphous Calcium Carbonate and Its Roles in Biomineralization. *Advanced Materials*, *15*(12), 959–970. https://doi.org/10.1002/adma.200300381

Aizenberg, J. (1996). Stabilization of amorphous calcium carbonate by specialized macromolecules in biological and synthetic precipitates. *Advanced Materials*, *8*(3), 222–226. https://doi.org/10.1002/adma.19960080307

Aizenberg, J., Addadi, L., Weiner, S., & Lambert, G. (1996). Stabilization of amorphous calcium carbonate by specialized macromolecules in biological and synthetic precipitates. *Advanced Materials*, *8*(3), 222–226. https://doi.org/10.1002/adma.19960080307

Aizenberg, J., Lambert, G., Weiner, S., & Addadi, L. (2002). Factors Involved in the Formation of Amorphous and Crystalline Calcium Carbonate: A Study of an Ascidian Skeleton. *Journal of the American Chemical Society*, *124*(1), 32–39. https://doi.org/10.1021/ja016990l

Aizenberg, J., Weiner, S., & Addadi, L. (2003). Coexistence of amorphous and crystalline calcium carbonate in skeletal tissues. *Connective Tissue Research*, *44*(SUPPL. 1), 20–25. https://doi.org/10.1080/03008200390152034

Ajikumar, P. K., Ling, G. W., Subramanyam, G., Lakshminarayanan, R., & Valiyaveettil, S. (2005). Synthesis and characterization of monodispersed spheres of amorphous calcium carbonate and calcite spherules. *Crystal Growth and Design*, *5*(3), 1129–1134. https://doi.org/10.1021/cg049606f

Akiva-Tal, A., Kababya, S., Balazs, Y. S., Glazer, L., Berman, A., Sagi, A., & Schmidt, A. (2011). In situ molecular NMR picture of bioavailable calcium stabilized as amorphous

CaCO 3 biomineral in crayfish gastroliths. *Proceedings of the National Academy of Sciences of the United States of America*, *108*(36), 14763–14768. https://doi.org/10.1073/pnas.1102608108

Al-Horani, F. A., Al-Moghrabi, S. M., & De Beer, D. (2003). The mechanism of calcification and its relation to photosynthesis and respiration in the scleractinian coral Galaxea fascicularis. *Marine Biology*, *142*(3), 419–426. https://doi.org/10.1007/S00227-002-0981-8/FIGURES/7

Albéric, M., Bertinetti, L., Zou, Z., Fratzl, P., Habraken, W., & Politi, Y. (2018). The Crystallization of Amorphous Calcium Carbonate is Kinetically Governed by Ion Impurities and Water. *Advanced Science*, *5*(5), 1701000. https://doi.org/10.1002/advs.201701000

Atkins, E. (1978). Elements of X-ray Diffraction. *Physics Bulletin*, *29*(12), 572–572. https://doi.org/10.1088/0031-9112/29/12/034

Beck, W. C., Grossman, E. L., & Morse, J. W. (2005). Experimental studies of oxygen isotope fractionation in the carbonic acid system at 15°, 25°, and 40°C. *Geochimica et Cosmochimica Acta*, *69*(14), 3493–3503. https://doi.org/10.1016/j.gca.2005.02.003

Becker, A., Bismayer, U., Epple, M., Fabritius, H., Hasse, B., Shi, J., & Ziegler, A. (2003). Structural characterisation of X-ray amorphous calcium carbonate (ACC) in sternal deposits of the crustacea Porcellio scaber. *Journal of the Chemical Society. Dalton Transactions*, *3*(4), 551–555. https://doi.org/10.1039/b210529b

Becker, A., Ziegler, A., & Epple, M. (2005). The mineral phase in the cuticles of two species of Crustacea consists of magnesium calcite, amorphous calcium carbonate, and amorphous calcium phosphate. *Dalton Transactions*, *10*, 1814. https://doi.org/10.1039/b412062k

Beniash, E., Addadi, L., & Weiner, S. (1999). Cellular Control Over Spicule Formation in Sea

Urchin Embryos: A Structural Approach. *Journal of Structural Biology*, *125*(1), 50–62. https://doi.org/10.1006/jsbi.1998.4081

Beniash, E., Aizenberg, J., Addadi, L., & Weiner, S. (1997). Amorphous calcium carbonate transforms into calcite during sea urchin larval spicule growth. *Proceedings of the Royal Society of London. Series B: Biological Sciences*, *264*(1380), 461–465. https://doi.org/10.1098/rspb.1997.0066

Beniash, E., Metzler, R. A., Lam, R. S. K., & Gilbert, P. U. P. A. (2009). Transient amorphous calcium phosphate in forming enamel. *Journal of Structural Biology*, *166*(2), 133–143. https://doi.org/10.1016/j.jsb.2009.02.001

Bentov, S., Brownlee, C., & Erez, J. (2009). The role of seawater endocytosis in the biomineralization process in calcareous foraminifera. *Proceedings of the National Academy of Sciences of the United States of America*, *106*(51), 21500–21504. https://doi.org/10.1073/pnas.0906636106

Bentov, S., Weil, S., Glazer, L., Sagi, A., & Berman, A. (2010). Stabilization of amorphous calcium carbonate by phosphate rich organic matrix proteins and by single phosphoamino acids. *Journal of Structural Biology*, *171*(2), 207–215. https://doi.org/10.1016/j.jsb.2010.04.007

Bergwerff, L., & van Paassen, L. A. (2021). Review and recalculation of growth and nucleation kinetics for calcite, vaterite and amorphous calcium carbonate. In *Crystals* (Vol. 11, Issue 11, p. 1318). Multidisciplinary Digital Publishing Institute. https://doi.org/10.3390/cryst11111318

Bewernitz, M. A., Gebauer, D., Long, J., Cölfen, H., & Gower, L. B. (2012). A metastable liquid precursor phase of calcium carbonate and its interactions with polyaspartate. *Faraday*

Discussions, *159*, 291–312. https://doi.org/10.1039/c2fd20080e

Blue, C. R., Rimstidt, J. D., & Dove, P. M. (2013). A Mixed Flow Reactor Method to Synthesize Amorphous Calcium Carbonate Under Controlled Chemical Conditions. In *Methods in Enzymology* (Vol. 532, pp. 557–568). Academic Press Inc. https://doi.org/10.1016/B978-0-12-416617-2.00023-0

Brecevic, L., & Kralj, D. (2008). ChemInform Abstract: On Calcium Carbonates: From Fundamental Research to Application. *ChemInform*, *39*(5), 467–484. https://doi.org/10.1002/chin.200805226

Cai, G. Bin, Zhao, G. X., Wang, X. K., & Yu, S. H. (2010). Synthesis of polyacrylic acid stabilized amorphous calcium carbonate nanoparticles and their application for removal of toxic heavy metal ions in water. *Journal of Physical Chemistry C*, *114*(30), 12948–12954. https://doi.org/10.1021/jp103464p

Cartwright, J. H. E., Checa, A. G., Gale, J. D., Gebauer, D., & Sainz-Díaz, C. I. (2012). Calcium Carbonate Polyamorphism and Its Role in Biomineralization: How Many Amorphous Calcium Carbonates Are There? *Angewandte Chemie International Edition*, *51*(48), 11960–11970. https://doi.org/10.1002/anie.201203125

Chen, S. F., Cölfen, H., Antonietti, M., & Yu, S. H. (2013). Ethanol assisted synthesis of pure and stable amorphous calcium carbonate nanoparticles. *Chemical Communications*, *49*(83), 9564–9566. https://doi.org/10.1039/c3cc45427d

Cohn, M., & Urey, H. C. (1938). Oxygen Exchange Reactions of Organic Compounds and Water. *Journal of the American Chemical Society*, *60*(3), 679–687. https://doi.org/10.1021/ja01270a052

Cölfen, H. (2010). A crystal-clear view. In *Nature Materials* (Vol. 9, Issue 12, pp. 960–961).

https://doi.org/10.1038/nmat2911

Coplen, T.B., & Schlanger, S. O. (1973). Oxygen and Carbon Isotope Studies of Carbonate Sediments from Site 167, Magellan Rise, Leg 17. In *Initial Reports of the Deep Sea Drilling Project, 17*. U.S. Government Printing Office. https://doi.org/10.2973/dsdp.proc.17.115.1973

Coplen, Tyler B. (2007). Calibration of the calcite-water oxygen-isotope geothermometer at Devils Hole, Nevada, a natural laboratory. *Geochimica et Cosmochimica Acta*, *71*(16), 3948–3957. https://doi.org/10.1016/j.gca.2007.05.028

Coronado, I., Fine, M., Bosellini, F. R., & Stolarski, J. (2019). Impact of ocean acidification on crystallographic vital effect of the coral skeleton. *Nature Communications*, *10*(1). https://doi.org/10.1038/s41467-019-10833-6

Costa, S. N., Freire, V. N., Caetano, E. W. S., Maia, F. F., Barboza, C. A., Fulco, U. L., & Albuquerque, E. L. (2016). DFT Calculations with van der Waals Interactions of Hydrated Calcium Carbonate Crystals CaCO3·(H2O, 6H2O): Structural, Electronic, Optical, and Vibrational Properties. *Journal of Physical Chemistry A*, *120*(28), 5752–5765. https://doi.org/10.1021/acs.jpca.6b05436

Cullity, B. D. (Bernard D. (2001). Elements of x-ray diffraction / B.D. Cullity, S.R. Stock. In *Book*. Prentice Hall,. https://discovery.mcmaster.ca/iii/encore/record/C__Rb1167916__SElements of x-ray diffraction__Orightresult__U__X6?lang=eng&suite=def

Darkins, R., Côté, A. S., Freeman, C. L., & Duffy, D. M. (2013). Crystallisation rates of calcite from an amorphous precursor in confinement. *Journal of Crystal Growth*, *367*, 110–114. https://doi.org/10.1016/j.jcrysgro.2012.12.027

De Nooijer, L. J., Toyofuku, T., & Kitazato, H. (2009). Foraminifera promote calcification by elevating their intracellular pH. *Proceedings of the National Academy of Sciences*, *106*(36), 15374–15378. https://doi.org/10.1073/PNAS.0904306106

De Yoreo, J. J., Gilbert, P. U. P. A., Sommerdijk, N. A. J. M., Penn, R. L., Whitelam, S., Joester, D., Zhang, H., Rimer, J. D., Navrotsky, A., Banfield, J. F., Wallace, A. F., Michel, F. M., Meldrum, F. C., Cölfen, H., & Dove, P. M. (2015). Crystallization by particle attachment in synthetic, biogenic, and geologic environments. In *Science* (Vol. 349, Issue 6247). https://doi.org/10.1126/science.aaa6760

Demény, A., Czuppon, G., Kern, Z., Leél-Őssy, S., Németh, A., Szabó, M., Tóth, M., Wu, C. C., Shen, C. C., Molnár, M., Németh, T., Németh, P., & Óvári, M. (2016). Recrystallization-induced oxygen isotope changes in inclusion-hosted water of speleothems – Paleoclimatological implications. *Quaternary International*, *415*, 25–32. https://doi.org/10.1016/j.quaint.2015.11.137

Demény, A., Németh, P., Czuppon, G., Leél-Ossy, S., Szabó, M., Judik, K., Németh, T., & Stieber, J. (2016). Formation of amorphous calcium carbonate in caves and its implications for speleothem research. *Scientific Reports*, *6*(1), 39602. https://doi.org/10.1038/srep39602

Devriendt, L. S., Watkins, J. M., & McGregor, H. V. (2017). Oxygen isotope fractionation in the CaCO3-DIC-H2O system. *Geochimica et Cosmochimica Acta*, *214*, 115–142. https://doi.org/10.1016/j.gca.2017.06.022

Dietzel, M., Purgstaller, B., Kluge, T., Leis, A., & Mavromatis, V. (2020). Oxygen and clumped isotope fractionation during the formation of Mg calcite via an amorphous precursor. *Geochimica et Cosmochimica Acta*, *276*, 258–273. https://doi.org/10.1016/j.gca.2020.02.032

DIFFRAC.EVA | Bruker. (n.d.). Retrieved December 3, 2021, from https://www.bruker.com/en/products-and-solutions/diffractometers-and-scattering-systems/x-ray-diffractometers/diffrac-suite-software/diffrac-eva.html

Douglas, R. C., & Savin, S. M. (1975). Oxygen and Carbon Isotope Analyses of Tertiary and Cretaceous Microfossils from Shatsky Rise and Other Sites in the North Pacific Ocean. In *Initial Reports of the Deep Sea Drilling Project, 32*. U.S. Government Printing Office. https://doi.org/10.2973/dsdp.proc.32.115.1975

Emiliani, C. (1966). Isotopic Paleotemperatures. *Science*, *154*(3751), 851–857. https://doi.org/10.1126/science.154.3751.851

Epstein, S., & Mayeda, T. (1953). Variation of O18 content of waters from natural sources. *Geochimica et Cosmochimica Acta*, *4*(5), 213–224. https://doi.org/10.1016/0016-7037(53)90051-9

Epstein, Samuel, Buchsbaum, R., Lowenstam, H., & Urey, H. C. (1951). Carbonate-water isotopic temperature scale. *Bulletin of the Geological Society of America*, *62*(4), 417–426. https://doi.org/10.1130/0016-7606(1951)62[417:CITS]2.0.CO;2

Erez, J. (1978). *Vital Effect in Coral & Foram*.

Evans, D., Webb, P. B., Penkman, K., Kröger, R., & Allison, N. (2019). The Characteristics and Biological Relevance of Inorganic Amorphous Calcium Carbonate (ACC) Precipitated from Seawater. *Crystal Growth and Design*, *19*(8), 4300–4313. https://doi.org/10.1021/acs.cgd.9b00003

Fairchild, I. J., Smith, C. L., Baker, A., Fuller, L., Spötl, C., Mattey, D., & McDermott, F. (2006). Modification and preservation of environmental signals in speleothems. *Earth-Science Reviews*, *75*(1–4), 105–153. https://doi.org/10.1016/j.earscirev.2005.08.003

Farhadi Khouzani, M., Chevrier, D. M., Güttlein, P., Hauser, K., Zhang, P., Hedin, N., & Gebauer, D. (2015). Disordered amorphous calcium carbonate from direct precipitation. *CrystEngComm*, *17*(26), 4842–4849. https://doi.org/10.1039/c5ce00720h

Frisia, S., Borsato, A., Fairchild, I. J., McDermott, F., & Selmo, E. M. (2002). Aragonite-Calcite Relationships in Speleothems (Grotte De Clamouse, France): Environment, Fabrics, and Carbonate Geochemistry. *Journal of Sedimentary Research*, *72*(5), 687–699. https://doi.org/10.1306/020702720687

Gabitov, R. I., Watson, E. B., Sadekov, A., Watson, B. E., & Sadekov, A. (2012). Oxygen isotope fractionation between calcite and fluid as a function of growth rate and temperature: An in situ study. *Chemical Geology*, *306–307*, 92–102. https://doi.org/10.1016/j.chemgeo.2012.02.021

Gago-Duport, L., Briones, M. J. I., Rodríguez, J. B., & Covelo, B. (2008). Amorphous calcium carbonate biomineralization in the earthworm's calciferous gland: Pathways to the formation of crystalline phases. *Journal of Structural Biology*, *162*(3), 422–435. https://doi.org/10.1016/j.jsb.2008.02.007

Gal, A., Weiner, S., & Addadi, L. (2010). The stabilizing effect of silicate on biogenic and synthetic amorphous calcium carbonate. *Journal of the American Chemical Society*, *132*(38), 13208–13211. https://doi.org/10.1021/ja106883c

Gayathri, S., Lakshminarayanan, R., Weaver, J. C., Morse, D. E., Manjunatha Kini, R., & Valiyaveettil, S. (2007). In vitro study of magnesium-calcite biomineralization in the skeletal materials of the seastar Pisaster giganteus. *Chemistry - A European Journal*, *13*(11), 3262–3268. https://doi.org/10.1002/chem.200600825

Gebauer, D., Gunawidjaja, P. N., Ko, J. Y. P., Bacsik, Z., Aziz, B., Liu, L., Hu, Y., Bergström,

L., Tai, C. W., Sham, T. K., Edén, M., & Hedin, N. (2010). Proto-calcite and proto-vaterite in amorphous calcium carbonates. *Angewandte Chemie - International Edition*, *49*(47), 8889–8891. https://doi.org/10.1002/anie.201003220

Gebauer, D., Völkel, A., & Cölfen, H. (2008). Stable prenucleation calcium carbonate clusters. *Science*, *322*(5909), 1819–1822. https://doi.org/10.1126/science.1164271

Ghosh, P., Adkins, J., Affek, H., Balta, B., Guo, W., Schauble, E. A., Schrag, D., & Eiler, J. M. (2006). 13C-18O bonds in carbonate minerals: A new kind of paleothermometer. *Geochimica et Cosmochimica Acta*, *70*(6), 1439–1456. https://doi.org/10.1016/j.gca.2005.11.014

Giuffre, A. J., Gagnon, A. C., De Yoreo, J. J., & Dove, P. M. (2015). Isotopic tracer evidence for the amorphous calcium carbonate to calcite transformation by dissolution-reprecipitation. *Geochimica et Cosmochimica Acta*, *165*, 407–417. https://doi.org/10.1016/j.gca.2015.06.002

Given, R. K., & Wilkinson, B. H. (1985). Kinetic control of morphology, composition, and mineralogy of abiotic sedimentary carbonates. *Journal of Sedimentary Petrology*, *55*(1), 109–119. https://doi.org/10.1306/212f862a-2b24-11d7-8648000102c1865d

Goldstein, J. I., Yakowitz, H., Newbury, D. E., Lifshin, E., Colby, J. W., & Coleman, J. R. (1975). Practical Scanning Electron Microscopy. In *Practical Scanning Electron Microscopy*. https://doi.org/10.1007/978-1-4613-4422-3

Gower, L. B. (2008). Biomimetic model systems for investigating the amorphous precursor pathway and its role in biomineralization. *Chemical Reviews*, *108*(11), 4551–4627. https://doi.org/10.1021/cr800443h

Günther, C., Becker, A., Wolf, G., & Epple, M. (2005). In vitro Synthesis and Structural

Characterization of Amorphous Calcium Carbonate. *Zeitschrift Für Anorganische Und Allgemeine Chemie*, *631*(13–14), 2830–2835. https://doi.org/10.1002/zaac.200500164

Hasse, B., Ehrenberg, H., Marxen, J. C., Becker, W., & Epple, M. (2000). Calcium carbonate modifications in the mineralized shell of the freshwater snail Biomphalaria glabrata. *Chemistry - A European Journal*, *6*(20), 3679–3685. https://doi.org/10.1002/1521-3765(20001016)6:20<3679::AID-CHEM3679>3.0.CO;2-#

Henini, M. (2000). Scanning electron microscopy: An introduction. *III-Vs Review*, *13*(4), 40–44. https://doi.org/10.1016/S0961-1290(00)80006-X

Hillaire-Marcel, C., Kim, S.-T., Landais, A., Ghosh, P., Assonov, S., Lécuyer, C., Blanchard, M., Meijer, H. A. J., & Steen-Larsen, H. C. (2021). A stable isotope toolbox for water and inorganic carbon cycle studies. *Nature Reviews Earth & Environment*, *2*(10), 699–719. https://doi.org/10.1038/s43017-021-00209-0

Hodson, M. E., Benning, L. G., Demarchi, B., Penkman, K. E. H., Rodriguez-Blanco, J. D., Schofield, P. F., & Versteegh, E. A. A. (2015). Biomineralisation by earthworms – an investigation into the stability and distribution of amorphous calcium carbonate. *Geochemical Transactions*, *16*(1), 4. https://doi.org/10.1186/s12932-015-0019-z

Huang, S. C., Naka, K., & Chujo, Y. (2007). A carbonate controlled-addition method for amorphous calcium carbonate spheres stabilized by poly(acrylic acid)s. *Langmuir*, *23*(24), 12086–12095. https://doi.org/10.1021/la701972n

ICDD. PDF-2+. (2002). *ICDD Database Search – ICDD*. International Centre for Diffraction Data, Newtown Square. https://www.icdd.com/pdfsearch/

Ihli, J., Kim, Y. Y., Noel, E. H., & Meldrum, F. C. (2013). The effect of additives on amorphous calcium carbonate (ACC): Janus behavior in solution and the solid state. *Advanced*

Functional Materials, *23*(12), 1575–1585. https://doi.org/10.1002/adfm.201201805

Ihli, J., Kulak, A. N., & Meldrum, F. C. (2013). Freeze-drying yields stable and pure amorphous calcium carbonate (ACC). *Chemical Communications*, *49*(30), 3134–3136. https://doi.org/10.1039/c3cc40807h

Immenhauser, A., Schöne, B. R., Hoffmann, R., & Niedermayr, A. (2016). Mollusc and brachiopod skeletal hard parts: Intricate archives of their marine environment. *Sedimentology*, *63*(1), 1–59. https://doi.org/10.1111/sed.12231

Jacob, D. E., Soldati, A. L., Wirth, R., Huth, J., Wehrmeister, U., & Hofmeister, W. (2008). Nanostructure, composition and mechanisms of bivalve shell growth. *Geochimica et Cosmochimica Acta*, *72*(22), 5401–5415. https://doi.org/10.1016/j.gca.2008.08.019

Jacob, D. E., Wirth, R., Soldati, A. L., Wehrmeister, U., & Schreiber, A. (2011). Amorphous calcium carbonate in the shells of adult Unionoida. *Journal of Structural Biology*, *173*(2), 241–249. https://doi.org/10.1016/j.jsb.2010.09.011

Jung, G. Y., Shin, E., Park, J. H., Choi, B. Y., Lee, S. W., & Kwak, S. K. (2019). Thermodynamic Control of Amorphous Precursor Phases for Calcium Carbonate via Additive Ions. *Chemistry of Materials*, *31*(18), 7547–7557. https://doi.org/10.1021/acs.chemmater.9b02346

Kellermeier, M., Melero-García, E., Glaab, F., Klein, R., Drechsler, M., Rachel, R., García-Ruiz, J. M., & Kunz, W. (2010). Stabilization of Amorphous Calcium Carbonate in Inorganic Silica-Rich Environments. *Journal of the American Chemical Society*, *132*(50), 17859–17866. https://doi.org/10.1021/ja106959p

Kim, S.-T., Coplen, T. B., & Horita, J. (2015). Normalization of stable isotope data for carbonate minerals: Implementation of IUPAC guidelines. *Geochimica et Cosmochimica Acta*, *158*,

276–289. https://doi.org/10.1016/j.gca.2015.02.011

Kim, S.-T., Hillaire-Marcel, C., & Mucci, A. (2006). Mechanisms of equilibrium and kinetic oxygen isotope effects in synthetic aragonite at 25 °C. *Geochimica et Cosmochimica Acta*, *70*(23 SPEC. ISS.), 5790–5801. https://doi.org/10.1016/j.gca.2006.08.003

Kim, S.-T., & O'Neil, J. R. (1997). Equilibrium and nonequilibrium oxygen isotope effects in synthetic carbonates. *Geochimica et Cosmochimica Acta*, *61*(16), 3461–3475. https://doi.org/10.1016/S0016-7037(97)00169-5

Kim, S. T., O'Neil, J. R., Hillaire-Marcel, C., & Mucci, A. (2007). Oxygen isotope fractionation between synthetic aragonite and water: Influence of temperature and Mg2+ concentration. *Geochimica et Cosmochimica Acta*, *71*(19), 4704–4715. https://doi.org/10.1016/j.gca.2007.04.019

Kimura, T., & Koga, N. (2011). Monohydrocalcite in comparison with hydrated amorphous calcium carbonate: Precipitation condition and thermal behavior. *Crystal Growth and Design*, *11*(9), 3877–3884. https://doi.org/10.1021/cg200412h

Kitano, Y., Okumura, M., & Idogaki, M. (1979). Behavior of dissolved silica in parent solution at the formation of calcium carbonate. *Geochemical Journal*, *13*(6), 253–260. https://doi.org/10.2343/geochemj.13.253

Koga, N., Nakagoe, Y., & Tanaka, H. (1998). Crystallization of amorphous calcium carbonate. *Thermochimica Acta*, *318*(1–2), 239–244. https://doi.org/10.1016/S0040-6031(98)00348-7

Koga, N., & Yamane, Y. (2008). Thermal behaviors of amorphous calcium carbonates prepared in aqueous and ethanol media. *Journal of Thermal Analysis and Calorimetry*, *94*(2), 379–387. https://doi.org/10.1007/s10973-008-9110-3

Köhler-Rink, S., & Kühl, M. (2007). The chemical microenvironment of the symbiotic

planktonic foraminifer Orbulina universa. *Http://Dx.Doi.Org/10.1080/17451000510019015*, *1*(1), 68–78. https://doi.org/10.1080/17451000510019015

Kojima, Y., Sakama, K., Toyama, T., Yasue, T., & Arai, Y. (1994). Dehydration of the Water Molecule in Amorphous Calcium Phosphate. *Phosphorus Research Bulletin*, *4*, 47–52. https://doi.org/10.3363/prb1992.4.0_47

Konrad, F., Gallien, F., Gerard, D. E., & Dietzel, M. (2016). Transformation of Amorphous Calcium Carbonate in Air. *Crystal Growth and Design*, *16*(11), 6310–6317. https://doi.org/10.1021/acs.cgd.6b00906

Kontoyannis, C. G., & Vagenas, N. V. (2000). Calcium carbonate phase analysis using XRD and FT-Raman spectroscopy. *The Analyst*, *125*(2), 251–255. https://doi.org/10.1039/a908609i

Labuhn, I., Genty, D., Vonhof, H., Bourdin, C., Blamart, D., Douville, E., Ruan, J., Cheng, H., Edwards, R. L., Pons-Branchu, E., & Pierre, M. (2015). A high-resolution fluid inclusion δ18O record from a stalagmite in SW France: Modern calibration and comparison with multiple proxies. *Quaternary Science Reviews*, *110*, 152–165. https://doi.org/10.1016/j.quascirev.2014.12.021

Lachniet, M. S. (2009). Climatic and environmental controls on speleothem oxygen-isotope values. *Quaternary Science Reviews*, *28*(5–6), 412–432. https://doi.org/10.1016/j.quascirev.2008.10.021

Lam, R. S. K., Charnock, J. M., Lennie, A., & Meldrum, F. C. (2007). Synthesis-dependant structural variations in amorphous calcium carbonate. *CrystEngComm*, *9*(12), 1226–1236. https://doi.org/10.1039/b710895h

Lee, H. S., Ha, T. H., & Kim, K. (2005). Fabrication of unusually stable amorphous calcium carbonate in an ethanol medium. *Materials Chemistry and Physics*, *93*(2–3), 376–382.

https://doi.org/10.1016/j.matchemphys.2005.03.037

Lee, M. R., Hodson, M. E., & Langworthy, G. N. (2008). Crystallization of calcite from amorphous calcium carbonate: earthworms show the way. *Mineralogical Magazine*, *72*(1), 257–261. https://doi.org/10.1180/minmag.2008.072.1.257

Levi-Kalisman, Y., Raz, S., Weiner, S., Addadi, L., & Sagi, I. (2002). Structural differences between biogenic amorphous calcium carbonate phases using X-ray absorption spectroscopy. *Advanced Functional Materials*, *12*(1), 43–48. https://doi.org/10.1002/1616-3028(20020101)12:1<43::AID-ADFM43>3.0.CO;2-C

Levi-Kalisman, Yael, Raz, S., Weiner, S., Addadi, L., & Sagi, I. (2000). X-Ray absorption spectroscopy studies on the structure of a biogenic "amorphous" calcium carbonate phase †. *Journal of the Chemical Society, Dalton Transactions*, *21*, 3977–3982. https://doi.org/10.1039/b003242p

Lewis, I. R., & Edwards, H. (2001). Handbook of Raman Spectroscopy. *Handbook of Raman Spectroscopy*. https://doi.org/10.1201/9781420029253

Li, J., Chen, Z., Wang, R. J., & Proserpio, D. M. (1999). Low temperature route towards new materials: solvothermal synthesis of metal chalcogenides in ethylenediamine. *Coordination Chemistry Reviews*, *190–192*, 707–735. https://doi.org/10.1016/S0010-8545(99)00107-1

Lowenstam, H. A, & Epstein, S. (1954). Paleotemperatures of the Post-Aptian Cretaceous as Determined by the Oxygen Isotope Method. *The Journal of Geology*, *62*(3), 207–248. https://doi.org/10.1086/626160

Lowenstam, Heinz A. (1972). Phosphatic hard tissues of marine invertebrates: Their nature and mechanical function, and some fossil implications. *Chemical Geology*, *9*(1–4), 153–166. https://doi.org/10.1016/0009-2541(72)90053-8

Mass, T., Giuffre, A. J., Sun, C. Y., Stifler, C. A., Frazier, M. J., Neder, M., Tamura, N., Stan, C. V., Marcus, M. A., & Gilbert, P. U. P. A. (2017). Amorphous calcium carbonate particles form coral skeletons. *Proceedings of the National Academy of Sciences of the United States of America*, *114*(37), E7670–E7678. https://doi.org/10.1073/pnas.1707890114

Mavromatis, V., Purgstaller, B., Dietzel, M., Buhl, D., Immenhauser, A., & Schott, J. (2017). Impact of amorphous precursor phases on magnesium isotope signatures of Mg-calcite. *Earth and Planetary Science Letters*, *464*, 227–236. https://doi.org/10.1016/j.epsl.2017.01.031

McConnaughey, T. (1989a). 13C and 18O isotopic disequilibrium in biological carbonates: I. Patterns. *Geochimica et Cosmochimica Acta*, *53*(1), 151–162. https://doi.org/10.1016/0016-7037(89)90282-2

McConnaughey, T. (1989b). 13C and 18O isotopic disequilibrium in biological carbonates: II. In vitro simulation of kinetic isotope effects. *Geochimica et Cosmochimica Acta*, *53*(1), 163–171. https://doi.org/10.1016/0016-7037(89)90283-4

McCrea, J. M. (1950). On the Isotopic Chemistry of Carbonates and a Paleotemperature Scale. *The Journal of Chemical Physics*, *18*(6), 849–857. https://doi.org/10.1063/1.1747785

McDermott, F. (2004). Palaeo-climate reconstruction from stable isotope variations in speleothems: A review. *Quaternary Science Reviews*, *23*(7–8), 901–918. https://doi.org/10.1016/j.quascirev.2003.06.021

Meldrum, F. C. (2003). Calcium carbonate in biomineralisation and biomimetic chemistry. In *International Materials Reviews* (Vol. 48, Issue 3, pp. 187–224). https://doi.org/10.1179/095066003225005836

Meldrum, F. C., & O'Shaughnessy, C. (2020). Crystallization in Confinement. In *Advanced*

Materials (Vol. 32, Issue 31, p. 2001068). John Wiley & Sons, Ltd. https://doi.org/10.1002/adma.202001068

Michel, F. M., MacDonald, J., Feng, J., Phillips, B. L., Ehm, L., Tarabrella, C., Parise, J. B., & Reeder, R. J. (2008). Structural characteristics of synthetic amorphous calcium carbonate. *Chemistry of Materials*, *20*(14), 4720–4728. https://doi.org/10.1021/cm800324v

Nakashima, Y., Takai, C., Razavi-Khosroshahi, H., Suthabanditpong, W., & Fuji, M. (2018). Synthesis of ultra-small hollow silica nanoparticles using the prepared amorphous calcium carbonate in one-pot process. *Advanced Powder Technology*, *29*(4), 904–908. https://doi.org/10.1016/j.apt.2018.01.006

Navrotsky, A. (2004). Energetic clues to pathways to biomineralization: Precursors, clusters, and nanoparticles. *Proceedings of the National Academy of Sciences of the United States of America*, *101*(33), 12096–12101. https://doi.org/10.1073/pnas.0404778101

Neumann, M., & Epple, M. (2007). Monohydrocalcite and its relationship to hydrated amorphous calcium carbonate in biominerals. *European Journal of Inorganic Chemistry*, *2007*(14), 1953–1957. https://doi.org/10.1002/ejic.200601033

Njegić-Džakula, B., Brečević, L., Falini, G., & Kralj, D. (2011). Kinetic Approach to Biomineralization: Interactions of Synthetic Polypeptides with Calcium Carbonate Polymorphs. *Croatica Chemica Acta*, *84*(2), 301–314. https://doi.org/10.5562/cca1809

Northrop, D. A., & Clayton, R. N. (1966). Oxygen-Isotope Fractionations in Systems Containing Dolomite. *The Journal of Geology*, *74*(2), 174–196. https://doi.org/10.1086/627153

O'Day, P. A., Rehr, J. J., Zabinsky, S. I., & Brown, G. E. (1994). Extended X-ray Absorption Fine Structure (EXAFS) Analysis of Disorder and Multiple-Scattering in Complex Crystalline Solids. *Journal of the American Chemical Society*, *116*(7), 2938–2949.

https://doi.org/10.1021/ja00086a026

Ogino, T., Suzuki, T., & Sawada, K. (1987). The formation and transformation mechanism of calcium carbonate in water. *Geochimica et Cosmochimica Acta*, *51*(10), 2757–2767. https://doi.org/10.1016/0016-7037(87)90155-4

Ostwald, W. (1901). Reviews-On the assumed isomerism between red and yellow mercuric oxide and on the surface-tension of solids. *The Journal of Physical Chemistry*, *5*(1), 75–75. https://doi.org/10.1021/j150028a603

Paquin, F., Rivnay, J., Salleo, A., Stingelin, N., & Silva, C. (2015). Multi-phase semicrystalline microstructures drive exciton dissociation in neat plastic semiconductors. *J. Mater. Chem. C*, *3*, 10715–10722. https://doi.org/10.1039/b000000x

Pérez-Huerta, A., & C. Fred, T. A. (2010). Vital effects in the context of biomineralization. *Seminarios de La Sociedad Española de Mineralogía*, *7*, 35–45.

Ping, H., Xie, H., Wan, Y., Zhang, Z., Zhang, J., Xiang, M., Xie, J., Wang, H., Wang, W., & Fu, Z. (2016). Confinement controlled mineralization of calcium carbonate within collagen fibrils. *Journal of Materials Chemistry B*, *4*(5), 880–886. https://doi.org/10.1039/C5TB01990G

Politi, Y., Batchelor, D. R., Zaslansky, P., Chmelka, B. F., Weaver, J. C., Sagi, I., Weiner, S., & Addadi, L. (2010). Role of Magnesium Ion in the Stabilization of Biogenic Amorphous Calcium Carbonate: A Structure−Function Investigation. *Chemistry of Materials*, *22*(1), 161–166. https://doi.org/10.1021/cm902674h

Politi, Y., Levi-Kalisman, Y., Raz, S., Wilt, F., Addadi, L., Weiner, S., & Sagi, I. (2006). Structural Characterization of the Transient Amorphous Calcium Carbonate Precursor Phase in Sea Urchin Embryos. *Advanced Functional Materials*, *16*(10), 1289–1298.

https://doi.org/10.1002/adfm.200600134

Purgstaller, B., Mavromatis, V., Immenhauser, A., & Dietzel, M. (2016). Transformation of Mg-bearing amorphous calcium carbonate to Mg-calcite - In situ monitoring. *Geochimica et Cosmochimica Acta*, *174*, 180–195. https://doi.org/10.1016/j.gca.2015.10.030

Radha, A. V., Forbes, T. Z., Killian, C. E., Gilbert, P. U. P. A., & Navrotsky, A. (2010). Transformation and crystallization energetics of synthetic and biogenic amorphous calcium carbonate. *Proceedings of the National Academy of Sciences*, *107*(38), 16438–16443. https://doi.org/10.1073/pnas.1009959107

Rao, A., Vásquez-Quitral, P., Fernández, M. S., Berg, J. K., Sánchez, M., Drechsler, M., Neira-Carrillo, A., Arias, J. L., Gebauer, D., & Cölfen, H. (2016). PH-Dependent Schemes of Calcium Carbonate Formation in the Presence of Alginates. *Crystal Growth and Design*, *16*(3), 1349–1359. https://doi.org/10.1021/acs.cgd.5b01488

Raz, S., Hamilton, P. C., Wilt, F. H., Weiner, S., & Addadi, L. (2003). The Transient Phase of Amorphous Calcium Carbonate in Sea Urchin Larval Spicules: The Involvement of Proteins and Magnesium Ions in Its Formation and Stabilization. *Advanced Functional Materials*, *13*(6), 480–486. https://doi.org/10.1002/adfm.200304285

Raz, S., Testeniere, O., Hecker, A., Weiner, S., & Luquet, G. (2002). Stable amorphous calcium carbonate is the main component of the calcium storage structures of the crustacean Orchestia cavimana. *Biological Bulletin*, *203*(3), 269–274. https://doi.org/10.2307/1543569

Rodriguez-Blanco, J. D., Shaw, S., Bots, P., Roncal-Herrero, T., & Benning, L. G. (2012). The role of pH and Mg on the stability and crystallization of amorphous calcium carbonate. *Journal of Alloys and Compounds*, *536*(SUPPL.1), S477–S479. https://doi.org/10.1016/j.jallcom.2011.11.057

Rodriguez-Blanco, Juan Diego, Shaw, S., & Benning, L. G. (2011). The kinetics and mechanisms of amorphous calcium carbonate (ACC) crystallization to calcite, viavaterite. *Nanoscale*, *3*(1), 265–271. https://doi.org/10.1039/C0NR00589D

Rodriguez-Navarro, C., Kudłacz, K., Cizer, Ö., & Ruiz-Agudo, E. (2015). Formation of amorphous calcium carbonate and its transformation into mesostructured calcite. *CrystEngComm*, *17*(1), 58–72. https://doi.org/10.1039/c4ce01562b

Ross, E. E., Mok, S. W., & Bugni, S. R. (2011). Assembly of lipid bilayers on silica and modified silica colloids by reconstitution of dried lipid films. *Langmuir*, *27*(14), 8634–8644. https://doi.org/10.1021/la200952c

Roy, R. N., Roy, L. N., Vogel, K. M., Porter-Moore, C., Pearson, T., Good, C. E., Millero, F. J., & Campbell, D. M. (1993). The dissociation constants of carbonic acid in seawater at salinities 5 to 45 and temperatures 0 to 45°C. *Marine Chemistry*, *44*(2–4), 249–267. https://doi.org/10.1016/0304-4203(93)90207-5

Saenger, C., & Wang, Z. (2014). Magnesium isotope fractionation in biogenic and abiogenic carbonates: Implications for paleoenvironmental proxies. In *Quaternary Science Reviews* (Vol. 90, pp. 1–21). Elsevier Ltd. https://doi.org/10.1016/j.quascirev.2014.01.014

Savin, S. M. (1977). The History of the Earth's Surface Temperature During the Past 100 Million Years. *Annual Review of Earth and Planetary Sciences*, *5*(1), 319–355. https://doi.org/10.1146/annurev.ea.05.050177.001535

Schmidt, M., Xeflide, S., Botz, R., & Mann, S. (2005). Oxygen isotope fractionation during synthesis of CaMg-carbonate and implications for sedimentary dolomite formation. *Geochimica et Cosmochimica Acta*, *69*(19), 4665–4674. https://doi.org/10.1016/j.gca.2005.06.025

Schwartz, A. M. (2002). Handbook of Industrial Crystallization - Chapter 01 - Solutions and solution properties. *Handbook of Industrial Crystallization*, *7*, 1–31. http://www.sciencedirect.com/science/article/pii/B9780750670128500033

Seo, K. S., Han, C., Wee, J. H., Park, J. K., & Ahn, J. W. (2005). Synthesis of calcium carbonate in a pure ethanol and aqueous ethanol solution as the solvent. *Journal of Crystal Growth*, *276*(3–4), 680–687. https://doi.org/10.1016/j.jcrysgro.2004.11.416

Setoguchi, H. (1989). Origin, Evolution, and Modern Aspects of Biomineralization in Plants and Animals. *Origin, Evolution, and Modern Aspects of Biomineralization in Plants and Animals*, *December*. https://doi.org/10.1007/978-1-4757-6114-6

Simkiss, K. (1991). Amorphous Minerals and Theories of Biomineralization. In *Mechanisms and Phylogeny of Mineralization in Biological Systems* (pp. 375–382). Springer Japan. https://doi.org/10.1007/978-4-431-68132-8_60

Smith, B. C. (2011). Fundamentals of fourier transform infrared spectroscopy, second edition. In *Fundamentals of Fourier Transform Infrared Spectroscopy, Second Edition*.

Stephens, C. J., Ladden, S. F., Meldrum, F. C., & Christenson, H. K. (2010). Amorphous calcium carbonate is stabilized in confinement. *Advanced Functional Materials*, *20*(13), 2108–2115. https://doi.org/10.1002/adfm.201000248

Swart, P. K. (2015). The geochemistry of carbonate diagenesis: The past, present and future. *Sedimentology*, *62*(5), 1233–1304. https://doi.org/10.1111/sed.12205

Taylor, M. G., Simkiss, K., Greaves, G. N., Okazaki, M., & Mann, S. (1993). An X-ray absorption spectroscopy study of the structure and transformation of amorphous calcium carbonate from plant cystoliths. *Proceedings of the Royal Society B: Biological Sciences*, *252*(1333), 75–80. https://doi.org/10.1098/rspb.1993.0048

Tester, C. C., Brock, R. E., Wu, C.-H., Krejci, M. R., Weigand, S., & Joester, D. (2011). In vitro synthesis and stabilization of amorphous calcium carbonate (ACC) nanoparticles within liposomes. *CrystEngComm*, *13*(12), 3975. https://doi.org/10.1039/c1ce05153a

Tester, C. C., Whittaker, M. L., & Joester, D. (2014). Controlling nucleation in giant liposomes. *Chemical Communications*, *50*(42), 5619–5622. https://doi.org/10.1039/c4cc01457j

Tobler, D. J., Rodriguez-Blanco, J. D., Sørensen, H. O., Stipp, S. L. S., & Dideriksen, K. (2016). Effect of pH on Amorphous Calcium Carbonate Structure and Transformation. *Crystal Growth and Design*, *16*(8), 4500–4508. https://doi.org/10.1021/acs.cgd.6b00630

Tompa, A. S., & Watabe, N. (1977). Calcified arteries in a gastropod. *Calcified Tissue Research*, *22*(1), 159–172. https://doi.org/10.1007/BF02010355

Townsend, D., Lahankar, S. A., Lee, S. K., Chambreau, S. D., Suits, A. G., Zhang, X., Rheinecker, J., Harding, L. B., & Bowman, J. M. (2004). The Roaming Atom: Straying from the Reaction Path in Formaldehyde Decomposition. *Science*, *306*(5699), 1158–1161. https://doi.org/10.1126/science.1104386

Travis, D. F. (2006). Structural features of mineralization from tissue to macromolecular levels of organization in the decapod crustacea. *Annals of the New York Academy of Sciences*, *109*(1), 177–245. https://doi.org/10.1111/j.1749-6632.1963.tb13467.x

Venn, A., Tambutté, E., Holcomb, M., Allemand, D., & Tambutté, S. (2011). Live tissue imaging shows reef corals elevate pH under their calcifying tissue relative to seawater. *PLoS ONE*, *6*(5). https://doi.org/10.1371/JOURNAL.PONE.0020013

Versteegh, E. A. A., Black, S., & Hodson, M. E. (2017). Carbon isotope fractionation between amorphous calcium carbonate and calcite in earthworm-produced calcium carbonate. *Applied Geochemistry*, *78*, 351–356. https://doi.org/10.1016/j.apgeochem.2017.01.017

Vinogradov, A. P. (1953). *The elementary chemical composition of marine organisms / A.P. Vinogradov.* https://discovery.mcmaster.ca/iii/encore/record/C__Rb2252090__SVinogradov, A. P. The Elementary Chemical Composition of Marine Organisms__Orightresult__U__X2?lang=eng&suite=def

Voorhees, P. W. (1985). The theory of Ostwald ripening. *Journal of Statistical Physics*, *38*(1–2), 231–252. https://doi.org/10.1007/BF01017860

Wang, S. S., & Xu, A. W. (2013). Amorphous calcium carbonate stabilized by a flexible biomimetic polymer inspired by marine mussels. *Crystal Growth and Design*, *13*(5), 1937–1942. https://doi.org/10.1021/cg301759t

Wang, Y., Zeng, M., Meldrum, F. C., & Christenson, H. K. (2017). Using confinement to study the crystallization pathway of calcium carbonate. *Crystal Growth and Design*, *17*(12), 6787–6792. https://doi.org/10.1021/acs.cgd.7b01359

Wang, Z. L., & Lee, J. L. (2008). Electron Microscopy Techniques for Imaging and Analysis of Nanoparticles. In *Developments in Surface Contamination and Cleaning: Second Edition* (Vol. 1, pp. 395–443). William Andrew Publishing. https://doi.org/10.1016/B978-0-323-29960-2.00009-5

Weiner, S. (2003). An Overview of Biomineralization Processes and the Problem of the Vital Effect. *Reviews in Mineralogy and Geochemistry*, *54*(1), 1–29. https://doi.org/10.2113/0540001

Weiner, S., Levi-Kalisman, Y., Raz, S., & Addadi, L. (2003). Biologically Formed Amorphous Calcium Carbonate. *Connective Tissue Research*, *44*(1), 214–218. https://doi.org/10.1080/03008200390181681

Weiss, I. M., Tuross, N., Addadi, L., & Weiner, S. (2002). Mollusc larval shell formation: amorphous calcium carbonate is a precursor phase for aragonite. *Journal of Experimental Zoology*, *293*(5), 478–491. https://doi.org/10.1002/jez.90004

Whittaker, M. L., Dove, P. M., & Joester, D. (2016). Nucleation on surfaces and in confinement. *MRS Bulletin*, *41*(5), 388–392. https://doi.org/10.1557/mrs.2016.90

Wombacher, F., Eisenhauer, A., Böhm, F., Gussone, N., Regenberg, M., Dullo, W. C., & Rüggeberg, A. (2011). Magnesium stable isotope fractionation in marine biogenic calcite and aragonite. *Geochimica et Cosmochimica Acta*, *75*(19), 5797–5818. https://doi.org/10.1016/j.gca.2011.07.017

Xto, J. M., Borca, C. N., van Bokhoven, J. A., & Huthwelker, T. (2019). Aerosol-based synthesis of pure and stable amorphous calcium carbonate. *Chemical Communications*, *55*(72), 10725–10728. https://doi.org/10.1039/c9cc03749g

Xu, N., Li, Y., Zheng, L., Gao, Y., Yin, H., Zhao, J., Chen, Z., Chen, J., & Chen, M. (2014). Synthesis and application of magnesium amorphous calcium carbonate for removal of high concentration of phosphate. *Chemical Engineering Journal*, *251*, 102–110. https://doi.org/10.1016/j.cej.2014.04.037

Xu, X. R., Cai, A. H., Liu, R., Pan, H. H., Tang, R. K., & Cho, K. (2008). The roles of water and polyelectrolytes in the phase transformation of amorphous calcium carbonate. *Journal of Crystal Growth*, *310*(16), 3779–3787. https://doi.org/10.1016/j.jcrysgro.2008.05.034

Zeebe, R. E. (1999). An explanation of the effect of seawater carbonate concentration on foraminiferal oxygen isotopes. *Geochimica et Cosmochimica Acta*, *63*(13–14), 2001–2007. https://doi.org/10.1016/S0016-7037(99)00091-5

Zeebe, R. E., & Wolf-Gladrow, D. A. (2001). CO2 in Seawater: Equilibrium, Kinetics, Isotopes.

In *Elsevier*. https://linkinghub.elsevier.com/retrieve/pii/S0924796302001793

Zeebe, R. E., Wolf-Gladrow, D. A., & Jansen, H. (1999). On the time required to establish chemical and isotopic equilibrium in the carbon dioxide system in seawater. *Marine Chemistry*, *65*, 135–153.

Zhang, H., Cai, Y., Tan, L., Qin, S., & An, Z. (2014). Stable isotope composition alteration produced by the aragonite-to-calcite transformation in speleothems and implications for paleoclimate reconstructions. *Sedimentary Geology*, *309*, 1–14. https://doi.org/10.1016/j.sedgeo.2014.05.007

Zhang, M., Li, J., Zhao, J., Cui, Y., & Luo, X. (2020). Comparison of CH4and CO2Adsorptions onto Calcite(10.4), Aragonite(011)Ca, and Vaterite(010)CO3Surfaces: An MD and DFT Investigation. *ACS Omega*, *5*(20), 11369–11377. https://doi.org/10.1021/acsomega.0c00345

Ziveri, P., Stoll, H., Probert, I., Klaas, C., Geisen, M., Ganssen, G., & Young, J. (2003). Stable isotope "vital effects" in coccolith calcite. *Earth and Planetary Science Letters*, *210*(1–2), 137–149. https://doi.org/10.1016/S0012-821X(03)00101-8

Zou, Z., Bertinetti, L., Politi, Y., Jensen, A. C. S., Weiner, S., Addadi, L., Fratzl, P., & Habraken, W. J. E. M. (2015). Supplementary - Opposite Particle Size Effect on Amorphous Calcium Carbonate Crystallization in Water and during Heating in Air. *Chemistry of Materials*, *27*(12), 4237–4246. https://doi.org/10.1021/acs.chemmater.5b00145